

From somites to vertebral column

Elizabeth Ward

University College London

A thesis submitted for the degree of
Doctor of Philosophy

PhD supervisors:

Prof. Claudio D. Stern & Prof. Susan E. Evans

January 2016

Declaration

I, Elizabeth Ward, confirm that the work presented in this thesis is my own. Where information has been derived from other sources, I confirm that this has been indicated in the thesis

Abstract

Vertebrates build their bodies in segments. This segmentation is established in the embryo when the paraxial mesoderm becomes segmented into the somites, which contain the precursors of the axial skeleton (sclerotome) and muscles (dermomyotome). The number and size of somites, and later the morphology of the vertebrae they go on to form, are both thought to be determined by information intrinsic to the paraxial mesoderm. This has led to the general understanding that the final segmental pattern of the vertebral column is a direct read-out of the segmentation established during somitogenesis. This study explores the role of signals external to the somite in segmentation of the vertebral column. Using fluorescent markers, the fate of somites was traced from anterior-posterior along the chick vertebral column, revealing a region-specific shift between the dorsal and ventral sclerotome, possibly mediated by external signals during sclerotome migration. Next, I identify the notochord as a potential source of these signals, and show that the notochord is required for segmentation of the vertebral bodies. Furthermore, an ectopic notochord is sufficient to alter the spatial periodicity of sclerotome set up in the somites. Inter-regional notochord grafts and somite tracing suggests that this change in somite segmentation is achieved by a previously unidentified attraction of the sclerotome towards the notochord, which compresses somitic segments. I go on to test whether Sonic hedgehog signalling from the notochord provides a directional cue by attracting sclerotome cells to the midline. This study indicates that a role for the notochord in vertebral segmentation is present in amniotes, highlighting a much-overlooked aspect of the development and evolution of vertebral patterning.

Acknowledgements

My first thanks go to my supervisors, Susan and Claudio, for introducing me to the wonderful world of somites and for their continued support and guidance throughout my PhD.

I am also indebted to my colleagues in the Stern lab, for their valuable ideas and input to this project, their help day-to-day in the lab and for making it such an enjoyable place to work. Special mentions go to Nidia (without whom the lab would collapse), Claire, Anna and Kat for their friendship and occasional embryology madness.

Outside of the lab, I would like to say a huge thank you to my family: Mum, Dad, Martin, Nat, Toby, Pete, Sue and Mel. Eight of the most hilarious people I know - I am very lucky to have you. To my parents I extend a particular thank you, for making it possible for me to pursue what I want to in life, but thankfully for being more concerned with my happiness than any career-based success. I cannot stress enough how much they have done for me over the years.

To all my friends, thank you for generally being brilliant. A special mention goes to Vicky (the Lou to my Harold), Harriet "you're not that rubbish" Muncey and to Laurie and Ratchet - always there for a chat, despite the best efforts of the Atlantic Ocean to come between us.

Last, but certainly not least, my biggest thanks go to my husband, Jue, for so many things I cannot even begin and who may never want to hear the word 'somites' again after this.

Table of Contents

Table of Contents	5
List of Figures	12
List of Tables	13
CHAPTER 1 : GENERAL INTRODUCTION	14
1.1. Segmentation	14
1.1.1. Many animals build their bodies in segments	14
1.1.2. Why study the development of segmentation? An evolutionary perspective	14
1.1.3. Segmentation in vertebrates	15
1.2. Establishing segmentation in the vertebrate embryo	16
1.2.1. The somites	16
1.2.2. The notochord	16
1.2.3. Formation and patterning of the mesoderm	17
1.2.4. Somitogenesis	19
1.2.5. The clock and wavefront model	20
1.2.6. The molecular basis of the “clock”	21
1.2.7. The period of the clock and segmentation	22
1.2.8. The molecular basis of the “wavefront”	23
1.2.9. Rostro-caudal patterning of the somite	24
1.2.10. The clock and wavefront cannot explain all aspects of somitogenesis	25
1.3. Antero-posterior patterning of the vertebrate body axis	28
1.3.1. Morphological variation along the vertebrate A-P axis	28
1.3.2. The Hox genes	28
1.3.3. Hox genes and vertebrate axial identity	29
1.3.4. When is axial identity determined?	31
1.4. Specification of somite compartments	32
1.4.1. Dorso-ventral patterning of the somite	32
1.4.2. Medio-lateral patterning of the somite	33

1.5. From sclerotome to vertebral column	35
1.5.1. Migration of the sclerotome	35
1.5.2. Rearrangement of the sclerotome and dermomyotome	36
1.5.3. The fate of sclerotome in the vertebrae: insights from anatomical studies	37
1.5.3.1. Model 1: Resegmentation	37
1.5.3.2. Model 2: Shifting of sclerotomes	37
1.5.3.3. Discontinuity in segmental patterning between sclerotomes and vertebrae	38
1.5.3.4. Tracing morphological boundaries in the sclerotome	40
1.5.4. The fate of sclerotome in the vertebral column: insights from experimental embryology	41
1.5.4.1. Quail-chick somite grafts	41
1.5.4.2. Tracing of somites in situ	42
1.5.5. Resegmentation: Outstanding questions	42
1.6. A role for external signals in vertebral segmentation.	43
1.6.1. Evidence for external signals in amniote vertebral segmentation	43
1.6.2. The notochord plays a key role in vertebral segmentation in teleost fish	45
1.6.3. Does the notochord play a role in vertebral patterning in amniotes?	48
1.7. Aims of the thesis	50
CHAPTER 2 : GENERAL MATERIALS AND METHODS	51
2.1. Embryology	51
2.1.1. Embryos	51
2.1.2. Harvesting embryos for fixation	51
2.1.3. Embryo fixation	51
2.1.4. Preparation of embryos for in-ovo manipulation	52
2.1.5. Preparation of embryos for 'New' culture	52
2.1.6. Counting of somites and vertebrae	52
2.1.7. Dil and DiO labelling	53
2.2 Molecular Biology	53
2.2.1. Isolation and purification of embryonic mRNA	53
2.2.2. Single-stranded cDNA synthesis	54

2.2.3. Primer design	54
2.2.4. Cloning of Uncx4.1 mRNA by PCR	55
2.2.5. Ligation and transformation	56
2.2.6. Preparation of ampicillin X-gal/IPTG selection plates	56
2.2.7. Preparation and purification of recombinant plasmid DNA	57
2.2.7.1. Mini-prep	57
2.2.7.2. Midi-prep	57
2.2.8. Diagnostic digest	57
2.2.9 Gel electrophoresis and sequencing of cloned DNA	58
2.2.10. Measurement of DNA and RNA concentration	58
2.3. Whole-mount In-Situ Hybridisation (WMISH)	58
2.3.1. Linearisation of plasmid DNA	58
2.3.2. PCR amplification of cDNA insert	59
2.3.3. Transcription of anti-sense RNA probes	60
2.3.4. WMISH protocol	62
2.4. Immunohistochemistry and histology	64
2.4.1. Whole-Mount immuno-staining	64
2.4.2. Whole-mount immuno-staining following WMISH	65
2.4.3. Skeletal preparations	67
2.4.4. Microtome sectioning of paraffin-embedded embryos	67
2.5. Imaging	68
2.5.1. Imaging of whole-mount embryos	68
2.5.2. Time-lapse imaging of live embryos	68
2.5.3. Imaging of sections	68
2.5.4. Optical Projection Tomography (OPT)	68
2.5.4.1. Preparation of specimens	68
2.5.4.2. OPT scanning	69
CHAPTER 3 : A “RESEGMENTATION-SHIFT” MODEL FOR VERTEBRAL FORMATION	70
3.1. Introduction	70
3.2. Materials and methods	71
3.2.1. Dil and DiO labelling of somites in different regions of the axis	71
3.2.2. Measurements of neural arch tilt	72

3.3. Results	72
3.3.1. Somite contribution to the vertebral bodies	72
3.3.2. Somite contribution to the occipital region, atlas and axis	75
3.3.3. Somite contribution to the neural arches	78
3.4. Discussion	82
3.4.1. A “resegmentation-shift” model for vertebral patterning	82
3.4.2. Positioning of intervertebral discs	84
3.4.3. The fate of the somites in the occipital region, atlas and axis	85
3.5. Summary	86
CHAPTER 4 : SIGNALS FROM THE NOTOCHORD ARE INVOLVED IN VERTEBRAL PATTERNING	88
4.1. Introduction	88
4.2. Materials and Methods	90
4.2.1. Notochord ablation	90
4.2.2. Notochord graft	91
4.2.3. Notochord and somite graft	91
4.2.4. Notochord grafts between different axial regions	92
4.2.5. Notochord and neural tube graft	92
4.2.6. Quantification of segment length	92
4.3. Results	93
4.3.1. The periodic pattern of vertebral bodies is lost when the notochord is ablated	93
4.3.2. Notochord grafts result in ectopic sclerotome lateral to the host somites	96
4.3.3. A notochord graft results in ectopic sclerotome in a different periodicity to that of the host sclerotome	99
4.3.4. Ectopic sclerotome is derived from the host	102
4.3.5. Ectopic sclerotome forms cartilage	105
4.3.6. The periodicity of the ectopic sclerotome is dependent upon somite size, not the axial region of the notochord	109
4.3.7. A notochord and neural tube graft gives rise to ectopic cartilage that resembles vertebral bodies and neural arches	115

4.4. Discussion	118
4.4.1. Two distinct roles for the notochord in vertebral development: Attraction and segmental patterning	118
4.4.2. The origin of ectopic sclerotome	121
4.4.3. Variation in the formation and segmentation of ectopic sclerotome	122
4.4.4. Does the notochord influence segmentation of other somitic compartments?	122
4.4.4.1. Dermomyotome	122
4.4.4.3. Syndetome	123
4.4.5. A possible role for the neural tube in neural arch patterning	123
4.5. Summary	126
 CHAPTER 5 : ATTRACTION OF THE SCLEROTOME TOWARDS THE NOTOCHORD	 127
5.1. Introduction	127
5.2 Materials and methods	129
5.2.1. Notochord graft plus Dil and DiO labelling in-ovo	129
5.2.2. Notochord graft in culture	130
5.2.3. DiO labelling of somites in culture	130
5.2.4. Calculating somite area	130
5.2.5. Preparation of Shh beads	131
5.2.6. Preparation of cell pellets	131
5.2.7. Western blot	131
5.2.8. Shh bead validation graft	132
5.2.9. Grafting of beads or pellets adjacent to the caudal-most somites in New culture	132
5.3. Results	133
5.3.1. Somite tracing suggests attraction of somite cells towards a grafted notochord	133
5.3.2. Notochord grafts give rise to ectopic sclerotome after 24 hours	136
5.3.3. Time-lapse imaging reveals an expansion of the somites in response to a notochord graft after 8 hours in culture	137
5.3.4. Identifying the attractant: A Shh bead is sufficient to give rise to a change in shape and size of the somites, but this effect is variable	142

5.3.5. Identifying the attractant: DiO-labelling suggests a migration of somites towards a SHH bead, but this effect is variable	146
5.3.6. Identifying the attractant: A cell pellet secreting Shh is sufficient to give rise to a change in shape and size of the somites, but this effect is still variable	147
5.4. Discussion	150
5.4.1. Somite cells are attracted to the notochord	150
5.4.2. Is this attraction specific to the sclerotome?	151
5.4.3. Somite expansion: Attraction, proliferation or both?	152
5.4.4. A notochord graft also disrupts medio-lateral and dorso-ventral patterning of the somite	154
5.4.5. Does Shh mediate the attraction? Lessons from the neural tube	155
5.4.6. Multiple roles for Shh from the notochord in somite development	155
5.4.7. Is Shh sufficient to mimic the attractive effect of a notochord in culture?	156
5.4.8. Is Shh required for the notochord to exert its attraction?	157
5.4.9. Do other factors play a role in regulating sclerotome migration and attraction?	158
5.5. Summary	159
CHAPTER 6 : EXPLORING AN ALTERNATIVE METHOD FOR STUDYING THE ROLE OF THE NOTOCHORD IN VERTEBRAL SEGMENTATION	160
6.1. Introduction	160
6.2. Materials and Methods	161
6.2.1. Grafts of Hensen's node notochord precursors	161
6.2.2. Preparation of FGF4 beads	161
6.2.3. FGF4 bead positive control graft	162
6.3. Results	162
6.3.1. An ectopic notochord expands the adjacent host paraxial mesoderm	162
6.3.2. Time-lapse movies show a transient stage at which somite cells appear to be attracted towards the ectopic notochord	165
6.3.3. Are somite cells attracted to FGF4 from the early notochord?	169

6.4. Discussion	172
6.4.1. Notochord precursor grafts as an assay for studying the role of the notochord in vertebral segmental patterning	172
6.4.2. The formation of ectopic somites	173
6.4.3. Notochord precursor grafts as an assay for studying somitogenesis	175
6.4.4. Does the ectopic notochord attract paraxial mesoderm cells?	176
6.4.5. Is FGF4 a long-range attractant?	177
6.5. Summary	178
CHAPTER 7 : DISCUSSION AND FUTURE DIRECTIONS	179
7.1. Introduction	179
7.2. Relationship between somite and vertebral segmentation	179
7.2.1. Resegmentation confirmed in the chick	179
7.2.2. Resegmentation and caudal autotomy	180
7.3. Resegmentation is not the whole story	181
7.3.1. Shifting sclerotomes and regionalisation of the vertebral column	181
7.4. The amniote notochord plays an important role in segmentation of the vertebral bodies	182
7.4.1. The notochord can influence sclerotome segmentation	182
7.4.2. Attraction: A new role for the notochord in vertebral development	183
7.5. Is the notochord intrinsically segmented?	184
7.6. A model for vertebral segmentation	185
7.7. Final remarks	187
References	188
Supplementary Material	217

List of Figures

Figure 1.1: Models of vertebral development	39
Figure 3.1: Tracing somite fate in the vertebral bodies	74
Figure 3.2: Summary of somite/vertebral body relationships	77
Figure 3.3: Tracing somite fate in the neural arches	79
Figure 3.4: Measurements of neural arch tilt	81
Figure 3.5: The “resegmentation-shift” model	82
Figure 4.1: Notochord ablation leads to a loss of segmentation in the vertebral bodies	96
Figure 4.2: An ectopic notochord graft leads to the formation of ectopic sclerotome	98
Figure 4.3: Ectopic sclerotome has a different segmental periodicity to host sclerotome	101
Figure 4.4: Ectopic sclerotome is derived from the host	104
Figure 4.5: A notochord graft leads to formation of ectopic cartilage	107
Figure 4.6: Two models by which the notochord could alter segmental periodicity of the sclerotome	110
Figure 4.7: Inter-regional notochord grafts suggest that the periodicity of ectopic sclerotome is dependent upon somite size, not the axial region of the notochord	114
Figure 4.8: Ectopic cartilage after a notochord and neural tube graft	117
Figure 5.1: Tracing somites in response to a notochord graft	135
Figure 5.2: Ectopic sclerotome is seen in response to a notochord graft after 24 hours	137
Figure 5.3: A lateral expansion of somites is seen in response to a notochord graft after eight hours	141
Figure 5.4: Can Shh beads attract somite cells?	145
Figure 5.5: Can cell pellets expressing Shh attract somite cells?	149
Figure 6.1: A notochord precursor graft generates an ectopic notochord, which expands the adjacent paraxial mesoderm	164
Figure 6.2: Time-lapse microscopy of notochord precursor grafts	168
Figure 6.3: Does FGF4 mediate the long-range attraction between the paraxial mesoderm and secondary notochord?	171
Figure 7.1: A model for vertebral segmentation	186

List of Tables

Table 2.1: Reagents and conditions used in the synthesis of sscDNA	54
Table 2.2: Reagents and cycle conditions used in PCR cloning	55
Table 2.3: Primer sequences and annealing temperatures used in PCR cloning	55
Table 2.4: Reagents used in ligation reaction	56
Table 2.5: Reagents and conditions used in diagnostic restriction digest reaction	58
Table 2.6: Reagents and conditions of the restriction digest reaction used to linearise recombinant plasmids	59
Table 2.7: Reagents and cycle conditions used in the amplification of cDNA insert from recombinant plasmid	60
Table 2.8: Reagents and conditions used in the transcription of cDNA probes	61
Table 2.9: Details of the restriction enzyme and RNA polymerase used in the synthesis of cDNA probes	61
Table 2.10: Details of primary and secondary antibody pairs	66
Table 3.1: Summary of somite tracing in different regions of the vertebral column using Dil and DiO	73
Table 4.1: The predicted segmental pattern of ectopic sclerotome that would result from inter-regional notochord grafts	112
Table 4.2: Summary of the mean percentage difference in segment length between the endogenous and ectopic sclerotome after inter-regional notochord grafts	113
Table 5.1: Details and results of embryos in which somites were traced in response to a notochord graft using Dil and DiO	133

Chapter 1 : General Introduction

1.1. Segmentation

1.1.1. Many animals build their bodies in segments

Repeating patterns are everywhere in the animal kingdom, and the word “segmentation” is often used to describe them. However, defining what constitutes a true “segment” has been a topic of much debate amongst biologists and is one that is still contested (Bateson, 1894; for reviews see Davis and Patel, 1999; Hannibal and Patel, 2013). It is generally accepted that true body plan segmentation is seen in only three extant clades in the animal kingdom: Chordata (the clade to which the vertebrates belong), Panarthropoda (onychophorans, insects, myriopods and crustaceans) and Annelida (segmented worms) (Bateson, 1894; Davis and Patel, 1999). In these animals, the body is divided into segments along the head-tail (anterior-posterior, A-P) axis. Furthermore, each segment contains muscular, neural, vascular and excretory elements either in the adult or at some point in its development, and so acts as close to a complete functional unit as possible (Bateson, 1894; Goodrich, 1930). In all three clades, these segmented structures are derived from both the mesoderm and ectoderm, another of the essential criteria for a functional unit to be regarded as a true segment (Bateson, 1894).

1.1.2. Why study the development of segmentation? An evolutionary perspective

That segmentation occurs in three clades of animals that are more distant to each other than to groups with no apparent segmentation (Grobbe, 1908; Eernisse et al., 1992; Aguinaldo et al., 1997) has led many to consider how the segmented body plan may have arisen. There are two main possibilities (for reviews, see Davis and Patel, 1999; Tautz, 2004; Peel et al., 2005; McGregor et al., 2009): first, that segmentation is an ancestral characteristic in all three lineages, present in the last common ancestor to all bilaterian animals (the hypothetical “urbilaterian”; De Robertis and Sasai, 1996), which has been conserved in the three segmented phyla and lost in others. Second, that segmentation arose separately in each of the three lineages, and is therefore

an example of convergent evolution. To begin to answer this question, we must first understand the developmental and molecular mechanisms that underlie the final pattern of segmented structures in the adult animal. As a result, the study of segmentation during embryonic development has been the subject of intense investigation in the field of developmental biology for centuries. This thesis is concerned with the development of segmentation in vertebrates.

1.1.3. Segmentation in vertebrates

The vertebrates are a large and diverse clade of animals. From their aquatic origins in the early Cambrian (Janvier, 1999; Shu et al., 1999), they have adapted to occupy a vast range of lifestyles and habitats. Despite the dramatic morphological variation seen across this group, all vertebrates share a common segmented body plan. This arrangement is visible in the muscles, blood vessels and nervous system of the adult, but is perhaps mostly clearly seen in the vertebral column, the defining feature of the vertebrate clade. The vertebral column is comprised of a series of repetitive elements (the vertebrae) extending from the base of the skull to the caudal end of the body.

Development of the segmented vertebral column can be simplified into two steps:

1. Establishment of segmentation in the vertebrate embryo (somite formation)
2. Translation of the primary segmentation of the somites into the final segmental pattern of the vertebral column.

This thesis addresses the second step. How is the original pattern of segments in the vertebrate embryo converted into the final segmental pattern of vertebrae that we see along the spine? To address this question, I will first outline the current understanding of step 1. How is segmentation established in the vertebrate embryo?

1.2. Establishing segmentation in the vertebrate embryo

1.2.1. *The somites*

In vertebrates, segmentation is set up in the embryo by subdivision of the paraxial mesoderm into the somites. Segments in the vertebrate embryo were first documented by the Italian biologist Marcello Malpighi in the 17th century (Malpighi, 1672; 1686), but according to Verbout (1976), it was not until the work of Francis Balfour in the late 19th century that the term “somite” was first used to describe them (Balfour, 1881). Somites form sequentially from rostral to caudal along the embryo, budding off in bilateral pairs from the unsegmented paraxial mesoderm on either side of the midline. In amniotes, they form as an epithelial sphere of cells surrounding a central lumen that contains a number of mesenchymal cells (the “somitocoele”; Williams, 1910; Huang et al., 1994). These simple structures contain the precursor cells of the axial skeleton, musculature, connective tissue, blood vessel endothelium and dermis of the vertebrate trunk (Christ and Ordahl, 1995; Christ and Scaal, 2008). Their formation lays the foundation on which the final segmented pattern of the adult animal is built.

1.2.2. *The notochord*

The notochord is a flexible rod of mesoderm that runs from rostral to caudal along the axial midline, beneath the neural tube on the dorsal side of the embryo. Its presence is considered diagnostic for Chordata (Haeckel, 1874; Nielsen, 2012) although a recent study has drawn similarities between this structure and the annelid axochord, and suggested a common origin for them (Lauri et al., 2014). The cells of the notochord are highly vacuolated, creating an outward force of osmotic pressure that is resisted by the thick extracellular matrix or sheath that surrounds it (Adams et al., 1990; Stemple, 2005). This makes the notochord both strong and flexible, properties that are essential for locomotion of the animal. In cephalochordates (Gee, 1996; Delsuc et al., 2006), the notochord persists into adulthood as the primary axial structure of the animal, where it not only provides tensile strength and flexibility but also serves as a point of muscle attachment. Therefore, the notochord precedes the vertebral column both in development and in evolution.

In vertebrates, most of these structural roles are taken over by the vertebral column after it forms around the notochord and neural tube during development. In many 'higher' vertebrates such as mammals and birds, the vertebral bodies completely replace the notochord in the adult, which persists only as the central portion (the mammalian nucleus pulposus) of the intervertebral disc (Walmsley, 1953; Choi et al., 2008). The outer portion of the intervertebral disc (the annulus fibrosus) is derived from the somites. As described in section 1.4, the notochord also plays an important signalling role during embryonic development.

1.2.3. Formation and patterning of the mesoderm

The mesoderm is formed during gastrulation as the middle of the three germ layers (Kimelman and Bjornson, 2004). Gastrulation begins in the chick with the formation of the primitive streak, a thickening of tissue that defines the midline of the epiblast. At the tip of the streak sits the primary organiser, known as Hensen's node in amniotes (Hensen, 1876; Viebahn, 2001). The notochord and medial somites form from distinct precursor populations in the node. As the node retracts caudally during neurulation, notochord precursors move out of the node, laying down the notochord from rostral to caudal along midline of the embryo. At the same time, precursors of the medial somites move out of the node and enter the pre-somitic mesoderm (PSM) on either side of the notochord (Spratt, 1955; Spratt and Condon, 1947; Selleck and Stern, 1991; 1992a). The more lateral mesoderm (lateral somites, intermediate mesoderm and lateral plate mesoderm) form from epiblast cells which ingress into the streak (Spratt, 1946) before moving laterally and rostrally out of the streak (Psychoyos and Stern, 1996; Yang et al., 2002), settling on either side of the axial midline. After their formation, development of both the notochord and paraxial mesoderm then progresses in a rostro-caudal direction along the embryo.

The decision of a somite precursor to enter the PSM is closely linked to the turnover of cells within the progenitor populations in the node. Labelling a single somite precursor within the chick node with a fluorescent dye, has revealed that the progeny of the single labelled cell become distributed in clusters. These clusters sit at regular intervals, around 6-7 somites in length,

along the A-P axis of the PSM (and later in the medial somites). This suggests that every time a somite precursor cell divides, one cell differentiates and enters the PSM, whilst the other remains in the node. Subsequent proliferation of each daughter cell within the PSM leads to the formation of small clusters in a periodic arrangement along the A-P axis (Selleck and Stern, 1991; 1992b). The idea that the notochord and medial somites form from stem cells in the node has also been corroborated by single-cell labelling studies in mouse (Nicolas et al., 1996; Cambray and Wilson, 2002; Tzouanacou et al., 2009).

The mesoderm is patterned across its medio-lateral (M-L) axis. The notochord sits at the midline, whilst the somites/paraxial mesoderm, intermediate mesoderm (IM) and lateral plate mesoderm (LPM) occupy progressively more lateral positions in the embryo. In chick, the mesoderm flanking the notochord later moves ventro-medially, eventually fusing together converting the flat embryo into a tube. The original M-L axis is therefore converted into the dorso-ventral (D-V) axis.

M-L (or D-V) patterning is established whilst prospective mesoderm cells are still in the streak. Cells in the node (as discussed above) and the rostral streak give rise to the axial and paraxial mesoderm, whilst more caudal streak cells give rise to mesoderm of a more lateral fate (Nicolet, 1965; Nicolet, 1970a; Psychoyos and Stern, 1996). It was first shown in *Xenopus* that this spatial arrangement of D-V mesoderm identity is due to the expression of a number of 'dorsalising' signals from the organiser, which results in a gradient of TGF β , Wnt and BMP signalling along the length of the streak (Harland and Gerhart, 1997). In chick, it has been shown that the expression of BMP inhibitors by the node leads to low levels of BMP signalling in the node and rostral streak, specify these cells as medial (dorsal/axial). Higher BMP levels in the caudal streak, away from these inhibitory signals, specify cells to a more lateral (ventral) fate (Tonegawa et al., 1997). Exposure of the caudal primitive streak to signals from the node causes these cells to adopt a dorsal (somatic) fate (Nicolet, 1970b; Streit and Stern, 1999), whilst the application of an ectopic source of BMP4 to the node and rostral streak converts these cells to a lateral fate (Streit and Stern, 1999).

Importantly, the M-L identity of the mesoderm, although specified in the streak, remains plastic for some time after cells exit the streak. It has been shown that

if a portion of PSM is grafted to the lateral-plate mesoderm, it does not form somites, but instead is converted into LPM. This suggested that a mechanism exists to maintain the M-L pattern established in the streak (Tonegawa et al., 1997). It is now known that M-L identity is reinforced in the mesoderm according to the relative levels of BMP4 expression in medial and lateral domains. The expression of Noggin, a BMP antagonist, results in low levels of BMP4 expression in the paraxial mesoderm, maintaining the somitic fate of these cells. High levels of BMP4 in the lateral mesoderm specify this tissue as lateral plate mesoderm (Tonegawa et al., 1997; Tonegawa and Takahashi, 1998; Streit and Stern, 1999; Dias et al., 2014). The inhibition of BMP4 in the lateral mesoderm by an ectopic source of Noggin results in the formation of ectopic somites (Tonegawa and Takahashi, 1998; Streit and Stern, 1999; Dias et al., 2014)

1.2.4. Somitogenesis

Somite formation occurs in a rhythmic fashion from rostral to caudal along the primary axis of the vertebrate embryo. As somites form in the rostral PSM, the process of axis elongation simultaneously replenishes the PSM by adding cells caudally. The dynamics of somitogenesis are remarkably conserved across the vertebrates. The total number of somites formed in the embryo varies dramatically between species, but is relatively fixed between individuals of the same species despite intra-specific variation in overall body size (Maynard Smith, 1960; Cooke, 1975; Richardson et al., 1998). The same is true of the rate of somite formation. A pair of somites forms every 120 minutes in mouse (Tam, 1981), 90 minutes in chick (Palmeirim et al., 1997) and 30 minutes in zebrafish (Schroter et al., 2008). The rate of somite formation, like development as a whole, varies with temperature in anamniotes but always generates the same number and size of segments (Pearson and Elsdale, 1979; Schroter et al., 2008), ensuring that the final segmentation pattern of the embryo remains relatively constant despite a fluctuating external environment.

One major question is how the variables of PSM length, somite size, and somite number are related in the embryo. The first insight came from a study in which a portion of the tail bud in *Xenopus* was surgically ablated to reduce the amount of PSM available for segmentation (Cooke, 1975). Cooke found that truncated embryos formed the same number of somites as their wild-type

counterparts, but that each somite was smaller, containing fewer cells than normal somites. This result highlighted an important point, that regardless of the amount of the PSM (which varies between individuals; Cooke, 1975), the total number of segments in the embryo is kept constant by alteration of the spatial periodicity of the segments. What, then, modulates the spatial periodicity of somites with respect to PSM length, and how is the rhythmic formation of the somites regulated?

1.2.5. The clock and wavefront model

In 1976, shortly after the study by Cooke described above, a theoretical model was proposed to explain the dynamics of somitogenesis, known as the 'Clock and Wavefront' model (Cooke and Zeeman, 1976). The model proposes that cells of the PSM possess a molecular oscillator (the 'clock'), which peaks and troughs in a smooth sinusoidal curve in time, the phase of which is synchronised locally between cells. In addition to the clock, a 'wavefront' traverses the PSM, regressing caudally down its length as the body axis elongates. As it passes down the PSM, the wavefront interacts with the clock to specify cells within the same period of an oscillation to form part of the same segment. This interaction activates a developmental programme that results in changes in cell behaviour within the specified segment, culminating in the formation of an epithelial somite in the rostral PSM. According to this model, the size of somites and the rate at which they form are the combined output of the interaction between the clock and wavefront, and are therefore determined by both the speed at which the wavefront progresses down the PSM and the period of clock oscillations within cells. This interaction could therefore translate the temporal periodicity of oscillations into a spatially periodic pattern of segmentation from rostral to caudal along the PSM. In turn, the speed of the wavefront was proposed to be a readout of the total body length, so that the model could account for how anamniote embryos regulate the total number of somites (Cooke and Zeeman, 1976; Slack, 1991). For this model to be compatible with the observation of Cooke (Cooke, 1975), both the period of the clock and the speed of the wavefront must be regulated in proportion to the overall length of the PSM (Cooke and Zeeman, 1976). In this way, the correct somite number will form, regardless of differences in embryo size.

1.2.6. The molecular basis of the “clock”

The original clock and wavefront model was compatible with the known dynamics of somitogenesis. However, the lack of evidence for either an oscillator or a wavefront within the embryo meant that it remained purely hypothetical for some time after its proposal. The first example of a molecular oscillator within the PSM came from the experiments of Palmeirim et al. (1997) who analysed the expression of *hairy1* (a homologue of the *Drosophila* segmentation gene *hairy*) in explants of chick embryos in which one half of the PSM was fixed, and the other half cultured in vitro for a longer period of time. Comparison between the two halves showed that *Hairy1* expression was highly dynamic, adopting a repetitive sequence of expression patterns within the PSM. Expression begins in the caudal PSM, sweeps rostrally and stabilises in a single stripe that corresponds to the caudal half of the most recently formed somite, before the whole sequence starts again. Crucially, the time taken to complete one sequence of expression was 90 minutes, the period of somite formation in the chick. By labelling PSM cells, the authors showed that cell migration could not explain the waves of expression. Furthermore, isolated pieces of PSM cultured in vitro still exhibited waves of dynamic *hairy1* expression and formed somites. Altogether, this suggested that the dynamic of *hairy1* expression is the result of synchronised oscillations within the cells of the PSM, and that these oscillations are an intrinsic property of the PSM.

Following this, many more studies sought to uncover other molecular oscillators within the PSM of chick and other vertebrates. There are now many genes known to exhibit cyclic or dynamic expression in the PSM, a group collectively referred to as the ‘clock genes’ (reviewed in Pourquié, 2011; Oates et al., 2012). Many of these are components of the Notch signalling pathway of which transcription factors such as *Lunatic fringe* (Forsberg et al., 1998; McGrew et al., 1998) and other members of the hairy/enhancer-of-split family (Holley et al., 2000; Jouve et al., 2000; Leimeister et al., 2000; Henry et al., 2002; Oates and Ho, 2002; Bessho et al., 2003) are transcriptional targets and effectors. In addition, many components and transcriptional targets of the Wnt and FGF pathways exhibit oscillatory expression within the PSM (Aulehla et al., 2003; Ishikawa et al., 2004; Dale et al., 2006; Dequéant et al., 2006; Hayashi et al., 2009).

Visualisation of clock gene expression in real-time using fluorescent reporters have shown waves of expression progressing through the PSM (Masamizu et al., 2006; Aulehla et al., 2008; Takashima et al., 2011; Soroldoni et al., 2014), in agreement with the earlier results from fixed embryos (Palmeirim et al., 1997; Aulehla and Johnson, 1999). The cyclical dynamics of the segmentation clock has been shown to be, at least in part, a result of negative feedback loops within the network (Holley et al., 2000; Oates and Ho, 2002; Bessho et al., 2003; Dale et al., 2003). These oscillations run freely in individual cells of PSM cultures but cell-cell signalling is required to synchronise them between cells in the PSM (Maroto et al., 2005; Masamizu et al., 2006).

Attempts to assemble individual genes into a network have revealed an overall picture of the segmentation clock as a complex interplay of signals and factors (Dequéant et al., 2006; González and Kageyama, 2010). The similarities between species in the pathways involved, particularly concerning Notch signalling, suggests that the segmentation clock is a conserved mechanism for the regulation of rhythmic somite formation across vertebrates, the details of which have been modified throughout vertebrate evolution to generate species-specific modules within the overall network (Krol et al., 2011).

1.2.7. The period of the clock and segmentation

According to the clock and wavefront model, somite size (and therefore total somite number) should be a read-out of two factors: the period of the clock and the speed of the wavefront (Cooke and Zeeman, 1976). In addition, both of these variables must be coupled to the overall length of the PSM that will segment (Cooke, 1975; Cooke and Zeeman, 1976). To test this in a biological system, therefore, these variables must be uncoupled.

By altering the intronic composition or otherwise mutating certain clock genes in zebrafish and mouse, mutant lines have been generated with an altered oscillation period, whilst leaving growth rate of the embryo constant (Schroter and Oates, 2010; Harima et al., 2013). In these mutants, the size of somites and the rate at which they form differ from wild-type animals, leading to a change in total somite number. Importantly, this change in the number of somites is translated up to the level of adult segmentation, with mutants possessing a different number of vertebrae in total compared to wild type

animals (Schroter and Oates, 2010; Harima et al., 2013). This suggests that the period of the clock can influence the spatial and temporal periodicity of segmentation. However it remains to be established whether changes to somite size are also translated up to the level of vertebrae. In other words, is vertebral length (which varies along the A-P axis in many species) also influenced by the period of the segmentation clock?

1.2.8. The molecular basis of the “wavefront”

For oscillations within the PSM to confer a segmental pattern, a mechanism must exist to convert this temporal periodicity into a spatial pattern, a role that Cooke and Zeeman speculated could be performed by interaction of the clock with a regressing ‘wavefront’ (Cooke and Zeeman, 1976). This wavefront represents a point of ‘rapid cell change’, which regresses from A-P along the PSM (Cooke and Zeeman, 1976). In this model, the interaction of the clock with the wavefront results in a disruption to the progress of the wavefront along the axis at regular intervals, thereby specifying groups of cells to form a somite. The authors speculated that a regressing wavefront could be set up by morphogen gradients that confer positional information to cells along the PSM. By coupling the gradients to overall growth rate of the embryo, the rate at which the wavefront regresses would be proportional to growth (Cooke and Zeeman, 1976; Slack, 1991), linking the dynamics of segmentation to the overall length of the PSM (Cooke, 1975).

During somitogenesis, a gradient of FGF (Crossley and Martin, 1995; Dubrulle et al., 2001) and Wnt (Takada et al., 1994; Aulehla et al., 2003) signalling is established, which is highest in the caudal PSM. Simultaneously, an opposing gradient of retinoic acid (RA) signalling is set up by the synthesis of RA in the somites (Neiderreither et al., 1997; Diez del Corral et al., 2003). When the levels of these signals are altered experimentally, the position of somite boundaries and the size of somites also change (Dubrulle et al., 2001; Sawada et al., 2001; Aulehla et al., 2003; 2008; Diez del Corral et al., 2003; Moreno and Kintner, 2004), suggesting that the gradients do affect somite size, presumably by controlling the number of cells that segment together to form a somite.

Surgical rotation of fragments of the PSM along its length have suggested that cells of the caudal PSM are flexible with regards to their segmentation, whereas those located in the rostral third are committed to a specific segmental pattern (Dubrulle et al., 2001). The expression of key somite markers such as *Paraxis* (Burgess et al., 1995) and *Mesp2*-like genes (Saga et al., 1997; Buchberger et al., 1998; Sawada et al., 2000) begins rostral to the point at which segmentation becomes determined. It has been shown that their expression, and subsequent commitment of cells to segmentation, is promoted by RA and suppressed by FGF signalling (Dubrulle et al., 2001; Sawada et al., 2001; Moreno and Kintner, 2004; Delfini et al., 2005). Thus, according to the principle of positional information (Wolpert, 1969), it has been proposed that at this point along the PSM (known as the “determination front”) the opposing gradients reach a balance, activating the developmental program that commits PSM cells to form a somite (Dubrulle et al., 2001; Diez del Corral et al., 2003).

As these gradients regress rostro-caudally along the PSM during body axis elongation, so does the determination front. Attempts to measure the rate at which the determination front regresses have suggested that it travels the length of a single somite during one period of the clock (Gomez et al., 2008). This has led to the proposal that the determination front is the wavefront of Cooke and Zeeman (1976), which through its interaction with the clock determines somite size.

1.2.9. Rostro-caudal patterning of the somite

Each somite is divided into distinct rostral and caudal halves possessing different molecular properties (Keynes and Stern, 1984; Stern et al., 1986; Norris et al., 1989). These properties ensure that the motor and sensory axons of the spinal nerves, and streams of neural crest cells from the neural tube are only permitted to migrate through the rostral half of each somite (Keynes and Stern, 1984; Rickmann et al., 1985; Bronner-Fraser, 1986; Bronner-Fraser and Stern, 1991). Rostro-caudal (R-C) patterning of the somite therefore confers a segmental pattern upon the nervous system and derivatives of the neural crest.

The distinct properties of each half are also essential for the maintenance of somite boundaries. When sclerotome halves of the same R-C identity are placed adjacent to each other (i.e. rostral next to rostral, or caudal next to

caudal), cells of similar identity have been shown to mix, whereas a boundary forms between those of different identity (i.e. rostral next to a caudal) (Stern and Keynes, 1987). This is also seen in the zebrafish *fused somite (fss)* mutant, in which R-C patterning of the somite is lost and adjacent somites are fused together (van Eeden et al., 1996). R-C polarity is therefore essential for somitic and non-somitic segmented structures to develop in concert to generate a working body plan.

When the PSM is rotated about its R-C axis, the polarity of the somites formed by the inverted PSM is also reversed, indicating that the PSM does not require signals from external tissues for its R-C patterning (Keynes and Stern, 1984; Aoyama and Asamoto, 1988). Furthermore, this intrinsic R-C polarity is already established when the somite forms, as some markers of the rostral somite such as *EphA4* (Schmidt et al., 2001; Barrios et al., 2003), *Mesp2* (Saga et al., 1997) and caudal markers such as *Uncx4.1* (Mansouri et al., 1997; Neidhardt et al., 1997), *hairy1* (Palmeirim et al., 1997) and *Lunatic fringe* (McGrew et al., 1998), are already expressed in their respective domains in the forming somite at the rostral tip of the PSM. Many of these markers are either clock genes themselves, or genes known to be regulated by the clock. It has been demonstrated that the *Mesp* family of transcription factors, such as *Mesp2* in mouse and *mespb* in zebrafish, are key regulators of both somite boundary formation and R-C somite polarity (Takahashi et al., 2000; Nomura-Kitabayashi et al., 2002). *Mesp2/mespb* regulate the expression of several other markers of somite polarity by acting as mediators of the Notch signalling pathway in the rostral PSM (Takahashi et al., 2000; 2003). Therefore, somite polarity is thought to be an intrinsic property of the somite, and coupled to somitogenesis itself.

1.2.10. The clock and wavefront cannot explain all aspects of somitogenesis

Based on the literature reviewed above, there is no doubt that a complex network of factors regulates molecular oscillations and gradients within the PSM, and that changes to this network result in disruption to somite periodicity and patterning (reviewed in Pourquié, 2011; Oates et al., 2012). However, it is difficult to see how this mechanism can fully explain Cooke's experiment, in which normal somite numbers were maintained in truncated embryos in

Xenopus (Cooke, 1975). According to these results, the embryo must be able to control somite number by somehow “measuring” the length of the PSM and dividing it up accordingly. The regression of the so-called “determination front” goes some way to linking body axis elongation (and thus PSM length) to somite boundary positioning (Dubrulle et al., 2001; Gomez et al., 2008). However, this cannot apply to *Xenopus*, since axis elongation in anurans does not exhibit the same dynamic and the PSM is already at its full length by the time the first somite forms (Stern and Piatkowska, 2015). Perhaps the results of Cooke (1975) in *Xenopus* are specific to this species, or anurans in general. If so, a mechanism by which embryos can scale somite size to overall PSM length to maintain a conserved number of somites may not be operating in other species.

The role of BMP inhibition in somite formation is often overlooked. In chick, it has long been known that the BMP antagonist Noggin can induce somite formation from both posterior primitive streak (Streit and Stern, 1999; Dias et al., 2014) and from the lateral plate mesoderm derived from it (Tonegawa et al., 1997; Tonegawa and Takahashi, 1998). Noggin is expressed by the notochord during embryonic development and it has been proposed to maintain the paraxial mesoderm in a somitic fate (Tonegawa et al., 1997; Tonegawa and Takahashi, 1998; Dias et al., 2014). Recently, it was shown that when explants of posterior primitive streak are exposed to Noggin, the resulting somites form simultaneously and in the absence of clock gene oscillations (Dias et al., 2014). This suggests that the clock is not required for somite formation. Also, since the somites form in three dimensions, like a “bunch of grapes”, gradients and wavefronts are unlikely to be involved in regulating their size (Dias et al., 2014). The authors proposed an alternative model in which somites self-assemble as a result of changes in cell-cell interactions within the PSM, activated by BMP inhibition.

How can we reconcile this model with the clock and wavefront model? First, ectopic somites which form in the absence of a clock are not patterned into a rostral and a caudal half, suggesting that the clock is at least required for this aspect of somite patterning (Dias et al., 2014) as previously reported (Takahashi et al., 2000; Takahashi et al., 2003). Second, ectopic somites form simultaneously, not periodically like normal somites (Dias et al., 2014), which

suggests that the clock and wavefront may be required to regulate the timing of somite formation.

The only credible alternative to the clock and wavefront model is the “cell cycle model” (Primmatt et al., 1989; Stern and Piatkowska, 2015). This model links somitogenesis to the turnover of self-renewing somite stem cells in the node, discussed in section 1.2.3. The model was proposed as a result of experiments in which chick embryos were subjected to a single pulse of heat shock during somitogenesis (Primmatt et al., 1988; 1989). It was found that this heat shock led to malformations in somites and their skeletal derivatives in a spatially periodic pattern, with a malformation observed in regular intervals along the axis. Critically, the distance between each malformation was approximately 6-7 somites in length, the same distance that the progeny of a single somite precursor were found to be spaced along the PSM (Selleck and Stern, 1991; 1992b). Furthermore, measurements of the rate of mitosis using a pulse-chase experiment confirmed that somite precursors complete a single cell cycle in approximately 10 hours, the same amount of time that it takes to form 6-7 somites in the chick (Primmatt et al., 1989; Selleck and Stern, 1991; 1992b). It was proposed that the heat shock led to disruption of somite precursors in the node, such that those at a critical point in the cell cycle at the time of the heat shock were irreversibly damaged. As a result, this led to defects in their progeny at regular intervals along the axis, which became apparent when those cells were unable to properly form somites (Primmatt et al., 1988; 1989).

The “cell cycle model” was therefore proposed, in which somite cells that enter the caudal PSM are synchronised with respect to their cell cycle. Entry into the caudal PSM marks the beginning of a cascade of autonomous signalling events, which eventually lead to the cellular changes required for somite formation. Cells that entered the PSM at a similar time are therefore at a similar level of maturity within the PSM, having undergone the same number of cell cycles as each other since leaving the stem cell niche in the node, and as a result these cells eventually group together to form a somite (Primmatt et al., 1989; Stern and Piatkowska, 2015). Like the clock and wavefront model (Cooke and Zeeman, 1976; Palmeirim et al., 1997), the cell cycle model suggests that segmentation is an intrinsic property of the PSM. Interestingly, heat shock in *Xenopus* and *Rana* results in only a single malformation along the axis (Elsdale et al., 1976; Cooke and Elsdale, 1980), suggesting that the

same spatial arrangement of somite stem cell progeny along the PSM does not exist in this group. This adds weight to the idea that the maintenance of segment number in truncated embryos (Cooke, 1975) is the result of key differences in the dynamics of somitogenesis in amphibians.

1.3. Antero-posterior patterning of the vertebrate body axis

1.3.1. Morphological variation along the vertebrate A-P axis

The process of somitogenesis establishes a pattern of serially homologous segments along the primary axis of the animal. Each somite gives rise to the same complement of adult tissues within a segment, but the morphology of these elements varies dramatically from segment to segment. This is perhaps most obvious in the vertebral column, in which vertebrae exhibit distinct morphologies along the A-P axis. In many amniotes, vertebrae can be grouped into regions of similar morphology along the vertebral column: cervical, thoracic, lumbar, sacral and caudal. These morphological regions are conserved between species, but the number of vertebrae in each region (known as the axial formula) varies dramatically between species (Gadow, 1933). This observation led to the theory that shifting of the boundaries between vertebral regions up and down the A-P axis during evolution could then give rise to the changing axial formulae of vertebrates (Goodrich, 1930).

1.3.2. The Hox genes

The role of *Hox* genes in conferring positional identity to cells along the A-P axis is well known. This was first brought to light in studies in *Drosophila* that linked genetic changes in genes located in clusters within the genome to mutant flies in which one segment adopts the morphological characteristics of another (Bridges and Hunt, 1923; reviewed in Akam, 1987), a so-called “homeotic transformation” (Bateson, 1894). The genes within these clusters are now known to belong to a large family of transcription factors known as the *Hox* genes, which possess a conserved DNA binding domain known as the ‘homeobox’, which is essential for their regulatory activity (McGinnis et al., 1984a; 1984b). *Drosophila* possesses two clusters of *Hox* genes, each of which contains a number of genes arranged sequentially along the

chromosome and therefore thought to have arisen by duplication of a single ancestral homeobox gene (Lewis, 1978; Lewis et al., 1980; Mcginnis et al., 1984b). *Hox* genes within a cluster display the unique property of being expressed during embryonic development in a spatial and temporal order that reflects their position along the chromosome (Lewis, 1978; Harding et al., 1985), a property known as “colinearity” (Harding et al., 1985). Moving from 3’ to 5’ along the cluster, *Hox* genes exhibit progressively more posterior domains of expression along the embryo and start to be expressed progressively later (Harding et al., 1985; Akam, 1987). The spatial expression of *Hox* genes during embryonic development therefore confers a positional identity to segments along the A-P axis in *Drosophila*.

Orthologues of *Drosophila Hox* genes have now been described across the animal kingdom, and the conservation of their sequence homology, clustered arrangement, collinear expression, and function has suggested that they represent a conserved gene or gene set for A-P patterning that was present at the base of the metazoans (Carrasco et al., 1984; Levine et al., 1984; Mcginnis et al., 1984b; Duboule and Dollé, 1989; Holland and Hogan, 1986; Graham et al., 1989; Kappen et al., 1993). Two whole-genome duplications at the base of the vertebrates, and another round at the base of the teleost lineage (Garcia-Fernandez and Holland, 1994; Amores et al., 1998; Prince et al., 1998a), has resulted in four (up to seven in teleost fish) paralogous *Hox* clusters in vertebrates (reviewed by Duboule, 2007). Individual gene duplications and losses within each cluster have led to considerable interspecific differences in the number of genes within each cluster. The basic plan of each cluster is a pattern of 13 genes (numbered 1-13 from 3’ to 5’ within the cluster), some of which may be missing. Genes within each cluster with the same number represent a “paralogous group”, and tend to be more similar in their regional pattern of expression than differently numbered genes in the same cluster (Duboule, 2007).

1.3.3. *Hox* genes and vertebrate axial identity

In vertebrates, *Hox* gene expression begins during gastrulation, in the primitive streak (Duboule and Dollé, 1989; Graham et al., 1989). Coupling expression to axis elongation, the temporal order in which *Hox* genes are expressed from 3’ to 5’ in the streak and later in the tail bud (temporal colinearity), is translated

into a spatial arrangement along the axis (spatial colinearity). 3' genes in a cluster are expressed first and therefore have a more anterior limit of expression. 5' genes are expressed later, and therefore are expressed within a more posteriorly-restricted domain. This results in *Hox* gene expression being organised in a series of nested domains along the A-P axis of the embryo. Somites are therefore grouped into regional domains that express a unique combination of *Hox* genes according to their position along the A-P axis (Burke et al., 1995).

The role of *Hox* genes in conferring positional identity to somites along the axis has been studied extensively, with much of the work focusing on the regulation of vertebral morphology in mouse. Although targeted mutations in individual *Hox* genes result in vertebral abnormalities specific to the region in which that *Hox* gene is expressed, the effects are often far less dramatic than the homeotic transformations seen in *Drosophila* (Chisaka and Capecchi, 1991; reviewed in Wellik, 2007). In contrast, knocking out all paralogous genes simultaneously results in more traditional homeotic transformations in vertebral morphology (Chen et al., 1998; McIntyre et al., 2007; Wellik and Capecchi, 2012). For example, knock-out of the three *Hox10* genes (present in the *HoxA,C* and *D* clusters), which normally begin to be expressed in the first lumbar somite, results in the transformation of lumbar and sacral vertebrae to a thoracic morphology (i.e. they develop ectopic ribs) (Wellik and Capecchi, 2012). It is therefore thought that *Hox* cluster duplication in vertebrates has led to a certain amount of functional redundancy between paralogous genes, and that axial identity is conferred by the combination of *Hox* genes (or '*Hox* code') expressed in a particular region, and not by a single *Hox* gene alone (Kessel and Gruss, 1991; Wellik, 2007).

The anterior boundaries of *Hox* gene expression in the somites align with the point of transition between axial regions of differing vertebral morphology, an alignment that is conserved between vertebrate species (Kessel and Gruss, 1991; Burke et al., 1995). For example, the anterior limit of *Hoxc6* expression lies at the transition between the cervical and thoracic regions in mouse and chick, despite the fact that this transition occurs at somite 12 in the former species and somite 19 in the latter (Burke et al., 1995). This suggests that the nested domains of *Hox* gene expression represent a conserved mechanism for conferring positional identity to somites along the A-P axis, the boundaries of

which have been shifted up and down the body axis to give rise to variations in axial formulae between species (Burke et al., 1995).

1.3.4. When is axial identity determined?

Classical experiments in which portions of PSM were transplanted between different axial regions showed that the graft formed vertebrae with the characteristic morphology of the region from which it was taken (Kieny et al., 1972). Later, a similar experiment showed that grafted PSM cells retain a Hox code specific to the axial region from which they were taken (Nowicki and Burke, 2000). Together, these experiments demonstrate that Hox expression and axial identity are an intrinsic property of the PSM. However, it is not certain exactly when axial fate becomes irreversibly determined during development.

One possible mechanism is that the Hox code of a cell is 'frozen' upon its entry into the PSM. This idea is perhaps most clearly conveyed in the "time-space translator" model (Durstun et al., 2012), which is based on previous reports in *Xenopus* that signals from the organiser are required to stabilise *Hox* expression in streak cells entering the PSM (Wacker et al., 2004). Due to the property of temporal colinearity, in which *Hox* genes are expressed in sequence from 3' to 5' within a cluster, cells that enter the PSM early will express more 3' (anterior) *Hox* genes than those that enter the PSM later. In this way, the temporally collinear pattern could be translated into a spatially collinear arrangement of *Hox* expression along the PSM.

The idea of *Hox* expression becoming fixed as cells enter the PSM is also suggested in the study described in section 1.2.10, where explants from the posterior primitive streak were induced to form somites by exposure to Noggin. It was found that the ectopic somites expressed the same Hox genes as were expressed by the streak tissue at the original point of excision (Dias et al., 2014). Based on this, the authors suggested that exposure of cells to BMP inhibitors from the notochord when they enter the PSM may "freeze" their Hox expression, committing them to a particular axial fate. However, it has also been suggested that the expression of Hox genes in cells of the epiblast may control the timing of ingress into the streak, and thus determine the ultimate

position that cells will occupy along the A-P axis prior to gastrulation (Iimura and Pourquie, 2006).

1.4. Specification of somite compartments

1.4.1. Dorso-ventral patterning of the somite

Shortly after its formation, the amniote somite differentiates into two populations of cells: a ventro-medial compartment of mesenchymal cells known as the sclerotome, which gives rise to the vertebral column and ribs, and a dorso-lateral compartment known as the dermomyotome, which remains as an epithelial sheet of cells overlying the sclerotome and gives rise to the postcranial musculature and dermis. These populations are marked by the expression of specific members of the paired-box (*Pax*) family of transcription factors. *Pax3* and *Pax7* are expressed in the dermomyotome, and later in the myotome, where they regulate the differentiation of these cells into muscle (Goulding et al., 1991; Jostes et al., 1991; Williams and Ordahl, 1994). *Pax1* and *Pax9* are expressed in the sclerotome, where they specify cells to form the axial skeleton (Deutsch et al., 1988; Ebensperger et al., 1995; Neubüser et al., 1995).

In contrast to R-C polarity, D-V patterning is not determined until after somite formation, as newly-formed somites which are rotated around their D-V axis by 180° form sclerotome and dermomyotome in normal positions (Keynes and Stern, 1986; Aoyama and Asamoto, 1988). This experiment also demonstrated that D-V patterning is not intrinsic, but is controlled by signals external to the somite. A number of studies in which surrounding structures were ablated or transplanted to ectopic positions have revealed that the somite is patterned across its D-V axis by a combination of signals from dorsal and ventral structures. Ventrally, Sonic Hedgehog (*Shh*) emanating from the notochord and floor plate (Brand-Saber et al., 1993; Pourquie et al., 1993; Fan and Tessier-Lavigne, 1994; Goulding et al., 1994; Fan et al., 1995; Dietrich et al., 1997) and the BMP antagonist *Noggin* from the notochord (McMahon et al., 1998) induce the expression of *Pax1* in the ventral somite, converting cells to a sclerotomal fate. This is counteracted by the “dorsalising” activity of canonical Wnt signalling from the dorsal neural tube and adjacent ectoderm, which

induces expression of *Pax3* in the dorsal somite, specifying this domain as dermomyotome (Christ et al., 1992; Fan and Tessier-Lavigne, 1994; Hirano et al., 1995; Dietrich et al., 1997; Capdevila et al., 1998; Olivera-martinez et al., 2001).

After initial D-V patterning of the somite, the dermomyotome itself forms two subcompartments. Cells at the medial edge undergo an epithelial to mesenchymal transition (EMT) and migrate underneath the dermomyotome to form a second layer, known as the myotome (Christ et al., 1976). The remaining dorsal layer, known as the dermatome, goes on to form the dorsal dermis of the trunk. The ventral layer, which sits between the dermatome and the sclerotome, gives rise to the postcranial epaxial skeletal muscles of the animal (Christ and Ordahl, 1995). At this medial position in the somite, Shh from the notochord and floor plate and Wnt signalling from the dorsal neural tube and ectoderm act together to induce a cascade of transcription factors such as *MyoD* and *myf5* that regulate myogenic differentiation in cells of the myotome (Pownall & Emerson, 1992; Münsterberg and Lassar, 1995; Dietrich et al., 1997; Borycki et al., 1998).

1.4.2. Medio-lateral patterning of the somite

In addition to R-C and D-V patterning, the somite is also patterned across its medio-lateral (M-L) axis. As discussed above (section 1.2.3), precursors of the somite are pre-patterned into medial and lateral domains even before they enter the paraxial mesoderm. Cells of the medial somite are formed from a precursor population in the lateral Hensen's node, whilst future lateral cells reside in the rostral primitive streak (Spratt, 1955; Selleck and Stern, 1991; 1992b; Psychoyos and Stern, 1996). However, when the positions of the medial and lateral half of a newly-formed somite are switched, the half-somites are re-specified according to their new position (Ordahl and Le Douarin, 1992). This demonstrates that, despite arising from distinct precursor populations, cells of the somite are not committed to a medial or lateral fate when they form a somite.

It is now known that BMP signalling from the LPM induces the expression of lateral somite markers such as *Sim1* (Pourquié et al., 1996), whilst repressing markers of the medial somite such as *Swip1* and *En1* (Vasiliauskas et al.,

1999; Cheng et al., 2004). Simultaneously, the expression of BMP antagonists such as Noggin by the notochord inhibits the “lateralising” signals of the LPM in the medial somite, whilst Shh induces this domain to adopt a medial identity (Pourquié et al., 1996; Vasilias et al., 1999). As a result, the same suite of signals from axial tissues mediates both dorso-ventral and medio-lateral patterning of the somite. Noggin and Shh in the notochord act both as “medialising” and “ventralising” signals, inducing sclerotome in the adjacent somite at the expense of the dermomyotome. Therefore the sclerotome is induced in the ventro-medial compartment of the somite, whilst the dermomyotome occupies a more dorso-lateral position.

Medio-lateral patterning is maintained by cells of the dermomyotome when they form the myotome, leading to subdivision of the myotome into a medial and lateral domain (Cheng et al., 2004). Later, after rotation of the somite by 45°, and ventral closure of the lateral embryo, the somite becomes re-oriented across the dorso-ventral axis of the body. The former lateral domain of the dermomyotome gives rise to the ventral (hypaxial) musculature of the trunk (and also the muscles of the limb). The medial domain sits above, forming the dorsal (epaxial) muscles associated with the axial skeleton (Ordahl and Le Douarin, 1992). The opposing medial and lateral signals are also involved at this later stage in the control of muscle differentiation in the myotome. A cascade of myogenic differentiation factors is induced in the medial myotome by the combined action of Shh from the notochord and Wnt signalling in the dorsal neural tube and ectoderm (see section 1.4.1 above). At the same time, BMP4 signalling from the lateral plate maintains the expression of *Pax3* in the lateral myotome, preventing it from entering myogenic differentiation. These opposing medial and lateral signals delay the onset of myogenic differentiation in the lateral (hypaxial) domain (Pourquié et al., 1995; Pourquié et al., 1996). Therefore, myogenesis proceeds from medial to lateral (now dorsal to ventral) across the myotome.

1.5. From sclerotome to vertebral column

1.5.1. *Migration of the sclerotome*

After specification, the sclerotome undergoes an epithelial to mesenchymal transition (EMT) and moves medially to invade the notochordal sheath and surround the notochord and neural tube (Remak, 1855). Here the cells give rise to the vertebral bodies and annulus fibrosus of the intervertebral discs (Christ and Scaal, 2008). At this point, therefore, the final segmentation pattern of the vertebral column is established.

Although sclerotome specification is reliant upon signals from axial structures (section 1.4.1), EMT of the ventro-medial somite has been reported to take place as normal in the absence of the notochord and neural tube (Christ et al., 1972; Hirano et al., 1995), suggesting that these structures are not required for de-epithelialisation. The first sign of this transition appears to involve a lengthening of the ventro-medial cells of the epithelial somite along their apical-basal axis, which begins at around the fifth caudal-most somite (Solursh et al., 1979). By the tenth most caudal somite, the sclerotome is truly mesenchymal, with increased extracellular space between cells (Solursh et al., 1979).

The movement of the sclerotome into the space surrounding the notochord is in part a result of a general expansion of this compartment, which is caused by a number of factors. EMT itself leads to a dispersal of the cells from their tight epithelial arrangement in the somite, increasing the space occupied by the sclerotome (Solursh et al., 1979). It has also been shown that Shh from the notochord stimulates proliferation of the sclerotome, leading to its expansion (Johnson et al., 1994; Fan et al., 1995). In addition, extracellular matrix components have been shown to play a role in expansion of the sclerotome. The onset of EMT has been correlated with an increase in expression of matrix metalloproteases, and chemical inhibition of these enzymes reduces, but does not completely abolish, sclerotome cell dispersal (Duong and Erickson, 2004). Cells of the sclerotome also secrete an ECM rich in hyaluronic acid, allowing extracellular spaces to become hydrated, expanding the sclerotome (Solursh et al., 1979).

Movement of the sclerotome cells towards the midline has been shown to be a result of active cell migration as well as expansion. This was first suggested by the results of a relatively crude experiment in which embryos were treated with a chemical inhibitor of cytoskeletal contraction, which prevented subsequent dispersal of sclerotome cells (Chernoff and Lash, 1981). Extracellular matrix secreted by the notochord and sclerotome cells is essential for migration. The notochordal sheath acts as a substrate for the sclerotome cells as they invade the space around the notochord prior to formation of the ventral vertebral cartilages (Christ and Scaal, 2008). Sclerotome cells have been shown to migrate in-vitro if cultured on a collagen matrix, but chemically inhibiting the synthesis of several ECM components leads to a reduction in this migratory behaviour (Sanders et al., 1988). This result suggests that the sclerotome cells themselves modulate the ECM of the space surrounding the notochord in order to migrate through it (Dockter, 2000). A similar culture system has been used to demonstrate that sclerotome cells actively migrate towards notochord explants in vitro, suggesting that as well as secreting a substrate upon which to migrate, the notochord may also provide a directional cue in the migration process (Newgreen et al., 1986).

1.5.2. Rearrangement of the sclerotome and dermomyotome

At the time of their formation, the sclerotome and dermomyotome sit within the same somitic segment. However, for the vertebral column to bend, each axial muscle must insert into two successive vertebrae. Therefore, the vertebral precursors of the sclerotome must shift by half a segment with respect to the muscle-precursors of the myotome during development. This also becomes apparent when the relationship between somite, vertebral, and spinal nerve segmentation is considered. The dorsal root of the spinal nerve projects through the rostral portion of the somite in the embryo, but sits caudal to the neural arch of each vertebra in the adult (Remak, 1855). This arrangement of adult tissues has been defined clinically as a “motion segment”, reflecting its functional importance (Schmorl and Junghanns, 1968). The translation of the simple “somitic segment” into the complex “motion segment” is therefore critical in establishing a working vertebrate body plan. How this rearrangement is achieved is a long-standing question in the field of developmental biology, and one that even now is not fully resolved.

1.5.3. The fate of sclerotome in the vertebrae: insights from anatomical studies

1.5.3.1. Model 1: Resegmentation

In 1855, Robert Remak proposed his “resegmentation” (Neugliederung) model to explain the rearrangement of the sclerotome with respect to the myotome, after he observed that the sclerotome is subdivided into a rostral and caudal half with differing cell density. He suggested that each half-sclerotome joins with the half-sclerotome from the next adjacent somite to form a vertebra comprised of cells from two successive somites (Fig. 1.1A) (Remak, 1855).

After the proposal of the resegmentation model, numerous attempts were made to address the relationship between somite and vertebral segmentation using careful observations of embryos at different developmental stages (reviewed in Baur, 1969; Verbout, 1976). Perhaps most notable amongst these was the work of von Ebner, who extended Remak’s identification of two separate sclerotome halves by reporting the presence of an “intrasegmental fissure” separating the two half-sclerotomes of a somite (Von Ebner, 1889). Von Ebner proposed that this fissure marked the future boundary between two vertebrae, suggesting that a vertebral pre-pattern exists within the sclerotome at this early stage. Following this, many authors argued for resegmentation on the basis of the discovery of similar fissures within the sclerotome of other specimens, or the argument that the rearrangement must occur to generate the final arrangement of all the elements of the motion segment (Schultze, 1896; Manner, 1899; Sensenig, 1949).

1.5.3.2. Model 2: Shifting of sclerotomes

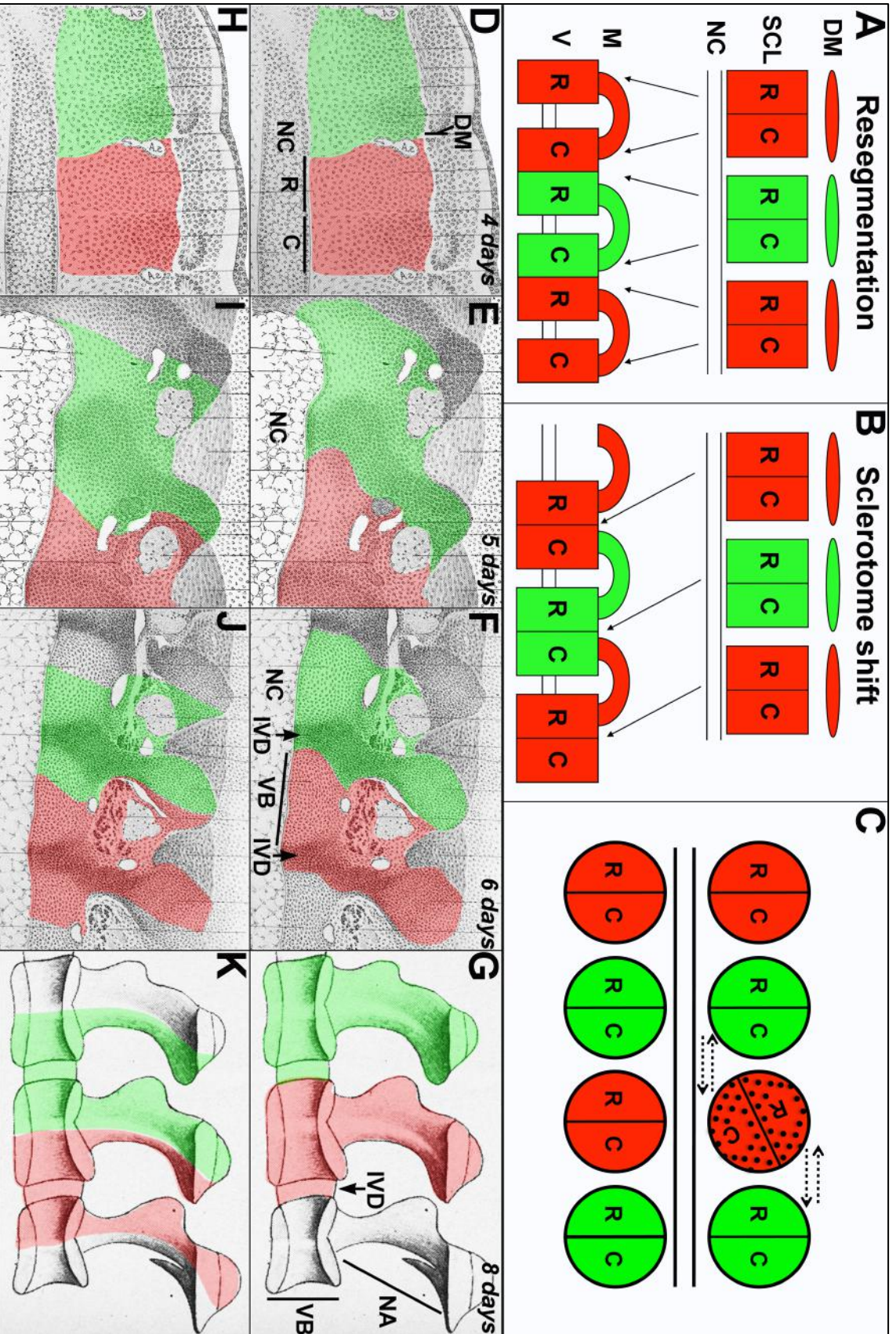
Among the complex anatomical descriptions that followed the publication of the resegmentation model, another notable observation was that rearrangements of the sclerotome are achieved by gradual shifts during development, rather than dramatic leaps in organisation (Kollman, 1891; Sensenig, 1949). On the basis of this concept, a second model can be suggested for vertebral column formation. Instead of a rearrangement of sclerotome halves, the sclerotome could be offset with respect to the myotome by a simple shift of the entire

sclerotome by half a segment as it migrates to the midline. In this model, sclerotome and vertebral segments are in a direct 1:1 relationship (Fig. 1.1B).

1.5.3.3. Discontinuity in segmental patterning between sclerotomes and vertebrae

Rearrangement of the myotome and sclerotome both require the segmental pattern to be maintained in the somitic tissue as it forms the vertebral column. However, a number of authors observed that when the sclerotome initially migrates to the midline, it forms an unsegmented mass around the notochord prior to vertebral formation (Kölliker, 1861; Frioriep, 1883; 1886; Baur, 1969; Verbout, 1985). On this basis, it was suggested that the original segmental pattern of the sclerotome breaks down entirely and vertebral boundaries are later specified *de novo* within this unsegmented mass (Williams, 1908; Verbout, 1976; Verbout, 1985). This mechanism would completely disconnect the segmentation of the somites from that of the vertebral column, and remove any need for either a resegmentation or shift of the sclerotome (Verbout, 1976).

Figure 1.1. Models of vertebral development. A. “Resegmentation” model. **B.** Sclerotome shift model. **C.** The orientation of a grafted somite (stippled) can influence the result: even a slight deviation from the correct R-C orientation will result in “like” sclerotome cells mixing, appearing like artefactual resegmentation. **D-F.** Illustrated sections through the sclerotome at 4, 5, 6 and 8 days (modified from Hamilton, 1953). Tracing of two consecutive somites (Red and Green) based on cell density boundaries. **G.** Interpretation of somite contribution to vertebrae based on cell density tracing (No resegmentation, 1 somite= 1 vertebra). **H-J.** Sections as in D-F, but tracing of two consecutive somites is independent of cell density and based on resegmentation. **K.** Interpretation of somite contribution to vertebrae based on resegmentation. (R=rostral sclerotome, C= caudal sclerotome, DM= dermomyotome, SCL = sclerotome, NC = notochord, M= muscle, V= vertebra, VB=vertebral body, NA=neural arch, IVD=intervertebral disc).



1.5.3.4. *Tracing morphological boundaries in the sclerotome*

In Verbout's review of vertebral column development, the author cautions against the problems associated with using morphological landmarks (such as a fissure or cell density boundary) as evidence of a vertebral pre-pattern within the sclerotome (Verbout, 1976). The cellular arrangements that form these landmarks may be transient within a tissue, making them unsuitable for use as indicators of cell lineage. This point is emphasised in Figure 1.1 D-K, which illustrates two rows of sections through the developing vertebral column of the chick (modified from Hamilton, 1953). The top (Fig. 1.1 D-F) and bottom (Fig. 1.1 H-J) rows show the same series of oblique coronal sections through the somites at progressively older stages, culminating in a sagittal section through the centre of the final vertebral column (Fig. 1.1 G, K). The sclerotomal tissue is highlighted in each section; clear differences in cell density within this tissue can be seen at each stage of development. At the start of each series, two consecutive sclerotomes are shown in red and green (Fig. 1.1 D, H). In the top row (Fig. 1.1 D-F), cell density boundaries are assumed to correspond to sclerotome boundaries throughout development and, based on this interpretation, the sclerotome gives rise to an entire vertebra and intervertebral disc (i.e. no resegmentation; Fig. 1.1G). Interestingly, these density boundaries appear to tilt, such that the more medial sclerotome is shifted along the R-C axis with respect to the lateral somite, supporting the shifting sclerotome model of vertebral formation (Fig. 1.1B). However, in the bottom row (Fig. 1.1 H-J), cell density boundaries are considered independent of sclerotome boundaries, and in this case the sections have been interpreted so that a single sclerotome contributes to two successive vertebrae (i.e. resegmentation; Fig. 1K). These sections illustrate how the same morphological information is open to two very different interpretations. Considering this, it is not surprising that anatomical studies yielded such a range of opposing views.

It is also important to note that the anatomical studies described above were carried out on embryonic material from a range of amniote species, including avians (Remak, 1855; Frieriep, 1883; Frieriep, 1886; Hamilton, 1953), reptiles (Von Ebner, 1889; Manner, 1899), and mammals (Kölliker, 1861; Kollman, 1891; Schultze, 1896; Sensenig, 1949; Verbout, 1985). Although a comparative study reported no significant differences between species in all three groups (Baur, 1969), anatomical descriptions alone cannot rule out the possibility that

the relationship between sclerotome and vertebral segmentation varies between amniote groups.

1.5.4. The fate of sclerotome in the vertebral column: insights from experimental embryology

1.5.4.1. Quail-chick somite grafts

Advances in the study of cell fate during avian embryogenesis came with the development of the chick-quail chimaera method (Le Douarin, 1972). Quail and chick cells can be differentiated on the basis of nucleolar morphology after staining with Feulgen's method (Le Douarin, 1972) or by immunocytochemistry for quail-specific proteins (Selleck and Bronner-fraser, 1995), thus allowing the tracing of quail tissue grafted within a chick host. This method provided a system in which to trace sclerotome cells from the somite to the vertebral column.

The first study to trace sclerotome fate in the vertebrae using this method was that of Beresford (Beresford, 1983), in which brachial quail somites were transplanted into the equivalent position of a chick host. The author was more concerned with the fate of the myotome in the brachial muscles. However, in a brief analysis of the vertebral column, cells from the grafted quail somite were found in two successive vertebrae in ten-day old embryos, supporting the resegmentation model (Remak, 1855). More comprehensive studies using the same technique in the cervical and/or thoracic region were later conducted, further supporting resegmentation in the formation of the vertebral body, neural arch, spinous process and rib (Bagnall et al., 1988; Huang et al., 1996). These studies demonstrated a remarkable agreement with Remak's original model and observations. However, there are concerns about the reliability of the grafting method used. As described previously (section 1.2.9), it has been shown that sclerotome halves of the same R-C identity have a tendency to mix when placed adjacent to each other (Stern and Keynes, 1987). In consequence, somite grafting is reliant upon precise orientation within the host. Even a modest deviation from the correct R-C orientation could lead to juxtaposition of "like" cells and therefore cause artificial resegmentation (Fig. 1.1C). To circumvent this problem, the study was repeated using grafts of 1.5 somites where the R-C polarity can be more easily controlled (Huang et al.,

2000a). The results showed all elements to be derived from two successive somites as previously described. However, variation was seen in the composition of the rib along the proximo-distal axis. The costal head was derived from cells of only one somite, whereas further distally the rib was derived from two.

The fate of each half-sclerotome has also been studied by replacing just the rostral or caudal half-sclerotome in the chick with a quail half of the same type (Aoyama and Asamoto, 2000). Here, the authors concluded that the rostral and caudal sclerotome gives rise to the caudal and rostral half of the vertebral body respectively, confirming resegmentation. Confusingly, the rostral sclerotome was found to have the capacity to contribute to both the rostral and caudal neural arch, whilst the caudal sclerotome only ever gave rise to the rostral neural arch. The apparent flexibility in the boundary between rostral and caudal sclerotomes in the neural arch could be explained by potential contamination of rostral cells within the caudal sclerotome graft and vice versa.

1.5.4.2. Tracing of somites in situ

An alternative approach is to label somites in situ. This has been attempted in chick using fluorescent dextrans (Bagnall, 1992) or retroviral transduction of a LacZ marker (Ewan and Everett, 1992). However, problems with fluorescent signal persistence after long incubation periods in the former, and the inability to contain the retrovirus in a single somite in the latter, render the results inconclusive. Peanut agglutinin (PNA), which preferentially stains the caudal sclerotome half (Stern et al., 1986; Davies et al., 1990) has also been used as a marker (Bagnall, 1989), but molecular markers cannot be used as indicators of lineage relationships because they may be expressed by different cells at different stages. Recently, labelling of somites in situ has been more successfully carried out in mouse using an *Uncx4.1-LacZ* transgenic reporter to trace the caudal sclerotome (Takahashi et al., 2013). The results are consistent with the idea that the vertebral bodies form by resegmentation.

1.5.5. Resegmentation: Outstanding questions

As a result of the many studies mentioned above, resegmentation is now generally accepted as the correct model of vertebral formation, particularly in

amniotes (Christ and Scaal, 2008). In avians, due to the failure of in situ somite labelling studies to yield conclusive results, this conclusion is almost entirely based on evidence from quail-chick grafting studies. However, because of problems associated with this technique, there remains some doubt as to whether resegmentation is the correct model in chick. First, the aforementioned risk of graft and host cells artificially mixing due to mis-orientation of the quail somite has never been satisfactorily addressed. Second, the quail-chick chimaera technique may not be ideal for cell tracing, since there is a risk that quail-chick differences (Bellairs et al., 1981) and/or disruption to ECM proteins surrounding the somite (which are involved in sclerotome development; Solursh et al., 1979; Duong and Erickson, 2004) may result in abnormal cell behaviour. Changes in sclerotome behaviour and mis-orientation of the grafted somite may explain the high incidence rate of malformed vertebrae reported in one of these studies (Bagnall et al., 1988). As a result, resegmentation has not been demonstrated conclusively in chick.

A recent study in mouse has shown that regional variation exists in the relative contribution of the caudal sclerotome to vertebrae along the R-C axis (Takahashi et al., 2013). This highlights a question that has been overlooked in the literature: does the relationship between sclerotome and vertebral segmentation vary along the vertebral column in chick? Chapter three of this thesis addresses these outstanding questions by using carbocyanine dyes to trace endogenous somites in different regions along the R-C axis in chick.

1.6. A role for external signals in vertebral segmentation.

1.6.1. Evidence for external signals in amniote vertebral segmentation

According to classical descriptions, resegmentation is dependent upon R-C patterning of the sclerotome (Remak, 1855; Von Ebner, 1889). As described in section 1.2.9, this R-C patterning is established prior to somite formation (Aoyama and Asamoto, 1988) and is thought to be dependent upon the oscillating expression of clock genes (Takahashi et al., 2003), an autonomous property of the PSM (Palmeirim et al., 1997). In contrast, the sclerotome is not specified until after somite formation (Aoyama and Asamoto, 1988), and is dependent upon signals from surrounding tissues (Brand-Saberi et al., 1993;

Pourquie et al., 1993; Fan and Tessier-Lavigne, 1994; see section 1.4.1 for further references). Thus, polarity of the sclerotome is determined prior to formation of the sclerotome itself. This has led to the general consensus that in amniotes, the information required for generating the final segmental pattern of the vertebral column is intrinsic to the somites, although external signals are required to induce vertebral differentiation from the somite. However, a number of lines of evidence suggest that external signals may play an important role in vertebral segmentation.

First, if segmentation of the vertebral column is directly translated from that of the somites, it follows that larger somites should give rise to larger vertebrae. In section 1.2.7, two studies were described which suggest that in both fish and mammals, changing the period of clock gene oscillations results in alterations to somite, and therefore vertebral, number (Schroter and Oates, 2010; Harima et al., 2013). These studies also showed that by changing somite number, the size of the somites was also altered. However, it has never been demonstrated whether or not this change in somite size results in a similar alteration in the length of vertebrae. Indeed, the situation in wild type chick embryos suggests that somite and vertebra size do not always correlate, particularly in the case of vertebral length. For example, the brachial somites in the chick are larger than those in the cervical region, but the vertebrae that arise from them are not dramatically different in length (E. Ward et al., unpublished observation). Here, something other than the size of the somites must determine the spatial periodicity of vertebral segmentation.

A second line of evidence comes from recent work on a line of mice in which R-C somite patterning was lost due to knockout of *Mesp2* or double knockout of *Ripply1* and *Ripply2* (Takahashi et al., 2013). In wild type embryos these genes act as a molecular switch to establish and maintain R-C compartment boundaries (Morimoto et al., 2007; Takahashi et al., 2010). In the mutant mice, segmentation of the vertebral column was partially maintained in the absence of R-C patterning (Takahashi et al., 2013). It is possible that some aspects of R-C somite patterning still remain in these mutants, independent of the *Mesp2/Ripply* system. However, if it is completely abolished as the authors claim, this could indicate that R-C patterning is in fact dispensable for vertebral column segmentation. In these mutants, something else must compensate for R-C patterning to instruct vertebral segmentation. Together, these

considerations hint at the possibility that at least some aspects of vertebral patterning are determined by signals external to the somite. What the source of these signals is, and how they act to confer a segmental pattern upon the vertebral column is not clear. These questions are addressed in chapters four to six of this thesis.

1.6.2. The notochord plays a key role in vertebral segmentation in teleost fish

The processes of sclerotome induction and vertebral column formation described in this chapter have focused almost entirely on amniotes. However, recent studies have led to a clearer understanding of how segmentation is generated in the vertebral column of teleost fish, and may provide an insight into a possible source of segmental information external to the somite in amniotes.

Zebrafish (like amniote) somites are subdivided into distinct rostral and caudal domains, a pattern that is established and maintained by *mesp-a* and *mesp-b*, orthologues of the murine *Mesp2* (Sawada et al., 2000). As described in section 1.2.9, this rostro-caudal patterning is lost in the zebrafish *fss* mutant (van Eeden et al., 1996), a phenotype that has been attributed to a loss-of-function mutation in the *Tbx24* locus, a transcription factor upstream of *mesp-a* (Nikaido et al., 2002). In amniotes, rostro-caudal polarity is required in the sclerotome for segmentation of the motor and sensory axons of the spinal nerves (Keynes and Stern, 1984; Rickmann et al., 1985; Bronner-Fraser and Stern, 1991). In *fss* mutants, it has been reported that motor axons show various fusions and irregularities, pointing towards a conserved role for R-C patterning in nervous system segmentation in fish (van Eeden et al., 1996). In contrast, sclerotome ablation experiments in wild-type zebrafish have reported no effect on the segmentation of the spinal nerves (Morin-Kensicki and Eisen, 1997). In this experiment, staining for sclerotome markers was carried out immediately after ablation to ensure the sclerotome had been completely removed, but crucially it was never analysed later than this. It is possible that ventralising signals from the notochord re-induced sclerotome cells after ablation, and that these cells conferred a segmental pattern upon the migrating motor axons.

In contrast to avians and mammals, the sclerotome in teleost fish is relatively small compared to the myotome (Sunier, 1911; Morin-Kensicki and Eisen, 1997). This is an adaptation to an aquatic lifestyle: The movements associated with swimming mean that the animal is more reliant upon segmented musculature for its locomotion than tetrapods, and less reliant upon the strength provided by a bulky vertebral column due to the support provided by the notochord (which persists into adulthood) and by the water through which it swims. However, despite these differences, the sclerotome is thought to be induced by a similar process of ventralising and dorsalising signals from the notochord and neural tube (Stickney et al., 2000).

In zebrafish, lineage analysis of single sclerotome cells has been carried out to address whether their progeny are subject to strict rostro-caudal compartmentalisation during vertebral development (Morin-Kensicki et al., 2002). In this study, Dil-labelled cells from a single somite were often found to be distributed across two consecutive vertebral segments, supporting resegmentation of the sclerotome, but suggesting that sclerotome cells are not subject to the strict compartmentalisation that results from the non-miscible properties of the rostral and caudal sclerotome in chick (Stern and Keynes, 1987). This process was termed 'leaky resegmentation' (Morin-Kensicki et al., 2002).

Analysis of the vertebral column in *fss* mutants (like in the mouse *Mesp2/Ripply* transgenic line) has provided an insight into whether R-C somite patterning is required for segmentation of the vertebrae in zebrafish. A clear difference is seen between vertebral elements. Neural and hemal arches are highly disorganised and often fused together, whereas the vertebral bodies show no abnormal phenotype, forming in a regularly spaced, segmented arrangement (van Eeden et al., 1996; Fleming et al., 2004). This suggests that whilst R-C patterning of the sclerotome is required for segmental patterning of the neural and hemal arches, something else controls segmentation of the vertebral bodies.

As well as variation at the somitic level, there are distinct differences in vertebral body morphology between amniotes and teleosts. Amniote vertebral bodies form by the formation of cartilaginous 'perichordal' centra around the notochord by sclerotomal chondrblasts, which are gradually replaced by bone

during endochondral ossification. In contrast, the vertebral bodies of teleost fish are comprised of two layers: The inner 'chondracentra' which initially form within the ECM of the notochordal sheath, and the 'perichondral centra' which directly ossify as a ring of bone surrounding the chordacentra (Gadow & Abbott, 1895; Fleming et al., 2015). It has been demonstrated that in both zebrafish (Fleming et al., 2001; 2004) and Atlantic salmon (Grotmol et al., 2003; Wang et al., 2013), the chordacentra are not derived from the sclerotome, but instead by the secretion of a bony matrix from the outer layer of cells in the notochord (the so-called chordablasts), laying down the initial segmental pattern. The sclerotome of the somites in these species only gives rise to the perichordal centra (which follow the same segmental pattern as the underlying chordacentra), as well as the neural and hemal arches (Grotmol et al., 2003; Fleming et al., 2004). The finding that the chordacentra and arches have different developmental origins in the zebrafish may explain why segmentation is disrupted in the latter, but not in former in the fused somite (fss) zebrafish mutants (Fleming et al., 2004). The differences in vertebral body development between teleosts and amniotes may suggest that they are not homologous structures, but represent two different responses to an evolutionary pressure to reinforce the notochord (Fleming et al., 2004; Fleming et al., 2015).

If the initial chordacentra in teleosts are formed by the notochord, how does the segmental pattern arise? Laser ablation of notochord cells in zebrafish only leads to a loss of vertebral bodies if it is carried out at distinct "segmentally reiterated" positions (Fleming et al., 2004). Furthermore, the first sign of segmentation in the axial skeleton of the Atlantic salmon is a change in the polarity of chordablast cells in bands around the notochord, which appear in a segmented pattern along the R-C axis (Grotmol et al., 2003). The secretion of the bony matrix by these bands of cells is preceded by the expression of Alkaline Phosphatase, a marker of osteoblasts (Grotmol et al., 2005). This suggests that the notochord in these species possesses an intrinsic segmental pattern that determines segmentation of the vertebral bodies. This raises a number of important questions: First, is notochord segmentation a derived trait of the teleosts, or was a segmented notochord present at the base of the vertebrates? If the latter, has segmentation of the notochord been retained in amniotes? And finally, could the notochord be a source of external segmental information that influences vertebral column segmentation in amniotes?

1.6.3. Does the notochord play a role in vertebral patterning in amniotes?

Unlike teleosts, there is currently no evidence to suggest that the cells of the amniote notochord contribute to vertebral column cartilage or bone. However, several studies suggest that it may be required for segmental patterning of the vertebral column. Some have analysed the role of the notochord in vertebral formation in chick by surgical ablation of a portion of the notochord (Watterson et al., 1954; Strudel, 1955; Teillet and Le Douarin, 1983). Absence of the notochord appears to have no effect on the formation of the neural arches, suggesting that after induction of the sclerotome, the notochord plays no further role in formation or segmental patterning of the neural arches (Watterson et al., 1954; Strudel, 1955). However, in the absence of a notochord, the position normally occupied by the vertebral bodies and intervertebral discs is replaced by a continuous strip of unsegmented cartilage (Watterson et al., 1954; Strudel, 1955). This result suggests that the notochord is not required for sclerotome to form cartilage in the ventral vertebral column, but is required for this cartilage to form segmentally. Together, this points towards a role for the notochord in segmentation of the vertebral bodies in the chick.

As well as being implicated in the segmentation of vertebral bodies, the notochord also plays a key role in development of the intervertebral discs (IVDs) that form between them. Indeed, the absence of IVDs in the unsegmented ventral cartilage of notochord-ablated embryos (Watterson et al., 1954; Strudel, 1955) suggests that the notochord is required for IVD development in chick. In mouse and human, the notochord is replaced by bone in the vertebral bodies, but persists as the central portion of the intervertebral discs (the nucleus pulposus). The outer ring of the intervertebral disc (known as the annulus fibrosus) is derived from the sclerotome. Recent studies in mouse have used a tamoxifen-inducible cre/lox system to specifically knock out *Shh* in the notochord or floor plate (Choi and Harfe, 2011; Choi et al., 2012). This allowed the timing of knockout to be controlled so that *Shh* was removed just before the onset of IVD differentiation, and after the sclerotome had been induced in the somite. The authors reported that *Shh* in the notochord (and not the floor plate) is required for formation of both the nucleus pulposus and annulus fibrosus of the IVD, as well as formation of the vertebral bodies. This

suggests that in mouse, the notochord is critical in the formation of the ventral vertebral column, and that Shh is essential for this function. It is not certain whether the same is true in chick.

Together, these studies suggest that although the notochord may not contribute to the vertebral bodies as they do in teleost fish, it may confer a segmental pattern upon the sclerotome, challenging the existing dogma that vertebral column segmentation in amniotes is generated entirely by segmental information within the sclerotome.

1.7. Aims of the thesis

In this thesis, I investigate how segmentation of the vertebral column is established from the initial spatial periodicity of the sclerotome set up during somitogenesis. I first re-visit resegmentation in chick, addressing the question of whether resegmentation is the correct model for vertebral column formation, and whether this process is variable along the R-C axis. I then go on to investigate the role of external signals in segmental patterning of the amniote vertebral column, specifically focusing on the notochord as a potential source of these signals.

Chapter 2 : General Materials and Methods

2.1. Embryology

2.1.1. Embryos

Eggs from domestic fowl (*Gallus gallus*, Brown Bovan Gold; Henry Stewart & Co., UK) and Japanese quails (*Coturnix japonica*; B.C. Potter, Rosedean Farm, UK) were incubated at 38°C in a humidified incubator and staged (Hamburger and Hamilton, 1951). Ca²⁺/Mg²⁺-free Tyrode's saline solution (henceforth referred to as 'Tyrode's saline') was used for *in ovo* manipulations and Pannett-Compton saline was used for manipulations in modified 'New' culture (Chapter 6.4, Stern and Holland, 1993).

The methods for preparation of embryos for manipulation *in ovo* and 'New' culture are described below. Details of manipulations for each experiment are described in the relevant chapter.

2.1.2. Harvesting embryos for fixation

After incubation to the desired stage, embryos were harvested at room temperature in Ca²⁺/Mg²⁺-free phosphate-buffered saline (PBS). In cases where embryos were harvested after experimental manipulation, embryos were collected in PBS as above or whichever saline solution was used during the experimental manipulation (Chapter 6.4, Stern and Holland, 1993).

2.1.3. Embryo fixation

4% paraformaldehyde (PFA) was used as a fixative in all experiments apart from those being processed for skeletal preparation (section 2.4.3). 4% PFA was prepared by dissolving PFA powder (Sigma) in PBS, preheated to 70°C and adjusted to approximately pH7.5 with 1M aqueous sodium hydroxide solution (NaOH; Sigma). The solution was placed at 70°C and agitated occasionally until the powder had completely dissolved.

Embryos were fixed overnight at 4°C, or for one hour at room temperature. From HH8 onwards, embryos were always fixed overnight to ensure full penetration of the fixative to deeper tissues and a number of holes made in the head using a fine tungsten needle to avoid trapping of probes and/or antibodies during staining. After fixation, embryos were either transferred to absolute methanol and stored at -20°C for up to a week (minimum overnight), or washed in PBS three to four times before further processing.

2.1.4. Preparation of embryos for *in-ovo* manipulation

Chicken eggs were incubated on their side so that the embryo sat in the centre of the egg immediately below the uppermost surface of the shell. The egg was first sterilised with 70% ethanol and prepared for *in ovo* manipulation as described (Chapter 12.3, Stern and Holland, 1993). After manipulation, embryos were lowered into the egg by removal of 2-4 ml albumen using a syringe needle inserted into the blunt end of the egg. A drop of albumen was placed on top of the embryo and 100 µl of 100x antibiotic-antimycotic (Gibco™; Life Technologies) added inside the egg, away from the embryo, to prevent bacterial and fungal growth during incubation. The egg was sealed using electrical tape and returned to the humidified incubator.

2.1.5. Preparation of embryos for 'New' culture

Embryos were prepared for 'New' culture (New, 1955) according to the modified protocol described (Stern and Ireland, 1981; Stern and Holland, 1993, Chapter 12.3).

2.1.6. Counting of somites and vertebrae

It was necessary to define an initial set of criteria for counting somites and the vertebrae to which they give rise. For this experiment, the fate map of Burke et al. (1995) was used as a guide (Fig. 3.1A). This fate map takes into account two main criteria: (1) that a somite contributes to two successive vertebrae (Huang et al., 2000b; Remak, 1855) and (2) that the most anterior 4.5 somites contribute to the occipital region of the skull (de Beer, 1937; Huang et al., 2000c). The first somite is a transient structure, being incorporated into the cranial mesoderm shortly after formation (Hamilton and Hinsch, 1956; Huang et

al., 1997), therefore the number of visible somites was counted and one added to reach the final somite number.

2.1.7. Dil and DiO labelling

Stock solutions of CellTracker™ CM-Dil and SP-DiOC₁₈(3) (Molecular Probes™; henceforth referred to as Dil and DiO) were prepared at 2mM in dimethylformamide (DMF; Sigma) and stored at -20°C according to the manufacturer's instructions. These were diluted immediately prior to labelling to the desired working concentration in 0.3 M sucrose and 0.002% Tween-20 (Sigma) (see individual chapter materials and methods sections for working concentration used in each experiment). Prior to dilution, the Dil and DiO stock solutions were heated for 15 minutes at 60°C and vortexed several times to ensure the dye was fully suspended. The carbocyanine dyes above were chosen as they contain thiol-reactive and sulfonated side-chains, which have been reported to improve their water solubility and persistence after fixation in other contexts, including in vivo cell tracing (Andrade et al., 1996).

2.2 Molecular Biology

2.2.1. Isolation and purification of embryonic mRNA

Embryos at HH25 were harvested in ice cold PBS (made with DEPC-treated water), and the heads removed. Total RNA was extracted by resuspending the trunk of the embryo in 1 ml TRIzol® reagent (Invitrogen). Embryos were homogenised by pipetting several times and incubating for 10 minutes at room temperature. 200 µl chloroform (Sigma) was added, mixed well and the phases separated using a micro-centrifuge. The aqueous phase was collected, 500 µl isopropanol added and the RNA precipitated for 10 minutes at room temperature. RNA was pelleted using a micro-centrifuge, washed in 75% ethanol, air-dried at 37°C and dissolved in DEPC-treated water. DNA was removed by adding RQ1 RNase-free DNase (Promega) at a concentration of 0.1 µg/µl and 5 µl of 10x RQ1 DNase reaction Buffer (Promega) at 37°C for 30 minutes. 5 µl DNAase Stop solution (Promega) were then added and incubated for ten minutes at 65°C to inactivate the DNAase.

Purified total RNA was diluted to a concentration of 2.5 µg/µl in DEPC-treated water, stored at -80°C or used immediately for cDNA synthesis (section 2.2.2 below).

2.2.2. Single-stranded cDNA synthesis

Single-stranded cDNA (sscDNA) was synthesised by reverse-transcription of the HH25 trunk mRNA using a Superscript™ III cDNA synthesis kit (Life Technologies). The reaction mix was set up as shown in Table 2.1, and the reaction carried out in a Bio-Rad T100™ Thermal Cycler PCR machine pre-programmed to the cycle conditions outlined.

Component	Amount (µl)	Cycle
HH25 trunk RNA (2.5 µg/µl)	1	1. Reverse transcription: 55°C – 30' 2. Denature: 94°C – 2' 3. 4°C - ∞
2x SSIII reaction mix	25	
Primers: Oligo (dT) 12-18 (0.5 µg/µl)	1	
Primers: random hexamers (50 ng/µl)	1	
ssIII RT/Taq enzyme mix	2	
DEPC-water	20	

Table Error! No text of specified style in document..1. Reagents and conditions used in the synthesis of single-stranded cDNA

A sample of the reaction was analysed using gel electrophoresis to check the strength of the cDNA product synthesised. The remaining volume was diluted in water at a ratio of 1:5 to 1:10 depending on the amount of product (estimated by the intensity of staining of the band on the gel). cDNA was stored at -20°C until use.

2.2.3. Primer design

Primers were designed against the mRNA sequence of the gene of interest using the online Primer3 interface (Koressaar and Remm, 2007; Untergasser et al., 2012). Primers were obtained from Life Technologies.

2.2.4. Cloning of *Uncx4.1* mRNA by PCR

A 650 base-pair fragment of the *Uncx4.1* mRNA sequence was amplified using HH25 trunk sscDNA (as prepared above) as a template. The optimised conditions used in the reaction are shown in Table 2.2. As a positive control, a plasmid containing the *Fibulin 7* (*Fbln7*) clone was used as a template, along with primers designed against the *Fbln7* mRNA sequence, which were originally used to clone this fragment. As a negative control, the DNA polymerase was replaced by an equivalent volume of sterile ultrapure water. Primer pairs and the optimised annealing temperature (T_m) used are shown in Table 2.3.

Component	Amount (μ l)	Cycle
cDNA template	1	1. Hot start: 95°C – 30 sec 2. Denaturing: 95°C – 10 sec 3. Annealing: 50-55°C – 30 sec 4. Extension: 72°C – 1.5 min 5. Go to Step 2 – 39x 6. Final extension - 72°C – 1.5 min 7. Hold: 12°C - ∞
Forward primer (100 μ M)	1	
Reverse primer (100 μ M)	1	
PCR nucleotide mix (10 mM) (Promega)	1	
5x Flexi Taq reaction buffer (Promega)	10	
MgCl ₂ (25 mM; Promega)	2	
GoTaq G2 DNA polymerase (Promega)	0.5	
Sterile ultrapure water	33.75	

Table 2.2. Reagents and cycle conditions used in the cloning of *Uncx4.1* mRNA by PCR.

mRNA target	Forward primer	Reverse primer	T_m (°C)
<i>Uncx4.1</i>	GGTGGGGTAGAGCAAGAAGT	CGGACGTGTTTATGCGAGAG	50
<i>Fibulin 7</i>	GAGCCCCTGAAATCCAGC	CTCAGAACTCATACTGGGACAG	55

Table 2.3. Primer sequences and corresponding annealing temperatures used in the cloning of a 650bp fragment of *Uncx4.1* cDNA by PCR. Primers designed against the *Fibulin 7* mRNA was used as a positive control in this reaction, using a plasmid containing the *Fibulin 7* cDNA as a template.

The presence of a cDNA product of the correct size was analysed by gel electrophoresis from a sample of the reaction.

2.2.5. Ligation and transformation

The cDNA PCR product was ligated into the PGEM[®]-T Easy vector (Promega) for fifteen minutes on ice, using the reaction mix shown in Table 2.4.

Component	Volume (µl)
Purified PCR product	3
2x rapid ligation reaction buffer (Promega)	10
PGEM [®] -T Easy vector (50 ng/µl) (Promega)	2
T4 DNA ligase (Promega)	2
Sterile ultrapure water	3

Table 2.4. Reagents used in the ligation reaction.

Competent DH5α *E. coli* cells were transformed with recombinant plasmids by heat shock. 1-2 µl of purified stock plasmid, or 10 µl of the ligation reaction above was added to 50 µl of competent bacteria, incubated on ice for 15 minutes, heat-shocked at 42°C for 45 seconds, then cooled on ice for two minutes. 800 µl of SOC medium (Super Optimal Broth with Catabolite repression; Sigma) was added to the transformation, and bacteria were cultured at 37°C for one hour with shaking at 250 RPM.

After culture, bacteria were pelleted and 750 µl of the SOC medium removed. The bacteria were re-suspended in the remaining 50 µl, plated on ampicillin X-gal/IPTG blue/white selection plates (see preparation method below) and cultured overnight at 37°C. White colonies were selected and cultured in lysogeny broth (LB; Sigma) to amplify the plasmid for diagnostics (see mini-culture and purification method in section 2.2.7.1).

2.2.6. Preparation of ampicillin X-gal/IPTG selection plates

Ampicillin plates were prepared by inoculating 1% LB Agar (Sigma) with ampicillin (Ampicillin sodium salt dissolved according to manufacturer's instructions; Cabiochem, Millipore) at a concentration of 100 µg/ml, which was

then poured into RNase-free Petri dishes and allowed to set at room temperature.

X-gal/IPTG (blue/white) selection plates were prepared by coating ampicillin plates with 4 µl of 200 mg/ml isopropyl-beta-D-thiogalactopyranoside (IPTG; eppendorf) and 20 µl of 50 mg/ml 5-bromo-4-chloro-3-indolyl-β-D-galactopyranoside (X-gal; Sigma). Plates were left to absorb the coating for at least 30 minutes prior to use.

2.2.7. Preparation and purification of recombinant plasmid DNA

2.2.7.1. Mini-prep

To amplify plasmids for sequence diagnostics, selected white colonies were cultured overnight at 37°C in 3 ml of lysogeny broth (LB; Sigma) containing ampicillin at a concentration of 100 µg/ml (henceforth referred to as 'ampicillin LB'). Plasmid DNA was extracted and purified from 1.5 ml of the culture using a QIAGEN® mini-prep kit according to the protocol outlined by the manufacturer. Purified DNA was eluted in 50 µl sterile ultrapure water.

2.2.7.2. Midi-prep

To grow larger quantities of plasmids for synthesis of antisense probes, 1 ml of the remaining 3 ml culture, or a scraping from a stored bacterial glycerol stock, was added to 50 ml of ampicillin LB and cultured overnight at 37°C. Plasmid DNA was extracted and purified using a QIAGEN® midi-prep kit according to the protocol outlined by the manufacturer. Purified DNA was eluted in 50-100 µl sterile ultrapure water and stored at -20°C.

2.2.8. Diagnostic digest

To check for the presence of a clone of the expected size in recombinant plasmids, a restriction digest reaction was carried out as outlined in Table 2.5 and incubated for two hours at 37°C. The EcoR1 restriction sites flank the insert in the multiple cloning site of the PGEM®-T Easy vector and are not present within the *Uncx4.1* clone sequence. Therefore, digestion of a

recombinant plasmid using the EcoR1 restriction enzyme should release the insert. The size of the insert was analysed by gel-electrophoresis.

Component	Volume (μl)
Purified mini-prep DNA	1
10x restriction digest buffer H (Promega)	1
BSA (1 mg/ml; Promega)	1
EcoR1 restriction enzyme (Promega)	0.5
Sterile ultrapure water	6.5

Table 2.5. Reagents and conditions used in restriction digest reaction to determine the presence and size of cloned DNA fragment in recombinant plasmid.

2.2.9 Gel electrophoresis and sequencing of cloned DNA

1% agarose gels containing ethidium bromide at a concentration of 0.4 μ g/ml were used to separate DNA and RNA. A 1 kb standard DNA ladder (Promega) was run alongside all samples.

Positive cDNA clones were sequenced by Source Biosciences Sanger sequencing facility, using universal primers against T7 or T3 promoter sites.

2.2.10. Measurement of DNA and RNA concentration

The concentration of DNA and RNA in aqueous solutions was measured using a NanoDrop 2000 spectrophotometer (Thermo Scientific).

2.3. Whole-mount In-Situ Hybridisation (WMISH)

2.3.1. Linearisation of plasmid DNA

Recombinant plasmid DNA was linearised by a restriction digest reaction using an enzyme with a unique restriction site within the plasmid. The restriction digest reaction was prepared as shown in Table 2.6, and incubated at 37°C for four hours. The specific restriction enzyme used to linearise each plasmid is shown in Table 2.9. The buffer used in each reaction was chosen according to

the efficiency guidelines of the enzyme manufacturer (Promega or New England Biolabs). Bovine serum albumin (BSA) (Promega) was added to the reaction at a concentration of 0.1mg/ml, if guidelines stated efficiency of the reaction was increased by its presence. In cases where BSA was not required, the equivalent volume of water was added to the reaction instead.

Component	Volume (μ l)
Plasmid DNA (1 mg/ml)	10
10x reaction buffer	5
Restriction enzyme	3
BSA (1 mg/ml) or water	5
Water	27

Table 2.6. Reagents and conditions of the restriction digest reaction used to linearise recombinant plasmids prior to transcription of antisense probes.

After restriction enzyme digestion, a sample of the reaction was analysed by gel electrophoresis alongside the undigested plasmid to ensure a single linear product.

The linearised plasmid was purified by phenol:chloroform extraction. An equal volume of phenol:chloroform (phenol:chloroform:isoamyl alcohol 25:24:1; Sigma) was added to the reaction mix. After vortexing, the aqueous and organic phases were separated using a micro-centrifuge and the aqueous phase containing the DNA collected. DNA was precipitated by adding 5 μ l 3 M sodium acetate and 125 μ l absolute ethanol and incubating overnight at -20°C. The precipitate was pelleted using a microcentrifuge at maximum speed for one minute, washed in 70% ethanol and air-dried at 37°C. Purified linear DNA was dissolved in sterile ultrapure water at a concentration of 1 μ g/ μ l (approximately calculated as the total amount of DNA linearised, allowing for loss during the purification process) and stored at -20°C.

2.3.2. PCR amplification of cDNA insert

In the case of the *Uncx4.1* plasmid, no unique restriction sites could be found in the vector that were not also present in the cloned fragment, and therefore linearisation of the plasmid by restriction digest was not possible. The probe

template insert was therefore amplified directly from the plasmid DNA by PCR using M13 forward and reverse primers (M13F: GTAAAACGACGGCCAGT; M13R: GCGGATAACAATTTTCACACAGG), sequences of which flank the cloning site of the PGEM®-T Easy vector. The PCR reaction mix and cycle conditions used are shown in Table 2.7. A sample of the PCR reaction was analysed by gel electrophoresis to ensure that a single product of the correct size had been amplified. The amplified probe template was used directly in the transcription of an antisense RNA probe without purification.

Component	Volume (µl)	Cycle
Plasmid DNA (5 ng/µl)	1	1. Hot start: 95°C – 3 min 2. Denature: 95°C – 1 min 3. Anneal: 50°C – 45 sec 4. Extension: 72°C – 1.5 min 5. Go to step 2 – 30x 5. Final extension: 72°C – 1.5 min 6. Hold: 12°C - ∞
M13 Forward primer (10 µM)	0.5	
M13 Reverse primer (10 µM)	0.5	
5x Flexi Taq reaction buffer (Promega)	2	
MgCl ₂ (25 mM; Promega)	1	
PCR nucleotide mix (10 mM) (Promega)	0.2	
GoTaq G2 DNA polymerase (Promega)	0.2	
DEPC-Water	0.2	

Table 2.7. Reagents and cycle conditions used in the amplification of cDNA insert from recombinant plasmid, in cases where linearisation of circular DNA by restriction digest is not possible due to the lack of a unique restriction site.

2.3.3. Transcription of anti-sense RNA probes

Digoxigenin (DIG)-labelled antisense RNA probes were transcribed from 3 µg of linear plasmid DNA at 37°C for three hours using the reaction mix shown in table 2.8. The RNA polymerase sequences located 5' to the DNA insert vary according to the vector and orientation of the insert. The RNA polymerase used to transcribe antisense RNA for each clone is shown in Table 2.9.

Component	Volume (μ l)
Template DNA (1 μ g/ μ l)	3
Water	22
5x transcription optimised buffer (Promega)	10
10x DIG RNA-labelling mix	5
Dithiothreitol (DTT) (100 mM; Promega)	5
Recombinant RNAsin® Ribonuclease inhibitor (Promega)	1
RNA polymerase (Promega)	4

Table 2.8. Reagents and conditions used in the transcription of anti-sense cDNA probes for in-situ hybridisation.

Clone	mRNA target	Linearisation of template by restriction digest or PCR amplification?	Restriction enzyme	RNA polymerase
15.24	Pax1	RD	Xba1	T3
2.53	Paraxis	RD	Pst1	T7
15.16	Uncx4.1	PCR	-	Sp6
13.73	Scleraxis	RD	HindIII	T3
2.56	Pax3	RD	SacI	T3
3.5	Patched 1	RD	Kpn1	T3
2.40	Nodal	RD	SacII	T7
2.88	Sox3	RD	Pst1	T7

Table 2.9. Details of the restriction enzyme and RNA polymerase used in the synthesis of cDNA probes from recombinant plasmids containing cloned DNA fragments of target gene mRNA.

Following transcription, 2 μ l of RQ1 RNase-Free DNase enzyme (Promega) was added to the reaction and incubated for a further 40 minutes at 37°C to remove the DNA template. A sample of the reaction mix was analysed by gel electrophoresis to check the strength of the RNA product synthesised, and that the DNA template had been completely digested.

Water was added to the remaining transcription reaction to a total volume of 80 μ l, and 8 μ l of 0.5 M EDTA (pH 8) added to inhibit the RNA polymerase. To purify the synthesised probe, the product was precipitated twice overnight at -20°C by adding of 10 μ l 4 M lithium chloride and 250 μ l absolute ethanol. After each precipitation, the precipitate was pelleted using a microcentrifuge, washed in 70% ethanol, 100% ethanol, then air-dried at 37°C. Purified probe was dissolved in water at a concentration of 1 mg/ml (calculated approximately, as the transcription reaction should yield eight times the weight of the template used). The dissolved probe was denatured at 95°C for three minutes before being cooled on ice for five minutes.

The denatured probe was dissolved in 1 ml hybridisation buffer, mixed well and stored indefinitely at -20°C. Before use, probes were diluted in a final volume of 10-15 ml hybridisation buffer (Stern, 1998), depending on the strength of the product

2.3.4. WMISH protocol

After fixation, embryos were transferred to absolute methanol and stored at -20°C at least overnight (no more than one week) to improve the permeability of the tissue. In-situ hybridisation was carried out as described by Stern (1998) using DIG-labelled antisense RNA probes prepared as above. PTW (Ca²⁺/Mg²⁺-free PBS containing 0.1% Tween-20) was used for all pre-hybridisation washes, and TBST (TBS containing 0.1% Tween-20) used for all washes after the hybridisation step. Throughout all washes, embryos were gently rocked. The procedure was as follows:

Fixed, methanol-stored embryos (see section 2.1.3 above) were rehydrated through 70%, 50% and 25% methanol in PTW and washed three times in PTW (ten minutes per wash). The embryos were then digested in 10 μ g/ml Proteinase K (Sigma) diluted in PTW, the duration of which was optimised according to the stage of the embryo and the probe to be used. As a general rule, embryos were digested for a minute per stage (Hamburger and Hamilton, 1951). For example, HH5 embryos were digested for 5 minutes. However, for embryos above HH17/18 it was found that a longer digestion time was required. HH18 embryos were digested for 25 minutes and HH24/25 embryos digested for 40 minutes. HH10-12 embryos harvested after 'New' culture were

found to be much more fragile, and were only digested for 6 minutes. After digestion, embryos were then washed briefly in PTW, before post-fixing in 4% PFA (section 2.1.3) containing 0.1% glutaraldehyde (Sigma) for 30 minutes at room temperature.

Embryos were then washed three times in PTW (ten minutes per wash) and transferred to hybridisation buffer (Stern, 1998). Pre-hybridisation was carried out for three hours at 70°C. Hybridisation buffer was then replaced with pre-warmed DIG-labelled RNA probes diluted in hybridisation buffer and hybridisation carried out overnight at 70°C. The next morning, the probe solution was removed and embryos were rinsed three times and washed in two changes of hybridisation buffer (30 minutes per wash) at 70°C. Embryos were then washed in a 1:1 solution of hybridisation buffer and TBST for 20 minutes at 70°C, before being washed five times in TBST at room temperature (one hour per wash). To decrease non-specific binding of the antibody, embryos were blocked in blocking buffer (TBST containing 1 mg/ml BSA (Sigma) and 5% goat serum (Sigma) that had previously been heat-inactivated at 55°C) for three hours at room temperature. Embryos were then incubated overnight at 4°C in primary antibody solution (alkaline phosphatase (AP)-conjugated anti-DIG Fab fragments (Roche) diluted in blocking buffer at a concentration of 1:5000). The next morning, embryos were rinsed in TBST, washed five times in TBST at room temperature (one hour per wash). Embryos were then transferred to NTMT solution (Stern, 1998) which acts as a substrate in the alkaline phosphatase reaction and incubated for twenty minutes. The stain was then developed by adding nitro blue tetrazolium (NBT; Roche) and 5-Bromo-4-chloro-indolyl phosphate (BCIP; Roche) to the NTMT substrate, at concentrations of 0.23mg/ml and 0.12mg/ml respectively and incubating in the dark, until the desired colour had developed. Embryos were then washed at least three times in PTW and post-fixed for one hour in 4% PFA at room temperature before imaging or further processing.

For all embryos of stage HH10 or above, the following modifications were made to the standard protocol: Prior to rehydration, embryos were bleached in 6% hydrogen peroxide (30% H₂O₂; Sigma) in methanol for one hour at room temperature both to inactivate endogenous peroxidases (if DAB staining was to be used in a later immunostain) and phosphatases (mainly present in blood cells) and to remove any pigment. Post-antibody TBST washes were increased

to six one-hour washes at room temperature, then overnight at 4°C. Finally, the time incubated in NTMT substrate prior to developing was increased to one hour.

2.4. Immunohistochemistry and histology

The details of primary and secondary antibody pairs and the concentration used for each application are listed in Table 2.10.

2.4.1. Whole-Mount immuno-staining

After fixation, embryos were transferred to absolute methanol and stored at -20°C. Staining was then carried out using HRP-conjugated secondary antibodies and peroxidase detection using 3,3-diaminobenzidine (DAB) as substrate as described by Stern (1998). As all immunostains in this thesis were carried out on embryos over HH10, modifications were made to incubation times and to the number and duration of washes to account for the large size of the embryos and the specific antibody used. PBS containing 1% Triton-X100 (Fisher) and 0.002% thimerosal (Sigma) was used in all solutions and washes (henceforth referred to as PBS-Triton). The protocol was then carried out as follows:

Embryos were first bleached in 6% H₂O₂ in methanol for one hour at room temperature. Embryos were then washed three times in PBS-Triton (one hour per wash) before incubating overnight in blocking buffer at 4°C (PBS-Triton containing 1 mg/ml BSA and 5% goat-serum that had been heat-inactivated at 55°C). The next morning, blocking buffer was replaced with primary antibody diluted to the desired concentration in blocking buffer and embryos were incubated in the primary antibody solution for at least three days (maximum five) at 4°C. Embryos were then washed five times in PBS-Triton (one hour each wash) at room temperature, before incubating in secondary antibody diluted to the desired concentration in blocking buffer for at least two days (maximum three) at 4°C. Embryos were then washed five times in PBS-Triton (one hour per wash) and a sixth wash overnight at 4°C. The next morning, embryos were transferred to 0.1M Tris (pH7.5), which buffers the peroxidase reaction, and incubated for one hour at room temperature. DAB substrate was

then added to the Tris solution to a final concentration of 0.75mg/ml and incubated in the dark at room temperature for thirty minutes.

Immunoperoxidase detection was then carried out by adding H₂O₂ to the DAB substrate solution to a final concentration of 0.03%. After the stain had developed to the desired colour, embryos were washed three times in tap water, followed by at least three washes in PBS-Triton (ten minutes each). Embryos were then post-fixed in 4% PFA overnight.

2.4.2. Whole-mount immuno-staining following WMISH

Following WMISH, embryos were post-fixed for one hour at room temperature in 4% PFA. Embryos were then washed five times (one hour per wash) in PBS-Triton at room temperature to ensure removal of all traces of ISH developing solution and PFA. The protocol above was then followed from the blocking step onwards.

Protein target	Application	Primary antibody					Secondary Antibody				
		Antibody	Source	Host species	Antigen species	Conc.	Antibody	Source	Host species	Antigen species	Conc.
Quail nuclear protein (QCPN)	WMIHC	QCPN quail cell marker	DSHB	Mouse	Quail	1 in 5	HRP-conjugated IgG	Jackson Immuno	Goat	Mouse	1 in 1000
Sonic Hedgehog N-terminus	WB	SHH (5E1)	DSHB	Mouse	Rat	1 in 500	HRP-conjugated IgG	Jackson Immuno	Goat	Mouse	1 in 5000
GFP	WMIHC	Anti-GFP	Invitrogen	Rabbit	Jellyfish	1 in 2000	HRP-conjugated IgG	Santa cruz	Goat	Rabbit	1 in 2000

Table 2.10. Details of the primary and secondary antibody pairs used in immunostaining and Western blot experiments. Antibody pairs are listed in the order in which they appear in the text. Sources: DSHB= Developmental Studies Hybridoma Bank. Applications: WMIHC = Whole-mount immunohistochemical stain, WB = Western blot. Conjugations: AP = Alkaline phosphatase, HRP = Horseradish Peroxidase

2.4.3. Skeletal preparations

Embryos were fixed in 95% ethanol for three days at 4°C. Skeletal preparations were carried out using Alcian Blue and Alizarin Red S (Sigma) according to the protocol described by McLeod (1980) for staining of E17/18 mouse embryos.

2.4.4. Microtome sectioning of paraffin-embedded embryos

If sectioning after WMISH and/or immunocytochemistry, post-fixed embryos were washed extensively in PBS prior to processing for sectioning.

Embryos were dehydrated in absolute methanol for ten minutes, then transferred to isopropanol for five minutes. Embryos were cleared in tetrahydronaphthalene (Sigma) for thirty minutes, before transferring to a 1:1 mixture of tetrahydronaphthalene and melted Paraplast® (Sigma) and placed at 60°C for 20 minutes or until the wax had melted. The embryos were then placed in fresh wax at 60°C and this replaced at least three times. Embryos were embedded in plastic moulds and the block allowed to set for at least one hour at 4°C.

10 µm sections were cut using a microtome (Microm) and collected on glass microscope slides (Super Premium Microscope Slides; VWR) coated in glycerine albumin (VWR) immediately before use. Sections were dried completely, de-waxed in HistoClear™ (National Diagnostics) and mounted using borosilicate glass cover slips (thickness no.1; VWR) in a solution of 3:1 Canada balsam (Merck) and HistoClear™.

2.5. Imaging

2.5.1. Imaging of whole-mount embryos

Whole embryos were viewed and photographed in PTW using an Olympus SZX10 upright dissecting microscope, QImaging RETIGA 2000R camera and QCapture Pro software, with epi-fluorescence illumination when required. Raw images were processed and figures assembled using Adobe® Photoshop® CS2 version 9.0. The only changes made to the raw images were adjustments to the brightness, contrast and colour balance and were applied to the entire image.

2.5.2. Time-lapse imaging of live embryos

The petri dish containing the embryo in culture was sealed using Parafilm® M and incubated at 37°C. Time-lapse imaging was carried out using an Olympus inverted microscope and Simple PCI software with epifluorescent illumination when required. Images were taken at ten-minute intervals.

2.5.3. Imaging of sections

Mounted sections were viewed and photographed using an Olympus VANOX-1 microscope and the same camera and software as used for imaging of whole-mount embryos (section 2.6.1). Where necessary, Nomarski Interference Contrast was used to better visualise the morphology of sections.

2.5.4. Optical Projection Tomography (OPT)

2.5.4.1. Preparation of specimens

Embryos were prepared for scanning in accordance with the protocol described in the Bioptonics microscopy OPT scanner user manual version 1.11.3 (MRC technology©), which is based on the preparation procedure described (Sharpe et al., 2002). Embryos were washed in PBS and embedded in 1% Ultrapure low melting-point agarose (Life Technologies) in water and set overnight at 4°C. Agarose blocks were trimmed using a fine blade, dehydrated in absolute

methanol and cleared in a 2:1 solution of benzyl benzoate (Sigma) and benzyl alcohol (Sigma) (BABB)

2.5.4.2. OPT scanning

Embryos were scanned using a Biotronics OPT scanner 3001M and Biotronics OPT scanning software. As scans were carried out only on skeletal preparation specimens, only the bright field channel (no filter) was used during scanning. Datasets were reconstructed using NRecon and processed for analysis using Biotronics Viewer. Apart from adjustments to brightness and contrast, the 'threshold' function was used to eliminate noise in the background, strictly following the manufacturers' instructions.

Chapter 3 : A “resegmentation-shift” model for vertebral formation

3.1. Introduction

Development of the vertebral column and axial musculature involves a rearrangement of the somite compartments from which they derive. The sclerotome must shift by half a segment with respect to the dermomyotome in order for a single muscle to insert into two adjacent vertebrae. Two main models have been proposed for this. The “resegmentation” model states that each half-sclerotome joins with the half-sclerotome from the next adjacent somite to form a vertebra (Fig. 1.1A; Remak, 1855). In this model, the vertebrae are comprised of cells from two successive somites. The second model suggests that the sclerotome shifts with respect to the myotome by half a segment (Fig. 1.1B). This model could also establish the required rearrangement of tissues, but here each vertebra is comprised of cells from a single somite. The conflicting evidence for these two models from over a century of anatomical studies was discussed in chapter one (section 1.5).

In recent years, lineage analysis by quail-chick somite grafts has led the resegmentation model to be generally accepted in amniotes (Bagnall et al., 1988; Huang et al., 1996; 2000b; Aoyama and Asamoto, 2000). However, there are a number of problems with these studies. First, somite grafting relies on precise orientation of the somite so that “like” sclerotome halves do not come to lie adjacent to each other. This would allow the cells to mix, causing artefactual resegmentation (Stern and Keynes, 1987). Second, the technique relies on the assumption that the grafted quail tissue recapitulates endogenous somite behaviour, which may not be the case (Bellairs et al., 1981). Finally, there are a number of discrepancies between these studies concerning the contribution of a single somite to certain vertebral elements such as the neural arch (Aoyama and Asamoto, 2000; Huang et al., 2000b). There is therefore no definitive evidence in the chick that the vertebrae form by resegmentation. Furthermore, many of the previous studies test resegmentation in one region alone, and do not take into account the possibility of regional variation. That some such regional variation exists has been suggested by a recent study using a transgenic approach to trace sclerotome fate in mouse, which reported

resegmentation in this species but observed differences in the relative contribution of each sclerotome half to the vertebral bodies along the A-P axis (Takahashi et al., 2013).

Here I re-examine the questions surrounding vertebral formation without relying on grafting, using Dil and DiO to trace somite contributions to the vertebral bodies and neural arches along the vertebral column. By tracing somites systematically along the A-P axis, I also test the possibility that the contribution of a single somite to a vertebra may vary in different regions of the vertebral column.

3.2. Materials and methods

3.2.1. Dil and DiO labelling of somites in different regions of the axis

To ensure that only somite cells were labelled, it was important to perform the dye injection into newly-formed somites still in their epithelial state, which had not yet been invaded by motor axons or neural crest cells (Keynes and Stern, 1984; Bronner-Fraser, 1986). For this reason, embryos were incubated to a stage at which the three caudal-most somites (somites I, II and III according to roman numeral nomenclature; Ordahl, 1993) corresponded to the axial region that was intended to be fate-mapped (Fig. 3.1A).

Embryos were prepared for *in ovo* manipulation (section 2.1.4). 2 mM stock solutions of Dil and DiO (prepared as described in section 2.1.7) were diluted to 150 mM and 230 mM respectively in 0.3 M sucrose containing 0.002% Tween-20. Dil (red) or DiO (green) was injected into the somitocoele of the caudal-most three somites (red/green/red from rostral to caudal) on each side of the midline (Fig. 3.1B) using a fine pipette pulled from a 50 µl borosilicate capillary tube (Sigma) attached to an aspirator.

Labelled embryos were incubated for a further six days and fixed in 4% paraformaldehyde overnight at 4°C. Prior to sectioning, embryos were washed extensively in PBS. The embryo was then pinned out with its ventral surface uppermost, and the soft tissue dissected from around the region of the vertebral column corresponding to the somites labelled. The exposed vertebral

column was then cut sagittally through its centre and parted to reveal the inside of the vertebral bodies and inner face of the neural arches.

3.2.2. *Measurements of neural arch tilt*

Skeletal preparations of wild type embryos at HH30-32 were dissected so that all that remained was the vertebral column. Vertebral column skeletal preparations were then pinned out on their side on a Sylgard plate and photographed using a dissection microscope. The angle at which the neural arches projected from the horizontal axis of the vertebral body (Figure 3.4A) was measured from the two-dimensional bright field images using Fiji (Schindelin et al., 2012). Four consecutive vertebrae were measured in each region in six embryos. The four vertebrae sampled in each region corresponded to those labelled in Figure 3.3 A-C: Cervical: V6-9; Thoracic: V18-21; Lumbar/sacral: V25-28.

3.3. Results

3.3.1. *Somite contribution to the vertebral bodies*

Table 3.1 summarises the embryos that were successfully labelled and sectioned, and the vertebral elements analysed in each. In the cervical (n=3), thoracic (n=4) and lumbar/sacral regions (n=4), a single vertebral body (centrum) was comprised of cells from two successive somites, with the boundary between red and green labelled cells located in the middle of the vertebral body (Fig. 3.1E-G, K-M). Cells from a single somite were detected in the annulus fibrosus of the intervertebral disc (IVD) and in approximately half of the vertebral body rostral and caudal to it. These results support the resegmentation model (Fig. 3.2B).

The boundary marking the contribution of two adjacent somites was always sharp, with little mixing of labelled cells six days later (Fig. 3.1 E-G, K-M, yellow arrows). This is consistent with the properties of rostral and caudal sclerotome halves, which form a boundary when placed in close proximity (Stern and Keynes, 1987). These results confirm that this property is strictly maintained even after the extensive migration and proliferation that

accompanies vertebral development. Stronger labelling was always observed in the IVDs compared to the vertebral cartilages. There are two possible interpretations of this finding: either cells of the IVD divide less frequently, or injection of the dye into the somitocoele, which has been reported to give rise to the annulus fibrosus of the IVD (Huang et al., 1996), labels these cells more intensely.

Embryo	Axial region	Somite no. labelled			Vertebral element analysed	
		Dil	DiO	Dil	Vertebral bodies	Neural arches
090414(1)	Axis/Atlas	5	6	7	X	-
090414(2)	Axis/Atlas	5	6	7	X	-
281112(4)	Axis/Atlas	5	6	7	X	-
141112(4)	Cervical	9	10	11	X	-
210313(1)	Cervical	10	11	12	X	-
210313(3)	Cervical	10	11	12	X	-
190613(2)	Cervical	10	11	12	-	X
261113(1)	Cervical	10	11	12	-	X
261113(2)	Cervical	11	12	13	-	X
041013(1)	Thoracic	24	25	26	X	X
041013(3)	Thoracic	24	25	26	X	X
220313(3)	Thoracic	19	20	21	X	-
220313(1)	Thoracic	19	20	21	X	-
141013(3)	Lumbar	27	28	29	X	X
141013(1)	Lumbar/sacral	29	30	31	X	X
190413(2)	Lumbar	27	28	29	X	X
141013(4)	Lumbar/sacral	30	31	32	X	X

Table 3.1. Summary of embryos in which somites were traced in different regions of vertebral column using Dil and DiO. Embryos shown in figures 1 and 2 are highlighted in bold.

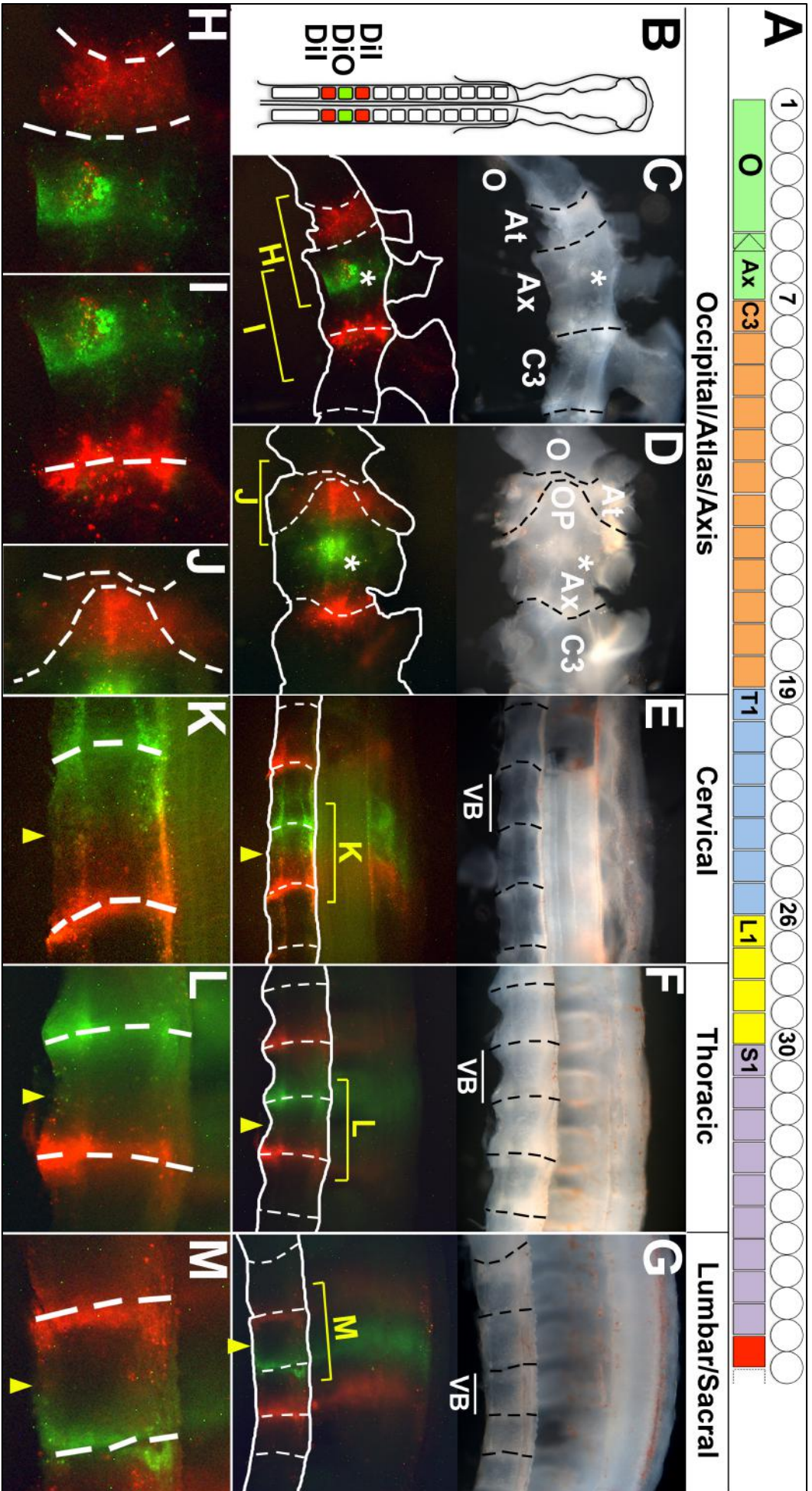


Figure 3.1. Tracing somite fate in the vertebral bodies. A. Diagram showing fate of each somite (circles) in the vertebrae (squares) used as a guide during labelling to ensure somites were labelled in all vertebral regions (adapted from Burke et al., 1995). Green=occipital, atlas and axis. Orange=cervical. Blue=thoracic. Yellow=lumbar. Purple=sacral. Red=caudal. **B.** Schematic showing the experimental design for tracing somites. The three caudal-most somite pairs (I, II and III) were labelled alternately with Dil and DiO. **C-M.** Somite fate in the vertebral bodies. Rostral to the left and dorsal to the top. C and E-G are sagittal sections through the vertebral column of 8-day-old embryos after labelling somites at two days with Dil and DiO. Bright field images (above) show the vertebral elements; Images in the red and green fluorescent channels (below) show labelled somite contributions to the vertebrae (Dil red, DiO green). The outline of the vertebral elements are shown on the fluorescent image. D is a dorsal view of the vertebral bodies in C. Yellow brackets show position of zoomed images in H-M. Yellow arrows indicate position of original somite boundary. (IVD=intervertebral disc O=occipital, At=atlas, Ax=axis, OP=odontoid process, C3=cervical vertebra 3, star= vestigial IVD, VB= vertebral body).

3.3.2. Somite contribution to the occipital region, atlas and axis

The morphology of the rostral-most vertebrae is distinctive. The atlas (C1) sits behind the occipital region of the skull, forming the atlanto-occipital joint, which allows flexion and extension of the head on the neck. The atlas has a ring-like morphology through which the odontoid process projects from the rostral face of the bulkier axis (C2) behind. Together, the atlas and axis form the atlanto-axial joint, which allows head rotation. As the projection of the odontoid process is not apparent in sagittal sections (Fig. 3.1C), the surrounding soft tissues were removed and the vertebrae were imaged from their dorsal side in this region (Fig. 3.1D), before sectioning sagittally.

The origin of the atlas and axis was studied by labelling somites five to seven in a red-green-red pattern from rostral to caudal with Dil and DiO. Cells from somite five (red) were found in the caudal occipital cartilage the entire atlas and the rostral tip of the odontoid process, which is fused to the axis (Fig. 3.1C, D, H). Cells from somite six (green) were found in the rostral portion of the axis body and the base of the odontoid process (Fig. 3.1C, D, H-J). Somite

seven (red) gives rise to the caudal portion of the axis body, the disc between the axis and C3, and the rostral portion of the C3 body (Fig. 3.1C, D, I). This apparent rearrangement of segments becomes clearer by considering the ventral (future vertebral bodies) and dorsal (future neural arches) aspects of the sclerotome individually (Fig. 3.3A). The body and arch that derive from the rostral half of somite five, fuse with the occipital region of the skull. The atlas is comprised of an arch derived from the caudal half of somite five, of which the corresponding body fuses to that of somite 6 to form the odontoid process, which in turn fuses to the axis body. The axis comprises of an arch and body derived from the caudal half of somite 6 and the rostral half of somite seven.

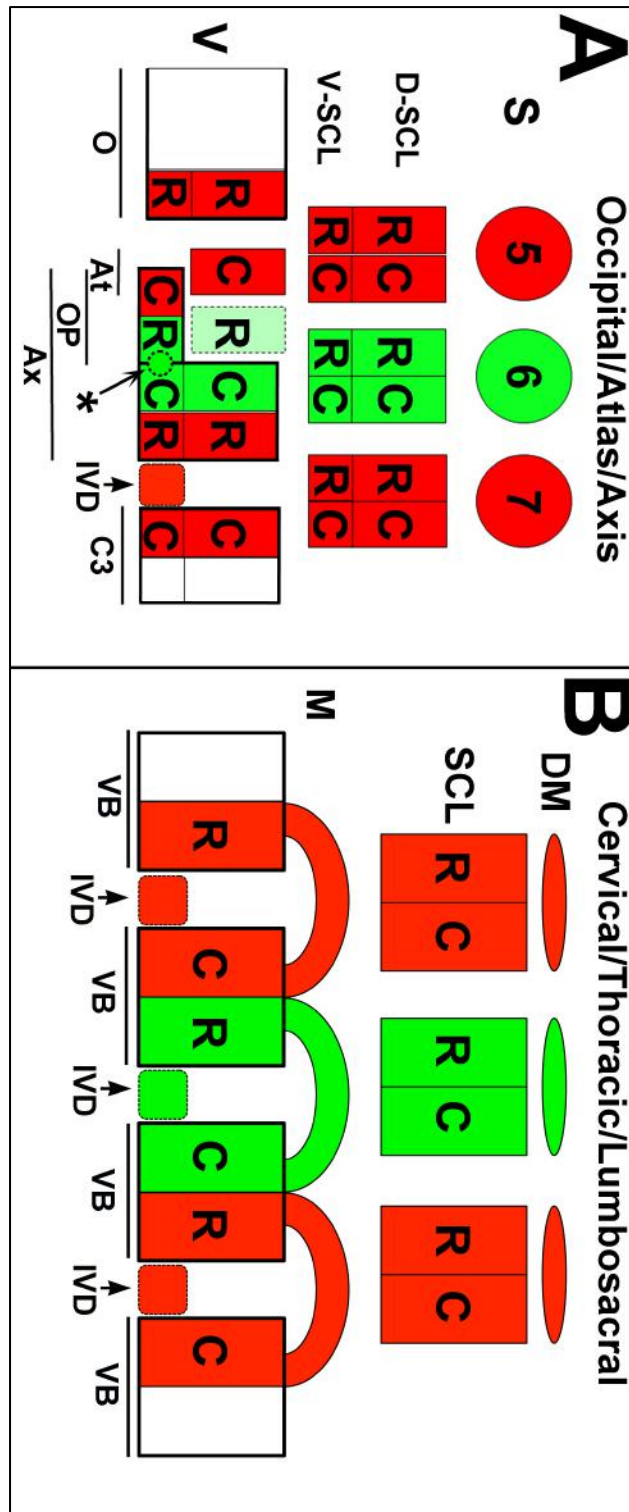


Figure 3.2. Summary of somite/vertebral body relationships along the body axis. **A.** Schematic summarising the contribution of somites 5-7 to the occipital-atlas-axis complex. (S=somites, D-SCL= dorsal sclerotome, V-SCL= ventral sclerotome, V= vertebrae, R=rostral sclerotome, C= caudal sclerotome, IVD=intervertebral disc O=occipital, At=atlas, Ax=axis, OP=odontoid process, C3= cervical vertebra 3, star= vestigial IVD) **B.** Schematic summarising the contribution of somites to the vertebral bodies in the cervical, thoracic and lumbosacral regions. (DM= dermomyotome, SCL=sclerotome, M= muscle, VB=vertebral body).

3.3.3. Somite contribution to the neural arches

To observe the contribution of Dil and DiO labelled somites to the neural arches, the same sectioning approach was used and the neural tube removed to reveal the inside face of the arch. At cervical (n=3), thoracic (n=4) and lumbar/sacral (n=4) levels, a single neural arch was comprised of cells from two successive somites (Fig. 3.3 A-F), with the red-green boundary located approximately in the centre of the arch (Fig. 3.3 A-F, yellow arrows). This confirms that the neural arches receive contributions from two successive somites as previously reported (Bagnall et al., 1988; Huang et al., 1996; Huang et al., 2000c). However, there is variation in the orientation of the boundary marking the contribution of the two adjacent somites. In the cervical and thoracic regions the boundary runs vertically from the centrum to the dorsal neural arch, as if cells from a single somite migrate to a similar level along the rostral-caudal (R-C) axis regardless of whether they give rise to ventral or dorsal structures (Fig. 3.3 A, B, D, E). However, in the lumbar/sacral region the red-green boundary tilts rostrally, suggesting that somite cells shift as they contribute to progressively more dorsal structures within the same segment (Fig. 3.3 C, F). This shows that the final R-C level at which cells are positioned at the midline varies between the dorsal and ventral sclerotome in a region-specific manner.

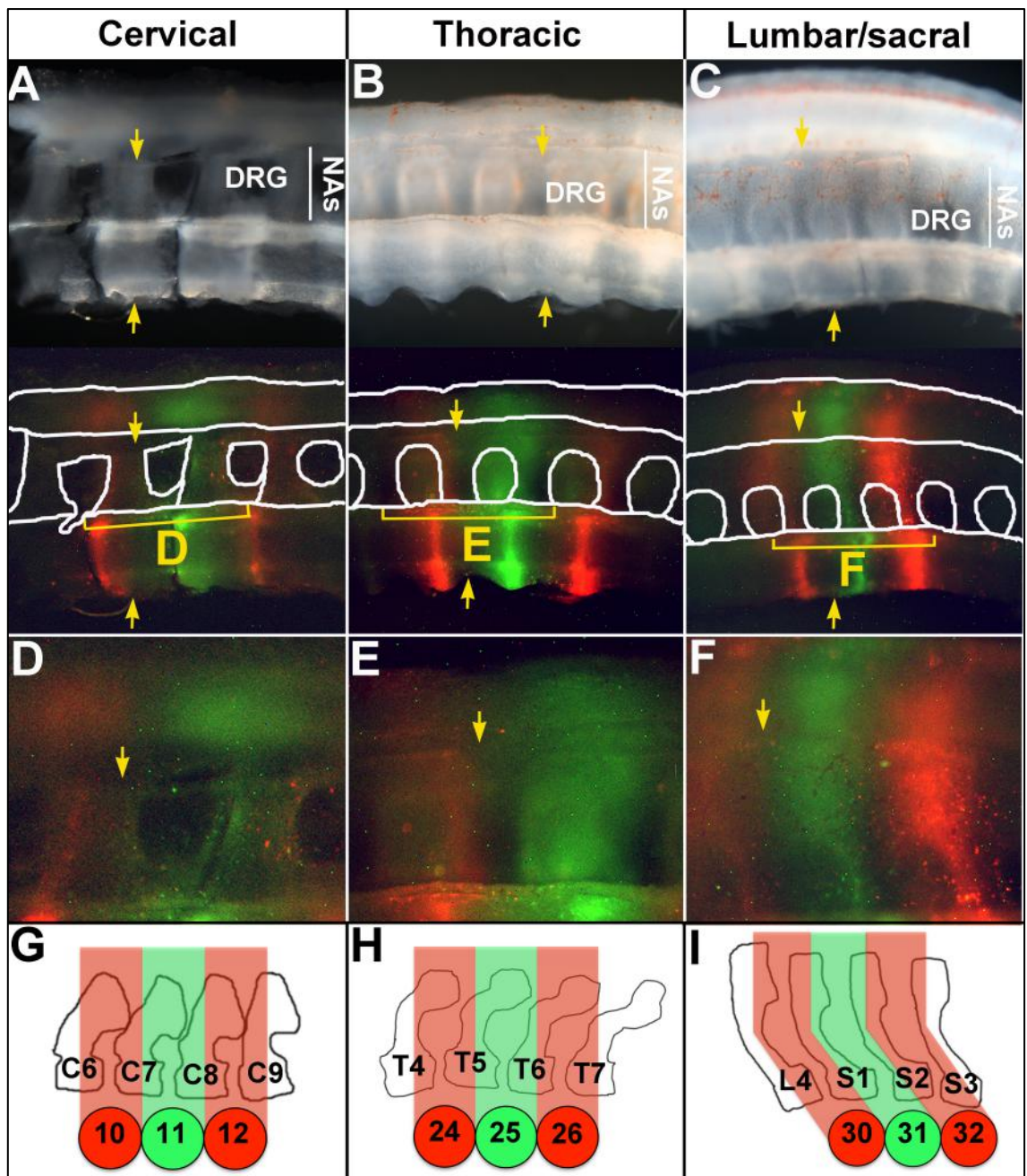


Figure 3.3. Tracing somite fate in the neural arches. A-F. Sagittal sections through the vertebral column of 8-day-old embryos after labelling somites with Dil and DiO at two days. Rostral to the left and dorsal to the top. Bright field images (above) show the vertebral elements; Images in the red and green fluorescent channels (below) show labelled somite contributions to the vertebrae (Dil red, DiO green). The outline of the vertebral elements are shown on the fluorescent image. D-F are zoomed images of regions indicated by yellow brackets in A-C (DRG=dorsal root ganglion, NT=neural tube; other labelling as in Fig. 3.1). **G-I.** Schematic showing the relationship between the inter-somitic boundary and the tilt of the NA in each region. Vertebral outlines drawn from a skeletal preparation of a HH32 embryo.

Skeletal preparations of eight-day old (HH30-32) embryos, illustrated by the outline of the cartilage corresponding to each labelled region, reveal that this variation in the “tilt” of the inter-somitic boundary is mirrored by a variation in the physical tilt of the neural arches (Fig. 3.3 G-I). Quantification of this tilt validates this observation (Fig. 3.4A). The angle of neural arch projection with respect to the horizontal axis of the body was measured across four consecutive vertebrae in each region, corresponding to the labelled vertebrae shown in figure 3.3 D-F. Across all vertebrae in each of the six embryos measured (a total of 24 vertebrae per region), neural arches in the cervical and thoracic region showed a mean angle of projection roughly perpendicular to the body (Cervical= $91 \pm 2^\circ$, Thoracic= $91 \pm 3^\circ$; Fig. 3.4B). In the lumbar/sacral region, neural arches had a more acute angle of projection, indicating that they are tilted rostrally (Lumbar/sacral = $72 \pm 6^\circ$; Fig. 3.4B). This correlation suggests a shift between dorsal and ventral elements of the sclerotome at the midline, which later goes on to influence the morphology of the vertebra it later forms.

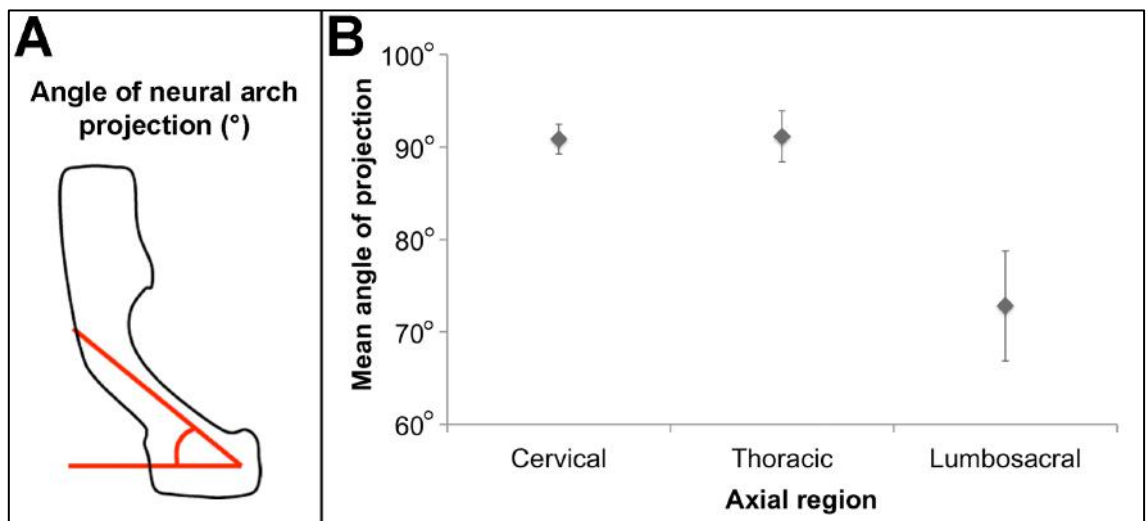


Figure 3.4. Measurements of the “tilt” of the neural arch. **A.** Schematic showing the measurement of the angle of neural arch projection. The angle at which the rostral face of the pedicle of the neural arch projects from the horizontal axis of the vertebral body was measured. **B.** Graph showing the mean angle \pm standard deviation of neural arch projection for each vertebral region. Measurements were taken from skeletal preparations of six embryos from HH30-32. In each region, the same four vertebrae were measured and the average angle calculated for all vertebrae measured across the six embryos (24 vertebrae/region). The graph shows the mean angle of NA projection for each region.

3.4. Discussion

3.4.1. A “resegmentation-shift” model for vertebral patterning

The results above demonstrate that the vertebral bodies and neural arches form by resegmentation of the sclerotome, in agreement with the resegmentation model proposed over 150 years ago (Remak, 1855). In addition, however, they reveal a “tilt” of the inter-somitic boundary that varies between axial regions, suggesting that sclerotome cells shift in a region-specific manner according to their dorso-ventral position within a segment. Based on these results, I propose a “resegmentation-shift” model, in which the final vertebral pattern is established by resegmentation of the sclerotome plus a shift that varies along the axis (Fig. 3.5). This new model reconciles Remak’s resegmentation model with the evidence from anatomical studies that appears to show a shift in sclerotome boundaries as they migrate (Fig. 1.1D-F; Hamilton, 1953). During resegmentation, a single somite gives rise to an intervertebral disc and half of the vertebral body and neural arch on either side. The results presented in this chapter show that there is little variation in this process along the vertebral column, indicating that the relative contribution of a somite to a vertebra is the same from segment to segment. This means that when the sclerotome shifts in the lumbosacral region, tilting the inter-somitic boundary, the cartilage from which it forms is also tilted resulting in variation in the projection of the neural arch between regions (Fig. 3.3I).

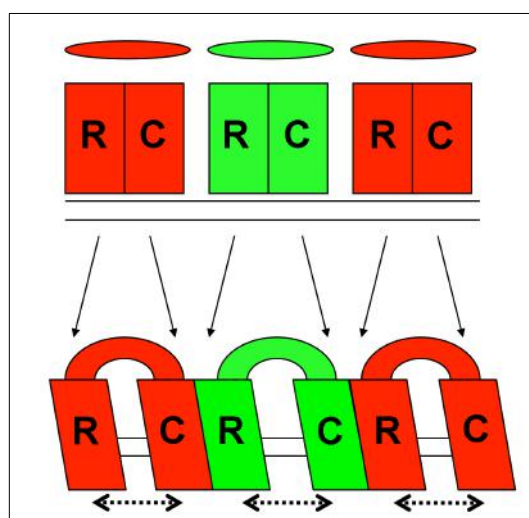


Figure 3.5. The “resegmentation-shift” model: Resegmentation of the sclerotome is accompanied by a shift between the dorsal and ventral sclerotome of variable extent along the axis (dashed arrows). Shapes and labels as in Fig. 3.1.

The classical description of resegmentation (Remak, 1855; Von Ebner, 1889) relies only upon intrinsic R-C patterning of each sclerotome half, from which the final segmentation pattern of the vertebral column is translated. However, in zebrafish (Van Eeden et al., 1996; Fleming et al., 2004) and mouse mutants (Takahashi et al., 2013) where R-C patterning of the somite has been abolished, vertebrae and intervertebral discs still retain a segmented pattern. This suggests that R-C patterning is dispensable for segmentation of the vertebral column and that some segmental information may exist external to the somites. The region-specific sclerotome shift outlined above points towards the same conclusion. Such a shift could be mediated by external signals, perhaps from the notochord or neural tube, which vary in a region-specific manner.

Vertebral morphology is highly regionalised along the vertebral column, with each vertebra possessing unique morphological characteristics according to its A-P position. This axial identity is regulated by the regionalised expression of *Hox* genes along the rostro-caudal axis of the body, which convey a 'positional address' to the sclerotome cells (Kessel and Gruss, 1991). The regional identity of the sclerotome is specified prior to somite formation (Kieny et al., 1972; Nowicki and Burke, 2000), or perhaps even earlier in the primitive streak (Iimura and Pourquie, 2006; Schroter and Oates, 2010; Dias et al., 2014). For example, cervical paraxial mesoderm will give rise to cervical vertebrae after it is transplanted to the thoracic region (Kieny et al., 1972). Regional identity, and the resulting morphology, is therefore an intrinsic property of the somite.

Our results indicate that the degree to which the dorsal and ventral sclerotome cells shift with respect to each other has a direct effect on vertebral morphology, namely in the tilt of the neural arch. If this shift is mediated by signals external to the somite (as predicted), this would suggest an aspect of vertebral morphology that is not regulated by information intrinsic to the somite. In the numerous studies describing homeotic transformations in vertebral morphology after either mis-expression of *Hox* genes (reviewed by Wellik, 2007; discussed in section 1.3.3), or heterotopic transplantation of paraxial mesoderm (Kieny et al., 1972), vertebral morphology is typically assigned to a regional identity by easily identifiable features such as the presence or absence of a rib (Wellik and Capecchi, 2012). It is possible that more subtle variations in morphology, such as the degree to which the neural

arch tilts, may have been missed in these experiments, masking elements of vertebral morphogenesis that may be controlled by signals external to the somite. Transplantation of lumbosacral somites to cervical regions and vice versa (between which the tilt of the neural arch varies the most; Fig. 3.4B), and analysis of the resulting neural arch tilt by skeletal preparation, would identify whether the projection of the neural arches is determined by information intrinsic or extrinsic to the somite.

3.4.2. Positioning of intervertebral discs

The results of somite tracing in the ventral vertebral column clearly show that the IVDs occupy a central position within a somitic segment. It would be logical, therefore, to assume a link between the formation of an IVD, and the boundary between rostral and caudal sclerotome halves, which also sits in the centre of the somite. However, previous studies have indicated that the two do not, in fact, coincide. The fate of individual half-sclerotomes has been investigated using quail-chick grafts (Goldstein and Kalcheim, 1992; Aoyama and Asamoto, 2000) and using a transgenic approach to label the caudal sclerotome in mice (Takahashi et al., 2013). These studies suggested that the somitic portion of the IVD is entirely derived from the caudal sclerotome. Furthermore, the finding that IVDs still form in a segmented pattern in the absence of R-C patterning (Goldstein and Kalcheim, 1992; van Eeden et al., 1996; Takahashi et al., 2013), as discussed in chapter one (section 1.2.1), suggests that R-C patterning is not required for IVD segmentation.

If not the R-C boundary within the somite, what does determine IVD position? By transgenic manipulation of the *Mesp2*/Ripply feedback loop, which maintains R-C patterning of the somite, Takahashi et al. (2013) generated mouse lines in which somites had either an entirely caudal or entirely rostral identity. Goldstein and Kalcheim (1992) fundamentally achieved the same result, by replacing somites with multiple sclerotome halves of the same identity. Both found that IVDs only formed in embryos containing sclerotome of a caudal identity. This suggests that although R-C boundaries are not required for IVD formation, caudal identity is. This led the authors of the former study to propose a mechanism for IVD patterning in which the opposing molecular properties of the two sclerotome halves stimulate IVD differentiation in the caudal half and suppress it in the rostral half (Takahashi et al., 2013).

However, a second mechanism has been proposed in which IVD could be segmentally patterned in the absence of any R-C patterning at all: If somitocoelomic cells are fated to become intervertebral disc (as their transplantation has suggested), their central position in the somite would naturally place the disc between the two halves later in development (Huang et al., 1996).

Alternatively, it is also possible that the chick notochord may have some degree of intrinsic segmental information which influences where vertebral elements are positioned (Stern, 1990), as has been suggested to be the case in teleost fish (Fleming et al., 2001; 2004; Grotmol et al., 2003; 2005). This, again, suggests a role for signals external to the somite in segmental patterning of the vertebral column in amniotes. The role of the amniote notochord in vertebral column segmentation is the subject of chapter four to six of this thesis.

3.4.3. The fate of the somites in the occipital region, atlas and axis

The occipital region, atlas and axis have distinct morphologies compared to more posterior vertebrae. The results of somite tracing in the occipital region and anterior cervical vertebrae are in agreement with the predicted homology of the elements based on anatomical studies (de Beer, 1937). The normal process of resegmentation still occurs in this region. However, the elements undergo a number of fusions, which gives them their distinct characteristics. These rearrangements are summarised in Fig. 3.2A. The atlas is formed from the caudal 'arch' element of somite five. The odontoid process is formed from the missing atlas 'body' (derived from the caudal half of somite five and the rostral half of somite six), which fuses to the anterior face of the axis. The axis itself is formed from the body and arch of the caudal half of somite six, and the rostral half of somite seven. From this point caudally, the contribution of a single somite to an IVD and half a vertebra either side begins.

The above results are also in agreement with those of lineage analysis by quail-chick somite grafts (Huang et al., 2000c), except that no evidence was found for a contribution of somite six to the posterior arch of the atlas, which would be expected according to the normal process of resegmentation (Fig 3.2A; light green rectangle with dashed border). This raises a question as to

the fate of this element. It is possible that the labelling and sectioning method was not sensitive enough to detect DiO-labelled cells from somite six in the atlas arch, as DiO signal was typically weaker than Dil after long incubation periods. Repeating the labelling experiment in somites five to seven, using the inverse colours (i.e. green-red-green) so that somite six was labelled with Dil, may show whether this somite contributes to the atlas as previously reported (Huang et al., 2000c).

Strong DiO fluorescence similar to that seen in the IVDs was present in a small area at the posterior edge of the odontoid process (Fig. 3.1C, D; white star). As this sits at the boundary between the rostral and caudal halves of somite six, it probably represents a vestigial disc, the development of which is suppressed by fusion of the odontoid process to the axis (Fig. 3.2A, dashed circle indicated by star). The fusions of vertebral elements that give rise to the distinctive morphology of the posterior occipital region, atlas and axis are regulated by anterior *Hox* gene expression (Kessel et al., 1990; Kessel and Gruss, 1991). In mouse, gain of function of *HoxA7* in the more anterior somites gives rise to homeotic transformations of the atlas and axis to morphologies reminiscent of more posterior cervical vertebrae (Kessel et al., 1990). Among other changes, the odontoid process (often referred to as the 'dens' in mammals) fails to fuse to the anterior face of the axis, and instead forms an atlas vertebral body. In the absence of this fusion, an intervertebral disc develops between the atlas and axis bodies. This supports the conclusion that that the bright DiO signal observed represents a vestigial disc at the base of the chick odontoid process.

3.5. Summary

The tracing of endogenous somites using Dil and DiO in this chapter shows definitively that the midline cartilages of the vertebra (the vertebral bodies and neural arches) form by resegmentation of the sclerotome. Furthermore, I have shown that the contribution of a single somite to its respective vertebrae is conserved between different regions of the vertebral column. However, these results also show that the resegmentation process is accompanied by a "shift" between dorsal and ventral elements of the same somite that varies along the vertebral column. Based on these findings, an alternative model for segmented vertebral patterning was proposed known as the "resegmentation-shift model".

An important implication of this model is that this shift could be regulated by signals external to the somite, which influence the final position of sclerotome cells at the midline.

Chapter 4 : Signals from the notochord are involved in vertebral patterning

4.1. Introduction

The vertebrae form a segmented pattern along the A-P axis. Although each vertebral unit shares a number of characteristics, their morphology is variable both between species and along the vertebral column within the same individual. It is well established that this morphology is regulated by the regionalised expression of *Hox* genes in the paraxial mesoderm, which confer a positional identity to somites along the A-P axis (see section 1.3.3). *Hox* gene expression is determined within cells of the PSM prior to somite formation (Nowicki and Burke, 2000), or even earlier whilst cells are still in the streak (Dias et al., 2014). The morphology of the vertebrae that somites will go on to form is therefore determined prior to somite formation (Kieny et al., 1972). As a result, vertebral morphology is thought to be an intrinsic property of the sclerotome.

In the study of vertebral morphology, one aspect that is often overlooked is the length of each vertebral body. Vertebral length varies considerably between species, and along the axis, and it is this property that gives the vertebral column its characteristic spatial periodicity. How is this pattern determined? In Chapter three, somite tracing showed definitively that in chick, the vertebral bodies and neural arches form by resegmentation of the sclerotome (Remak, 1855). Resegmentation establishes the arrangement of vertebral precursors along the axis, laying down the spatially periodic pattern of sclerotome cells from which the vertebrae develop. The resegmentation process, according to classical descriptions, is dependent upon R-C patterning of the somite (Remak, 1855; Von Ebner, 1889), which is determined prior to somite formation in the PSM by the oscillating expression of clock genes in the PSM (Takahashi et al., 2003). As the 'segmentation clock' has been shown to be an autonomous property of the PSM (Palmeirim et al., 1997), it is generally accepted that the spatial periodicity of the vertebral column (like vertebral morphology) is determined by information intrinsic to the somite. However, there are a number

of pieces of evidence that suggest a role for external signals in determining the length of each vertebra.

First, if segmentation of the vertebral column is translated from that of the somites, it follows that larger somites would give rise to larger vertebrae. However this is not always the case, at least in the case of vertebral length in the chicken (E. Ward et al., unpublished observation). Second, segmentation is partially maintained in the vertebral column of mutant animals where R-C patterning of the somites has been abolished (Zebrafish: Van Eeden et al., 1996; Mouse: Takahashi et al., 2013). This suggests that rostro-caudal patterning, and therefore resegmentation, is dispensable for formation of the vertebrae in a segmented pattern. Finally, results in the previous chapter revealed that resegmentation is accompanied by a region-specific shift of sclerotome cells along the A-P axis of the vertebral column. It was suggested that this shift is regulated by signals external to the somite, guiding cells to different positions at the midline. These arguments challenge the idea that all segmented information is intrinsic to the somite.

If external signals are involved in vertebral patterning, where do they come from? Two obvious candidates are the notochord and the neural tube, as these are the structures around which the sclerotome migrates to form the vertebral bodies, IVDs and neural arches. Signals from both these structures play an earlier role in somite patterning (see section 1.4). Furthermore, ablation studies have suggested that both the notochord and neural tube are required for normal formation of the vertebral column in chick (Watterson et al., 1954; Strudel, 1955).

The notochord precedes the vertebral column both developmentally and evolutionarily. It is a defining characteristic of the chordates and has been suggested to be the “archetypal segmented structure” (Stern, 1990), which in the vertebrates has gradually become dominated by the increasing size of the sclerotome and the intrinsic metamerism it brings with it to the vertebral column (Stern, 1990; Fleming et al., 2015). In contrast to birds and mammals, it has been shown that in teleost fish, the notochord contributes directly to the vertebral bodies by secreting a bony matrix (Grotmol et al., 2003; Fleming et al., 2004; Wang et al., 2013). It has also been shown that a segmental pattern within the teleost notochord may underlie the spatial periodicity of the vertebral

bodies (Fleming et al., 2004; Grotmol et al., 2005). The notochord in this group has therefore retained an important role in formation and patterning of the vertebral column.

Has a role for the notochord in segmental patterning of the vertebral column been conserved in the amniotes? In this chapter, I investigate the role of the notochord in determining the spatial periodicity of vertebral column in chick. I go on to conduct a preliminary study into the role of the neural tube in the same process.

4.2. Materials and Methods

4.2.1. Notochord ablation

The notochord ablation procedure is illustrated in Fig. 4.1A. Embryos at HH11-12 were prepared *in ovo* (section 2.1.4). Tyrode's saline was removed from the raised embryo and replaced with a standing drop of 0.12% trypsin (Sigma) diluted in $\text{Ca}^{2+}/\text{Mg}^{2+}$ -free Tyrode's saline. The vitelline membrane was peeled away dorsal to the caudal-most somites and rostral PSM. Two cuts were then made in the ectoderm from rostral to caudal on either side of the neural tube using a 25 gauge syringe needle. Using the convex side of the needle, the neural tube was moved gently from left to right, allowing trypsin to enter the space around the neural tube and notochord, until the neural tube could be freed from the notochord in a region around six somites in length along the A-P axis. The underlying notochord was then moved from left to right in the same way until it lifted free from the endoderm beneath, taking care to ensure that the endoderm remained intact. The free portion of notochord was cut at each end using the syringe needle and removed from the embryo using a pipette. The trypsin solution was then removed and replaced with a standing drop of Tyrode's saline and the neural tube replaced into its original position at the midline. The embryo was lowered and sealed as previously described (section 1.2.4) and incubated for a further six days to HH32-33 before fixing for skeletal preparation. Embryos were scanned by optical projection tomography (OPT) to visualise the three-dimensional morphology of the skeleton.

Sham notochord ablation experiments were also carried out. In these experiments, the same procedure as above was followed. However, the notochord was not excised after it was detached from the underlying endoderm.

4.2.2. Notochord graft

The notochord graft procedure is illustrated in Figure 4.2A. Quail donor and host chick embryos were incubated to HH10-11 and host chick embryos prepared *in ovo* (section 2.4.1). A small hole was made in the vitelline membrane adjacent to the PSM, and a slit made from rostral to caudal, adjacent and parallel to the paraxial mesoderm at the level of the caudal-most somites and rostral PSM. Donor quail embryos were collected in Tyrode's saline as described in section 2.1.2, and pinned flat on a Petri dish with a silicone (Sylgard, Dow Corning) coated base, with their ventral surface facing up. The embryo was submerged in 0.12% trypsin solution (prepared as above; section 4.2.1), and a piece of notochord five to six somites in length, spanning the caudal-most somites and rostral PSM was gently eased from the neural tube below using a fine tungsten needle attached to a glass Pasteur pipette. The loose portion of notochord was then cut at each end using the syringe needle. The notochord graft was transferred to the host embryo in a 1:3 mix of albumen and Tyrode's saline using a pipette, the albumen/saline mixture being essential to avoid the graft sticking to the inside of the pipette tip. The notochord was inserted into the slit made in the host and the vitelline membrane was replaced over the grafted region. Embryos were harvested at either three (HH24-25: for whole mount in-situ hybridisation) or six to seven days after grafting (HH32-35: for skeletal preparation).

Sham notochord graft experiments were also carried out, in which the host was prepared as above, a slit made lateral to the somites, but no notochord inserted. Like notochord grafts, these embryos were harvested at either three or six days after the operation was carried out.

4.2.3. Notochord and somite graft

The same procedure was carried out as in the notochord graft experiment described above (section 4.2.2), but in addition to the notochord, one of the most newly-formed quail somites was removed from the donor quail embryo

and transplanted lateral to the grafted notochord in the medial lateral plate mesoderm. This procedure is illustrated in Figure 4.4F.

4.2.4. Notochord grafts between different axial regions

The same procedure was carried out as in the notochord graft experiment described above (section 4.2.2), but the axial region from which the notochord was taken and the position into which it was grafted varied. Embryos at HH10-11 (10-13 somites) were used for grafts to and from the cervical region, whereas embryos at HH13-14 (19-21 somites) were used for grafts to and from the brachial region. The notochord graft experiments to and from different axial levels are illustrated in Fig. 4.7 A-D (Graft1: cervical to cervical; Fig. 4.7A. Graft2: Brachial-cervical; Fig. 4.7B. Graft 3: Cervical-brachial; Fig. 4.7C. Graft 4: Brachial-brachial; Fig.4.7D).

4.2.5. Notochord and neural tube graft

The notochord and neural tube graft was carried out using the same procedure described for grafts of the notochord alone (section 4.2.2). Here, the neural tube was grafted along with the notochord ensuring the tissues remained attached to each other throughout the procedure. Grafted embryos were incubated to HH33 and analysed by skeletal preparation as previously described. The procedure is shown in Figure 4.8A.

4.2.6. Quantification of segment length

The A-P length of endogenous and ectopic segments was measured from images of embryos stained for *Uncx4.1* or *Scleraxis*, three days after a notochord graft. Both markers are expressed in stripes. *Uncx4.1* is a marker of the caudal sclerotome, therefore the caudal limit of each *Uncx4.1* stripe marks the boundary between two sclerotome segments. *Scleraxis* marks a population of tendon progenitors that occupies the anterior and posterior-most edge of the dorsal sclerotome, therefore the caudal-most limit of each stripe marks the same point in each sclerotome segment. The length of each segment was therefore measured as the space between the caudal boundary of each stripe.

Expression of each marker in the endogenous somites extends from the dorsal to the ventral sclerotome (Fig. 4.3B, G). It was therefore important to define the D-V level at which the segment length measurements were taken. Given that ectopic segments form adjacent to an ectopic notochord, it was reasoned that the equivalent point in the endogenous sclerotome was at the level of the endogenous notochord. The endogenous notochord can be identified as a white stripe that runs from anterior to posterior, transecting the stripes of staining, along the dorsal side of the embryo (Fig. 4.3B, G; ENC=endogenous notochord). Endogenous segment length was therefore measured at this level.

Embryos were imaged in whole mount, maintaining the same resolution across all images. The space between consecutive ectopic segments was measured (in pixels) along with that of the endogenous segments immediately adjacent using Fiji (Schindelin et al., 2012). Ectopic and endogenous segment length was then compared using a paired-sample student T-test in IBM® SPSS® Statistics. To visualise this comparison in graph form, ectopic segment length was expressed as a percentage of endogenous segment length. The mean and standard deviation percentage length was then averaged across all embryos. The results are displayed as bar charts in Fig. 4.3 and 4.7.

4.3. Results

4.3.1. The periodic pattern of vertebral bodies is lost when the notochord is ablated

Previous ablation studies have suggested that the notochord is required for segmentation of the ventral vertebral column in chick (Watterson et al., 1954; Strudel, 1955). The ablation was carried out in these studies by removing both the notochord and neural tube and replacing the neural tube back to its original position. This successfully removed the notochord, but it is unclear how disruption to the neural tube as a result of the procedure may have also influenced the results. I therefore repeated the ablation experiment by removing the notochord from beneath the neural tube *in ovo*, reducing disruption to the neural tube. A portion of the notochord four to six somites in length was removed surgically from the posterior cervical/anterior thoracic region of a chick embryo (Fig. 4.1A). At HH32-33 (six days after grafting),

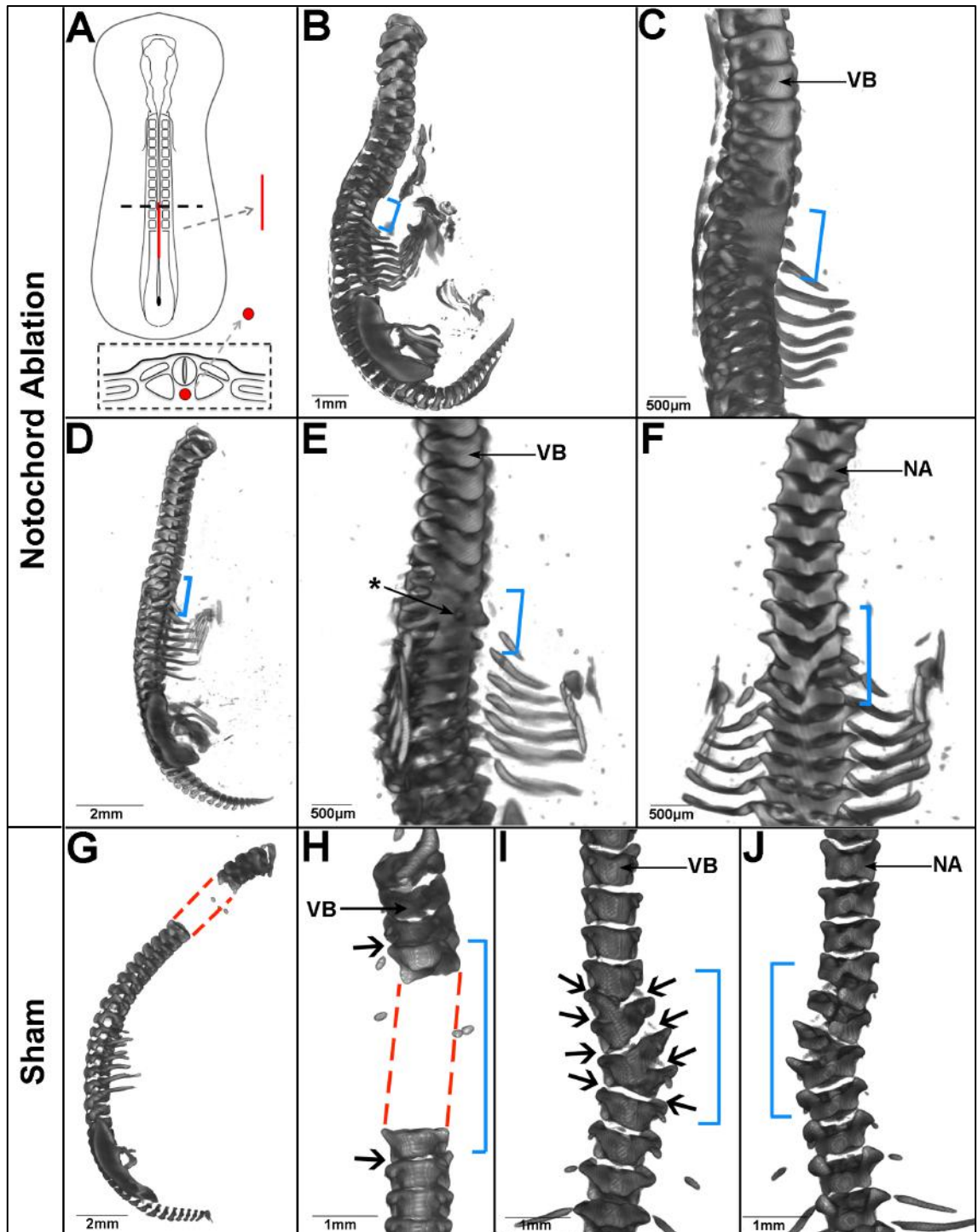
skeletal preparations were made of the ablated embryos and the stained skeleton was scanned using OPT to visualise its three-dimensional morphology. In 7/7 embryos, there was a fusion of the vertebral bodies in the region where the notochord had been removed (Fig. 4.1 B-F). Normal segmentation of the vertebral bodies was seen in the regions rostral and caudal to the ablated region. Segmentation of the neural arches in the ablated region was maintained in all embryos, with 3/7 embryos showing normal neural arch morphology throughout the vertebral column (Fig. 4.1B). The remaining 4/7 embryos showed some degree of disruption to neural arch morphology including fusions and/or absence of cartilage (Fig. 4.1 D, F). When the operation was carried out in the thoracic region, no change was seen in the periodicity or morphology of the ribs.

As a control, 'Sham' notochord ablation experiments were carried out in which a section of neural tube was lifted free from the notochord, the notochord beneath lifted free from the underlying endoderm, but not ablated. At this point, both the notochord and neural tube were tucked back into the space at the midline. After skeletal prep and analysis by OPT of embryos six days after grafting (HH32-33), 3/3 embryos showed no fusion of the vertebral bodies, with clear spaces in alcian blue staining in the operated region indicating the location of the intervertebral disks. In 1/3 of these embryos, vertebral morphology was completely normal (Fig. 4.1G-H; Unfortunately, the embryo shown here broke in the operated region prior to OPT scanning. This break is indicated in the panels with a red dotted line). However, in 2/3 of these embryos, neural arch morphology was abnormal (Fig. 4.1J), suggesting that the fusions and absences of neural arches in experimental embryos was the result of disruption to the neural tube, not due to the notochord ablation itself. In addition, in the embryos that showed disrupted neural arches, the vertebral bodies showed a misalignment between the right and left halves at the midline (4.1I). However, although misaligned, there were clear spaces in alcian blue staining, representing the position of intervertebral discs (4.1I). The reason for this misalignment is not clear, however it is not surprising that a certain amount of disruption to vertebral body morphology should occur due to the invasive nature of the operation. One important observation is that when the notochord is replaced to its position at the midline after being lifted from the endoderm, it was often no longer parallel to the axial midline. This may result in a shift of the sclerotome on either side as it migrates to the midline, causing a

misalignment of the vertebrae on either side. The misalignment effect seen in these sham ablation experiments requires further investigation. Nevertheless, the presence of segmentation in the vertebral bodies after the sham ablation suggests that the fusion of the ventral cartilage in experimental embryos was due to the absence of the notochord. These results support the hypothesis that the notochord is required for normal segmentation of the vertebral bodies, as also found by Watterson (1954) and Strudel (1955).

Figure 4.1. Notochord ablation leads to a loss of segmentation in the vertebral bodies.

A. Schematic showing the notochord ablation procedure. (Above = dorsal view, below = transverse section; ablated notochord shown in red). **B-F.** OPT reconstruction of two HH30-32 embryos, six days after notochord ablation and skeletal preparation. (Blue brackets = ablated region). **B.** First example, whole embryo (head removed). **C.** First example, ventro-lateral view of vertebral bodies of embryo in **B.** Zoomed on ablated region. **D.** Second example, whole embryo (head removed). **E.** Second example, ventro-lateral view of vertebral bodies of embryo in **D.** Zoomed on ablated region. (Star = hole/foramen). **F.** Second example, dorsal view of neural arches of embryo in **D.** Neural arches show abnormal morphology and disrupted segmented pattern. **G-J.** OPT reconstruction of HH30-32 embryo skeletal preparations, six days after a sham notochord ablation (blue brackets = operated region; black arrows = position of intervertebral disks). **G.** First example, whole embryo (head removed). Red dashed lines indicate point where skeleton was accidentally broken before OPT-scanning. **H.** First example, ventral view zoomed on operated region of embryo in **G.** Vertebral morphology is normal, with no fusion of the vertebral bodies. **I.** Second example of skeletal preparation of embryo, six days after a sham notochord graft. Ventral view, zoom on operated region. Vertebral bodies do not fuse, but intervertebral disks are misaligned on either side of the midline. **J.** Dorsal view of embryo in **I.**, showing misalignment of neural arches in the operated region. (NA = neural arch, VB = vertebral body).



4.3.2. Notochord grafts result in ectopic sclerotome lateral to the host somites

The next step was to test whether the notochord can influence the segmental patterning of the sclerotome during vertebral column development. An ectopic notochord was grafted from the posterior cervical region of a two-day old quail embryo (HH10-11) into a position lateral to the lower cervical somites in a chick host of the same stage (Fig. 4.2A). At HH24-25 (three days after

grafting), in situ hybridisation for the sclerotome marker *Pax1* showed that ectopic sclerotome was present in the grafted region just rostral to the forelimb (9/13 embryos) (Fig. 4.2 B, C; Black arrows). The ectopic *Pax1* expression had a segmented pattern with a more compressed spatial periodicity compared to the endogenous pattern of the sclerotome (Fig. 4.2 B, C). In all except one embryo, there was no apparent change to either the size or periodicity of the endogenous *Pax1* expression on the graft side (Fig. 4.2 B, C) or the contralateral side of the embryos (Fig. 4.2D).

As a control, 'Sham' notochord grafts were carried out in which a slit was made adjacent to the somites of the chick host, but no notochord inserted. In 4/4 embryos, in-situ hybridisation at HH24-25 showed normal *Pax1* expression on both sides of the embryo, with no ectopic expression in the operated region (Fig. 4.2. E-G). This confirms that the presence of ectopic sclerotome in experimental embryos was due to the presence of the ectopic notochord.

To assess whether the influence of the notochord is restricted to the sclerotome, the notochord graft experiment was repeated and HH24-25 embryos were stained for *Pax3*, a marker of the dermomyotome. In 4/4 embryos, *Pax3* staining showed no ectopic expression in the grafted region (Fig. 4.2 H, I). This shows that a notochord graft results in ectopic sclerotome with no ectopic dermomyotome. *Pax3* was seen in strong, dorsal stripes, with the degree of expression in more ventral regions varying between embryos. In 2/4 embryos, no change to endogenous *Pax3* expression was seen in the grafted embryos. However, in the remaining two embryos, the ventral extent of *Pax3* expression seemed to be reduced compared to ungrafted regions, giving the appearance of a "clearing" of expression in the region of the notochord graft (Fig. 4.2 H, I; Black bracket). This effect was seen only in the grafted region, with no change to endogenous *Pax3* expression seen on the contralateral side (Fig. 4.2J).

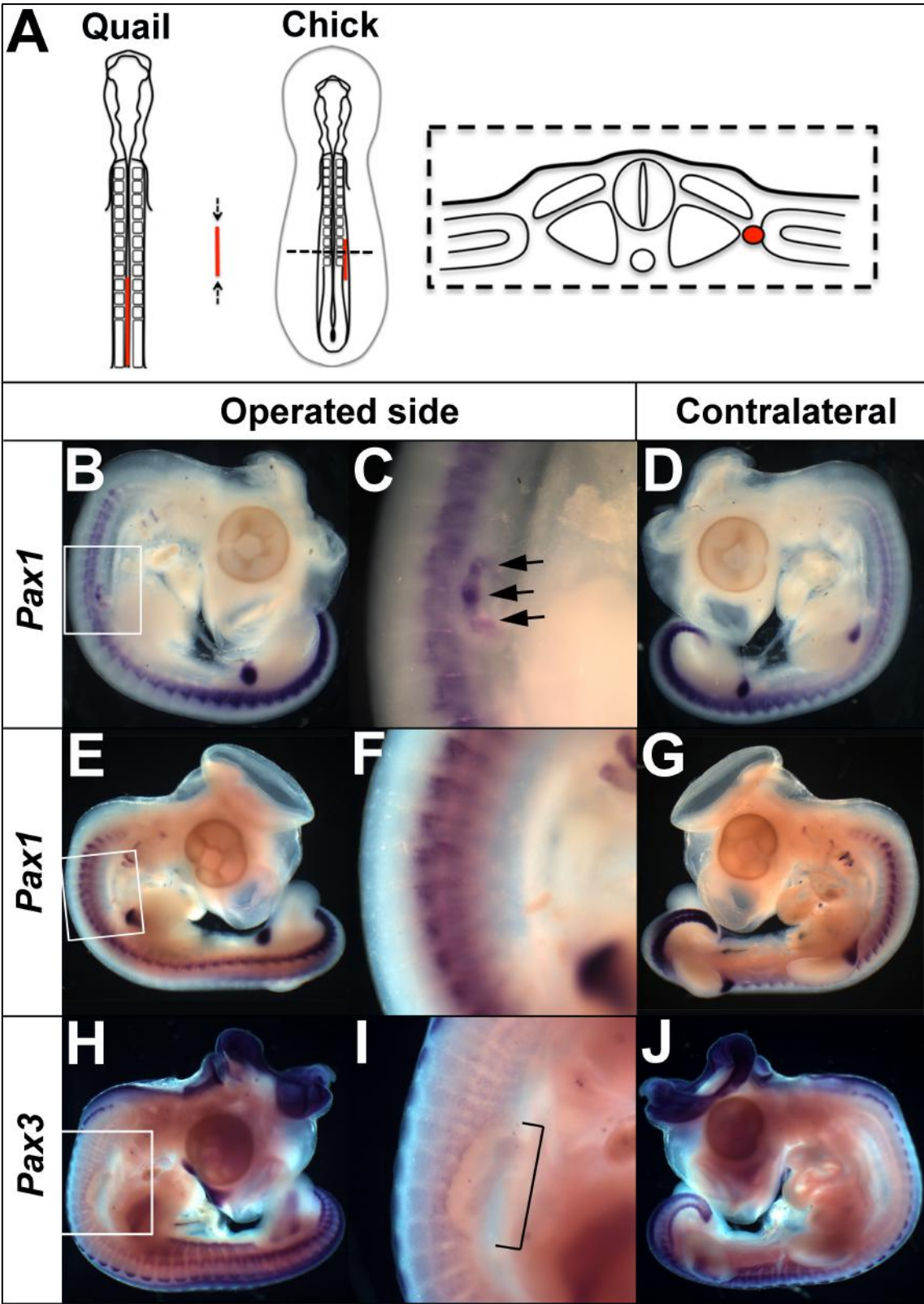


Figure 4.2. An ectopic notochord graft leads to the formation of ectopic sclerotome lateral to the endogenous somites **A.** Schematic showing the notochord graft procedure. (Left = quail donor, centre = chick host, right = transverse section; notochord graft shown in red). **B-D.** *Pax1* expression (a marker of the sclerotome) in a HH25 embryo, three days after the notochord graft. B,C. Ectopic *Pax1* expression is seen in the grafted region anterior to the forelimb (black arrows). D. No ectopic *Pax1* expression is seen on the contralateral side of the embryo. **E-G.** *Pax1* expression in a HH25 embryo, three days after a 'sham' notochord graft. No ectopic expression is seen in the operated region (E-F) or on the contralateral side of the embryo (G). **H-J.** *Pax3* expression (a marker of the dermamyotome) in a HH25 embryo, three days after a notochord graft. H, I. *Pax3* expression appears to be 'cleared' in the ventral somites, in the region of the notochord graft (black bracket). J. No apparent clearing of expression is seen on the contralateral side of the embryo. (Left=graft side, whole embryo. Centre=graft side, higher magnification of boxed portion in whole embryo. Right = contralateral, ungrafted side)

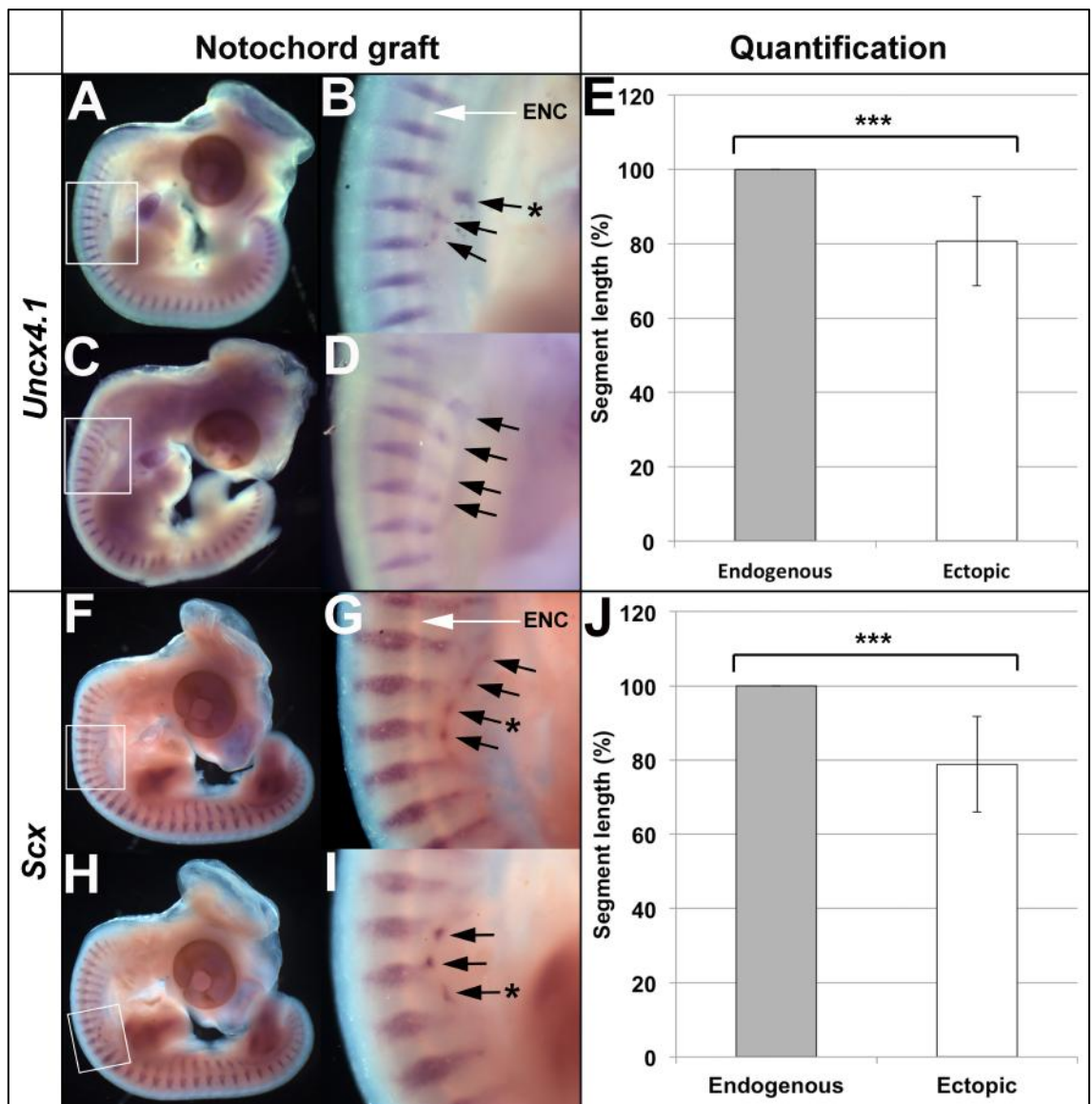
4.3.3. A notochord graft results in ectopic sclerotome in a different periodicity to that of the host sclerotome

To more clearly visualise the segmentation of the ectopic sclerotome, the same notochord graft procedure was carried out (Fig. 4.2A), and embryos analysed at HH24-25 by in situ hybridisation for *Uncx4.1*, a marker of the caudal sclerotome (Mansouri et al., 1997; Neidhardt et al., 1997). Ectopic *Uncx4.1* expression was seen in the grafted region (6/7 embryos) and clearly showed a more compact segmental pattern compared to that of the endogenous sclerotome (5/6 embryos) (Fig. 4.3 A-D; black arrows). In addition, a number of *Uncx4.1* stripes were found to occupy a position that was distinctly out-of-phase with the endogenous segmentation pattern (Fig. 4.3B; black star). Again, there was no visible change to endogenous *Uncx4.1* expression (Fig. 4.3 A-D).

The observed difference in periodicity was verified by quantification of segment length (i.e. the space between successive *Uncx4.1* stripes from anterior to posterior) in the ectopic sclerotome and the endogenous sclerotome immediately adjacent to it. The procedure for measuring segment length is described in section 4.2.6. On average, ectopic segments were 19% (S.D.=12%) shorter than that of the adjacent endogenous sclerotome (Fig. 4.3E). A pairwise student T-test, comparing ectopic and endogenous segment

length across all samples (14 pairs of segments in total), showed this difference to be statistically significant ($t(13) = 6.21$, $p = 0.000$).

Figure 4.3. A notochord graft leads to the formation of ectopic sclerotome with a different segmental periodicity to host sclerotome. A-D. Expression of *Uncx4.1* (a marker of the caudal sclerotome) in HH24-25 embryos three days after a notochord graft. Ectopic *Uncx4.1* expression is seen in the region of the notochord graft. A-B. Example one. C-D. Example two. **E.** Comparison of segment length (as indicated by *Uncx4.1*) between the endogenous and ectopic sclerotome. The mean segment length of the ectopic sclerotome is expressed as a percentage of the mean segment length of the adjacent endogenous somites. Ectopic segments are an average of 19% smaller compared to the adjacent endogenous segments. A pairwise student T-test shows this difference is statistically significant ($p < 0.005$, $n = 14$). **F-I.** Expression of *Scleraxis* (a marker of a sclerotomal tendon progenitors) in HH24-25 embryos three days after a notochord graft. Ectopic *Scleraxis* expression is seen in the region of the notochord graft. F-G. Example one. H-I. Example two. **J.** Comparison of segment length (as indicated by *Scleraxis*) between the endogenous and ectopic sclerotome. The mean segment length of the ectopic sclerotome is expressed as a percentage of the mean segment length of the adjacent endogenous somites. Ectopic segments are an average of 21% smaller compared to the adjacent endogenous segment. (Black arrows = segments of ectopic expression, Black star = segments of expression that are significantly out of phase the endogenous expression pattern, ENC = endogenous notochord visible as white stripe extending from A-P along the axis)



Segmentation of the ectopic sclerotome after a notochord graft was also assessed by in-situ for *Scleraxis*, which marks a sub-compartment of tendon progenitors within the sclerotome defined as the ‘syndetome’ (Brent et al., 2003). At HH24-25, ectopic *Scleraxis* expression was seen in the region of the notochord graft in 4/4 embryos (Fig. 4.3 F-I; Black arrows). Similar to *Uncx4.1*, the segmented pattern of *Scleraxis* expression appeared to be in a more compact spatial periodicity compared to the endogenous tendon progenitor populations. The endogenous expression of *Scleraxis* was unchanged (Fig. 4.3F-G), with the exception of a slight decrease in the ventral extent of expression in the grafted region (Fig. 4.3G, I). The observed difference in spatial periodicity between the endogenous and ectopic syndetome was verified by quantification of segment length, in the same way as was carried out for *Uncx4.1*-stained embryos. On average, ectopic segments were 21%

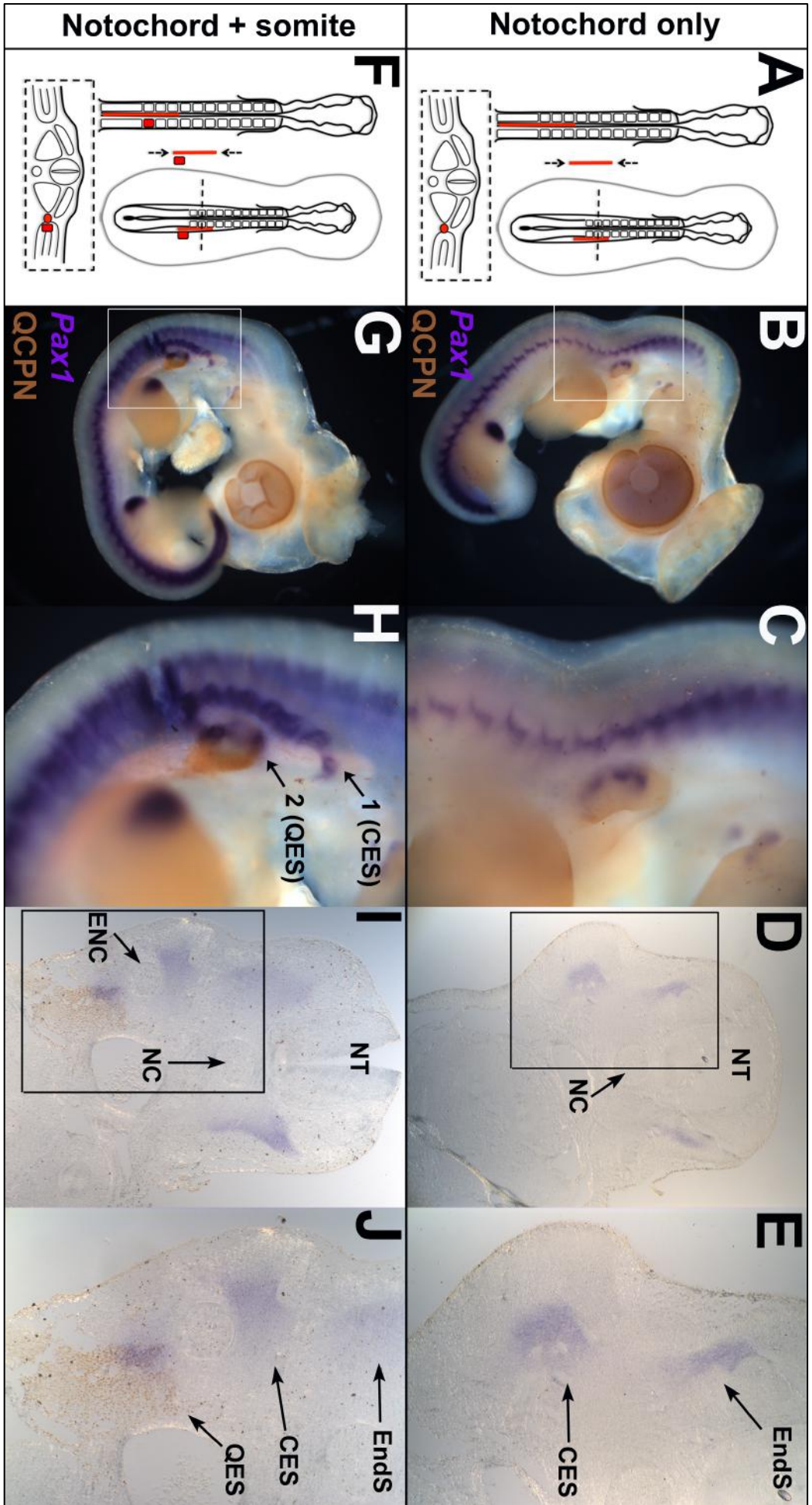
(S.D=13%) shorter than that of the adjacent endogenous sclerotome (Fig. 4.3J). A pairwise student T-test, comparing ectopic vs. endogenous segment length across all samples (11 pairs of segments in total), showed this difference to be statistically significant ($t(10)=5.53$, $p=0.000$).

4.3.4. Ectopic sclerotome is derived from the host

The difference in the segmentation of the ectopic and endogenous sclerotome suggests that the grafted notochord may attract host sclerotome towards it and somehow alter its spatial periodicity. However, it is possible that the *Pax1*-positive cells seen in the grafted region are not derived from the host, but from quail sclerotome cells that were transferred accidentally with the donor notochord during grafting. If this were the case, the change seen in sclerotome segmentation might not be due to signals from the notochord graft, but a result of intrinsic segmental information within contaminating quail sclerotome cells. To rule out this possibility, the origin of the ectopic sclerotome was traced in quail/chick chimaeras.

The QCPN antibody recognises a quail-specific perinuclear protein and is commonly used in analysis of quail-chick grafting experiments to identify graft from host cells (Selleck and Bronner-fraser, 1995). A QCPN immuno stain was therefore carried out on notochord grafted embryos at stage HH24/25 in order to determine whether the ectopic sclerotome was of chick or quail origin. The QCPN immuno showed no staining of the ectopic sclerotome (data not shown). However, the quail notochord graft, which provides an internal positive control in this experiment, also did not stain positive for the QCPN marker. Indeed, quail embryos at the same stage also showed no QCPN staining in the notochord, suggesting that the antibody is unable to penetrate the notochord at this stage (data not shown). As an alternative positive control, the original notochord graft experiment was repeated (Fig. 4.4A), but in half of the embryos a single quail somite was grafted lateral to the grafted notochord (Fig. 4.4F). Experimental and positive control embryos were processed in parallel.

Figure 4.4. Ectopic sclerotome is derived from the host. A-E. Notochord graft only. A. Notochord graft procedure schematic. B. WMISH for sclerotome marker *Pax1* (purple) and immuno stain for the quail-specific marker QCPN (brown) in HH24/25 embryos, three days after a notochord graft. C. Higher magnification of whole embryo in B. D. Transverse section of embryo in B shows endogenous and ectopic sclerotome. E. Higher magnification of section in D. Ectopic sclerotome contains no QCPN-positive staining, showing it is derived from the chick host. **F-J.** Notochord plus somite graft. F. Notochord plus somite graft procedure (positive control experiment). G. WMISH for *Pax1* and immuno for QCPN in HH24/25 embryos (as in B), three days after a notochord and somite graft. H. Higher magnification of whole embryo in G. Two rows of ectopic sclerotome can be seen. I. Transverse section of embryo in G shows endogenous sclerotome and two rows of ectopic sclerotome dorsal and ventral to the ectopic quail notochord. J. Higher magnification of section in I. Ectopic sclerotome below the quail notochord graft contains QCPN-positive cells, showing it is derived from the grafted somite. (NT=neural tube, NC=endogenous notochord, ENC=ectopic quail notochord, CES=chick-derived ectopic sclerotome, QES=quail-derived ectopic sclerotome, EndS=endogenous sclerotome)



In situ hybridisation for the sclerotome marker *Pax1* revealed ectopic sclerotome in the grafted region of all embryos (8/8 embryos; Fig. 4.4 B, C), confirming the previous results (section 4.3.2). In embryos with a notochord and somite graft, two populations of sclerotome were seen in the grafted region (2/3 embryos; Fig. 4.4 G, H; arrows 1 and 2). In the example shown, these populations form two separate rows of segments, which can be seen to sit dorsal and ventral to the grafted notochord in transverse sections (Fig. 4.4 I, J). The quail notochord, though visible morphologically, never stained for QCPN (Fig. 4.4 I, J; ENC= ectopic quail notochord), as found previously. A proportion of the ventral *Pax1*-expressing cells were QCPN-positive, indicating that they were derived from the grafted quail somite. The ectopic *Pax1*-expressing cells dorsal to the graft were QCPN-negative, and were therefore derived from the chick host (Fig. 4.4 I, J; CES=chick ectopic sclerotome, QES=quail ectopic sclerotome). In normal notochord grafted embryos processed in parallel (5/5 embryos), the ectopic sclerotome did not stain for QCPN, confirming that it was derived from the host (Fig. 4.4 D, E).

The accidental transfer of quail somite cells during the notochord grafting procedure can therefore be ruled out, indicating that the notochord that influences segmentation of host sclerotome.

4.3.5. Ectopic sclerotome forms cartilage

The previous results demonstrate that the notochord has the capacity to influence the segmental pattern of vertebral column precursors, but does this influence extend to the resulting vertebrae? To address this question, the same notochord graft experiment was carried out (Fig. 4.2A). Grafted embryos were incubated for a further six days and the resulting cartilage revealed by skeletal preparation and analysed using OPT. At HH32-34 (six days after grafting), skeletal preparations show that the endogenous vertebral elements are formed as cartilage (Fig. 4.5). Ectopic cartilage can be seen in the grafted region lateral to the endogenous host vertebral column on the right hand side (n=5) (Fig. 4.5; ectopic cartilage in OPT images has a semi-transparent blue overlay). It is not possible to locate the graft or confirm that the ectopic cartilage is host-derived, as whole mount QCPN staining is not possible after the clearing step of the skeletal preparation procedure. However, it is likely that the ectopic cartilage forms from ectopic sclerotome, which was shown previously to derive from the host (section 4.3.4).

Sham notochord grafts, as carried out in section 4.3.2, were also analysed for the presence of ectopic cartilage at the same stages as above (six days after grafting, HH32-34). In 3/3 embryos, no ectopic cartilage formed in the grafted region adjacent to the vertebrae immediately rostral to the forelimb (Fig. 4.5. E, F). The dark patch in the example shown (Fig. 4.5F), overlaid in red, is not cartilage but trapping of the alcian blue stain in the oesophagus and/or trachea. This demonstrates that ectopic cartilage, like ectopic sclerotome, is not an artifact of the operation, but results from the presence of a notochord graft.

Although morphological variation was seen across all embryos, ectopic cartilage was not continuous, displaying distinct regions of strong Alcian blue staining within the overall shape which may represent some degree of segmentation (Fig. 4.5 B-D; Red arrows). Various shapes and processes were often visible and in one embryo, the ectopic cartilage formed ring-like structures that appeared to wrap around a central cylindrical cavity (potentially the grafted notochord) (Fig. 4.5C; two rings indicated by red arrows). The endogenous vertebrae were unaffected by the graft, except in one embryo where fusions of some of the neural arches (Fig. 4.5D; white star) and vertebral bodies (Fig. 4.5D; red star) were seen posterior to the region of ectopic cartilage. This may be a result of damage to the endogenous somites or neural tube during the grafting procedure. Alternatively, it may be a consequence of the graft being placed closer to the somites than usual so that the final pattern of the endogenous sclerotome at the midline was an interpretation of signals from both the graft and endogenous notochord. Nevertheless, in all cases the aggregations of ectopic cartilage were spaced with a smaller periodicity than the endogenous vertebral cartilage. If these aggregations truly are segments, this suggests not only that the notochord influences segmentation of the sclerotome during migration but that this pattern is translated up to the level of cartilage condensation. However, the morphology of the ectopic cartilage was highly irregular and not a complete recapitulation of all vertebral elements, indicating that the notochord and somites alone are not sufficient to correctly pattern the sclerotome.

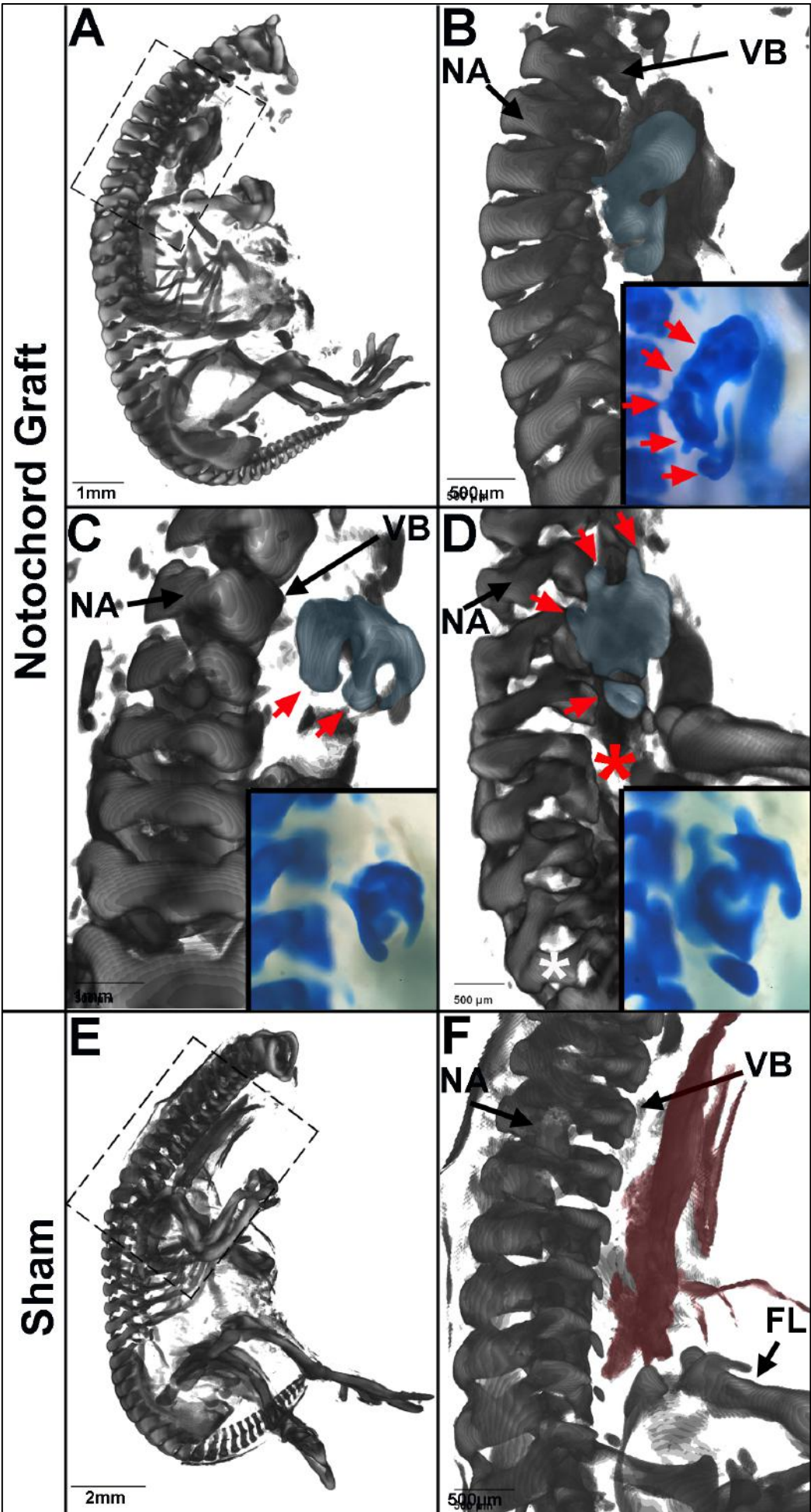


Figure 4.5. A notochord graft leads to formation of ectopic cartilage. A-D. OPT reconstructions of skeletal preparations of HH30-33 embryos, six days after a notochord graft. Ectopic cartilage is highlighted in blue. Inset images show bright field images of ectopic cartilage, stained with Alcian Blue. (NA=neural arch; VB=vertebral body, Red arrows= potential segmentation of cartilage) A. Lateral view of whole embryo (head removed) shows ectopic cartilage in grafted region. B. Zoom on boxed region of embryo shown in A. C. Second example of ectopic cartilage. Zoom on ectopic cartilage, which shows a ring-like morphology. C. Third example of embryo showing ectopic cartilage. Zoom on ectopic cartilage. This embryo shows disruption to the morphology of the endogenous vertebrae. (red star=fused vertebral bodies, white star = fused neural arches). **E-F.** OPT reconstruction of skeletal preparation of HH30-33 embryo, six days after a sham notochord graft. No ectopic cartilage is seen in the operated region. Red overlay indicates trapping of alcian blue stain, not cartilage. E. Lateral view of whole embryo. F. Zoom on operated region.

4.3.6. The periodicity of the ectopic sclerotome is dependent upon somite size, not the axial region of the notochord

Two likely mechanisms could explain how the notochord could bring about a change in the spatial periodicity of sclerotome segmentation.

Model 1: Segmental information within the notochord

The notochord could have a covert segmental pattern that can influence the positioning of sclerotome, or the differentiation of vertebral structures, at set points along the midline (Fig. 4.6A).

At the stage of grafting (HH10-12), the notochord is a continuous rod of vacuolated mesodermal cells that provide tensile strength at the midline of the embryo, with no reported morphological segmental pattern. It is anchored at the anterior end within the head, and the retraction of Hensen's node towards the posterior end means that the notochord is under tension. As a result, when the notochord graft is excised from the quail embryo during the notochord graft procedure, the excised portion visibly shrinks upon release of this tension. Any segmental information within the notochord at this point would also shrink to a more compact pattern, instructing the more compact segmentation seen in the ectopic sclerotome when it is grafted to the host.

Model 2: A uniform attractant secreted from the notochord

The notochord secretes an attractant molecule, specifically attracting sclerotome cells (Fig. 4.6B).

The secretion of a hypothetical "attractant" uniformly along the length of the grafted notochord would create a radius of the molecule around the notochord and a concentration gradient highest at the notochord, radiating outwards. Because of diffusion, the notochord would be shorter than the total length of somites within the radius of the attractant, so some cells from somites not immediately adjacent to the grafted notochord would also be attracted. These sclerotome cells moving towards the notochord would naturally compress the pattern as they migrate, leading to the reduction in spacing between sclerotome segments seen in the ectopic sclerotome.

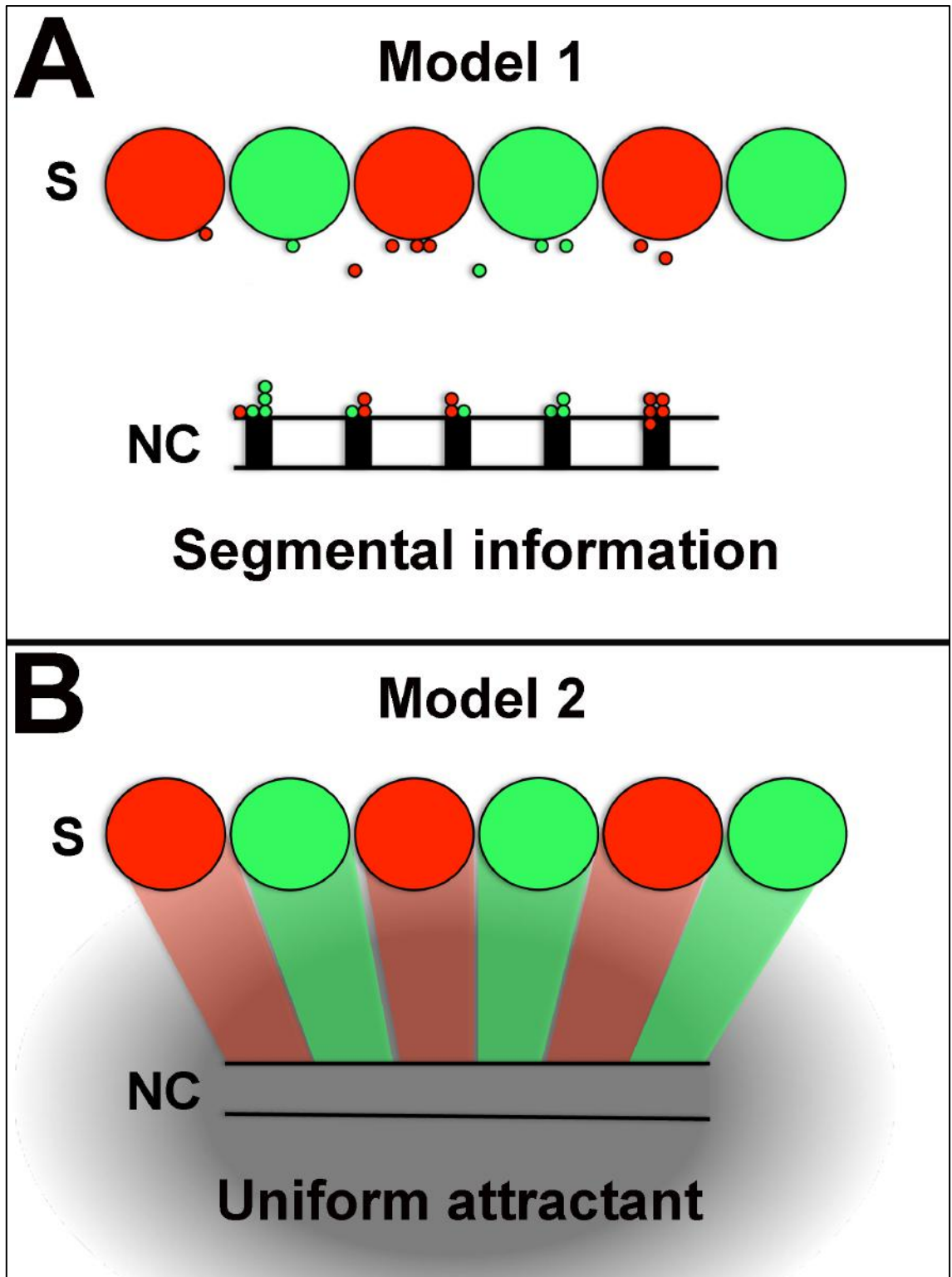


Figure 4.6. Two models by which the notochord could alter segmental periodicity of the sclerotome, as seen in notochord grafts. A. Model 1: Segmental information within the notochord is imposed on the migrating sclerotome. **B. Model 2:** An attractant is secreted uniformly from the notochord, towards which the sclerotome migrates. Segments compress as they move towards the notochord. (S=sclerotome; NC=notochord).

To distinguish between the two mechanisms, I took advantage of regional differences in somite size along the body axis of the embryo. The mid-cervical somites in the chick embryo are smaller than those in the brachial region. If the same length of notochord was grafted lateral to the somites in both of these regions, the radius of the hypothetical attractant secreted (model 2) would remain constant between the two grafts, but the number of somites that sit within this radius (and therefore able to respond to the attractant) would be fewer in the brachial region. In this case, it would be expected that the spatial periodicity of the ectopic sclerotome generated in each region would be different. Alternatively, if there is segmental information within the notochord (model 1), the spatial periodicity of the ectopic sclerotome should be identical regardless of the region to which the notochord is grafted, but should instead vary according to regional differences in segmental patterning of the notochord.

Notochord grafts were conducted to and from the cervical and brachial region, using embryos at HH10-11 (10-13 somites) and HH13-14 (19-21 somites) respectively (Fig. 4.7 A-D; Each graft is numbered to correspond with the result shown in Fig. 4.7 E-K). The segmental pattern of ectopic sclerotome at HH24-25 was compared across embryos by in-situ hybridisation for *Uncx4.1* (Fig. 4.7 E, G, I, K). Grafts of cervical notochords to cervical somites, previously carried out in the original notochord graft experiment (section 4.3.2), were used in this comparison. The length of donor notochord was kept constant between grafts, to ensure the number of segments within the notochord (model 1), or the length of the attractant source (model 2) was constant between grafts. Notochords were always removed at the level of the caudal-most somites and grafted lateral to the somites in the equivalent region of the chick host. In this way, the relative importance of segment size within the somites and signals from the notochord could be tested between regions, whilst keeping the 'age' of the notochord and somites (and therefore the timing of signals) the same between grafts. The predicted pattern of segmentation generated by each graft according to each model is outlined in Table 4.1. The layout of this table corresponds to that of the actual results for each graft in Figure 4.7E-K.

	Cervical Notochord	Brachial Notochord
Cervical somites	<ol style="list-style-type: none"> 1. <i>Many closely spaced segments</i> 2. <i>Many closely spaced segments</i> 	<ol style="list-style-type: none"> 1. <i>Few widely spaced segments</i> 2. <i>Many closely spaced segments</i>
Brachial somites	<ol style="list-style-type: none"> 1. <i>Many closely spaced segments</i> 2. <i>Few widely spaced segments</i> 	<ol style="list-style-type: none"> 1. <i>Few widely spaced segments</i> 2. <i>Few widely spaced segments</i>

Table 4. Error! No text of specified style in document. The predicted segmental pattern of ectopic sclerotome that would result from notochord grafts, if the notochord influences segmental patterning according to model 1 (segmented information model) or model 2 (uniform attractant model).

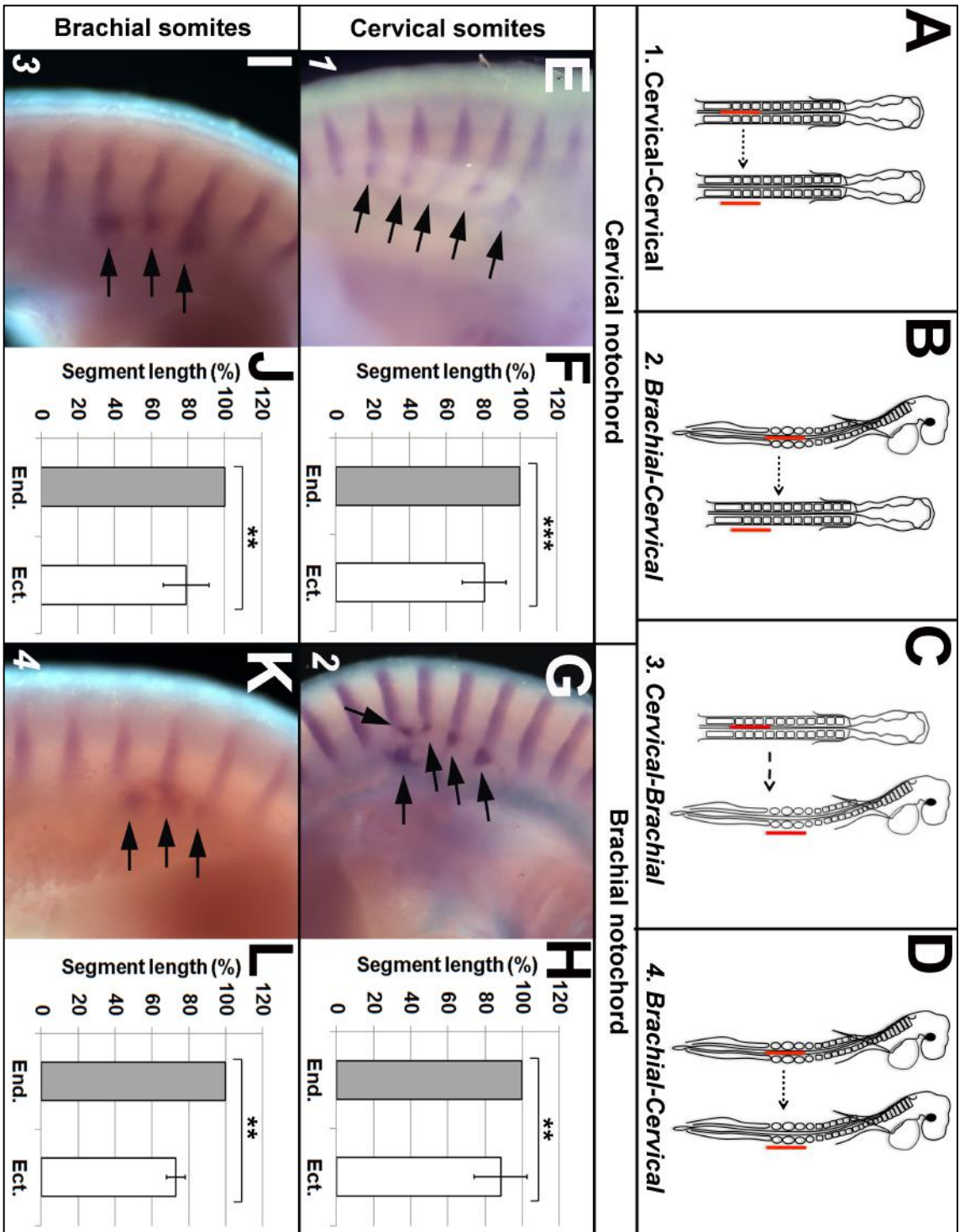
At HH24-25, 18/20 embryos across the four grafts showed ectopic sclerotome with a segmented pattern, revealed by the expression of *Uncx4.1* (Fig. 4.7 E, G, I, K; black arrows). The length of the ectopic and endogenous sclerotome was quantified as previously, the procedure for which is described in section 4.2.6. In all four grafts, the ectopic sclerotome segments were significantly shorter than the adjacent endogenous sclerotome segments (Fig. 4.7F, H, J, L). The average percentage decrease of the ectopic sclerotome segments compared to the endogenous sclerotome is summarised in table 4.2.

Furthermore, a number of ectopic segments were seen be distinctly out of phase with the endogenous segmentation pattern (Fig 4.3B, G, I; black stars). This corroborates the results of the cervical notochord grafts from section 4.3.3.

Graft	Mean % difference in segment length	SD (%)	Pairwise T-test
1 Cervical - Cervical	19	12	T(13)= 6.21 p=0.000
2 Brachial - Cervical	12	14	T(17)= 3.57 p=0.002
3 Cervical - Brachial	21	12	T(8)= 5.01 p=0.001
4 Brachial - Brachial	27	5	T(3)=9.95 p=0.002

Table 4.11. Summary of the mean percentage difference in segment length between the endogenous and ectopic sclerotome in HH24-25 embryos, three days after a notochord graft to and from the cervical and brachial axial regions. Grafts 1-4 are illustrated in Fig. 4.7A-D.

Figure 4.7. Inter-regional notochord grafts suggest that the periodicity of ectopic sclerotome is dependent upon somite size, not the axial region of the notochord. A-D. Schematics showing different permutations of inter-regional notochord grafts (red=grafted notochord). A. Graft 1: Cervical notochord grafted to cervical somites. B. Graft 2: Brachial notochord grafted to cervical somites. C. Graft 3: Cervical notochord grafted to brachial somites. D. Graft 4: Brachial notochord grafted to brachial somites. **E-L.** *Uncx4.1* WMISH (purple) shows the segmental pattern of ectopic sclerotome resulting from grafts 1-4 in HH24/25 embryos, three days after grafting. E. *Uncx4.1* expression after graft 1. F. Comparison of mean ectopic and endogenous segment length in graft 1 embryos. G. *Uncx4.1* expression after graft 2. H. Comparison of mean ectopic and endogenous segment length in graft 2 embryos. I. *Uncx4.1* expression after graft 3. J. Comparison of mean ectopic and endogenous segment length in graft 3 embryos. K. *Uncx4.1* expression after graft 4. L. Comparison of mean ectopic and endogenous segment length in graft 1 embryos. Images are high magnification of grafted region of whole-mount embryo (black arrows = segments of *Uncx4.1* expression. In all graphs, the mean segment length of the ectopic sclerotome is expressed as a percentage of the mean segment length of the adjacent endogenous somites.



In embryos where a cervical or brachial notochord was grafted adjacent to the cervical somites, *Uncx4.1* expression showed 3-6 segments of ectopic sclerotome in a more compact spacing (cervical-cervical (Fig. 4.7E): 5/5 embryos; brachial-cervical (Fig. 4.7G): 5/5 embryos). This was in comparison to embryos where notochords from either region were grafted to the brachial somites, which always showed three segments of ectopic sclerotome with wider spacing (cervical-brachial (Fig. 4.7I): 5/5 embryos; brachial-brachial (Fig. 4.7K): 2/2 embryos). The segmental patterning of ectopic sclerotome did not alter according to which region the notochord graft was taken from. This is illustrated most convincingly when the segmentation is compared between graft 3 and 4 embryos. The notochord graft that was taken from the cervical region (graft 3) spanned a greater number of somitic segments than that taken from the brachial region (graft 4). If segmental information within the notochord influenced periodicity of the sclerotome, it would be expected that the cervical notochord would give rise to a greater number of ectopic sclerotome segments than the thoracic notochord. However, the results show the reverse. Both grafts consistently resulted in only three segments of ectopic sclerotome adjacent to the brachial somites, regardless of whether the notochord was cervical or brachial in origin (Fig. 4.7. I and K). These results are consistent with the pattern predicted to result from a uniform attractant secreted from the notochord (Table 4.1, model 2), suggesting that if any segmental information exists within the notochord, the segmental periodicity of the somites is dominant.

4.3.7. A notochord and neural tube graft gives rise to ectopic cartilage that resembles vertebral bodies and neural arches

Although OPT reconstructions of skeletal preparations showed some degree of segmental patterning in the ectopic cartilage of notochord-grafted embryos, this cartilage never showed normal vertebral morphology (Fig. 4.5). This result suggests that the sclerotome and notochord are not sufficient to pattern all elements of the vertebral column. Cartilage resembling the morphology of vertebral bodies was observed in a number of embryos, but no cartilage of a neural arch-like morphology was ever observed. Therefore, it is reasonable to speculate that the notochord is only able to influence the morphology and periodicity of the vertebral bodies that form around it, and additional signals are required to pattern the more remote neural arches. If similar axial-derived signals also pattern the arches, a possible candidate source of these signals is

the neural tube. To address whether the neural tube plays a role in patterning the neural arches, the same procedure as the original quail-chick notochord graft experiment was carried out, but instead both the notochord and neural tube from the cervical region of a quail were transplanted lateral to the somites of a chick host of the same stage (Fig. 4.8A).

In a single grafted embryo at HH33, skeleton preparation revealed ectopic cartilage in the grafted region (Fig. 4.8 B, C; Blue overlay=ectopic cartilage). OPT allowed further analysis of the three-dimensional morphology of this cartilage. The cartilage was more extensive than in embryos of the same stage with a notochord graft alone, and contained four or five elements of a neural arch-like morphology (Fig. 4.8C; red arrows), with varying degrees of fusion between each element. The most anterior element contained a hole in the cartilage (Fig. 4.8C; star), that resembled a foramen through which a segmental vein or artery might project. This suggests that signals from the neural tube induces the sclerotome to form neural arches, consistent with the results of neural tube excision studies which reported that in the absence of a neural tube, no neural arches form (Watterson et al., 1954; Strudel, 1955; Teillet and Le Douarin, 1983).

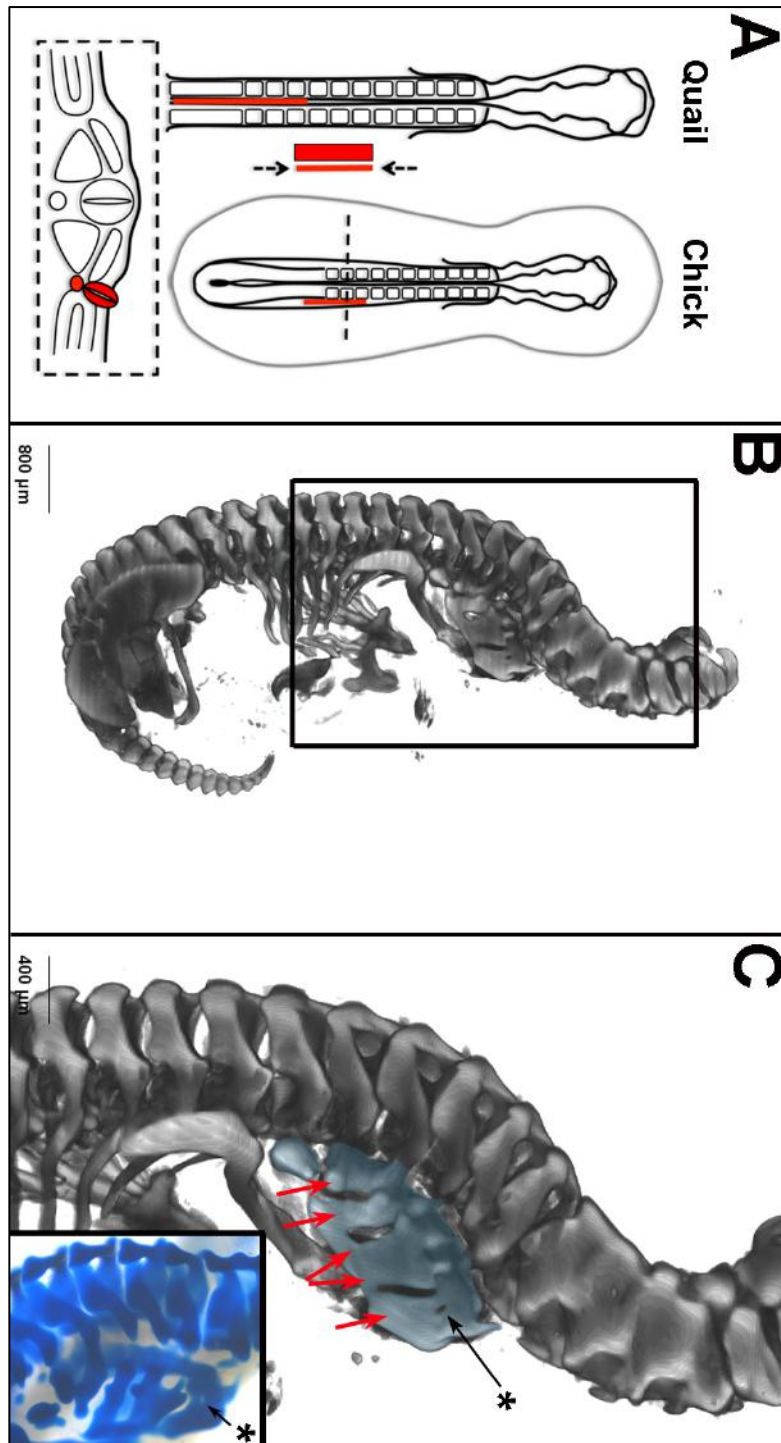


Figure 4.8. Ectopic cartilage resulting from a notochord and neural tube graft. A. Notochord and neural tube graft procedure (Neural tube and notochord shown in red). **B.** OPT reconstruction of HH33 embryo skeletal preparation, six days after a notochord and neural tube graft (Red bracket=ectopic cartilage). **C.** Zoom on boxed region of embryo in B. Inset image shows ectopic cartilage and adjacent endogenous vertebrae imaged in bright field after skeletal preparation alone. Ectopic cartilage contains elements of neural arch-like morphology and a hole that resembles a foramen (star). Red arrows indicate cartilage of a 'neural arch-like' morphology.

4.4. Discussion

4.4.1. Two distinct roles for the notochord in vertebral development: Attraction and segmental patterning

The above results demonstrate that the notochord is required for segmental patterning of the vertebral bodies. Furthermore, a notochord graft lateral to endogenous somites results in the formation of ectopic sclerotome in a different spatial periodicity than the endogenous sclerotome. The results of notochord grafts to and from axial regions of differing somite size support the presence of a chemoattractant, which is secreted from the notochord and towards which the sclerotome migrates. This suggests that the grafted notochord could alter the segmental pattern of the sclerotome, without necessarily possessing any intrinsic segmental information. Evidence from notochord grafts supports the uniform attractant model (Fig. 4.6B), but this mechanism cannot account for the results of notochord ablations. Vertebral bodies form but have no segmental pattern in the absence of a notochord, a result that was also found in previous notochord ablation studies (Watterson et al., 1954; Strudel, 1955; Teillet and Le Douarin, 1983). This suggests that as well as mediating an attraction, the notochord plays an additional role that is essential for segmental patterning of the vertebral bodies. It is possible that this latter role is mediated by segmental information within the notochord, as described in model one (Fig. 4.6A), the influence of which is masked in notochord grafts by the action of the attractant and the dominance of somite segmental patterning. The “attractant” and “segmental information” models are therefore not necessarily mutually exclusive.

The results of notochord ablations also appear to contradict the results of inter-regional notochord grafts in another way. If the notochord is required for segmental patterning of the vertebral bodies, why do notochord grafts from different regions not pattern ectopic sclerotome differently? There are two possible explanations for this. First, the information within the notochord that is required for vertebral body segmentation may have its effect at the later stage of cartilage formation. This might explain the results of another notochord ablation study in the chick, which found that the segmented pattern of *Pax1*-expressing sclerotome cells at HH29 was not affected by ablation of the

notochord (Senthinathan et al., 2012). My analyses of segmentation in inter-regional notochord grafts only extended to the segmentation of the sclerotome at HH24-25. It may be that differences in segmentation of ectopic cartilage would be observed in these embryos at a later stage. Second, in the inter-regional notochord graft experiment it was assumed that if the notochord does possess segmental information, it would have the same spatial periodicity as the somites that surround it (i.e. widely spaced in the brachial region, compact in the cervical region). However, this may not be the case, as the mature vertebrae of the cervical and brachial region are not dramatically different in length. Therefore, segmental information within the notochord may not be sufficiently different between these regions to cause an observable change in the ectopic sclerotome. Notochord grafts between regions where vertebral lengths differ dramatically would be more informative. The caudal-most part of the vertebral column is an obvious region to test this, as the caudal vertebrae are much smaller than the more anterior vertebrae. Notochord grafts were attempted from the caudal to the cervical region, but the results were inconclusive. The ventral closure of the embryo at this stage makes it very difficult to dissect the notochord graft cleanly from the donor quail embryo. Furthermore, this ventral closure and turning of the embryo makes it difficult to carry out the reciprocal graft of a cervical notochord to the tail bud somites *in ovo*.

All cartilage at the midline derives from *Pax1*-expressing sclerotome cells (Ebensperger et al., 1995) which are induced in the ventro-medial compartment of the somite due to exposure of these cells to high levels of Shh secreted from the adjacent notochord and floor plate (Johnson et al., 1994; Fan et al., 1995). In the PSM ablations, the notochord is excised from the PSM region prior to somite formation, raising the question of how somites in the ablated region subsequently become dorso-ventrally patterned to form the cartilage seen at the midline. It has been shown that the floor plate is sufficient to induce *Pax1* in the sclerotome, therefore this could compensate for the absence of a notochord (Brand-Saberi et al., 1993; Ebensperger et al., 1995). This result also adds another question to the “attraction model”. If attractive signals from the notochord were solely responsible for the medial migration of the sclerotome to the midline, it would be expected that vertebral bodies should be absent when the notochord is removed. Instead, a strip of unsegmented ventral cartilage forms in the absence of a notochord (also shown by Watterson et al.

1954; Strudel 1955). This suggests that although the notochord is attractive, it is not required for the formation of cartilage at the midline. Its absence could again be compensated for by signals from the floor plate, as has been suggested to be the case in mouse (Ando et al., 2010).

Movement of the sclerotome towards the notochord during vertebral column formation has been shown to be a result of both an expansion of the tissue and active migration of cells (Solursh et al. 1979; Chernoff & Lash 1981; see also section 1.5.1). The fact that cells migrate specifically towards the midline (and not at random) indicates that a mechanism must be acting to mediate the directionality of this movement (Chernoff and Lash, 1981). Surprisingly, however, no such mechanism appears to have been proposed before. A directional cue from the midline would be an obvious explanation, and the results in this chapter suggest that this might be mediated by a chemoattractant from the notochord. This proposed attractive property of the notochord is supported by a study in which sclerotome cells were found to migrate towards a notochord *in vitro* (Newgreen et al., 1986).

The notochord is known to play multiple roles during vertebral development; for example in the specification of the sclerotome as previously discussed, and later in the formation of the inter-vertebral discs (Choi and Harfe, 2011; Choi et al., 2012). The attraction of sclerotome to the midline and subsequent segmental patterning of the vertebrae proposed here, represent two possible further roles for the notochord in vertebral development.

Although a notochord graft was shown to lead to the formation of ectopic cartilage, the morphology of this cartilage was highly irregular. Aggregations of strong alcian blue staining, as well as spaces between regions of ectopic cartilage, may represent some degree of segmentation. However, whether this represents true segmentation is not certain. One important point is that the ectopic cartilage forms from only one row of ectopic sclerotome, whereas endogenous vertebrae form from bilateral rows of sclerotome that meet at the midline. The irregular morphology of the ectopic cartilage may be partially due to the absence of this second row of sclerotome. An experiment is currently in progress to analyse the presence and segmental pattern of ectopic intervertebral disks after a notochord graft. In this experiment, grafted embryos will be stained using an antibody against Fibromodulin, an extracellular matrix

protein expressed in intervertebral disks but not vertebral bodies. The results of this experiment will hopefully better elucidate the segmental pattern of ectopic cartilage.

4.4.2. The origin of ectopic sclerotome

The experiments described above show that the ectopic sclerotome seen in notochord graft experiments is derived from the host, but it is not clear from where in the host the ectopic sclerotome derives. There are a number of possibilities. Firstly, some cells in the lateral-most endogenous sclerotome may lie closer to the grafted notochord than to the endogenous one. These cells could respond to the attractant secreted from the grafted notochord and migrate towards it instead of migrating to the midline. A second possibility is that the notochord graft induces the expression of *Pax1* in lateral somite cells, which would normally form dermomyotome. Indeed, an ectopic induction of *Pax1* in the lateral somite was seen in studies using the same notochord graft assay technique to investigate dorso-ventral somite patterning (Brand-Saberi et al., 1993; Ebensperger et al., 1995). It is likely that induced sclerotome forms a proportion of the ectopic sclerotome in notochord-grafted embryos, along with a migration of some endogenous sclerotome cells towards the graft. The stripes of ectopic *Uncx4.1* were continuous with the endogenous sclerotome in several embryos, extending ventro-laterally towards the graft and compressing together as they do so (Fig. 5.5 G-J). This observation supports a continuous migration and compression of the endogenous sclerotome towards the graft.

A third possibility is that the grafted notochord induces ectopic somites from surrounding non-somitic mesoderm. In the normal embryo, the mesoderm forms somites through the inhibition of BMP signalling in the dorsal paraxial mesoderm, by the secretion of BMP inhibitors from Hensen's node and the notochord at the midline (Tonegawa and Takahashi, 1998; Streit and Stern, 1999). It has also been shown that beads expressing Noggin (one of the BMP inhibitors secreted by the notochord) can induce ectopic somites from lateral plate mesoderm through the inhibition of BMP-4 (Tonegawa and Takahashi, 1998; Streit and Stern, 1999; Dias et al., 2014). It is therefore possible that secretion of BMP inhibitors by the ectopic notochord leads to the induction of somites *de novo* from the lateral plate or intermediate mesoderm. After the induction of ectopic somites, the expression of Shh and Noggin by the graft

may subsequently pattern the somites dorso-ventrally, giving rise to ectopic sclerotome in a segmented pattern. If this third possibility were confirmed, it would weaken the attraction model, as an attraction of the endogenous sclerotome mediated by the grafted notochord would not be required to form ectopic sclerotome. Further work is therefore required to confirm the origin of the ectopic sclerotome. This question is addressed in chapter five.

4.4.3. Variation in the formation and segmentation of ectopic sclerotome

Analysis of *Uncx4.1* and *Pax1* expression showed that 15% of embryos did not develop ectopic sclerotome in response to a notochord graft. It is possible that in these cases the graft had been placed too lateral for signals from the notochord to reach the somite. If grafts were placed within the LPM, instead of between the LPM and the somites, the graft could sit in the space between the splanchnic and somatic mesoderm and be pulled further away from the somites during ventral closure of the embryo. It is also possible that some notochord grafts died during the grafting procedure.

There was also variation in the number of ectopic sclerotome segments seen in each embryo. The length of notochord grafted during each manipulation was kept relatively constant at five to six cervical somites (or three brachial somites), but variation in graft length may partly account for the variation seen in segment number. Even if the length of notochord excised was constant between embryos, there may have been variation in the amount of notochord shrinkage that occurred when the graft was removed, which could also result in differing graft lengths. Another contributing factor could be that the graft did not remain parallel to the A-P axis during development. The expression of various somitic markers in a number of embryos suggests a curvature of the notochord graft that may have positioned parts of the graft too far lateral for it to have an effect on the somite (e.g. Fig. 4.3G and 4.7G). However, without the ability to stain the grafted notochord at this stage (due to the failure of the QCPN immunostain), it is difficult to verify the size and shape of each graft.

4.4.4. Does the notochord influence segmentation of other somitic compartments?

4.4.4.1. Dermomyotome

Segmentation of the dermomyotome appears to be unaffected by a grafted notochord. However, half of the notochord graft embryos analysed for *Pax3* expression showed a “clearing” of *Pax3* expression around the graft. It is likely that this effect is due to induction of *Pax1* in the lateral somite at the expense of *Pax3*-expressing dermomyotome cells, as was observed in the original notochord graft experiments that were carried out to investigate D-V patterning of the somite (e.g. Brand-Saberi et al., 1993; Pourquié et al., 1993; see also section 1.4.1). Double staining using both *Pax1* and *Pax3* probes is required to verify their relative expression within the same embryo.

4.4.4.3. Syndetome

In a similar way to the sclerotome, ectopic syndetome (a tendon progenitor population within the sclerotome) is formed in response to a notochord graft. The ectopic syndetome, as visualised by the expression of *Scleraxis*, is in a more compressed segmental pattern than that of the endogenous compartment. In the normal embryo, the syndetome compartment is restricted to two regions where the sclerotome and myotome abut at the rostral and caudal edge of each somite, therefore forming in a position between the two tissues that the tendon will ultimately connect. The tendon progenitors are induced from sclerotome cells by FGF signalling from the adjacent myotome (Brent et al., 2003). It is likely that the induction of ectopic *Scleraxis* is a consequence of the formation of ectopic sclerotome by the grafted notochord. In the region of the notochord graft, the ectopic sclerotome may contact the lateral myotome, inducing ectopic syndetome at ectopic positions. Since the segmental pattern of ectopic sclerotome is more compressed than that of the endogenous sclerotome, it would follow that the induced syndetome would also have a more compact pattern. Supporting this, quantification of segment length for the ectopic sclerotome and syndetome, showed a similar percentage decrease compared to the endogenous segmental periodicity (21% for sclerotome, 19% for syndetome).

4.4.5. A possible role for the neural tube in neural arch patterning

The formation of more extensive ectopic cartilage in response to a combined neural tube and notochord graft suggests that the neural tube also plays a role

in vertebral patterning. Neural arch-like elements were not present in the ectopic cartilage of embryos with a notochord graft alone, suggesting that the neural tube patterns the dorsal elements of the vertebrae that form around it. However, this result is based upon only one grafted embryo, and further repeats are required. It is also important to note that the three axial structures present in the grafted region (the neural tube, notochord and somites) are still not sufficient to recapitulate normal formation and patterning of vertebrae in the ectopic cartilage. This suggests that other signals from surrounding tissues are required for complete vertebral patterning.

A role for the neural tube in vertebral patterning has been proposed previously. In the neural tube excision experiments of Strudel, neural arches did not form in the absence of a neural tube in either the cervical or thoracic region of the chick (Strudel, 1955). However, Strudel also observed a disruption to segmental patterning of the ventral cartilage (the vertebral bodies) that surrounds the notochord when the neural tube was ablated. The ventral cartilage did not segment into individual bodies, but rather formed a cartilaginous “manchon” (sleeve) around the notochord with repeated “étranglements” (constrictions) along the A-P axis that Strudel proposed was evidence of partial segmentation. This suggests that as well as being required for the formation and patterning of the neural arch cartilage that forms around it, the neural tube is also necessary for normal segmentation of the vertebral body cartilage that sits ventral to it.

However, Senthinathan et al. (2012) reported that excision of the neural tube had no effect on the segmental expression of *Pax1* in the ventral sclerotome surrounding the notochord. Although this appears to contradict the observations of Strudel, it could mean that the signals from the neural tube that influence vertebral segmentation act at the level of cartilage formation, and not during the earlier stages of sclerotome migration. However, Senthinathan et al. focused only on segmentation of the ventral sclerotome. As there is a potential role for the neural tube in patterning the dorsal cartilage, it remains to be seen whether removal of the neural tube disrupts the earlier segmented pattern of the more dorsal sclerotome from which the neural arch cartilage is derived (Christ and Scaal, 2008).

Another consideration is how spinal nerve projections from the grafted neural tube affect the cartilage that forms around them. During normal development, R-C patterning of the sclerotome imposes a segmented pattern on the axons of the spinal nerves by only permitting axon outgrowth through the rostral half (Keynes and Stern, 1984; Rickmann et al., 1985). As the ectopic sclerotome that forms around the notochord graft alone was shown to have an R-C pattern (as seen by the segmented expression of *Uncx4.1*), it follows that, with the addition of an ectopic neural tube, this pattern would influence the segmentation of the ectopic spinal nerves that project from it. Indeed, the presence of at least one spinal nerve projection is suggested by a foramen-like hole in one of the elements of the ectopic cartilage (Fig. 4.6C; foramen indicated by star). In the neural tube excision experiment previously discussed, spinal nerves were found to be absent from the operated region (Senthinathan et al., 2012). Therefore, it is possible that the spinal nerves later re-impose their segmented pattern back to the sclerotome, patterning the neural arch cartilage that forms around the ganglia.

If signals from both the notochord and neural tube could independently influence the segmentation of the vertebral elements that form around them, this might account for the region-specific shift between dorsal and ventral elements within a segment that was reported in Chapter three. The tilt of the inter-somitic boundary, and later the neural arch, could be achieved by a shift of the notochord relative to the neural tube (leading to a mis-alignment of the segmental information within them) along the A-P axis. One way to investigate this would be to conduct neural tube grafts between the cervical/thoracic and sacral regions and analyse the “tilt” of the neural arch cartilage that forms around them. The same question could be addressed by rotating a portion of the neural tube around the A-P axis by 180° and analysing the orientation of the neural arch cartilage that forms. It also remains to be answered how the notochord and neural tube individually influence segmental patterning of the vertebrae, whilst still retaining coherent development of each element within a segment.

4.5. Summary

In this chapter, I investigated whether the notochord in chick plays a role in segmentation of the vertebral column by conducting a series of notochord ablation and grafting experiments. I first repeated the notochord ablation experiments of previous authors (Watterson et al., 1954; Strudel, 1955), and by OPT analysis of the resulting skeleton, confirmed that the notochord is required for segmentation of the vertebral bodies. I then went on to show that a notochord, grafted lateral to the somites, results in the formation of host-derived sclerotome in a more compressed segmental pattern compared to the endogenous sclerotome of the host. This suggests that the notochord has the capacity to alter the spatial periodicity of the sclerotome. Through a series of notochord grafts between different axial regions, I showed that the spatial periodicity of the ectopic sclerotome was not dependent upon the axial region of the notochord, but on the size of the somites to which the notochord was grafted. These results suggest that the notochord possesses an attractive property, towards which the sclerotome migrates, resulting in compression of the ectopic sclerotome. However, the possibility that the chick notochord possesses an intrinsic segmentation cannot be ruled out, since the vertebral bodies do not segment in the absence of a notochord.

Chapter 5 : Attraction of the sclerotome towards the notochord

5.1. Introduction

The vertebral column runs along the midline of the animal, but the cellular precursors from which it forms (the sclerotome), originate in the somites lateral to the midline. To form the vertebrae, the sclerotome cells must relocate to the midline. There must, therefore, be a cue to direct sclerotome cells medially, but currently no mechanism is known that regulates this directed movement.

In the previous chapter, it was reported that a notochord, grafted lateral to the somites leads to the formation of ectopic sclerotome (and later cartilage) with a different spatial periodicity to that of the host. Furthermore, the periodicity of this ectopic sclerotome did not change according to the region from which the notochord was derived, but was dependent upon the spatial periodicity of the somites in the region to which the notochord was grafted. A “uniform attractant model” was proposed to explain this result (Fig. 4.5B). This model predicts that the notochord secretes a chemoattractant uniformly along its length, to which only cells of the sclerotome are competent to respond.

The uniform attractant model relies on the assumption that the ectopic sclerotome is formed by a portion of the sclerotome in the endogenous somites migrating laterally towards the grafted notochord, rather than towards the midline. However, it is possible that the ectopic sclerotome derives from new somites induced from the lateral plate mesoderm or intermediate mesoderm by the secretion of BMP inhibitors from the notochord graft (Tonogawa and Takahashi, 1998; Streit and Stern, 1999). If this were the case, no attraction mechanism would be necessary to generate the ectopic sclerotome. At the beginning of this chapter, I therefore investigate whether such an attraction mechanism exists, by tracing the migration of the endogenous somites adjacent to a notochord graft.

After providing evidence to support an attraction between the somites and notochord, the next step was to identify what mediates this attraction at a molecular level. I took a candidate approach to this question, reasoning that

the “attractant” and its downstream signalling mechanism must fulfill a number of criteria:

1. The attractant must be present in the notochord when the sclerotome begins to migrate.
2. The attractant must be able to signal across the distance between the notochord and sclerotome.
3. Downstream targets of the attractant, such as cell surface receptors and intracellular signalling pathway components, must be expressed by the sclerotome at the equivalent time in order for it to respond.

Shh is a secreted signalling molecule expressed by the notochord at its formation and throughout development (Echelard et al., 1993; Johnson et al., 1994). It is known to regulate a number of important processes during somite development, including specification of the sclerotome in the ventro-medial somite (Johnson et al., 1994; Fan et al., 1995) and the maintenance and proliferation of this tissue after its specification (Fan et al., 1995). Shortly after its specification, indicated by the expression of the sclerotome marker *Pax1* (Ebensperger et al., 1995), the specified sclerotome undergoes an epithelial to mesenchymal transition, allowing cells to break from the somite and migrate (Christ and Ordahl, 1995). Therefore, Shh is already signalling to the sclerotome upon initiation of sclerotome migration.

Although initiation of sclerotome migration occurs simultaneously (or shortly after) specification of the sclerotome, it is maintained over a much longer developmental time frame until all sclerotome cells have reached their final position. Shh continues to be synthesised in the notochord throughout this time (Echelard et al., 1993; Johnson et al., 1994), as are downstream components of the hedgehog signalling pathway in the sclerotome cells such as the *Patched* receptors and *Gli* transcription factors (Borycki et al., 1998). Shh signalling from the notochord, and the competence of the sclerotome to respond to this signal, are therefore maintained throughout sclerotome migration. Therefore, Shh fulfills all of the above criteria for a role in mediating the directed migration of sclerotome to the midline.

In the previous chapter, it was reported that when the notochord is ablated the vertebral bodies do form, but are not segmentally patterned. This raised a number of questions, such as how do sclerotome cells become specified in the absence of Shh from the notochord, and how do these sclerotome cells migrate to the midline to form the unsegmented ventral cartilage? The notochord plays an additional role in inducing Shh expression in the floor plate of the ventral neural tube (Placzek, 1995; Roelink et al., 1995), which in the absence of a notochord, is sufficient to induce *Pax1* in the sclerotome (Brand-Saberi et al., 1993; Ebensperger et al., 1995; Ando et al., 2010). Therefore, it seems likely that Shh from the floor plate compensates to specify the sclerotome after the notochord is ablated. Compensation by the floor plate could also be involved in sclerotome attraction, explaining how sclerotome cells reach the midline in embryos in which the notochord has been ablated. Indeed, in mouse it has been shown that the floor plate is sufficient to regulate sclerotome development and vertebral formation (Ando et al., 2010). This strengthens the argument for Shh as the predicted “attractant”. Later in this chapter, I therefore go on to test whether an ectopic source of Shh is sufficient to bring about a migration of somite cells towards it, therefore acting as a chemoattractant.

5.2 Materials and methods

5.2.1. Notochord graft plus Dil and DiO labelling in-ovo

The notochord graft and somite labelling procedure is illustrated in Fig. 5.1A. The notochord graft procedure was carried out as previously described (Section 4.2.2; Fig. 4.2A). However, the notochord was placed slightly more rostral, so that its entire length was adjacent to somites that could be labelled and traced in alternate colours. Following grafting, Dil and DiO were used to label four to six somites, both adjacent to the graft and on the contralateral side of the embryo, in an alternating red and green pattern, using the same procedure as described for the somite tracing experiments in chapter three (section 3.2.1; Fig. 3.1B).

5.2.2. Notochord graft in culture

Chick host embryos at HH9-10 were prepared for modified New culture as described previously (section 2.1.5). A quail notochord was grafted adjacent to the somites using the same technique as described for notochord grafts *in ovo*. However as the ventral surface of the host is uppermost in culture, the hole was made through the endoderm in order to insert the notochord graft lateral to the somites.

5.2.3. DiO labelling of somites in culture

The somites and rostral PSM adjacent to the notochord graft, bead or cell pellet were labelled with DiO at a concentration of 115 mM using the same technique as described for *in ovo* labelling experiments (section 3.2.1). DiO was preferred for labelling in New culture as it was found to form aggregates less readily than DiI. As the incubation period here was much shorter than for *in ovo* labelling experiments, cells undergo fewer divisions. As a result, negligible dilution of the DiO signal occurs during incubation. The concentration of DiO used was therefore lower than that used for *in ovo* experiments, as it was found that lower concentrations also aggregate less readily. Staining was therefore more evenly distributed throughout the somite.

Embryos were either imaged by time-lapse microscopy (section 2.5.2) or before and after incubation in the culture dish. Epifluorescent illumination was used to detect DiO-labelled somite cells.

5.2.4. Calculating somite area

To measure somite size after exposure to a grafted quail notochord for 8-9 hours, embryos were stained for *Paraxis* by whole-mount in situ hybridisation to mark the somites and then immunostained for the quail nuclear marker QCPN to detect the graft. Embryos were imaged in whole-mount, maintaining the same magnification across all images.

The four somites closest to the notochord graft were chosen for measurement. The projected total area of these four somites, identified by their *Paraxis* staining, was calculated in pixels from the 2D bright field image using Fiji (Schindelin et al., 2012). The four somites on the contralateral side of the

midline that had not been exposed to a notochord graft were also measured as a negative control.

The total area of the eight measured somites (four bilateral pairs) was calculated, and the data normalised for size variation between embryos by converting the somite area in pixels to a percentage of the total somite area for both the graft and contralateral side. The mean percentage area of the graft and control sides was compared across all samples by a paired-sample student T-test using IBM[®] SPSS[®] Statistics.

5.2.5. Preparation of Shh beads

Affi-Gel[®] Blue beads (100-200 mesh; Bio-Rad Laboratories Ltd.) were incubated overnight at 4°C in 1 mg/ml Human Sonic Hedgehog (Shh) protein (Sigma) in PBS with 0.1 µg/ml BSA. Beads incubated in PBS with 0.1 µg/ml BSA were used as negative controls.

5.2.6. Preparation of cell pellets

The pCAGGS-Shh-N (Niwa et al., 1991; Oberg et al., 2002) or empty pCA β expression constructs were transfected overnight into confluent human embryonic kidney 293T cells at a concentration of 0.13 µg/µl in Dulbecco's Modified Eagle Medium (DMEM; Life Technologies), using linear polyethylenimine (PEI; Polysciences) at a concentration of 0.43 µg/µl (Boussif et al., 1995). Transfection efficiency was analysed by eye using a Zeiss Axiovert 100 inverted microscope with epifluorescence illumination. Cells were trypsinised using 0.25% Trypsin-EDTA (Gibco), washed in PBS and re-suspended in 1ml of DMEM with 10% fetal bovine serum (FBS DMEM). Cells were counted using a haemocytometer, and 20 µl hanging drops of FBS DMEM, each containing 500 or 750 cells from the transfected cell populations, were formed on the lid of a Petri dish. Hanging drops were incubated within a humid Petri dish for 36-48 hours at 37°C until cells had coalesced into a single spherical pellet.

5.2.7. Western blot

To confirm that the cell pellets secreted Shh protein, a Western blot was carried out using the hanging drop FBS-DMEM medium surrounding the cell

pellets and probed with an antibody against the active domain of the Shh protein (SHH-N). Details of the primary and secondary antibodies used are shown in table 2.10. After incubation of hanging drops for 48 hours, the medium surrounding two 750-cell pellets was collected from Shh and control (pCA β -transfected) cells. The samples were run under reducing conditions at 105 V for 1.5 hours on a Novex 4-12% Bis-Tris protein gel (Life-tech), alongside Magic-Mark™ XP and MultiMark standard protein ladders. After transfer to a PROTRAN® 0.45 μ m nitrocellulose blotting membrane at 20 V for 2 hours, the sample was blocked for 30 minutes at room temperature in blocking buffer made from 5% milk powder (Marvel) dissolved in TBST, and incubated in primary antibody diluted in blocking buffer overnight at 4°C. After several washes in TBST, the blot was incubated in HRP-conjugated secondary antibody diluted in blocking buffer for 1.5 hours at room temperature. After several washes in TBST, the blot was developed using an Amersham™ ECL™ Prime Western Blotting Detection Reagent kit (GE Healthcare) and imaged using a Bio-rad ChemiDoc™ MP Imaging system.

5.2.8. Shh bead validation graft

As a positive control, Shh-loaded beads were assayed by their ability to induce the expression of *Nodal* ectopically on the right hand side of Hensen's node (Levin et al., 1995). HH3+/HH4- chick embryos were prepared for New culture as previously described (section 2.1.5), and a small pocket made in the epiblast on the right side of the embryo (ventral uppermost) adjacent to the Hensen's node. Individual Shh or negative control PBS beads, prepared as previously described, were placed in the pocket and embryos were cultured to HH6-7. The negative and positive control procedures are illustrated in Figure 5.4 A and C respectively.

5.2.9. Grafting of beads or pellets adjacent to the caudal-most somites in New culture

Chick embryos at HH9-10 were prepared for New culture as described previously (section 2.1.5). A small pocket was made in the lateral plate mesoderm lateral to the caudal-most somites and rostral PSM. Individual beads or pellets, washed briefly in saline, were transferred to the embryo using a pipette and placed in each pocket with Shh beads or pellets on the right and

control beads or pellets on the left. Embryos were cultured for 5-11 hours. This procedure is illustrated in Fig. 5.4E (beads) and Fig. 5.5B (cell pellets).

5.3. Results

5.3.1. Somite tracing suggests attraction of somite cells towards a grafted notochord

To test whether signals from the notochord do indeed mediate an attraction of somite cells, I traced somites in response to a notochord graft. Following the standard notochord graft procedure, the adjacent somites were labelled alternately with Dil and DiO on either side of the midline (Fig. 5.1A). The position of labelled cells was compared after three days incubation, between the graft and control side of the embryo at HH24-25. All notochord grafts were taken from the caudal cervical region of a quail donor, and grafted to the cervical region of a chick host. The results are summarised in Table 5.1.

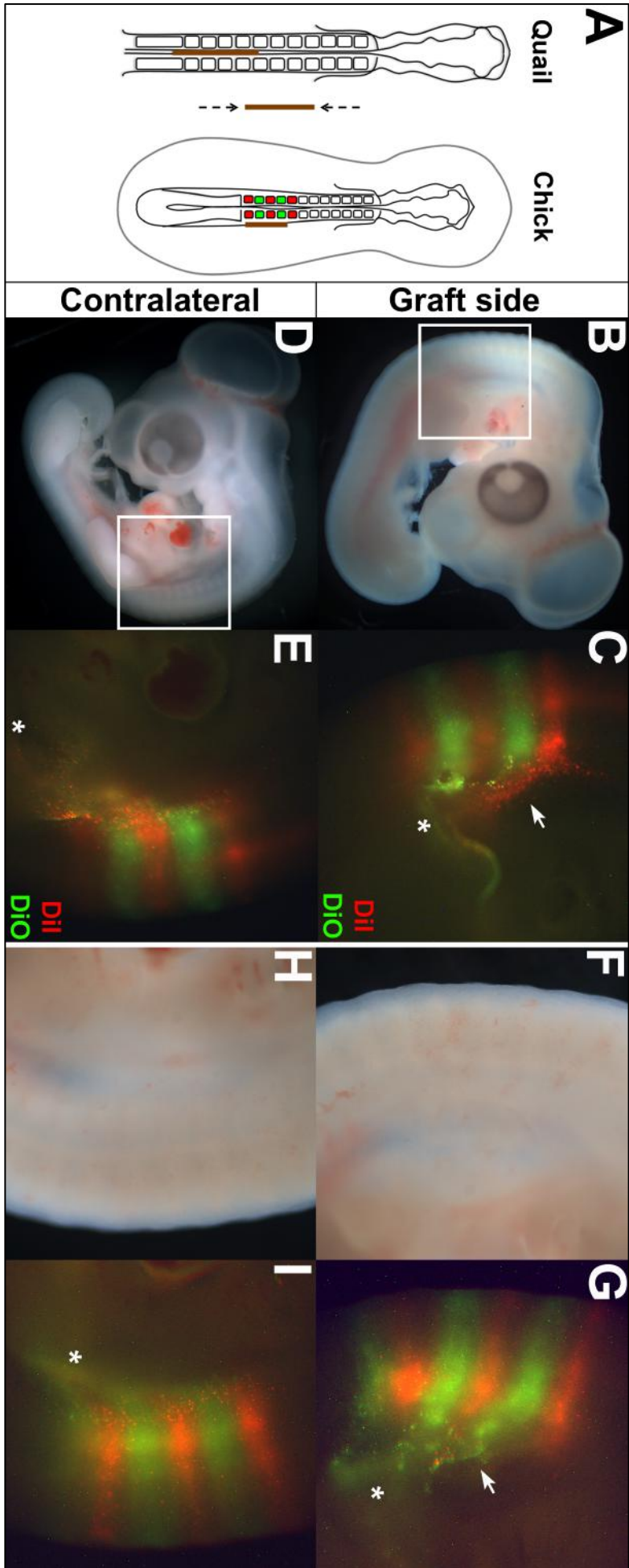
Embryo	Somites labelled	Expansion and compression of labelled somite segments? Y/N	Labelled cells found in the limb? Y/N
030613(2)	12-16	Y	Y
030613(4)	10-14	N	N
030613(5)	13-16	Y	Y
311013(2)	6-9	Y	N
311013(4)	8-15	Y	Y
190216(1)	7-12	N	N
190216(2)	7-12	Y	N
190216(3)	8-13	Y	N
190216(3)	7-12	Y	N

Table 5.1. Details and results of embryos in which somites were traced in response to a notochord graft using Dil and DiO, The embryos shown in figure 5.1 B-I is in bold.

Figure 5.1 shows two examples of embryos three days after the notochord graft and somite labelling was carried out. At HH24/25, clear stripes of labelled somite cells could be seen on either side of the embryo in the grafted region (9/9 embryos; Fig. 5.1 B-I). The boundary between Dil and DiO-labelled somites was still sharp at this stage, as previously found in the somite tracing experiments of chapter 3. In 7/9 embryos, a ventro-lateral expansion of the Dil

and DiO-labelled domain was seen on the graft side compared to the unoperated side of the embryo (Fig. 5.1 B-I). This suggests a migration of the labelled somites towards the grafted notochord. In all of the embryos in which a ventral expansion was observed, the expanded region seemed to bend posteriorly, suggesting a compression of somite segments closest to the graft compared to the dorsal region of the same somites. This is particularly clear in the rostral-most labelled somites of the examples shown. In example 1 (Fig. 5.1 B-E), the rostral-most red segment shows a progressive bend towards the posterior end of the embryo (Fig.5.1C; white arrow). In example 2 (Fig. 5.1F-I), the rostral-most red segment appears unaffected by the graft, however the adjacent green segment shows the same posterior bend as example 1. This is reminiscent of the “attraction and compression” of somite segments towards the grafted notochord predicted by the “uniform attractant” model (see Fig. 4.6B).

Figure 5.1. Tracing somites in response to a notochord graft. **A.** Notochord graft and labelling procedure. A notochord graft is performed, then the adjacent somites labelled alternately with Dil (red) and DiO (green) on either side of the midline. **B-I.** Two examples of labelled and grafted embryos, three days after a notochord graft (HH25). **B-E. Example 1:** B. Lateral view of whole embryo, graft side. C. Lateral view of embryo in B, higher magnification on boxed region, in red and green fluorescent channels. D-E. Ungrafted side of embryo in B and C. D. Bright field, whole embryo. E. Higher magnification view of labelled somites in red and green fluorescent channels. **F-I. Example 2:** F. High magnification image of operated region on graft side, lateral view. G. View as in F, in red and green fluorescent channels. H-I. Ungrafted side of embryo in F-G. H. Bright field, high magnification. E. View as in H, in red and green fluorescent channels. In both examples, Dil and DiO-labelled somite cells are seen in stripes, with ventro-lateral expansion of labelled region towards the graft, seen clearest in the more anterior-labelled somites (white arrow). On the ungrafted side, the corresponding labelled region is not expanded. (White star = contribution of labelled somites to the limb).



In 3/9 embryos, some labelled cells were found in the proximal region of the limb (Fig. 5.1 C, E; white star). However, no variation in the contribution of the somites to the limb was seen between the graft and control sides, suggesting that the migration of somite cells into the limb is likely to be unaffected by the notochord graft. The contribution of labelled somites to the limb here is not unexpected, since somites 16-21 contribute to the limb musculature (Beresford, 1983). In 2/3 embryos in which labelling was found in the limb, the somites labelled included somite 16. In the remaining embryo, labelling extended to somite 15. It is very likely that some of the dye leaked into somite 16 in this embryo, or that the somites were incorrectly counted. In the two examples shown, a faint band of fluorescent signal extends laterally and posteriorly from the three posterior-most labelled segments on both the graft and ungrafted side of the embryo (Figure 5.1 C, E, G, I; white star). In the case of the first example, this can be explained by migration of some cells from these somites into the limb. However, in the second example, the labelled somites are further anterior (somites 7-12) and therefore no contribution of these somites to the limb is expected. It is unclear if this faint band of fluorescent signal represents a migration of labelled cells. However, given that it was seen consistently on both sides of the embryo, regardless of which somites were labelled, it is more likely to be an artifact of the labelling technique or autofluorescence from blood vessels in the labelled region.

5.3.2. Notochord grafts give rise to ectopic sclerotome after 24 hours

The experiment above supports a directed movement of somite cells towards the notochord graft, consistent with an attraction mediated by signals from the notochord. However, the formation of ectopic sclerotome has so far only been analysed a minimum of three days after grafting (HH24/25). During this three-day period, extensive cell proliferation, limb outgrowth, ventral closure, and turning of the embryo all make the dynamics of somite cell movement difficult to observe. To investigate the finer dynamics of this process, and the mechanism by which it is mediated, it was necessary to identify a shorter time frame in which ectopic sclerotome could be followed in response to a notochord graft. The original notochord graft experiment (Fig. 4.2A) was therefore repeated, and analysed by whole-mount *in situ* hybridisation for *Pax1* after a shorter incubation period of 24 hours.

A single embryo was grafted at HH10 and analysed after 24 hours incubation at HH18. This embryo showed ectopic *Pax1* expression in the grafted region (Figure 5.2 A, B). This ectopic expression appeared as a ventro-lateral expansion of the endogenous expression domain (Fig. 5.2B; black bracket), in contrast to the separate domain of expression typically seen two days later at HH24/25 (see Fig. 4.2 B, C). Segmentation of the ectopic sclerotome was not obvious by *Pax1* expression alone, although light and dark patches of expression could be seen.

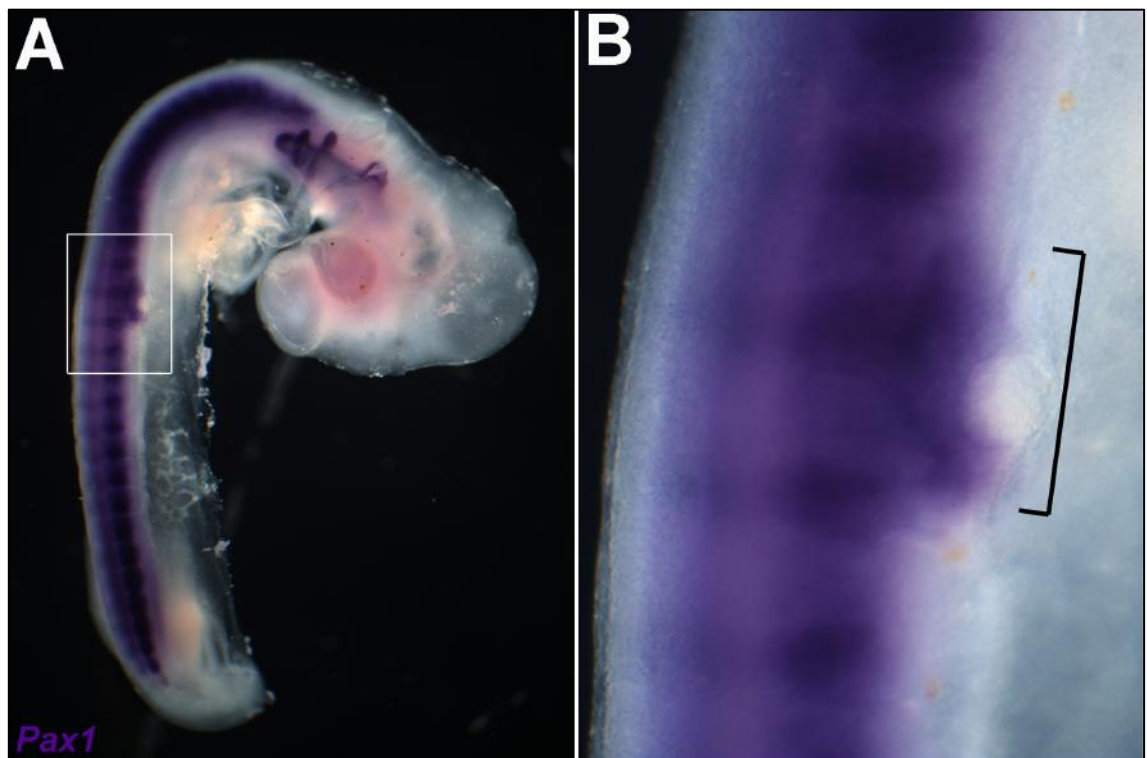


Figure 5.2. Ectopic sclerotome is seen in response to a notochord graft after 24 hours. **A.** WMISH for *Pax1* (purple) shows presence of ectopic sclerotome in a HH18 embryo, 24 hours after a notochord graft. Ectopic sclerotome is continuous with the endogenous sclerotome. **B.** Higher magnification on boxed region of A. Black bracket indicates expanded *Pax1* expression.

5.3.3. Time-lapse imaging reveals an expansion of the somites in response to a notochord graft after 8 hours in culture

The result above indicates that ectopic sclerotome has already formed 24 hours after a notochord graft. This provides a shorter time frame in which to study this process. Furthermore, this incubation period is within the upper time limit at which an embryo can survive in New culture (New, 1955), suggesting

that it may be possible to observe the response of somites to a notochord graft in real time. I therefore went on to analyse this process by time-lapse imaging of notochord grafts in culture. The notochord graft procedure was carried out in New culture and the adjacent somites and PSM on either side of the midline were labelled with DiO (Fig.5.3 A, D).

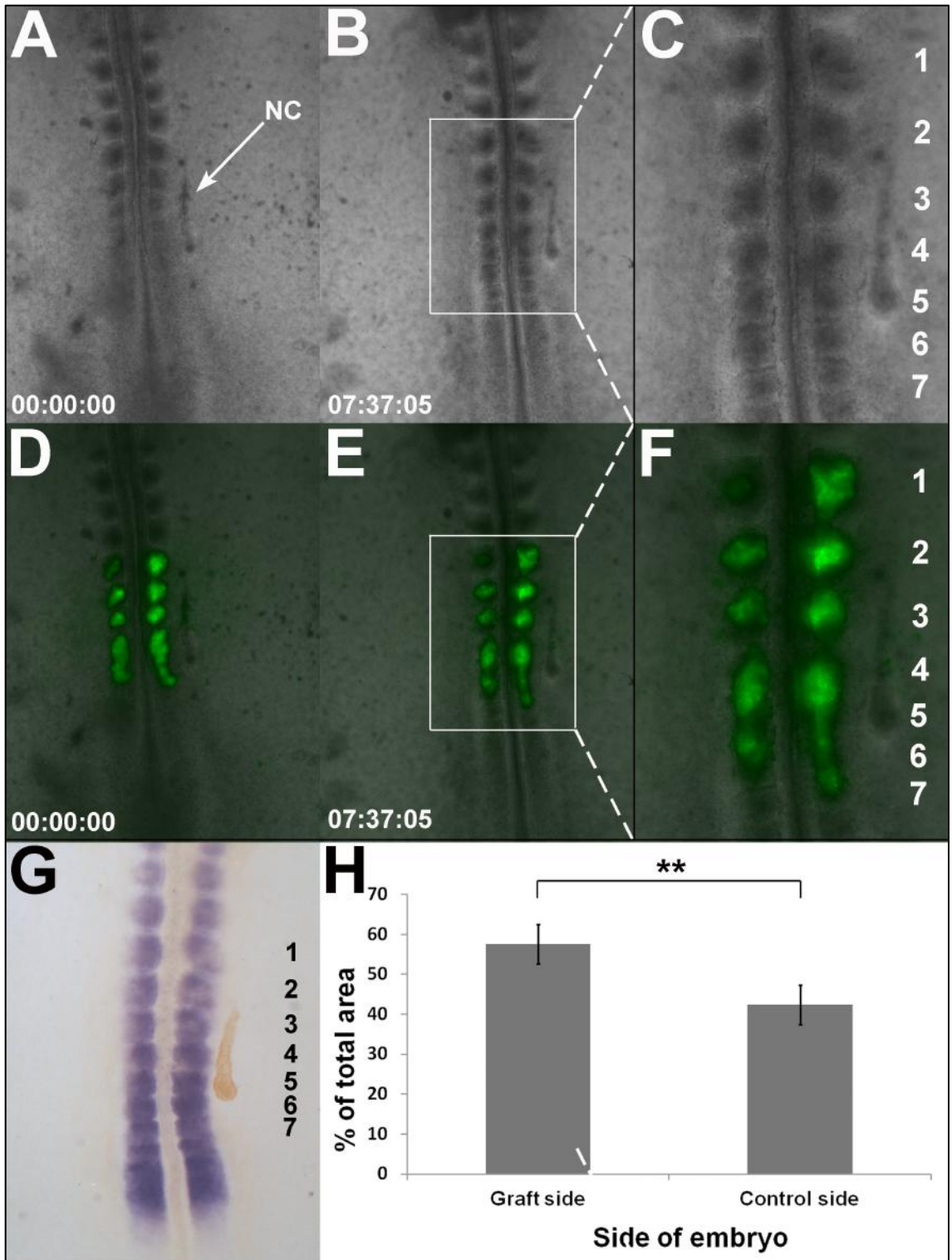
Still images at fixed time points during development are shown in Figure 5.3 A-F both in bright field (Fig 5.3 A-C), and overlaid with the fluorescent channel to show the DiO labelling (Fig. 5.3 D-F). The time-lapse movie can be seen in S1 and S2. Prior to incubation (0 hours), the grafted notochord can be seen lateral to the paraxial mesoderm on the right side of the embryo (Fig. 5.3 A, D). DiO-labelling is visible and confined to the somites and PSM at this point (Fig. 5.3D). After 7 hours 37 minutes, a further four somites had formed, all of which contained DiO-labelled cells from the rostral PSM (Fig. 5.3 B, E). In bright field, there was a clear change in the shape and size of the somites close to the notochord graft compared to the contralateral somites on the unoperated side (Fig. 5.3 B, C). This is most obviously seen in labelled somites 1-2 (rostral to the notochord graft), which show a lateral expansion towards the notochord graft, biased to the posterior part of the somite. An overall lateral expansion could be seen in labelled somites 3-5 (immediately adjacent to the notochord graft), which is most clearly visible in labelled somite four. However, in the fluorescent channel, no obvious change in the size or shape of the DiO-labelled domain accompanied the somite expansion seen in bright field (Fig. 5.3 E, F). This is most clearly seen in labelled somite one. Here, although the latero-posterior expansion of the somite can be seen in bright field (Fig. 5.3C), the expanded domain shows no visible DiO labelling (Fig. 5.3F). This indicates that the expanded domain is not derived from somite cells that were originally labelled with DiO.

After filming, the embryo was fixed and somite morphology further analysed by in situ hybridisation for *Paraxis*, a marker of the anterior PSM and epithelial somites (Burgess et al., 1995). QCPN immunostaining was then carried out to locate the quail notochord graft (Fig. 5.3G). Supporting the somite expansion observed in the bright field time-lapse images, *Paraxis* expression was also laterally expanded adjacent to the notochord graft compared to the contralateral somites on the unoperated side of the embryo. In labelled somites 1-2, this *Paraxis* expansion was biased to the posterior somite, reflecting the

shape of these somites observed in the bright field time-lapse images prior to staining. In labelled somites 3-5, *Paraxis* showed a much clearer expansion of the somites than was visible in time-lapse. Furthermore, a clear expansion of labelled somites 6-7 (caudal to the notochord graft) could also be seen, which was not visible previously. In these somites, *Paraxis* expression showed a lateral expansion that was greatest in the anterior part of the somite, the region of the somite closest to the grafted notochord.

To quantify somite expansion, notochord grafts in culture were repeated and *Paraxis* staining used to mark the somites as in Fig 5.3G. Guided by the results of time-lapse imaging and subsequent analysis of *Paraxis* expression in this embryo (Fig. 5.3 A-G), in which a visible change in somite size and shape was seen after approximately 7.5 hours, embryos were analysed after eight hours' incubation. The two-dimensional projected area of the four somites closest to the notochord graft (right) was compared to that of the contralateral somites that had not been exposed to a notochord graft (left). The measurements were carried out using bright field images of embryos stained for *Paraxis*, ensuring each image was taken at the same magnification and resolution. The area of the four somites on either side of the embryo was calculated as the number of pixels (px) containing the purple *Paraxis* stain. The purpose of these area measurements was to quantify the difference in size between somites exposed to a notochord and those that are not, and as a result the actual size of the somites is not important. Therefore, it was not necessary to convert this area measurement in pixels to SI units (e.g. μm^2). The area of the four somites measured on each side was normalised for individual size variation between embryos, by converting it to a percentage of the total area of all eight somites measured. The results are shown in Fig. 5.3H. The mean area of somites adjacent to the graft ($M= 30.1 \times 10^3 \text{ px}$ $SD= 6.9 \times 10^3 \text{ px}$; $M(\%)= 57.6$), was significantly greater than that of the control somites ($M= 22.5 \times 10^3 \text{ px}$ $SD= 6.8 \times 10^3 \text{ px}$; $M(\%)=42.4$) after 8 hours in culture (paired-sample T-test: $t(6)= 3.88$, $p=0.008$). This confirms a significant expansion of the somites in response to a notochord graft.

Figure 5.3. A lateral expansion of somites is seen in response to a notochord graft after eight hours. A-F. Time-lapse imaging of a developing embryo, in which somites adjacent to a notochord graft are labelled with DiO (green). A-C. Bright field channel only. D-F. Bright field channel overlayed with green fluorescent channel (DiO). A and D. Grafted and labelled embryo at 0 hours. B and E. Embryo approximately 7.5 hours after the graft. C and F. Zoom on boxed region in B and E. In bright field, somites adjacent to the notochord graft (numbered 1-7) are seen to expand towards the graft, but DiO is not seen in expanded part of somites. **G.** WMISH for somite marker *Paraxis* (purple) on embryo shown in A-F, eight hours after a notochord graft. The quail notochord graft (brown) was detected by an immuno-stain for the QCPN quail cell marker. *Paraxis* expression confirms that somites 1-7 are expanded towards the graft. **H.** Graph showing quantification of somite area in response to a notochord graft. The mean total area of the four somites closest to a notochord graft, across six embryos, was compared to contralateral somites (control side), after eight hours exposure to a notochord graft. The total area of somites on each side of the embryo is expressed as a percentage of the total area of all eight somites measured per embryo. A paired sample T-test shows that the greater percentage area of somites on the graft side compared to the control side is



These results demonstrate a general expansion of somites in response to a notochord graft. However, *Paraxis* staining was not always uniform within a single somite, indicating variability in the level at which it is expressed (Fig. 3G). In the normal somites not exposed to a notochord graft (left), *Paraxis* staining showed a domain of weaker expression at the lateral edge of the somite that begins at around the fifth caudal-most somite (i.e. labelled somite 3 in Fig. 5.3G) and progressively increases in size further rostrally. In the more immature somites caudal to this, *Paraxis* expression was relatively uniform throughout each somite. On the graft side, *Paraxis* staining in the four caudal-most somites (i.e. labelled somites 4-7) was consistently strong throughout the somite, similar to their contralateral partners. The domain of weaker expression was also present on this side rostral to labelled-somite 3. However, this domain of weaker expression was expanded compared to the contralateral side. This suggests not only that a notochord graft causes a general expansion of the adjacent somites, but also results in an expansion in the domain of weaker *Paraxis* expression.

5.3.4. Identifying the attractant: A Shh bead is sufficient to give rise to a change in shape and size of the somites, but this effect is variable

The results of the somite tracing experiments above demonstrate a directed migration of somite cells towards the notochord graft after three days, and an expansion of the somite after eight hours. This supports the notion of an attraction between the somites and notochord, directing the migration of sclerotome cells towards the midline to form the vertebral bodies. The next step, therefore, is to identify the nature of the postulated attractant. In the “uniform attraction” model (Fig. 4.5B), the compression of ectopic sclerotome segments was predicted to be achieved by the action of a chemoattractant secreted uniformly along the length of the notochord. The distance between the somites and notochord in normal embryos also suggests that this process is mediated by a diffusible or transportable factor that provides a directional cue in sclerotome migration. A strong candidate is the secreted signalling molecule Sonic Hedgehog (Shh).

To investigate Shh as an attractant for somite cells to the notochord, beads soaked in human Shh protein (Sigma) were used. Shh-loaded beads were first validated by their ability to induce ectopic *Nodal* expression on the right side of

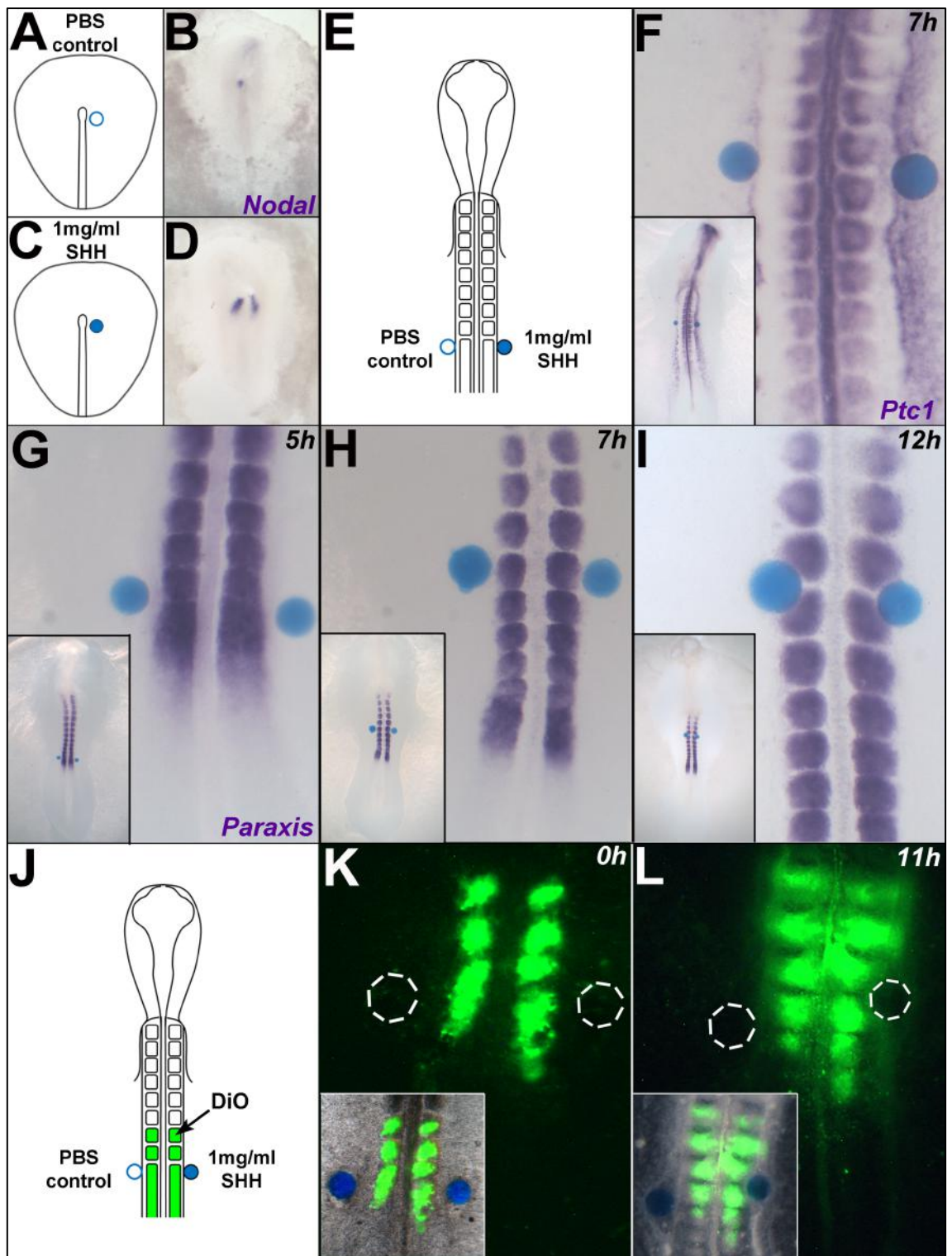
the embryo. In the normal embryo, Shh signalling in the left side of Hensen's node is known to induce left-handed expression of *Nodal* in the adjacent lateral mesoderm, a mechanism involved in the regulation of left-right organ asymmetries during development (Levin et al., 1995). A control (Fig. 5.4A) or Shh bead (Fig. 5.4C) was grafted on the right hand side of the node of HH3+/4- embryos in culture and incubated to HH6/7. Analysis by in situ hybridisation showed that in embryos grafted with control beads, asymmetric expression of *Nodal* on the left side of the embryo was maintained as normal (n=2; Fig. 5.4B). However, ectopic expression of *Nodal* on the right hand side of the embryo was seen in response to SHH-soaked beads (n=1; Fig. 5.4D). This result indicates that Shh protein secreted from the bead is able to activate downstream targets of the Shh signalling pathway in the surrounding host cells.

I then went on to test whether Shh beads can mimic the effect of a notochord graft. Single Shh and control beads were grafted to the LPM on the right and left side of the embryo respectively, adjacent to the rostral-most PSM (Fig. 5.4E). Beads were placed so that their position along the A-P axis, and distance from the paraxial mesoderm, was similar to that of the notochord graft in previous experiments. First, the ability of the beads to trigger a Shh response in the adjacent somites was assessed. The expression of the Shh receptors *Patched1* and *Patched2* (*Ptc1/2*) has been shown to be upregulated in response to Shh. Their expression can therefore be used as an indicator of hedgehog signalling (Pearse et al., 2001). After seven hours, in situ hybridisation showed ectopic expression of *Ptc1* in the lateral somites adjacent to the Shh bead on the right hand side of the embryo (Fig. 5.4F). This was seen in at least three somites rostral and caudal to the level of the bead. In the left somites adjacent to the control bead, expression was restricted to the medial somite, resembling the normal expression pattern of *Ptc1*. However, this effect was only seen in 1/3 embryos, with the remaining two embryos showing no *Ptc1* expression in the lateral somite in response to either control or Shh beads. This suggests that the ability of a bead to activate hedgehog signalling in the lateral somite is variable.

Despite this variable response, I proceeded to analyse whether Shh beads are sufficient to induce an expansion of the adjacent somites. After five hours, in situ hybridisation for *Paraxis* showed no observable difference in shape or size

of the somites adjacent to either the control or Shh bead (0/2 embryos; Fig. 5.4G). After seven hours, 2/3 embryos showed a slight expansion of the right somites adjacent to the Shh bead compared to the control side (Fig. 5.4H). This expansion was seen in the somite immediately adjacent to the bead, and at least one somite further rostral and caudal to this. After 12 hours, the shape and size of somites were more difficult to analyse, as the Shh beads had invariably moved medially (possibly by forces accompanying the early stages of ventral closure of the embryo), obscuring the lateral edge of the somites. Nevertheless, an expansion of the somites could be observed in 2/4 embryos. In both of these embryos, expansion was seen in the two somites adjacent to the bead, and in up to three somites caudal to the level of the bead. In addition to this expansion, these embryos also showed a change in the shape of somites, suggesting a 'bending' of somites towards or around the bead (Fig. 5.4I). 1/4 embryos showed no somite expansion, but did show a change in shape of somites adjacent to the bead. 1/4 embryos showed no change in the shape or size of somites adjacent to the control or Shh beads.

Figure 5.4. Can Shh beads attract somite cells? A-D. Positive control experiment. A and C. Schematics showing placement of control PBS (A) or Shh-loaded bead (C) on the right hand side of the node in HH3+/4- embryos. B After 5-6 hours, WMISH for *Nodal* (purple) shows normal asymmetric expression in response to PBS (negative control) bead. D. After 5-6 hours, Shh bead has induced ectopic *Nodal* expression on the right hand side of the embryo, confirming that Shh beads can activate Shh signalling in surrounding tissue. **E.** Schematic showing bead-graft procedure. Shh or control PBS-loaded beads were placed adjacent to the caudal-most somites on the either side of HH9-10 embryos. **F.** After 7 hours, WMISH showed up-regulation of the Shh receptor *Patched1* (purple) in the lateral somites adjacent to the Shh bead (right), but not adjacent to the PBS bead (left). **G-I.** WMISH for *Paraxis* (purple) in embryos grafted with Shh and control beads after 5, 7 and 12 hours incubation. After 7 hours, a slight expansion of somites adjacent to the Shh bead is seen. After 12 hours, embryos show an expansion and/or change in the shape of somite adjacent to the Shh bead. In F-I, main panel shows high magnification image of region of interest, inset shows lower magnification image of whole embryo. **J.** Tracing somites next to a bead graft. Caudal somites and rostral PSM adjacent to Shh and control beads were labelled with DiO (green). **K.** Embryo with bead graft and DiO-labelled somites prior to incubation (0 hours). **L.** After 11 hours incubation, DiO-labelled cells appear to surround the Shh bead, suggesting a migration of somite cells towards the Shh bead. In K and L, main panel shows green fluorescent channel alone, inset shows overlay of bright field and green fluorescent channels. Dotted circles = outline of beads.



5.3.5. Identifying the attractant: DiO-labelling suggests a migration of somites towards a SHH bead, but this effect is variable

The expansion of *Paraxis* expression in response to a Shh bead resembles the response of somites to a notochord graft after eight hours. However, this could also be indicative of an increase in somite proliferation (which is known to be mediated by Shh signalling from the notochord and floor plate; Fan et al., 1995) and not a result of an attraction of the somites towards the bead. To investigate how a bead affects the migration of somite cells, the somites adjacent to the beads were traced on either side of the embryo using DiO (Fig. 5.4J). Labelled embryos were imaged at 0 hours (i.e. immediately after labelling; Fig. 5.4K), and analysed after 10-11 hours in culture (Fig. 5.4L).

In 1/2 embryos, DiO-labelled somite cells surrounded the Shh bead after 10 hours in culture, an effect that was not seen on the control side. This is seen as a green fluorescent ring around the Shh bead on the right hand side of the embryo, which is clearest when viewed in the fluorescent channel alone (Fig. 5.4L). This is accompanied by an expansion and change in shape of the DiO-labelled somites adjacent to the Shh bead. The greatest effect is seen in the second and third most rostral labelled-somites in the example shown (Fig. 5.4L). The second labelled somite shows a lateral expansion of the DiO-labelled domain adjacent to the Shh bead. The next posterior somite (the third labelled somite) shows a change in shape of the DiO-labelled domain, which appears to tilt towards the bead. These expansions and changes in shape are not seen in the contralateral somites adjacent to the control bead. This result is indicative of an expansion of somites mediated by the Shh bead, and supports a migration of somite cells towards the bead. However, the second embryo analysed in the same way showed no expansion or migration of DiO labelled cells adjacent to either the Shh or control beads. Again, the response of somites to a Shh bead appears to be variable between embryos.

5.3.6. Identifying the attractant: A cell pellet secreting Shh is sufficient to give rise to a change in shape and size of the somites, but this effect is still variable

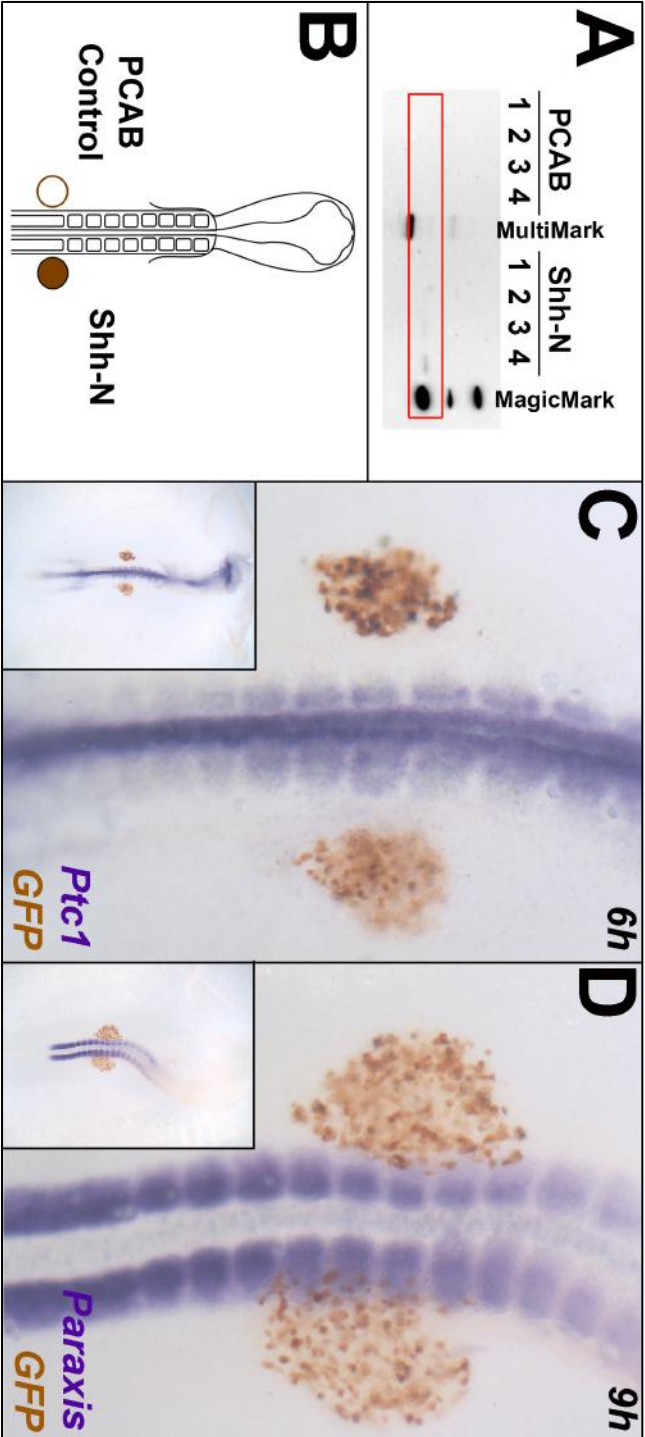
The results obtained from the bead experiments above are highly variable. One major technical problem with these experiments is that the affigel-blue beads have a tendency to move during culture. At best, this made it difficult to ensure that the distance between the bead and the somite, and the position of the bead along the A-P axis, was roughly equal between the control and Shh sides (see the difference between the bead positions at 0 and 10 hours in culture in Fig. 5.4 K, L). At worst, forces during development of the embryo would push the bead out of its pocket in the LPM and cause it to float away from the somites. These embryos were not included in the analysis, nor were those in which the difference in bead position between the right and left side was too great to be comparable. This exclusion made it difficult to obtain a sufficient number of repeats for thorough analysis, and could be a contributing factor to the variability seen in the results. Another drawback of using beads is that they can only hold a fixed amount of protein, and it is unclear at what point this protein runs out.

These problems can be improved by substituting protein-soaked beads with cell pellets transfected to express the protein of interest continuously. I therefore repeated the bead experiment above using pellets of 293T human embryonic kidney cells transfected with a PCAGGS expression plasmid (Niwa et al., 1991) containing the cDNA sequence of the N-terminal signalling domain of Shh (Shh-N) (Roelink et al., 1995; Oberg et al., 2002). In this plasmid, the *Shh-N* insertion is under the control of a β -actin promoter, and inclusion of an internal ribosomal entry site (IRES) upstream of an enhanced GFP (EGFP) reporter gene leads to the expression of both the insertion and GFP reporter from independent transcripts. Cells transfected with a PCA β expression vector (also containing an IRES linked to a GFP reporter gene) with no insertion were used as a negative control in place of PBS-soaked beads. All transfected cells therefore express the GFP reporter gene.

The secretion of the Shh-N protein from the transfected cell pellets was validated by a Western blot of the FBS-DMEM hanging drop medium surrounding the Shh and control cell pellets after incubation for 48 hours. The

total amount of medium collected (40 μ l) from each of the experimental and control pellets was loaded in ascending amounts across four lanes (Fig. 5.5A; 1= 5 μ l; 2= 7.5 μ l; 3= 15 μ l; 4= 30 μ l). The blot was probed with an antibody against the secreted domain of the Shh protein, SHH-N (Table 2.10). A band at around 20kDa (the predicted Mr of the Shh-N peptide) was seen in the third and fourth lane of the sample, taken from cells transfected with the PCAGGS-Shh-N expression construct. No bands were seen in any lanes containing the negative control sample. This verifies the secretion of Shh protein from the cell pellets.

Figure 5.5. Can cell pellets expressing Shh attract somite cells? **A.** Western blot of cell culture medium surrounding cell pellets transfected with PCAG-Shh-N or PCA β empty vector, two days after transfection, confirms expression of Shh-N from transfected cell pellets. The total amount of medium collected (40 μ l) from each of the experimental and control pellets was loaded in ascending amounts across four lanes (1= 5 μ l; 2= 7.5 μ l; 3= 15 μ l; 4= 30 μ l), and probed using an anti-SHH-N antibody **B.** Schematic showing pellet-graft procedure. Pellets of cells transfected with a PCAG-Shh-N expression plasmid were grafted adjacent to the caudal somites on the right side of HH9-10 embryos. Procedure is the same as Fig. 5.4E, using pellets instead of beads. **C.** After 6 hours incubation, WMISH shows *Patched1* (purple) is upregulated in the lateral somites adjacent to the Shh pellet (right), and not adjacent to PBS pellet (left). Transfected cells express GFP, and are detected by an anti-GFP immuno stain **D.** After 9 hours, WMISH for the somite marker *Paraxis* shows an expansion of somites towards the Shh cell pellet (brown). In C and D, main panel shows high magnification image of region of interest, inset shows lower magnification image of whole embryo.



I then went on to test whether a Shh cell pellet can mimic the effect of a notochord graft in culture. As in the bead experiments, Shh and control pellets were grafted to the LPM on the right and left side of the embryo respectively, adjacent to the rostral-most PSM (Fig. 5.5B). Again, the ability of the Shh pellet to activate hedgehog signalling in the adjacent somites was analysed by in situ hybridisation for the *Ptc1* receptor. In 1/2 embryos, *Ptc1* was upregulated in the lateral somites adjacent to the Shh pellet after six hours in culture (Fig. 5.5C). This was seen in at least three somites rostral and caudal to the level of the pellet. Adjacent to the control pellet, *Ptc1* expression was restricted to the medial somite. Although this suggests an upregulation of hedgehog signalling in the lateral somites in response to the cell pellet, the second embryo showed no change in expression of *Ptc1* in response to the Shh bead. Further repeats are required to verify this result. The shape and size of somites was also analysed in response to the cell pellets by *Paraxis* in situ after nine hours in culture. As with the bead experiments, the results were variable. In 2/4 embryos, a clear lateral expansion of the right side somites was seen adjacent to the Shh cell pellet compared to the control side (Fig. 5.5D). The remaining two embryos showed no difference in the shape and/or size of somites adjacent to the control or Shh pellets.

5.4. Discussion

5.4.1. Somite cells are attracted to the notochord

The results of somite tracing in notochord-grafted embryos demonstrate a movement of somite cells towards the ectopic notochord three days after grafting. This supports the notion of an attraction of somite cells towards the notochord. The dynamics of labelled segments, which bend and compress towards the grafted notochord, bear a strong resemblance to that predicted in the “uniform attractant” model, proposed in chapter 4. Overall, this adds to evidence that signals from the notochord somehow act as a directional cue for somite cells migrating to the midline to form the vertebral column.

The sharp boundaries between labelled somites in these embryos (seen as distinct red and green stripes) are consistent with the results of somite fate mapping in the vertebral column (in chapter 3), where somite boundaries were

maintained up to cartilage formation. As before, this is compatible with the opposing properties of the rostral and caudal sclerotome halves, which do not mix and form a boundary when placed adjacent to each other (Stern and Keynes, 1987). This is an essential component of the uniform attractant model, as discrete somite segments must be maintained throughout migration in order for them to be compressed in response to a notochord graft.

5.4.2. Is this attraction specific to the sclerotome?

During normal development, it is specifically the *Pax1*-expressing cells of the sclerotome that migrate to the midline to form the vertebral bodies (Ebensperger et al., 1995) This suggests that out of all the compartments of the somites, only the ventral sclerotome can respond to the predicted attractive signals from the notochord, either because only these cells are competent, or because the cells in other compartments are too far away to respond to the attractive signals. We can speculate that the labelled cells that migrate ectopically towards the grafted notochord are the same that form ectopic sclerotome. However, it is important to highlight that labelling whole somites with Dil and DiO in this experiment does not distinguish between different precursor populations within a single somite. Further work is therefore required to determine the identity of the ectopically migrating cells. This was attempted by subsequent analysis of labelled embryos by in situ hybridisation for the sclerotome marker *Pax1*. Unfortunately, lipophilic carbocyanine dyes (Dil and DiO) are largely washed out during the in situ procedure and therefore it could not be determined whether the labelled cells were of sclerotomal identity. An alternative approach would be to specifically label (and subsequently trace) individual somite compartments, rather than the whole somite. In principle, it may be possible to electroporate somite precursors in the node and primitive streak, with a fluorescent reporter construct driven by the regulatory elements of compartment marker genes (such as *Pax1* in the sclerotome) if these can be identified.

It is important to note that although all of the midline vertebral cartilages are formed by the sclerotome, not all sclerotome cells form the midline cartilages. The ribs, for example, have been shown to derive from a population of cells within the sclerotome (Huang et al., 2000a ; Evans, 2003). How do these cells evade the mechanism of attraction from the notochord? One possibility is that

the more dorso-lateral position of this subpopulation, close to the border between the sclerotome and dermomyotome (Christ and Scaal, 2008), means that the concentration of attractant it receives is too low to elicit a medial migration, or that opposing signals from lateral sources dominate in these cells. Alternatively, lateral somite cells may lack competence to respond to the attractive effects of Shh. These are interesting questions for the future.

5.4.3. Somite expansion: Attraction, proliferation or both?

As described above, the ventro-lateral migration of the labelled somites over three days in response to a notochord graft provides evidence for an attraction mechanism. Further to this, results over shorter time frames suggest that the notochord mediates a significant expansion of somites in response to a notochord graft after eight hours in culture. This expansion is reminiscent of the “bulging” of the ventro-medial somite towards the notochord that has been reported to occur as the basement membrane delaminates in this region to form the mesenchymal sclerotome (Christ and Ordahl, 1995). Further expansion of this tissue is caused by the secretion of an ECM rich in hydrated glycoproteins (Solursh et al., 1979), and an increase in sclerotome cell proliferation induced by Shh from the notochord (Fan et al., 1995; Teillet et al., 1998). It is therefore likely that the same process occurs ectopically in the lateral somite adjacent to the notochord graft, causing the observed expansion of the somites towards the graft. However, the epithelial to mesenchymal transition, whilst causing an overall expansion of the sclerotome, is also essential for the sclerotome to migrate. It is possible that the ectopic notochord is mediating both an expansion and an attraction of the sclerotome towards it. The result of *Pax1* staining 24 hours after a notochord graft supports this. At this earlier stage, the ectopic sclerotome was seen as an expansion of the endogenous sclerotome, whilst two days later this has separated into two separate domains of *Pax1* expression. This suggests that the notochord graft first expands the sclerotome laterally, before the opposing attractive forces from the endogenous and ectopic notochord eventually separates the ectopic sclerotome from the endogenous portion. .

However the laterally expanded portion of the somites adjacent to the notochord contained no DiO-labelled cells, suggesting that it does not form as a result of a “bulging” or migration of DiO-labelled somite cells towards the

graft. It is possible that the labelling and imaging method used was not sufficient to detect DiO signal in the expanded region. The epithelial to mesenchymal transition of the sclerotome, and subsequent migration towards the notochord, means that these cells will be more dispersed. The resolution at the magnification used (2x or 5x objective), or exposure in the fluorescent channel during imaging, may be insufficient to detect the signal from these more dispersed cells.

The DiO-labelling method was chosen as it allows the tracing of endogenous cells, but it brings with it a number of problems. Although the concentration of DiO was optimised to achieve relatively uniform labelling across the somites, the method unavoidably produces regions of lighter and darker signal. In this case, the transplantation of somites from transgenic GFP-expressing embryos (Sang, 2004) may be required to ensure complete and uniform labelling. This would enable the tracing of somite cell movements over the shorter time frame with greater accuracy, and would also allow further analysis of the location of somite cells in sections by anti-GFP immunostaining. However, the same problems apply to this technique as the studies that investigated the resegmentation process using quail-chick somite grafts (Beresford, 1983; Bagnall et al., 1988; Huang et al., 1996; Huang et al., 2000b). It is difficult to ensure that transplanted somites are placed in the correct orientation with respect to their rostro-caudal pattern. Mis-orientation of the grafted somite could cause “like” sclerotome halves to mix, disrupting their normal segmentation pattern (Stern and Keynes, 1987). However, for the purposes of tracing the movement of these cells towards the notochord graft, strict maintenance of normal segmentation is not essential.

Quantification of somite proliferation in response to a notochord will help to determine whether the degree to which proliferation increases can account for the expansion seen in the somites. An experiment to address this is in progress, in which eight-hour notochord grafted embryos are double-stained using antibodies against the phospho-histone H3 (ser10) mitosis marker to detect proliferating cells and Not1, a notochord marker. Transverse sections of stained embryos are then DAPI-stained, so that the proportion of proliferating cells (the mitotic index) in a somite can be manually counted for each somite and compared between the graft and control side.

5.4.4. A notochord graft also disrupts medio-lateral and dorso-ventral patterning of the somite

In the original studies which investigated dorso-ventral and medio-lateral patterning of the somite, it was found that an ectopic notochord grafted lateral to the somites induces *Pax1*-expressing sclerotome at the expense of *Pax3*-expressing dermomyotome in the lateral somite (Brand-Saberi et al., 1993; Pourquié et al., 1993; Fan and Tessier-Lavigne, 1994; Ebensperger et al., 1995; Vasiliasuskas et al., 1999). As I have used the same notochord graft assay here, it is likely that the notochord graft “ventro-medialises” the lateral somites to some extent, expanding the sclerotomal compartment laterally. The results described above support such a process. *Pax1* staining of embryos 24 hours after a notochord graft revealed a ventro-lateral expansion of the endogenous sclerotome. Furthermore, *Paraxis* staining in somites after eight hours exposure to a notochord graft was also indicative of an induction of sclerotome in the lateral somites. *Paraxis* is initially expressed in all somite cells, but is progressively downregulated in the sclerotome upon its differentiation (Burgess et al., 1995). The expanded domain of weak *Paraxis* expression in somites adjacent to a notochord graft could represent a domain of ectopic sclerotome induction in the lateral somite.

Although these results are suggestive of a disruption to dorso-ventral and medio-lateral patterning, further work is required to confirm this. WMISH for *Pax1* and *Pax3* after eight-hour notochord graft cultures will elucidate the relative proportion of sclerotome and dermamyotome that is specified adjacent to the notochord graft. Medio-lateral patterning of the somite could also be assessed through analysis of the expression of the early medial and lateral somite markers present before differentiation of the sclerotome and dermomyotome, *Sim1* (Pourquié et al., 1996) and *Swip1* (Vasiliasuskas et al., 1999).

One important point, however, is that newly-induced sclerotome in the lateral somite will still have the same spatial periodicity as the endogenous sclerotome upon its formation. Even if the ectopic sclerotome seen at HH24-25 is entirely derived from this newly-specified sclerotome, this still provides evidence that the notochord influences the spatial periodicity of the sclerotome and later cartilage.

5.4.5. Does *Shh* mediate the attraction? Lessons from the neural tube

Parallels have been drawn between dorso-ventral patterning of the somites and that of the neural tube (Fan and Tessier-Lavigne, 1994). The neural tube is patterned into specific domains of neural fate along its D-V axis by a concentration gradient of *Shh* secreted from the ventral floor plate and notochord (Echelard et al., 1993; Roelink et al., 1995; Briscoe and Ericson, 2001). After specifying ventral cell types in the neural tube, *Shh* plays further roles in the development of ventral neurons. *Shh* from the floor plate maintains the proliferation of these progenitor populations (Merchán et al., 2007), and acts as a chemoattractant to guide axon growth cones ventrally. This latter role has been demonstrated in commissural neurons (Charron et al., 2003) and oligodendrocytes in the optic region of the neural tube (Merchán et al., 2007). Indeed, there are many examples in which morphogens play additional roles in the development of the very cells that they originally specify (Boliventá and Martí, 2001).

In the somites, *Shh* expression is maintained in the notochord long after specification of the sclerotome, as is the expression of hedgehog signalling components such as *Ptc1* in the somite (Echelard et al., 1993; Borycki et al., 1998). This suggests that *Shh* plays further roles in somite development besides specification of somite compartments. As in the neural tube, *Shh* is known to play an additional role in maintaining survival and proliferation of the sclerotome after it has been specified (Fan et al., 1995; Teillet et al., 1998). Could *Shh* from the notochord act as a chemoattractant in this system too, providing a directional cue to sclerotome cells as they migrate to the midline?

5.4.6. Multiple roles for *Shh* from the notochord in somite development

It is clear from the discussion above that *Shh* from the notochord mediates a number of important processes in somite development. Complicating matters further, all these processes overlap in their timing, occurring from around the fourth caudal-most somite onwards in the chick. This makes designing experiments to dissect its role in one aspect alone very challenging.

Although results were variable, the bead and pellet graft experiments suggest that Shh is sufficient to expand the somites towards it, mimicking the effect of a notochord graft. However, as discussed in the case of notochord grafts, it is unclear to what extent an expansion of the somites is due to specification of ectopic sclerotome in the lateral somite, an increase in somite proliferation, or an attraction of sclerotome cells towards the Shh source.

5.4.7. Is Shh sufficient to mimic the attractive effect of a notochord in culture?

The migration of DiO-labelled somite cells towards a Shh bead after ten hours in culture (Fig. 5.4L) demonstrates that Shh alone may be sufficient to attract the sclerotome. However, this result was seen in only one of the two embryos analysed. Further tracing of somites in response to Shh beads and pellets is required to verify this result. Results from both the bead and pellet experiments were highly variable. This variability is seen across all parameters analysed. 33% to 50% of embryos showed an upregulation of hedgehog signalling in the lateral somites (as indicated by *Ptc1* expression) in response to a Shh bead or cell pellet respectively. A similar proportion of embryos showed an expansion, change in shape, or directed migration of the somites after 7-12 hours exposure to Shh from a bead or cell pellet. It is reasonable to speculate that those embryos in which hedgehog signalling is upregulated in the lateral somite, are the same which show a downstream response in somite cell behaviour. However, a greater number of cases are required across all experiments before conclusions can be drawn.

An important consideration in these experiments is that the migratory behaviour of the sclerotome may not be a simple binary response to the presence or absence of a chemoattractant, but according to the principle of positional information may be dependent upon the specific concentration of the attractant to which it is exposed (Wolpert, 1969). If this is the case, a response of the somite will not be observed unless the appropriate concentration of Shh is delivered by the bead or pellet. The concentration of Shh secreted by cell pellets can be measured by quantitative analysis of the Western blot. However, the rate of secretion cannot be easily altered aside from using pellets of different sizes (in this experiment, I used pellets comprised of 500 cells, but this can be altered). In the beads, it is difficult to measure the rate of secretion,

but it would be easier to alter this parameter by changing the initial concentration of protein that was loaded onto the bead. The concentration of 1 mg/ml that was used in this experiment was chosen as a starting point based on the concentration used in other studies (e.g. in digit duplication experiments in the limb; Sanz-Ezquerro and Tickle, 2000). Loading beads with progressively lower concentrations of Shh may be required to identify whether variability in the response of the somites is due to changes in Shh concentrations received by the cells.

Furthermore, the concentration gradient of the chemoattractant may also be an important factor determining whether or not a sclerotome cell migrates towards the source, as has been shown to be the case in the guidance of commissural neurons in the neural tube (Charron et al., 2003). It may be challenging to mimic the concentration gradient of Shh that is normally established by the notochord using beads or pellets. The gradient could vary between embryos as a result of a large number of factors other than the rate of Shh secretion by the bead. For example, the distance of the bead or pellet from the somites varies during culture; thereby affecting the distance the molecule has to travel to exert an effect. Another factor is a variation in the size (and therefore surface area) of the bead, which will affect not only the total amount of protein loaded onto the bead, but also the rate at which it is secreted. Changes to these factors from embryo to embryo could lead to altered Shh gradients, and could partially explain the variability that was seen in the response of somites to the bead or pellet.

5.4.8. Is Shh required for the notochord to exert its attraction?

Another approach is to test whether the notochord can exert its chemoattractive effect in the absence of Shh signalling. One way to address this question would be to conduct a normal notochord graft, whilst blocking signal transduction in the responding somites by exposing the embryo to inhibitors of the hedgehog signalling pathway, such as cyclopamine (Cooper et al., 1998; Incardona et al., 1998). Cyclopamine binds to Smoothed (Smo), blocking downstream activation of *Gli* and downstream transcription of target genes (Chen et al., 2002). However, experiments in which Shh signalling is disrupted bring similar problems to experiments in which an ectopic source of Shh is added. Inhibition of the response to hedgehog signalling in the somites

using cyclopamine will also inhibit the formation of sclerotome and its subsequent proliferation (Incardona et al., 1998). For the experiment to be meaningful, therefore, it must be designed to ensure the role of Shh in the migration of sclerotome is tested in isolation from its other effects. This is a major challenge to this study.

5.4.9. Do other factors play a role in regulating sclerotome migration and attraction?

This study has focused on testing the strongest attractant candidate, Shh, but there are a number of other candidate molecules that may either act alone, or in combination to regulate sclerotome migration.

The BMP inhibitors Noggin, Chordin and Follistatin, which are secreted by the node and notochord, play important early roles in embryonic patterning (Tonegawa and Takahashi, 1998; Streit and Stern, 1999; Dias et al., 2014) and do continue to be expressed in the more rostral notochord at lower levels. Noggin is sufficient to induce *Pax1* in the sclerotome, and probably acts through an alternative pathway to Shh, bringing about a quicker induction than either pathway could achieve alone (McMahon et al., 1998). Perhaps Noggin also plays a later role in sclerotome attraction. Another possible candidate is the hormonal peptide Elabela (Ela; aka Toddler), a recently discovered secreted signalling molecule that binds and activates Apelin receptors on the cell surface (Pauli et al., 2014). This peptide sequence is conserved across the vertebrates and has recently been cloned in chick (B. Reversade, 2015, unpublished). Interestingly, it has been shown that in zebrafish, Ela from the notochord acts as a chemoattractant to guide blood vessel precursors (angioblasts) from the LPM to the midline (Helker et al., 2015). Here they form the primary axial blood vessels: the dorsal aorta and cardinal vein. This process bears an obvious similarity both in terms of migratory dynamics and in timing, with sclerotome migration. In order to test whether Ela is a viable attractant candidate, it would first be necessary to determine whether Ela and Apelin receptors are expressed by the chick notochord and sclerotome at the appropriate time in development.

5.5. Summary

On the basis of the results of inter-regional notochord grafts, it was proposed in chapter four that the notochord plays an attractive role in the guidance of sclerotome cells to the notochord, where they form the vertebral bodies. In this chapter, I first investigated whether the notochord does indeed attract the sclerotome towards it. Tracing somites adjacent to a notochord graft showed a directed migration of labelled somite cells towards the ectopic notochord over three days, suggesting that the cells of the somite are attracted to the notochord. Using time-lapse microscopy, I attempted to trace the migration of labelled somite cells towards a notochord graft in real-time, however no such migration could be observed over a shorter time frame of 24 hours. However, an ectopic notochord was found to give rise to a significant expansion of the somites over this shorter time frame. It was proposed that as well as inducing the sclerotome (Brand-Saberi et al. 1993; Pourquié et al. 1993; see section 1.4.1) and mediating its expansion (Fan et al. 1995; Teillet et al. 1998), the notochord also plays an additional role in attracting the sclerotome towards the midline. I therefore went on to investigate what mediates this attraction. After identifying Shh as a potential chemoattractant candidate, I tested whether an ectopic source of Shh lateral to the somites can mimic the attractive effects of a notochord. Although results were variable, tracing of somites did suggest a movement of labelled cells towards ectopic sources of Shh. Further work is required to confirm whether Shh acts as a chemoattractant in this context, and whether it acts alone.

Chapter 6 : Exploring an alternative method for studying the role of the notochord in vertebral segmentation

6.1. Introduction

The notochord graft experiments of the previous two chapters isolate the notochord from the other axial tissues, providing a simple system in which to investigate its specific role in somite and vertebral development. However, the graft does not perfectly mimic the notochord in its native state, as its removal from the donor embryo results in a release from the tension that is generated by other tissues. This release of tension causes two main problems. First, the grafted notochord shrinks considerably in length. The effect of this on the cellular structure of the notochord has not been investigated, but it is likely to be altered dramatically by such a change. There is growing evidence that the mechanical forces experienced by cells during development are transduced to regulate a diverse range of cellular processes such as proliferation, differentiation and migration (reviewed by Mammoto and Ingber, 2010; Eyckmans et al., 2011). Changes in mechanical stress caused by release of tension in the notochord may therefore have consequences for the subsequent development of the notochord and its signalling activity. Second, the notochord tends to bend after excision, in the absence of the forces that keep it parallel to the midline. This means that some parts of the grafted notochord sit further from the adjacent somites than others. This may have a considerable effect on the local concentration of signals from the notochord received by the neighbouring somites. I therefore sought to develop an assay that corrects these problems.

It is well established that grafts of the primary organiser (Hensen's node in chick) to peripheral regions of the embryo leads to the formation of a secondary axis (Spemann and Mangold, 1924; Waddington, 1930; Waddington, 1932). This secondary axis is formed as a result of the ability of the node to self-differentiate to form an ectopic notochord (Spratt, 1955; Selleck and Stern, 1991; 1992a), to contribute to and recruit host cells to form ectopic somites (Nicolet, 1971; Hornbruch et al., 1979; Selleck and Stern, 1991), and (if the graft is young enough), to induce and pattern neural tissue in the host ectoderm (Waddington, 1932; Storey et al., 1992). The notochord is formed

from a precursor population in the rostral Hensen's node (Selleck and Stern, 1991; 1992), and is laid down as the node retracts caudally along the midline after gastrulation. Grafts of only the notochord precursor population within the node into the PSM have been found to retain their fate and generate an ectopic notochord (Selleck and Stern, 1992a). We therefore reasoned that a graft of this precursor population to the correct position in the early embryo would lay down an ectopic notochord lateral to the forming somites. The retraction of the node posteriorly should generate an ectopic notochord that is reasonably linear, parallel to the host somites, sidestepping the problems described above. In this chapter I investigate the suitability of the notochord precursor graft as an assay to study the role of the notochord in vertebral segmentation.

6.2. Materials and Methods

6.2.1. Grafts of Hensen's node notochord precursors

Chicken host embryos at stage HH4+ to HH5 were prepared for New culture as previously described (section 2.1.5). A small pocket was made in the epiblast adjacent to the primitive streak, at a level equivalent to the middle of the length of the primitive streak. Donor quail embryos at stage HH4/4+ were collected in Tyrode's saline and pinned flat on a Sylgard (Dow Corning) coated dish with the dorsal surface uppermost. A 'wedge' shape corresponding to the territory of prospective notochord cells (Selleck & Stern, 1991; 1992) was excised from the midline of the Hensen's node, anterior to the pit. The graft was transferred to the host embryo using a Gilson pipette in an albumen/saline mixture (section 4.2.2), and tucked into the pocket adjacent to the streak. Cultures were incubated for 24 hours. The procedure is shown in figure 6.1A.

6.2.2. Preparation of FGF4 beads

Heparin-coated acrylic beads (Sigma) were incubated overnight at 4°C in 0.1 µg/µl Human Fibroblast Growth Factor 4 (FGF4) protein (R&D systems) in PBS containing 0.1 µg/µl BSA. Beads incubated in PBS with 0.1 µg/µl BSA were used as negative controls.

6.2.3. FGF4 bead positive control graft

As a positive control, the release of *FGF4* from beads was assayed by their ability to induce the prospective neural marker *Sox3* in a competent region of the area opaca (Streit et al., 2000; Yardley and Garcia-Castro, 2012).

Individual beads were grafted to the area opaca of an embryo in New culture (section 2.1.5) at HH3+, at a level anterior to the node. FGF4-soaked beads were placed on the left and negative control beads in the equivalent position on the right. Cultures were incubated for 4-5 hours. This procedure is illustrated in figure 6.3A.

6.3. Results

6.3.1. An ectopic notochord expands the adjacent host paraxial mesoderm

A wedge-shaped portion of a quail donor's Hensen's node at stage HH4 was grafted adjacent to the primitive streak on the right hand side of a stage HH4+/HH5 chick embryo (Fig. 6.1A). The portion of the node to be grafted was carefully excised to ensure that it only contained medial cells rostral to the pit (the notochord progenitors) and no cells from the more lateral node, which are known to give rise to the medial somites (Selleck and Stern, 1991). Grafted embryos were incubated overnight. The paraxial mesoderm was then analysed by WMISH for the somite and rostral PSM marker *Paraxis*, followed by immunostaining with the quail-specific antibody QCPN to locate graft-derived cells.

The position of the graft was carefully chosen to ensure that the graft lay adjacent to the host somites and remained there despite the extensive cell movements of gastrulation and neurulation. This position was guided by the experiments of Hornbruch et al. (1979), who used node grafts at different positions to investigate the origin of somites induced during secondary axis formation. It was found that grafts placed adjacent to the primitive streak generate a secondary axis adjacent to the host somites (Hornbruch et al., 1979; the results of this study with regards to the origin of somites in the secondary axis is discussed in 6.4.2 of this chapter). Moreover, the axial level at which the graft was placed is adjacent to the boundary between the

position of somite progenitors anteriorly and the more lateral mesoderm progenitors posteriorly within the primitive streak (Psychoyos and Stern, 1996).

After 24 hours in culture, the notochord progenitor graft had generated an ectopic notochord that was typically positioned just lateral to the host somites (23/24 embryos; Fig. 6.1 B-D). In a minority (6/23) of these embryos, no difference in *Paraxis* expression was observed between the graft and control side of the embryo (not shown). However, in the majority of embryos (17/23), a clear expansion was seen on the graft side compared to the control side. The extent of this expansion was variable between the 17 embryos that showed an effect. Some embryos showed a general increase in the size of the right hand somites and/or PSM laterally towards the graft (6/17 embryos; Fig. 6.1 B, E), similar to (but typically more extensive than) the expansion of somites seen in response to a notochord graft in chapter 5 (Fig. 5.3). However, in the majority of embryos (11/17), this expansion was accompanied by the formation of segmented blocks of ectopic *Paraxis* expression running rostro-caudally, lateral to the notochord graft (11/17 embryos; Fig. 6.1 C, D). Transverse sections show that these ectopic structures have an epithelial arrangement with a central lumen (Fig. 6.1 F, G). This morphology and the fact that they express *Paraxis* suggests that these blocks are somites.

Figure 6.2. A notochord precursor graft generates an ectopic notochord, which expands the adjacent paraxial mesoderm. **A.** Notochord precursor graft procedure. Notochord precursors from a HH4 quail node (red triangle) were grafted on the right of the primitive streak of a HH5 chick host, as shown. **B-D.** After overnight incubation, a QCPN immunostain (brown) showed the graft had generated an ectopic notochord on the right side of the embryo. WMISH for *Paraxis* (purple) showed an expansion of paraxial mesoderm next to the ectopic notochord (right). The extent of this expansion was variable, indicated by the three example embryos shown. **B.** Lateral expansion of somites and PSM. **C and D.** Lateral expansion and formation of ectopic somites. Dotted line indicates plane if transverse section. **E-G.** Transverse sections of embryos in B-D. Ectopic somites have an epithelial organisation with a central lumen. (ENC=Ectopic notochord, ES= ectopic somites)



Cells in a wedge-shaped region rostral to the primitive pit are committed to a notochordal fate in the HH4 embryo. Immediately lateral to this compartment sits a mixed population of cells that will contribute to the somites and notochord, but are not committed to either fate at this stage (Selleck and Stern, 1991; 1992). It was important therefore, that only notochord progenitors were grafted in the experiment above, as somite precursors contaminating the graft may contribute to the ectopic somites. QCPN immunostaining was carried out on all embryos after *Paraxis* in situ hybridisation to locate quail (graft-derived) cells. In all embryos, quail cells were confined to the grafted node and secondary notochord, with no co-localisation of *Paraxis* and QCPN staining (Fig. 6.1B-G). This confirms that the ectopic and expanded somites are derived entirely from the chick host.

6.3.2. Time-lapse movies show a transient stage at which somite cells appear to be attracted towards the ectopic notochord

The results above raise a number of questions. First, does the grafted node retract from rostral to caudal, generating a notochord in the same orientation as the host, or vice versa? Second, from where in the host do the ectopic somites originate? As discussed in the previous chapters in the case of notochord grafts, they could be formed by a proliferation (Fan et al., 1995; Teillet et al., 1998) and/or attraction of the endogenous somites, or be induced de novo from more lateral mesoderm as a result of BMP inhibition (Tonegawa and Takahashi, 1998; Streit and Stern, 1999). Third, do the ectopic somites form simultaneously or sequentially from rostral to caudal, similar to endogenous somites? To begin to answer these questions, I repeated the experiment and followed it by time-lapse video microscopy of embryos from the ventral side of the embryo. Four movies were made in total, and two of these movies are shown in S3 and S4. Still images from set time points during the development of the embryos in movie S3 and S4 are shown in Fig. 6.2 A-E and G-K respectively.

In general, the development of embryos across all four movies was very similar, though the extent of paraxial mesoderm expansion and the timing at which critical events occur were somewhat variable. Immediately after grafting (0 hours), the graft of prospective notochord cells can be seen as a dark spot (white arrow) on the right hand side of the streak of the host embryo (Fig. 6.2

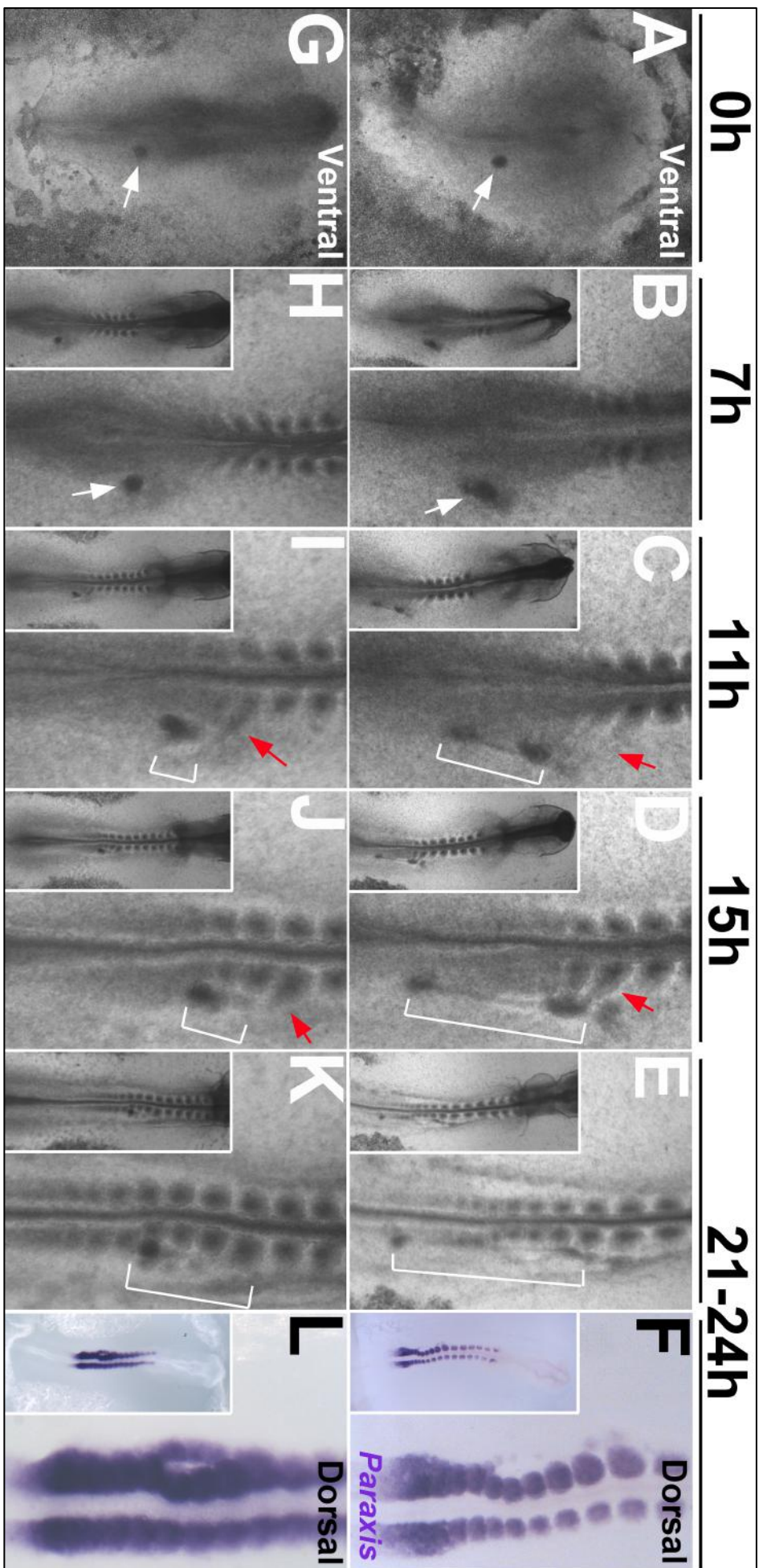
A, G). As the embryo develops, graft cells do not ingress into the streak, but follow an arc-like trajectory around the host node. At first, the graft moves laterally, until it passes the level of the host node (which is simultaneously retracting caudally). At this point, the graft begins to move towards the midline again, finally settling just lateral to the somites. During this time, the graft forms a notochord parallel to the host axis.

In movie S3, at 7 hours, the host embryo has reached HH8 and the new notochord begins to form rostral to the graft (Fig. 6.2B; white arrow). The graft retracts caudally, laying down the ectopic notochord in the same rostro-caudal orientation as the host. At around 11 hours, the host embryo had reached HH9- (6 somites), and the right hand paraxial mesoderm (which is seen as a dark region) adjacent to the ectopic notochord (white bracket) appears to have expanded laterally towards the graft (Red arrow, Fig. 6.2C). From this point, the morphology of the caudal somites is highly unusual. Their lateral edge is continuous with dark, segmented stripes that stretch towards the notochord (Red arrow, Fig. 6.2C and D), which at their longest, stretch laterally across a distance more than three times the somite's diameter (11 hours; Fig. 6.2C). As the notochord moves medially towards the somites, the stripes retract medially with it. After 24 hours, these somites had an expanded morphology (Fig. 6.2E), similar to the response of somites to a notochord graft seen in the previous chapter (section 5.3.3). At this point the embryo was fixed and analysed by *Paraxis* in situ hybridisation. This confirmed an expansion of the somites and PSM adjacent to the ectopic notochord compared to the left hand control somites (Fig. 6.2F; N.B. the embryo was filmed from the ventral side, but imaged from the dorsal side after in-situ. Therefore the expanded paraxial mesoderm is seen on the left side in F). QCPN also showed no contribution of the node graft to the somites, confirming the previous result (data not shown). However, *Paraxis* staining also reveals light patches of ectopic *Paraxis* expression adjacent to the expanded somites on the graft side, like small ectopic somites. However in movie S3, the process by which these somites form is difficult to see.

The formation of ectopic somites is more clearly visible in S4. In general, the timing of events was comparable to that of movie S3 (Fig. 6.2 G-K). *Paraxis* staining of the final embryo after 21 hours total incubation showed 3-4 ectopic somites in a row that runs parallel to the endogenous somites (Fig. 6.2L; N.B.

Again, this embryo is filmed from the ventral side but imaged after in-situ from the dorsal side, so the ectopic somites are seen on the left side in L). The ectopic somites can be seen to form between 15-19 hours. In this embryo, their formation appears to coincide with that of endogenous somites 9-11 adjacent to them. At first, the PSM that forms these somites is expanded towards the node, which at this time is “sweeping” past rostro-caudally, laying down the notochord adjacent to the PSM (Fig. 6.2J). The starting point of ectopic somite formation is obscured, as it seems to take place beneath the ectopic notochord. Somites 9-11 might arise as transient large somites, from which the ectopic somites “bud-off” laterally shortly after formation. Alternatively, the expanded PSM in this region may form two rows of somites parallel to each other with no transient large somite, the ectopic somites then move under the notochord and settle on the lateral side of the notochord.

Figure 6.2. Time-lapse microscopy of notochord precursor grafts reveal a transient attraction of somites to the ectopic notochord generated by the graft, followed by formation of ectopic somites from the expanded endogenous paraxial mesoderm. A-E, G-K. Still images from time-lapse movies of developing embryos with a notochord precursor graft (white arrow). A-E. Bright field images of movie S3, at 0, 7, 11, 15 and 24 hours. F. WMISH for *Paraxis* of embryo in A-E after 24 hours. G-K. Bright field images movie S4, at 0, 7, 11, 15 and 21 hours. L. WMISH for *Paraxis* of embryo in G-K after 21 hours. At 11 and 15 hours, somites appear to be attracted (red arrow) towards the ectopic notochord (white bracket). In all cases, the main image is zoomed on the region containing the graft and affected paraxial mesoderm. Inset images show whole embryo at the same stage. N.B. Embryos in time-lapse were imaged in ventral view (graft on the right side). Images after in-situ (F,L) are in dorsal view, so expanded paraxial mesoderm is seen on the left.



6.3.3. Are somite cells attracted to FGF4 from the early notochord?

The dark stripes that form between the ectopic notochord and endogenous somites stretch across a space normally occupied by the LPM. However, unlike the LPM, they are segmented, continuous with the normal host somites. It is therefore possible that the dark stripes are trails of cells attracted to the graft. What mediates this attraction? It has been shown that Fibroblast Growth Factor 4 (FGF4) is expressed in Hensen's node and early notochord, but is down-regulated in the more mature notochord, and that primitive streak cells (presumptive mesoderm and endoderm) grafted to the area opaca are attracted to a source of FGF4 (Yang et al., 2002). Could FGF4 in the emerging notochord of the graft be the attractant?

To test this, heparin-coated acrylic beads soaked in human FGF4 protein (Sigma) were used. Beads were first validated by their ability to induce the prospective neural marker *Sox3* in the area opaca (Streit et al., 2000; Yardley and Garcia-Castro, 2012). FGF4 and control PBS beads were placed at the medial edge of the area opaca of a stage HH3+ embryo in culture, on the left and right side of the embryo respectively (Fig. 6.3A). Embryos were then incubated for 4-5 hours and analysed for *Sox3* expression. In 2/2 embryos, the FGF4 bead led to an expansion of *Sox3* expression from the prospective neural plate, whilst no expansion was seen on the right side of the embryo adjacent to the PBS bead (Fig. 6.3B). This confirms that the FGF4 beads are active.

I next went on to test whether FGF4 beads can attract somites. Using the same approach as the Shh bead experiments of chapter five (section 5.3.4), FGF4 and control beads were grafted to the LPM on the right and left side of the embryo respectively (Fig. 6.3C). Grafted embryos were incubated and the paraxial mesoderm analysed after 5 and 10 hours by in situ hybridisation for *Paraxis*. After 5 hours, there was no difference in the shape or size of somites between the FGF4 and control side of the embryo (3/3 embryos; Fig. 6.3D). However, after 10 hours a slight lateral expansion could be seen in up to four somites adjacent to the FGF4 bead, as compared to the PBS control bead (3/3 embryos; Fig. 6.3E). This was accompanied by a decrease in *Paraxis* expression in the lateral somite, causing the sharp lateral edge of the stain (seen in the contralateral somites) to be lost. In general, the shape of the

somites was such that they appeared to bend towards the bead producing a “kink” in the paraxial mesoderm.

To investigate directly the movement of somite cells in response to an FGF4 bead, the experiment above was repeated, and the adjacent somites traced using DiO (Fig. 6.3F). Labelled embryos were photographed prior to incubation (Fig. 6.3G; 0 hours), and then analysed after 10 hours' incubation (Fig. 6.3H). Finally, embryos were stained for *Paraxis* (Fig. 6.3I). After 10 hours, the embryos had formed a further 7-8 somites. In 3/6 embryos, DiO labelling was found to form a ring around the FGF4 bead, suggesting that somite cells had moved to surround the bead (Fig. 6.3H). This was not seen on the contralateral side of the embryo around the PBS bead. *Paraxis* staining in these embryos (6.3I) revealed a similar change in the size and morphology of somites as seen previously (Fig. 6.3E). Importantly, the DiO labelling always extended further lateral than *Paraxis* staining, suggesting that *Paraxis* is downregulated in the cells that migrate towards the bead. In 1/6 embryos, a lateral expansion of the DiO-labelled somites was present but no ring of labelling was seen to surround the bead. In this embryo, the FGF4 bead was positioned further from the somite than normal. In this case, the DiO labelling still extended further lateral than *Paraxis* staining, suggesting again that *Paraxis* expression had been lost from the laterally expanded portion of the somite. In 2/6 embryos, no movement or expansion of DiO-labelled cells towards the FGF4 or control beads was seen after 10 hours.

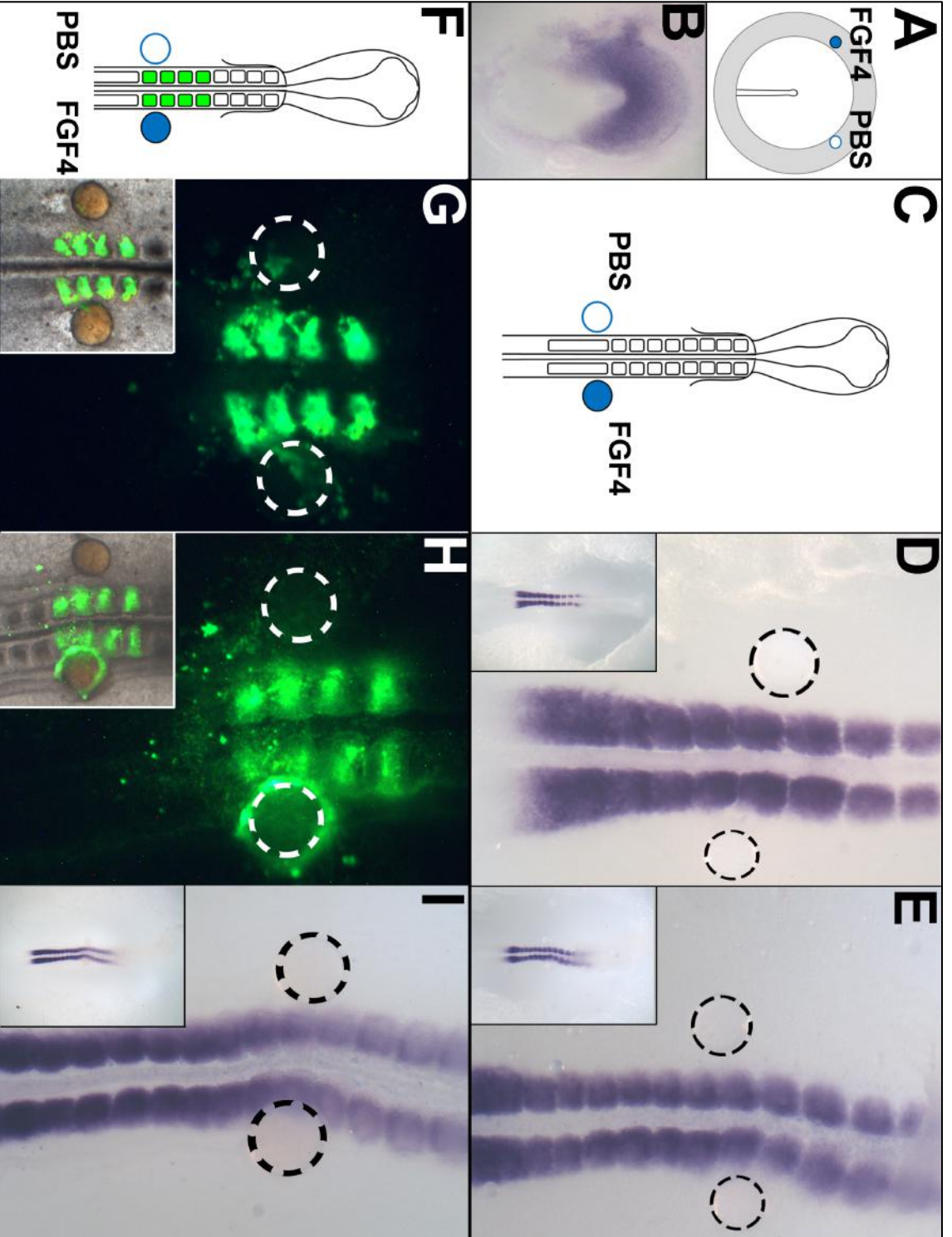


Figure 6.3. Does FGF4 mediate the long-range attraction between the paraxial mesoderm and secondary notochord? A-B. Positive control experiment confirming that FGF4 beads are capable of activating FGF signalling. A. Schematic showing positive control bead-graft procedure. PBS (right) or FGF4 (left) beads were placed in the area opaca of a HH3+ embryo. B. After 5 hours, WMISH for *Sox3* (early marker of neural plate), shows *Sox3* expression in the neural plate into the area opaca on the left (FGF4 bead) side, and not on the right (control) side. **C.** Schematic showing bead-graft procedure. PBS (left) and FGF4 (right) beads were placed adjacent to the somites on either side of HH9-10 embryos. **D-E.** WMISH for *Paraxis*, 5 and 10 hours after a bead-graft. D. After 5 hours, there is no difference in the shape and size of somites adjacent to the FGF4 and control bead. E. After 10 hours, somites adjacent to the FGF4 bead (right) are expanded and/or altered in shape compared to control side (left). In both D and E, main panel shows high magnification on region of interest, inset shows whole embryo. **F-H.** Tracing somites adjacent to FGF4 and PBS beads. F. Somite tracing procedure. Caudal somites and rostral PSM adjacent to FGF4 and control beads were labelled with DiO (green). G. Embryo with bead graft and DiO-labelled somites in bright field and green fluorescent channel prior to incubation (0 hours). H. After 10 hours, DiO-labelled somite cells accumulate in a ring around the FGF4 bead (right), suggesting a migration of somite cells towards the bead. In both G and H, main panel shows high-magnification image in green fluorescent channel only, inset shows overlay of bright field and fluorescent channel. (Dotted circle = outline of bead)

6.4. Discussion

6.4.1. Notochord precursor grafts as an assay for studying the role of the notochord in vertebral segmental patterning

The aim set out at the start of this chapter was to develop a notochord graft assay in which tension is maintained in the grafted notochord. The results above demonstrate that a graft of notochord precursors from Hensen's node results in the formation of an ectopic notochord, whilst still maintaining the mechanical forces that normally act upon the notochord during axis elongation. The movement of the graft during development follows the same trajectory as primitive streak cells, which follow highly organised cell movements as they migrate out of the streak to form the mesoderm and definitive endoderm underneath the epiblast (Psychoyos and Stern, 1996; Yang et al., 2002). This

suggests that the graft is either pulled passively by the flow of host cells during gastrulation and neurulation, or that it is subject to the same forces as cells of the primitive streak as they move out of the streak. Therefore, guided by the known migration paths and fates of cells in different regions of the primitive streak (Psychoyos and Stern, 1996; Yang et al., 2002), the final position of the ectopic notochord could in theory be altered by changing the position at which the notochord precursors are grafted.

After 24 hours incubation, the secondary notochord resulted in an extensive expansion of the host paraxial mesoderm adjacent to it, showing similarities to the response of somites to a notochord graft (section 5.3.3). However, further analysis indicated that the effect of the graft on host development was far more complex than a simple response of the somites to the notochord when it eventually settles adjacent to them. In the notochord precursor graft assay, the mature somites respond to signals from a relatively “young” notochord. This represents an interaction between two tissues that never actually occurs during development. Normally, only the posterior PSM is exposed to a young notochord. Although the response of the somites to the young notochord may be interesting with regards to general mechanisms of long-range signalling and chemotaxis (discussed below), it cannot tell us anything about how signals from the notochord influence migration of the normal sclerotome. By the time the secondary notochord has matured to the stage at which it would normally regulate this process, the host somites have been subject to too many changes by its earlier signals.

Therefore, it must be concluded that the assay is not a reliable system in which to study the role of the notochord in sclerotome migration and vertebral patterning. The original notochord graft assay is much more reliable in this respect. The graft is always removed and grafted to the same rostro-caudal level (adjacent to the newly-formed somites), ensuring the graft and responding somites are at a similar level of maturity, mimicking normal development as closely as possible. The problem of tension, however, remains unsolved.

6.4.2. The formation of ectopic somites

The response of the somites to the ectopic notochord generated by the precursor graft was typically much more extensive than the expansion of

somites seen in response to a notochord graft. Furthermore, in a large proportion of embryos, the secondary notochord also resulted in a row of ectopic somites forming adjacent to the notochord graft. These ectopic somites are not surprising given the known capacity of a node graft to generate somites (Spemann and Mangold, 1924; Waddington, 1932; Nicolet, 1971; Hornbruch et al., 1979). This capacity, however, is dependent on the region of the host to which it is grafted. If grafted to the area opaca, a notochord and neural plate form, but no somites (Storey et al., 1992). If grafted to the area pellucida, an entire secondary axis is generated including somites (Hornbruch et al., 1979). These ectopic somites have been shown to be a mixture of host and graft cells (Hornbruch et al., 1979).

In the above studies the whole node was grafted, which contains both notochord and medial somite precursors (Selleck and Stern, 1991). In this experiment, I grafted only the portion of the node that contains the notochord precursors and QCPN immunostaining showed that the ectopic somites were derived entirely from host tissue. Therefore, the graft does not contribute to the ectopic somites itself, but still has the capacity to induce somites in host tissue. Interestingly, in the study by Hornbruch et al. (1979), the distance from the midline at which the secondary axis was generated in the host embryo was found to determine whether the somites derived from host or graft tissue. In embryos in which the secondary axis was formed adjacent to the host somites, the rows of ectopic somites were typically comprised entirely of host cells. It seems likely therefore, that this study describes the same process as seen in our experiments: an expansion of the paraxial mesoderm and formation of ectopic somites in the host as a result of signals from the secondary notochord.

It is possible that the ectopic somites form, at least in part, from the lateral plate mesoderm adjacent to the ectopic notochord. The node and notochord are a source of BMP inhibitors such as Noggin, and at their normal position at the midline they generate a low-BMP environment, required for somite formation (Tonegawa and Takahashi, 1998; Streit and Stern, 1999). The inhibition of BMP more laterally with an ectopic source of Noggin is sufficient to induce the cells of the LPM to spontaneously organise into somites (Streit and Stern, 1999). It therefore cannot be ruled out at this stage that the LPM contributes to the ectopic somites seen in response to the secondary

notochord in my experiments. However, the time-lapse movies suggest that the ectopic somites derive instead from the somitic mesoderm. They appear to form in regions of the paraxial mesoderm that have already expanded in response to the ectopic node and notochord. This is seen in movie S3, in which the PSM and somites are greatly expanded prior to ectopic somite formation. Later, the ectopic somites appear to form from this expanded tissue: either directly (i.e. forming two somites side by side rather than a single row), or immediately after endogenous somite formation, budding off laterally from the single large somite formed from the paraxial mesoderm.

6.4.3. Notochord precursor grafts as an assay for studying somitogenesis

In a recent study, it was shown that a piece of posterior primitive streak from a stage HH5 embryo (a tissue not fated to become somites) will spontaneously form somite-like structures if cultured in an environment of BMP inhibition (Dias et al., 2014). The cellular organisation of these structures is that of an epithelial sphere of similar size to normal somites, and they express the somite marker *Paraxis*. Furthermore, if grafted in place of a somite, they will be patterned dorso-ventrally and differentiate into dermomyotome and sclerotome like normal somites. This suite of characteristics led the authors to conclude that they were, in fact, somites. However, these structures exhibit a number of characteristics that sets them apart from normal somites. Firstly, they form simultaneously (or in two or three “bursts”). Secondly, they do not form in a line, but in clustered arrangement compared to that of a “bunch of grapes” (Stern and Bellairs, 1984; Dias et al., 2014). Thirdly, they are not subdivided into rostral and caudal halves, and finally, no oscillatory expression of clock genes such as *hairy1* (Palmeirim et al., 1997) precedes their formation. This led the authors to conclude that although the waves and oscillations of the “segmentation clock” (Cooke and Zeeman, 1976; see section 1.2 for further details) are important for regulating the timing of somite formation (Herrgen et al., 2010; Schroter and Oates, 2010; Harima et al., 2013) and in its rostro-caudal patterning (Takahashi et al., 2003), they are not required for somite formation itself. Dias et al. (2014) proposed that somite size can be regulated at least in part by local cell-cell interactions, such as constraints to the packing arrangement of cells.

The dynamics of ectopic somite formation seen in the above study (Dias et al., 2014) and others (Stern and Bellairs, 1984) is very similar to the ectopic somites that I observed to form adjacent to the secondary notochord. The expanded PSM, rather than forming a single large somite, forms either two somites side-by-side, or a transient large somite, soon splitting into two smaller ones. This behaviour suggests that a somite becomes unstable above a certain threshold size, and is reminiscent of the self-organising property of somites demonstrated in the computational model of the study described above (Dias et al., 2014). Here, a group of mesenchymal cells will self-organise into epithelial balls of a relatively uniform size and cell number, based only on cell-cell interactions such as adhesion and packing constraints. The assay developed in this chapter, therefore, may provide another mechanism by which to study the property of a tissue to self-assemble into somites in response to BMP inhibition. However, if they do indeed form from the expanded paraxial mesoderm, it would be expected that the 'clock and wavefront mechanism' would operate prior to formation of the ectopic somites (Cooke and Zeeman, 1976; see section 1.2), in contrast to the ectopic somites of the above study (Dias et al., 2014).

6.4.4. Does the ectopic notochord attract paraxial mesoderm cells?

Observing the development of grafted embryos by time-lapse microscopy revealed an unexpected transient stage in which dark bands of tissue extended from the lateral edge of the host somites and PSM to the forming ectopic notochord. These bands were always continuous with the endogenous paraxial mesoderm, in rostral regions forming segmented 'stripes' radiating out from the somites, and in more caudal regions an unsegmented block adjacent to the PSM. The tissue had an unusual dynamic reminiscent of elastic (or a piece of chewing gum) being pulled between two points. The stripes 'stretched' and compressed over long distances and appeared to 'relax' and broaden as the notochord moved closer to the midline. Interestingly, the shape and arrangement of the stripes is similar to the predicted dynamics of somite cells being attracted to the notochord in the "uniform attractant" model (section 4.3.6; Fig. 4.6B). Overall, this is consistent with attraction of the paraxial mesoderm cells towards the ectopic notochord, and appears to compress the segmental pattern as it does so.

There are two questions still to be answered regarding this effect. First, from where do the stripes derive? The attraction of somite cells over long distances is the most likely possibility, given that the stripes are continuous with the somites. Also the non-miscible properties of cells in the rostral and caudal half of each somite may explain why the stripes are segmented (Stern and Keynes, 1987). However as the stripes stretch across a space normally occupied by the LPM it cannot be ruled out that this tissue also contributes. The first step to answering this question would be to trace the paraxial mesoderm in response to the graft. However, this experiment is not trivial, as at the point of grafting the paraxial mesoderm has not yet formed at this level. One approach may be to label the somite precursors at their point of origin in the endogenous node and streak before grafting (Selleck and Stern, 1991; Psychoyos and Stern, 1996). Another possibility would be to conduct the node graft as normal, and later to label the paraxial mesoderm at a point prior to the formation of the stripes. The second question is, what is the cellular structure of these stripes? The dark appearance of these expansions in bright field is similar to that of the somites, suggesting that they have a higher density of cells than the surrounding LPM and are therefore, perhaps, more epithelial. Analysis of sections through these structures would help to elucidate their cellular organisation.

6.4.5. *Is FGF4 a long-range attractant?*

The FGF family of secreted signalling molecules has an important role in the regulation of cell migration and chemotaxis in a diverse range of vertebrate developmental systems (reviewed in Bottcher and Niehrs, 2005; Dorey and Amaya, 2010). The results of the bead experiments tentatively suggest that a source of FGF4 is sufficient to cause a migration of paraxial mesoderm cells towards it. The strongest evidence for this comes from tracing of somites using DiO adjacent to an FGF4 bead, which after 10 hours in culture resulted in an accumulation of DiO-expressing cells around it. However, this was variable, with only 50% of embryos showing this result. To demonstrate that FGF4 does indeed mediate this attraction to the notochord, it is also necessary to perform a loss-of-function experiment: does the grafted notochord attract the paraxial mesoderm when FGF4 is inhibited? This could be tested using chemical inhibitors of FGF receptors such as SU5402 (Mohammadi et al., 1997) or FIIN

hydrochloride (Zhou et al., 2011), which bind at the tyrosine kinase domain of the receptor, preventing downstream signal transduction of the FGF signal.

FGF4 is expressed transiently in the emerging notochord at stages HH5-6, but from around HH7 it is not expressed in the posterior part, or any other region of the notochord (Shamim and Mason, 1999). The apparent attraction of the paraxial mesoderm seen in the time-lapse movies begins at a time when the notochord has just begun to emerge from the notochord precursor graft (which at the point of grafting was at stage HH4). If the graft follows the same developmental program as a normal notochord, it should express FGF4 at this stage. However, the attraction persists for several hours, at least until the graft reaches the midline. With FGF4 swiftly downregulated in the normal notochord, it is not clear for how long its expression is maintained in the graft. A more detailed study of the time-course of FGF4 expression during notochord development from the grafts was attempted but did not succeed because of technical difficulties.

6.5. Summary

This chapter explored a method to generate an ectopic notochord adjacent to the somites in which normal tension is maintained in the graft. Grafting notochord precursors from the node of a donor embryo, to a position adjacent to the primitive streak of a host, was found to generate an ectopic notochord adjacent to the host somites. Furthermore, it was found that the position of the ectopic notochord could be reliably predicted. However, this led to unexpected responses in the paraxial mesoderm adjacent to the graft, most notably a long-range attraction of somite cells towards the young ectopic notochord, possibly mediated by FGF4. The effect described is the result of the exposure of mature paraxial mesoderm to a 'young' notochord, an interaction that does not occur during normal development. This calls into question the reliability of this assay in the notochord in vertebral column segmentation (for which it was originally intended). Instead, the results suggest another use for this assay in the future study of diverse processes in embryonic development such as long-range chemotaxis and somitogenesis.

Chapter 7 : Discussion and future directions

7.1. Introduction

At first glance, the epithelial spheres of mesoderm that comprise the somites are remarkably simple. However, delving deeper into their development proves they are not. They give rise to the segmented muscles, connective tissue, dermis and vertebral column of the adult (Christ and Ordahl, 1995), and impose a segmented pattern upon surrounding tissues (Keynes and Stern, 1984; Rickmann et al., 1985; Bronner-Fraser, 1986; Lim et al., 1991). All the segmented elements of the vertebrate body must develop in concert to form functional units (or “motion segments”; Schmorl & Junghanns 1968) along the A-P axis that together permit locomotion. Although centuries of research have given us a remarkable insight into the mechanisms that give rise to this arrangement, crucial questions still remain. The work in this thesis addresses the broad question: how is segmentation of the somites translated into the final segmental arrangement of vertebrae along the A-P axis?

7.2. Relationship between somite and vertebral segmentation

7.2.1. Resegmentation confirmed in the chick

It is generally accepted that the vertebral column forms by “resegmentation” of the sclerotome, a model that was proposed over a century ago to account for the fact that the muscles (myotome) and vertebrae (sclerotome) come to be offset by half a segment (Remak, 1855). Over the past thirty years, support for the resegmentation model has been provided by a number of somite-tracing studies using quail-chick somite transplants (Bagnall et al., 1988; Huang et al., 1996; 2000b) or other labelling techniques (Bagnall, 1989; 1992; Ewan and Everett, 1992). However, because of problems with all of these methods (see section 1.5.5 and 1.5.6), resegmentation in the chick had never been convincingly demonstrated. Furthermore, no study had ever addressed whether this mechanism varies along the A-P axis.

I began this study by using Dil and DiO labelling to trace somites in different regions of the A-P axis in the vertebral column, a technique that eliminates the

problems associated with other studies. My results demonstrated that a single somite gives rise to the annulus fibrosus of the IVD, and half of the vertebral body and neural arch anterior and posterior to the disc. This was the case in all regions of the vertebral column tested and demonstrated definitively that the chick vertebrae form by resegmentation of the sclerotome. Another somite tracing study in mouse has recently confirmed resegmentation for the first time in a mammalian species (Takahashi et al., 2013). Together, these results support the idea that resegmentation is a common mechanism for vertebra formation in amniotes.

In anamniotes, the story is not so clear. A recent study, which used fluorescent dyes to label somites, has reported resegmentation in the Mexican axolotl (*Ambystoma mexicanum*) (Piekarski and Olsson, 2014). However, in the zebrafish (a teleost fish) a “leaky resegmentation” has been reported in which Dil-labelled sclerotome cells from a single somite were found to contribute to elements across five or six vertebral segments (Morin-Kensicki et al., 2002). On this basis, it is tempting to infer conservation of an ancestral “resegmentation” mechanism that appeared after the split of lobe-finned (sarcopterygian) and ray-finned (actinopterygian) fish and before the split of amphibians and amniotes. However, there are many other plausible explanations. Resegmentation may have evolved separately a number of times during vertebrate evolution. Alternatively, it may have been present at the very base of the vertebrates, and subsequently modified in the teleost lineage so that cells in each sclerotome half are able to subvert the strict rostro-caudal compartmentalisation that maintains somite boundaries (Stern and Keynes, 1987; van Eeden et al., 1996; Takahashi et al., 2013). Given that reliable somite tracing experiments have been carried out on only a few vertebrate species it is impossible to differentiate between these possibilities at present.

7.2.2. Resegmentation and caudal autotomy

A number of vertebrate species (including some salamanders and many lizards) have the remarkable ability to self-detach their tails, a mechanism known as “caudal autotomy” (Arnold, 1988). Among those lizard species that possess this ability, most sever their tails through the centre of the vertebral body and neural arch (Bellairs, 1985). The position of the fracture is predictable; where the tail has the ability to autotomise, a fracture plane is

seen in the centre of the caudal vertebra (Bellairs, 1985; Gilbert et al., 2014). This has led many to speculate that the fracture plane marks the original somite boundary within the vertebra and is the result of an incomplete fusion between half-sclerotomes during resegmentation (Albrecht, 1883; Werner, 1971; Bellairs, 1985). Despite this intriguing suggestion, no study has ever tested this. The Dil and DiO labelling method used in chapter three of this thesis (Fig. 3.1B) would be a simple method of addressing this. Due to the incubation time required between labelling and analysis, this would need to be carried out *in ovo*, but this is more difficult in reptiles as most lack a hard shell. However, the Madagascar ground gecko (*Paroedura pictus*), which lays eggs with a hard shell, has recently been identified as a promising model system (Noro et al., 2009). This species also displays intra-vertebral caudal autotomy, and may represent the perfect species in which to test the relationship between somite boundaries and fracture planes.

7.3. Resegmentation is not the whole story

7.3.1. Shifting sclerotomes and regionalisation of the vertebral column

The results of somite tracing in chick reported in this thesis show that the resegmentation process is conserved along the A-P axis of the vertebral column. This demonstrates that while vertebral morphology varies dramatically along the A-P axis, somitic composition does not. However, my analysis clearly showed that the dorsal and ventral sclerotome cells from a single somite do not necessarily migrate to the same A-P level along the midline, but rather shift with respect to each other along the A-P axis in a region-specific manner. This leads to a variable “tilt” in the boundary between somite cells within the vertebra, which correlates with the physical tilt of the neural arches in each region. This correlation suggests a causal relationship between the position of somite cells at the midline and the tilt of the neural arch, which varies along the axis. On the basis of these results, I proposed a modified version of the resegmentation model, the “Resegmentation-shift” model (Fig. 3.5), for vertebral formation.

What causes this shift? There are obvious parallels between the variability of the sclerotome shift along the A-P axis and collinear *Hox* expression, which

specifies regional vertebral morphology (Kessel and Gruss, 1991; Burke et al., 1995). However, it is difficult to see how *Hox* expression in the sclerotome cells (which is cell-autonomous) could determine the position to which they migrate at the midline. It is more likely that this process is governed by guiding signals external to the somite that vary regionally along the axis, possibly from the notochord and/or neural tube. This suggests a role for signals external to the somite in the regulation of vertebral segmentation and morphology.

Of course, regionalised *Hox* expression in the notochord and neural tube may underlie the variability in the guiding signals they emit along the A-P axis. It is well established that the vertebrate neural tube is patterned by collinear *Hox* expression along its A-P axis (Duboule and Dollé, 1989; Graham et al., 1989; Prince et al., 1998a). However, whether the notochord is regionalised in the same way is not clear. Collinear *Hox* expression has been reported in the notochord in zebrafish (Prince et al. 1998), however there is no report of a similar expression pattern in the chick notochord.

7.4. The amniote notochord plays an important role in segmentation of the vertebral bodies

7.4.1. The notochord can influence sclerotome segmentation

In teleosts, only the perichordal centra, neural and hemal arches are derived from the sclerotome, with the chordacentra (which form prior to the perichordal centra that surround them) being formed by the secretion of bone from the notochord (Grotmol et al., 2003; Fleming et al., 2004; Wang et al., 2013). In amniotes, all elements of the vertebrae (including the vertebral bodies) are derived from the sclerotome (Christ and Wilting, 1992). However, notochord ablation studies in chick have reported that the vertebral bodies cannot segment in the absence of a notochord (Watterson et al., 1954; Strudel, 1955), a result that I confirmed in chapter 4 of this thesis (section 4.3.1, Fig. 4.1). This suggests that a role for the notochord in segmental patterning of the vertebral bodies has been retained in chick. In chapter 4 of this thesis, I showed that an ectopic notochord, grafted lateral to the somites in a chick host, leads to the formation of ectopic sclerotome from host cells in a more compressed spatial periodicity to that of the host. This suggests that the notochord can influence

the spatial periodicity of sclerotome, and therefore may play a role in determining segmentation of the vertebral bodies.

7.4.2. Attraction: A new role for the notochord in vertebral development

After showing that the notochord can influence vertebral segmentation, I went on to investigate possible mechanisms for this. Through a series of notochord graft experiments between different axial regions, I showed that the segmentation of the ectopic sclerotome is dependent upon the spatial periodicity of the somites in the region it is grafted to. These results can be explained by a simple model, in which the notochord attracts sclerotome towards it by chemotaxis (the “uniform attractant” model; Fig. 4.6B). This hypothesis was supported by the results of somite tracing adjacent to a notochord graft, which showed a migration of labelled somite cells towards the notochord graft (Fig. 5.1), as well as evidence from a previous in-vitro study (Newgreen et al., 1986).

In chapter five, I explored the attraction mechanism in more detail, investigating whether Shh may be acting as the chemoattractant for the sclerotome. Although the results suggested that somite cells may be attracted to an ectopic source of Shh, these results were difficult to interpret due to the simultaneous roles of Shh in the induction (Fan and Tessier-Lavigne, 1994; Johnson et al., 1994; Ebensperger et al., 1995), proliferation (Johnson et al., 1994; Fan et al., 1995; Teillet et al., 1998), and survival (Teillet et al., 1998) of the sclerotome. Further work will seek to dissect the role of the notochord in sclerotome chemotaxis from these other processes, and to investigate further whether Shh acts alone as a chemottractant in this context. It also remains to be seen whether the attractive property of the notochord is present in other vertebrates. In chick, its role seems to be in the recruitment of sclerotome for vertebral body formation. However, in some teleost species the sclerotome-derived perichordal centra form later, after the formation of the primary chordacentra by the notochord (Grotmol et al., 2003; Fleming et al., 2015). Does the notochord also attract the sclerotome in these teleost species, and if so, is the timing of attraction delayed until after the chordacentra have formed? These are questions for the future.

7.5. Is the notochord intrinsically segmented?

Attraction of the sclerotome towards the notochord is an integral part of vertebral morphogenesis. However, it cannot explain my results (Fig. 4.1) or those of other studies (Watterson et al., 1954; Strudel, 1955), which demonstrate that the ventral vertebral column fails to segment in the absence of a notochord. The chick notochord is therefore required for generating the final segmentation of the vertebral column. However, the mechanism by which it does this remains a mystery.

Upon its formation, the notochord is a continuous rod of mesoderm, with no obvious morphological segmentation. However, later in development it begins to swell and constrict along its length in a regular pattern that coincides with that of the future vertebral column (Hamilton, 1953; Balfour, 1881). In mammals, the notochord is replaced by cartilage in the vertebral bodies, persisting only as the central portion of the adult intervertebral disk (IVD), a structure known as the nucleus pulposus (Human: Walmsley, 1953; Rat: Rufai et al., 1995; Mouse: Choi et al., 2008). It has also been shown that in mice, *Shh* in the notochord is required for formation of the IVDs (Choi and Harfe, 2011; Choi et al., 2012). In chick, the presence of a nucleus pulposus in the adult IVD has been contested (Bruggeman et al., 2012). However, whether or not it persists into adulthood, the notochord forms the central core of the ventral vertebral column up to hatching (Bruggeman et al., 2012).

If the notochord is segmented, there must be an underlying molecular pattern. Formation of the notochord-derived vertebral bodies in teleosts has been shown to be preceded by the formation of segmented bands of notochord cells that express alkaline phosphatase (Grotmol et al., 2005). However there is no example to date of any gene expressed in a segmented pattern within the amniote notochord. The ECM protein aggrecan has been shown to be present in a regular pattern within the notochordal sheath during vertebral column development (Bundya et al., 1998). It is not clear whether the notochord, or sclerotome cells invading the sheath, secrete this.

How does the notochord acquire its regular pattern of swellings? One possibility is that the surrounding somites impose the pattern upon the

notochord, as they do in the neural tube (Lim et al., 1991). Studies in Collagen II-deficient mice have shown that in the absence of normal vertebral body development, the notochord fails to break down in the vertebral bodies to form the nucleus pulposus in the IVDs (Aszódi et al., 1998). Based on this result, it has been suggested that the swellings in the notochord are the result of mechanical forces imposed by the forming vertebral bodies and resistance to this force by osmotic pressure within the heavily-vacuolated notochord (Aszódi et al., 1998; Choi and Harfe, 2011). This would explain how a segmented pattern could be achieved within the notochord even if an earlier molecular pre-pattern did not exist. However this hypothesis has never been tested. Another possibility is that the amniote notochord, like the paraxial mesoderm, is intrinsically segmented, and perhaps the “archetypal segmented structure” of the vertebral embryo (Stern, 1990).

The question therefore still remains: is the notochord intrinsically segmented, or is this pattern imprinted upon it (mechanically or otherwise) by the surrounding somites? An experiment is currently being developed to test this, in which somites are surgically ablated next to a portion of the notochord. Analysis of coronal sections through the notochord in the ablated region should be sufficient to determine whether segmented swellings develop in the absence of somites.

7.6. A model for vertebral segmentation

The experiment proposed above may elucidate whether the segmented swellings within the chick notochord are intrinsic to the notochord or imposed by the somites. However, the lack of evidence for molecular segmentation within the amniote notochord makes it more likely that its pattern comes from the somites. If true, this must be reconciled with the fact that the amniote notochord is required for vertebral body segmentation (Watterson et al., 1954; Strudel, 1955) and also for the formation of intervertebral discs, which form in a segmented pattern (Choi and Harfe, 2011; Choi et al., 2012).

Fig. 7.1 illustrates a model to account for these results. In the absence of intrinsic segmentation (Fig. 7.1A), the notochord emits a chemoattractant (possibly Shh) causing the sclerotome to migrate towards it (Fig. 7.1B). The

non-miscible properties of the rostral and caudal sclerotome halves maintain strict somite boundaries throughout vertebral formation (Stern and Keynes, 1987). Signals from the sclerotome impose a segmented pattern upon the notochord, specifying notochord cells at segmentally reiterated positions as the future nucleus pulposus (NP) of the IVD (Fig. 7.1C). The specified NP cells in the notochord then signal back to the sclerotome (possible via Shh; Choi et al. 2012) to specify the position of the annulus fibrosus (AF) within the sclerotome (7.1D). Vertebral bodies form between the IVDs. To form a coherent IVD, a relay of signals is therefore required between the sclerotome and notochord. In the absence of the notochord, the sclerotome cannot form the AF, and therefore the entire sclerotome forms a continuous strip of vertebral bodies, as seen in notochord ablation studies (Fig. 4.1 of this thesis; Watterson et al. 1954; Strudel 1955). This suggests an essential role for IVDs in the spacing of vertebral bodies. Further work will seek to test this model.

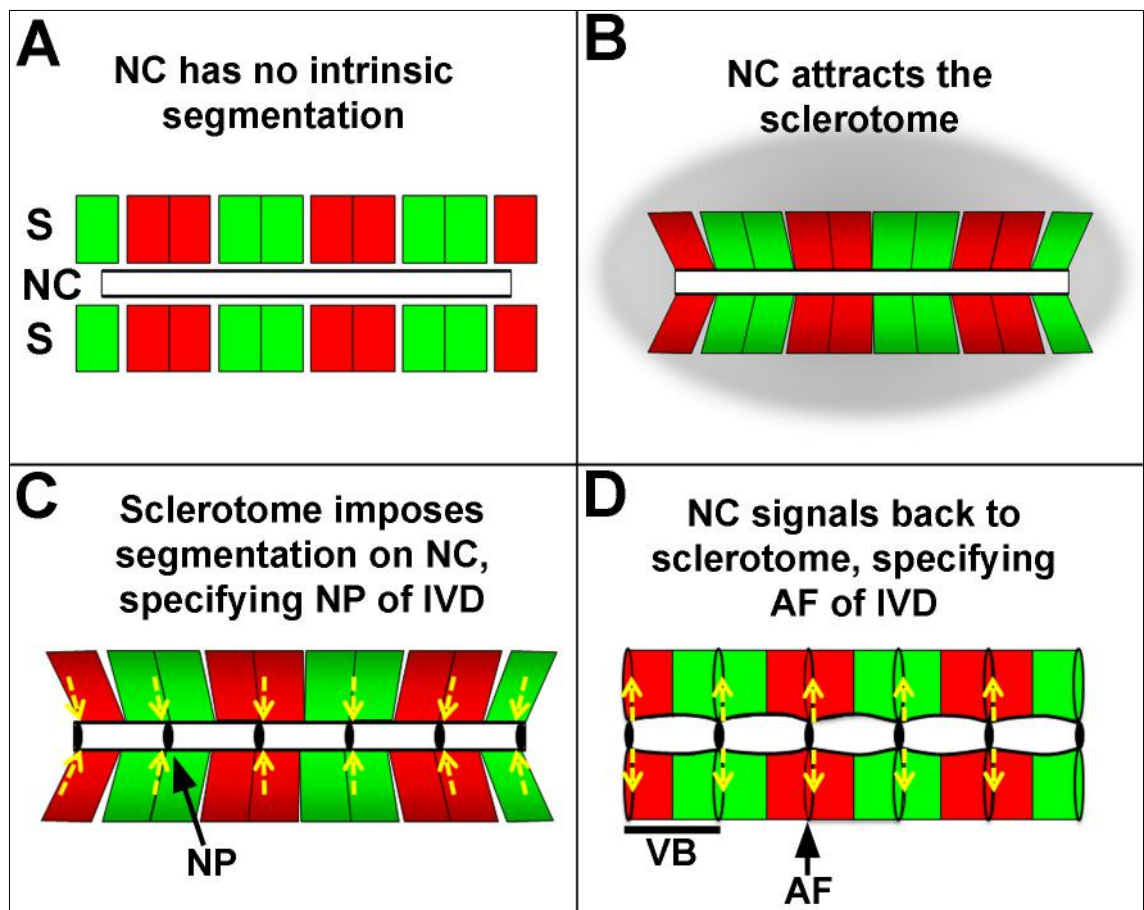


Figure 7.1. A model for vertebral segmentation. **A.** The notochord (NC) has no intrinsic segmentation. (surrounding sclerotome (S) is coloured alternately red and green. Each sclerotome is divided into a rostral and caudal half) **B.** The notochord emits a chemoattractant (possibly Shh) causing the sclerotome to migrate towards it. **C.** Signals from the sclerotome specify notochord cells at segmentally reiterated positions as the future nucleus pulposus (NP) of the IVD. **D.** NC signals back to the sclerotome, specifying the position of the annulus fibrosus (AF) within the sclerotome. Vertebral bodies (VB) form between the IVDs.

7.7. Final remarks

The formation of somites is a critical step in the development of the segmented body plan in vertebrates. As much of the information required to pattern the vertebral column is intrinsic to the somites, the role of external signals in this process is often overlooked. In this thesis, I have demonstrated the relationship between somite and vertebral segmentation in chick, and uncovered a hitherto unknown role for the notochord in the attraction of sclerotome during vertebral formation. Furthermore, this work adds to growing evidence that the notochord in amniotes plays an active role in vertebral segmentation.

References

- Adams, D. S., Keller, R. and Koehl, M. A. R.** (1990). The mechanics of notochord elongation, straightening and stiffening in the embryo of *Xenopus laevis*. *Development* **110**, 115–130.
- Aguinaldo, A. M. A., Turbeville, J. M., Linford, L. S., Rivera, M. C., Garey, J. R., Raff, R. A. and Lake, J. A.** (1997). Evidence for a clade of nematodes, arthropods and other moulting animals. *Nature* **387**, 489–493.
- Akam, M.** (1987). The molecular basis for metameric pattern in the *Drosophila* embryo. *Development* **101**, 1–22.
- Albrecht, P.** (1883). Note sur le presence d'un rudiment de proatlas sur un exemplaire de *Hatteria punctata* Gray. *Bull. Mus. R. Hist. Nat, Belg.* **2**, 185–192.
- Amores, A., Force, A., Yan, Y., Joly, L., Amemiya, C., Fritz, A., Ho, R. K., Langeland, J., Prince, V., Wang, Y., Westerfield, M., Ekker, M. and Postlethwait, J. H.** (1998). Zebrafish hox Clusters and Vertebrate Genome Evolution. *Science*. **282**, 1711–1715.
- Ando, T., Semba, K., Suda, H., Sei, A., Mizuta, H. and Yamamura, K.** (2010). The floor plate is sufficient for development of the sclerotome and spine without the notochord. *Mech. Dev.* **128**, 129–140.
- Andrade, W., Seabrook, T. J., Johnston, M. G. and Hay, J. B.** (1996). The use of the lipophilic fluorochrome CM-Dil for tracking the migration of lymphocytes. *J. Immunol. Methods* **194**, 181–189.
- Aoyama, H. and Asamoto, K.** (1988). Determination of somite cells: independence of cell differentiation and morphogenesis. *Development* **104**, 15–28.
- Aoyama, H. and Asamoto, K.** (2000). The developmental fate of the rostral/caudal half of a somite for vertebra and rib formation: experimental confirmation of the resegmentation theory using chick-quail chimeras. *Mech. Dev.* **99**, 71–82.

- Arnold, E. N.** (1988). Caudal Autotomy as a Defense. In *Biology of the Reptilia, vol. 16, Ecology B* (ed. Gans, C. and Huey, R. B.), pp. 235–275. New York: Alan R. Liss.
- Aszódi, A., Chan, D., Hunziker, E., Bateman, J. F. and Fässler, R.** (1998). Collagen II is essential for the removal of the notochord and the formation of intervertebral discs. *J. Cell Biol.* **143**, 1399–1412.
- Aulehla, A. and Johnson, R. L.** (1999). Dynamic Expression of Lunatic fringe Suggests a Link between notch Signaling and an Autonomous Cellular Oscillator Driving Somite Segmentation. *Dev. Biol.* **207**, 49–61.
- Aulehla, A., Wehrle, C., Brand-Saberi, B., Kemler, R., Gossler, A., Kanzler, B. and Herrmann, B. G.** (2003). Wnt3a Plays a Major Role in the Segmentation Clock Controlling Somitogenesis. *Dev. Cell* **4**, 395–406.
- Aulehla, A., Wiegraebe, W., Baubet, V., Wahl, M. B., Deng, C., Taketo, M., Lewandoski, M. and Pourquié, O.** (2008). A β -catenin gradient links the clock and wavefront systems in mouse embryo segmentation. *Nat. Cell Biol.* **10**, 186–193.
- Bagnall, K. M.** (1989). The binding pattern of peanut lectin associated with sclerotome migration and the formation of the vertebral axis in the chick embryo. *Anat. Embryol. (Berl)*. **180**, 505–513.
- Bagnall, K. M.** (1992). The migration and distribution of somite cells after labelling with the carbocyanine dye, Dil: the relationship of this distribution to segmentation in the vertebrate body. *Anat. Embryol. (Berl)*. **185**, 317–324.
- Bagnall, K. M., Higgins, S. J. and Sanders, E. J.** (1988). The contribution made by a single somite to the vertebral column: experimental evidence in support of resegmentation using the chick-quail chimaera model. *Development* **103**, 69–85.
- Balfour, F. M.** (1881). *A Treatise on Comparative Embryology, vol:II*. London: MacMillan.
- Barrios, A., Poole, R. J., Durbin, L., Brennan, C., Holder, N. and Wilson, S. W.** (2003). Eph/Ephrin Signaling Regulates the Mesenchymal- to-Epithelial Transition

of the Paraxial Mesoderm during Somite Morphogenesis. *Curr. Biol.* **13**, 1571–1582.

Bateson, W. (1894). *Materials for the study of variation treated with special regard to discontinuity in the origin of species*. London: MacMillan.

Baur, R. (1969). Zum Problem der Neugliederung der Wirbelsäule. *Acta Anat. (Basel)*. **72**, 321–356.

Bellairs, A. d'A (1985). Autotomy and Regeneration in Reptiles. In *Biology of the Reptilia, vol. 15, Development B* (ed. Gant, C. and Billett, F.), pp. 301–411. New York: John Wiley & Sons.

Bellairs, R., Ireland, G. W., Sanders, E. J. and Stern, C. D. (1981). The behaviour of embryonic chick and quail tissues in culture. *J. Embryol. Exp. Morphol.* **61**, 15–33.

Beresford, B. (1983). Brachial Muscles in the Chick Embryo: the fate of individual somites. *J. Embryol. Exp. Morphol.* **77**, 99–116.

Bessho, Y., Hirata, H., Masamizu, Y. and Kageyama, R. (2003). Periodic repression by the bHLH factor *Hes7* is an essential mechanism for the somite segmentation clock. *Genes Dev.* **17**, 1451–1456.

Boliventa, P. and Marti, E. (2001). Introduction: Unexpected Roles for Morphogens in the Development and Regeneration of the CNS. *J. Neurobiol.* **64**, 321–323.

Borycki, A., Mendham, L. and Emerson, C. P. (1998). Control of somite patterning by Sonic hedgehog and its downstream signal response genes. *Development* **125**, 777–790.

Bottcher, R. T. and Niehrs, C. (2005). Fibroblast Growth Factor Signaling during Early Vertebrate Development. *Endocr. Rev.* **26**, 63–77.

Boussif, O., Lezoualc'h, F., Zanta, M. a, Mergny, M. D., Scherman, D., Demeneix, B. and Behr, J. P. (1995). A versatile vector for gene and oligonucleotide transfer into cells in culture and in vivo: polyethylenimine. *Proc. Natl. Acad. Sci. U. S. A.* **92**, 7297–7301.

- Brand-Saberi, B., Ebensperger, C., Wilting, J., Bailing, R. and Christ, B.** (1993). The ventralizing effect of the notochord on somite differentiation in chick embryos. *Anat. Embryol. (Berl)*. **188**, 239–245.
- Brent, A. E., Schweitzer, R. and Tabin, C. J.** (2003). A somitic compartment of tendon progenitors. *Cell* **113**, 235–48.
- Bridges, C. B. and Hunt, M. T.** (1923). *The third-chromosome group of mutant characters of Drosophila melanogaster*. Washington: Carnegie Institute of Washington.
- Briscoe, J. and Ericson, J.** (2001). Specification of neuronal fates in the ventral neural tube. *Curr. Opin. Neurobiol.* **11**, 43–49.
- Bronner-Fraser, M.** (1986). Analysis of the Early Stages of Trunk Neural Crest Migration in Avian Embryos Using Monoclonal Antibody HNK-1. *Dev. Biol.* **115**, 44–55.
- Bronner-Fraser, M. and Stern, C. D.** (1991). Effects of Mesodermal Tissues on Avian Neural Crest Cell Migration. *Dev. Biol.* **143**, 213–217.
- Bruggeman, B. J., Maier, J. A., Mohiuddin, Y. S., Powers, R., Lo, Y., Guimarães-Camboa, N., Evans, S. M. and Harfe, B. D.** (2012). Avian intervertebral disc arises from rostral sclerotome and lacks a nucleus pulposus: implications for evolution of the vertebrate disc. *Dev. Dyn.* **241**, 675–83.
- Buchberger, A., Seidl, K., Klein, C., Eberhardt, H. and Arnold, H.** (1998). cMeso-1, a Novel bHLH Transcription Factor, Is Involved in Somite Formation in Chicken Embryos. *Dev. Biol.* **199**, 201–215.
- Bundya, J., Rogers, R., Hoffman, S. and Conway, S. J.** (1998). Segmental expression of aggrecan in the non-segmented perinotochordal sheath underlies normal segmentation of the vertebral column. *Mech. Dev.* **79**, 213–217.
- Burgess, R., Cserjesi, P., Ligon, K. L. and Olson, E. N.** (1995). Paraxis: A basic helix-loop-helix protein expressed in paraxial mesoderm and developing somites. *Dev. Biol.* **168**, 296–306.
- Burke, A. C., Nelson, C. E., Morgan, B. A. and Tabin, C.** (1995). Hox genes and the evolution of vertebrate axial morphology. *Development* **121**, 333–46.

- Cambray, N. and Wilson, V.** (2002). Axial progenitors with extensive potency are localised to the mouse chordoneural hinge. *Development* **129**, 4855–4866.
- Capdevila, J., Tabin, C. and Johnson, R. L.** (1998). Control of Dorsoventral Somite Patterning by Wnt-1 and B-Catenin. *Dev. Biol.* **193**, 182–194.
- Carrasco, E., Mcginnis, W., Gehring, W. J. and De Robertis, E. M.** (1984). Cloning of an *X. laevis* Gene Expressed during Early Embryogenesis Coding for a Peptide Region Homologous to *Drosophila* Homeotic Genes. *Cell* **37**, 409–414.
- Charron, F., Stein, E., Jeong, J., McMahon, A. P. and Tessier-Lavigne, M.** (2003). The Morphogen Sonic Hedgehog Is an Axonal Chemoattractant that Collaborates with Netrin-1 in Midline Axon Guidance. *Cell* **113**, 11–23.
- Chen, F., Greer, J. and Capecchi, M. R.** (1998). Analysis of *Hoxa7/Hoxb7* mutants suggests periodicity in the generation of the different sets of vertebrae. *Mech. Dev.* **77**, 49–57.
- Chen, J. K., Taipale, J., Cooper, M. K. and Beachy, P. A.** (2002). Inhibition of Hedgehog signaling by direct binding of cyclopamine to Smoothed. *Genes Dev.* **16**, 2743–2748.
- Cheng, L., Alvares, L. E., Ahmed, M. U., El-Hanfy, A. S. and Dietrich, S.** (2004). The epaxial-hypaxial subdivision of the avian somite. *Dev. Biol.* **274**, 348–369.
- Chernoff, E. A. G. and Lash, J. W.** (1981). Cell Movement in Somite Formation and Development in the Chick: Inhibition of Segmentation. *Dev. Biol.* **87**, 212–219.
- Chisaka, O. and Capecchi, M. R.** (1991). Regionally restricted developmental defects resulting from targeted disruption of the mouse homeobox gene *hox-1.5*. *Nature* **350**, 473–479.
- Choi, K.-S. and Harfe, B. D.** (2011). Hedgehog signaling is required for formation of the notochord sheath and patterning of nuclei pulposi within the intervertebral discs. *Proc Natl Acad Sci U S A* **108**, 9484–9489.
- Choi, K.-S., Cohn, M. J. and Harfe, B. D.** (2008). Identification of nucleus pulposus precursor cells and notochordal remnants in the mouse: implications for disk degeneration and chordoma formation. *Dev. Dyn.* **237**, 3953–3958.

- Choi, K.-S., Lee, C. and Harfe, B. D.** (2012). Sonic hedgehog in the notochord is sufficient for patterning of the intervertebral discs. *Mech. Dev.* **129**, 255–62.
- Christ, B. and Ordahl, C. P.** (1995). Early stages of chick somite development. *Anat. Embryol. (Berl)*. **191**, 381–396.
- Christ, B. and Scaal, M.** (2008). Formation and Differentiation of Avian Somite Derivatives. *Adx Exp Med Biol* **168**, 1–41.
- Christ, B. and Wilting, J.** (1992). From somites to vertebral column. *Ann. Anat.* **174**, 23–32.
- Christ, B., Jacob, H. J. and Jacob, M.** (1972). Experimental analysis of somitogenesis in the chick embryo. *Z Anat Entwicklungsgesch* **138**, 82–97.
- Christ, B., Jacob, H. J. and Jacob, M.** (1976). On the formation of the myotomes in avian embryos. An experimental and scanning electron microscope study 1. *Experientia* **34**, 514–516.
- Christ, B., Brand-Saberi, B., Grim, M. and Wilting, J.** (1992). Local signalling in dermomyotomal cell type specification. *Anat. Embryol. (Berl)*. **106**, 505–510.
- Cooke, J.** (1975). Control of somite number during morphogenesis of a vertebrate, *Xenopus laevis*. *Nature* **254**, 196–199.
- Cooke, J. and Elsdale, T.** (1980). Somitogenesis in amphibian embryos upon pattern abnormalities that follow short temperature shocks. *J. Exp. Morphol.* **58**, 107–118.
- Cooke, J. and Zeeman, E. C.** (1976). A Clock and Wavefront Model for Control of the Number of Repeated Structures during Animal Morphogenesis. *J. Theor. Biol.* **58**, 455–476.
- Cooper, M. K., Porter, J. A., Young, K. E. and Beachy, P. A.** (1998). Teratogen-Mediated Inhibition of Target Tissue Response to Shh Signaling. *Science*. **280**, 1603–1608.
- Crossley, P. H. and Martin, G. R.** (1995). The mouse *Fgf8* gene encodes a family of polypeptides and is expressed in regions that direct outgrowth and patterning in the developing embryo. *Development* **121**, 439–451.

- Dale, J. K., Maroto, M., Dequeant, M., Malapert, P. and McGrew, M.** (2003). Periodic Notch inhibition by Lunatic Fringe underlies the chick segmentation clock. *Nature* **421**, 275–278.
- Dale, J. K., Malapert, P., Maroto, M., Johnson, T., Jayasinghe, S., Trainor, P., Herrmann, B. and Pourquié, O.** (2006). Oscillations of the Snail Genes in the Presomitic Mesoderm Coordinate Segmental Patterning and Morphogenesis in Vertebrate Somitogenesis. *Dev. Cell* **10**, 355–366.
- Davies, J. A., Cook, G. M. W., Stern, C. D. and Keynes, R. J.** (1990). Isolation from chick somites of a glycoprotein fraction that causes collapse of dorsal root ganglion growth cones. *Neuron* **2**, 11–20.
- Davis, G. K. and Patel, N. H.** (1999). The origin and evolution of segmentation. *Trends Genet* **15**, M68–M72.
- De Beer, G. R.** (1937). *The development of the vertebrate skull*. Chicago: University of Chicago Press.
- De Robertis, E. M. and Sasai, Y.** (1996). A common plan for dorsoventral patterning in Bilateria. *Nature* **380**, 37–40.
- Delfini, M.-C., Dubrulle, J., Malapert, P., Chal, J. and Pourquié, O.** (2005). Control of the segmentation process by graded MAPK/ERK activation in the chick embryo. *Proc. Natl. Acad. Sci.* **102**, 11343–11348.
- Delsuc, F., Brinkmann, H., Chourrout, D. and Philippe, H.** (2006). Tunicates and not cephalochordates are the closest living relatives of vertebrates. *Nature* **439**, 965–968.
- Dequéant, M., Glynn, E., Gaudenz, K., Wahl, M., Chen, J., Mushegian, A. and Pourquié, O.** (2006). A Complex Oscillating Network of Signaling Genes Underlies the Mouse Segmentation Clock. *Science*. **314**, 1595–1598.
- Deutsch, U., Dressier, R. and Gruss, P.** (1988). Pax 1, A Member of a Paired Box Homologous Murine Gene Family, Is Expressed in Segmented Structures during Development. *Cell* **53**, 617–625.
- Dias, A. S., de Almeida, I., Belmonte, J. M., Glazier, J. A. and Stern, C. D.** (2014). Somites without a clock. *Science*. **343**, 791–795.

- Dietrich, S., Schubert, F. R. and Lumsden, A.** (1997). Control of dorsoventral pattern in the chick paraxial mesoderm. *Development* **124**, 3895–3908.
- Diez del Corral, R., Olivera-martinez, I., Goriely, A., Gale, E., Maden, M. and Storey, K.** (2003). Opposing FGF and Retinoid Pathways Control Ventral Neural Pattern, Neuronal Differentiation, and Segmentation during Body Axis Extension. *Neuron* **40**, 65–79.
- Dockter, J. L.** (2000). Sclerotome Induction and Differentiation. *Curr. Top. Dev. Biol.* **48**, 77–127.
- Dorey, K. and Amaya, E.** (2010). FGF signalling: diverse roles during early vertebrate embryogenesis. *Development* **137**, 3731–3742.
- Duboule, D.** (2007). The rise and fall of Hox gene clusters. *Development* **134**, 2549–2560.
- Duboule, D. and Dollé, P.** (1989). The structural and functional organization of the murine HOX gene family resembles that of Drosophila homeotic genes. *EMBO J.* **8**, 1497–1505.
- Dubrulle, J., Mcgrew, M. J. and Pourquié, O.** (2001). FGF Signaling Controls Somite Boundary Position and Regulates Segmentation Clock Control of Spatiotemporal Hox Gene Activation. *Cell* **106**, 219–232.
- Duong, T. D. and Erickson, C. A.** (2004). MMP-2 Plays an Essential Role in Producing Epithelial-Mesenchymal Transformations in the Avian Embryo. *Dev. Dyn.* **229**, 42–53.
- Durston, A. J., Wacker, S., Bardine, N. and Jansen, H. J.** (2012). Time Space Translation: A Hox Mechanism for Vertebrate A-P Patterning. *Curr. Genomics* **13**, 300–307.
- Ebensperger, C., Wilting, J., Brand-Saberi, B., Mizutani, Y., Christ, B., Balling, R. and Koseki, H.** (1995). Pax-I, a regulator of sclerotome development is induced by notochord and floor plate signals in avian embryos. *Anat. Embryol. (Berl)*. **191**, 297–310.
- Echelard, Y., Epstein, D. J., St-Jacques, B., Shen, L., Mohler, J., McMahon, J. A. and McMahon, A. P.** (1993). Sonic Hedgehog, a Member of a Family of Putative

Signaling Molecules, Is Implicated in the Regulation of CNS Polarity. *Cell* **75**, 1417–1430.

Eernisse, D. J., Albert, J. S. and Anderson, F. E. (1992). Annelida and Arthropoda Are Not Sister Taxa: A Phylogenetic Analysis of Spiralian Metazoan Morphology. *Syst. Biol. (Stevenage)*. **41**, 305–330.

Elsdale, T., Pearson, M. and Whitehead, M. (1976). Abnormalities in somite segmentation following heat shock to *Xenopus* embryos. *J. Exp. Morphol.* **35**, 625–635.

Evans, D. J. R. (2003). Contribution of somitic cells to the avian ribs. *Dev. Biol.* **256**, 114–126.

Ewan, K. B. and Everett, A. W. (1992). Evidence for resegmentation in the formation of the vertebral column using the novel approach of retroviral-mediated gene transfer. *Exp. Cell Res.* **198**, 315–20.

Eyckmans, J., Boudou, T., Yu, X. and Chen, C. S. (2011). A Hitchhiker's Guide to Mechanobiology. *Dev. Cell* **21**, 35–47.

Fan, C. and Tessier-Lavigne, M. (1994). Patterning of Mammalian Somites by Surface Ectoderm and Notochord: Evidence for Sclerotome Induction by a Hedgehog Homolog. *Cell* **79**, 1175–1186.

Fan, C., Porter, J. A., Chiang, C., Chang, D. T., Beachy, P. A. and Tessier-Lavigne, M. (1995). Long-Range Sclerotome Induction by Sonic Hedgehog: Direct Role of the Amino-Terminal Cleavage Product and Modulation by the Cyclic AMP Signaling Pathway. *Cell* **81**, 457–465.

Fleming, A., Keynes, R. and Tannahill, D. (2001). The role of the notochord in vertebral column formation. *J. Anat.* **199**, 177–180.

Fleming, A., Keynes, R. and Tannahill, D. (2004). A central role for the notochord in vertebral patterning. *Development* **131**, 873–80.

Fleming, A., Kishida, M. G., Kimmel, C. B. and Keynes, R. J. (2015). Building the backbone: the development and evolution of vertebral patterning. *Development* **142**, 1733–1744.

- Forsberg, H., Crozet, F. and Brown, N. A.** (1998). Waves of mouse Lunatic fringe expression, in four-hour cycles at two-hour intervals, precede somite boundary formation. *Curr. Biol.* **8**, 1027–1030.
- Froriep, A.** (1883). Zur Entwicklungsgeschichte der Wirbelsaule, insbesondere des Atlas und Epistropheus und der Occipitalregion. I. Beobachtungen an Hahnerembryonen. *Arch. Anat. Physiol.* **1883**, 177–234.
- Froriep, A.** (1886). Zur Entwicklungsgeschichte der Wirbelsaule, insbesondere des Atlas und Epistropheus und der Occipitalregion. II. Beobachtungen an Säugetierembryone. *Arch. Anat. Physiol.* **1886**, 69–150.
- Gadow, H. F. and Abbott, E. C.** (1895) On the evolution of the vertebral column of fishes. *Philos. Trans. R. Soc. Lond. B. Biol. Sci.* **186**, 168-221
- Gadow, H. F.** (1933). *The evolution of the vertebral column*. Cambridge, UK: Cambridge University Press.
- Garcia-Fernandez, J. and Holland, P. W. H.** (1994). Archetypal organization of the amphioxus Hox gene cluster. *Nature* **370**, 563–566.
- Gee, H.** (1996). *Before the Backbone: Views on the Origin of the Vertebrates*. London: Chapman & Hall.
- Gilbert, E. A. B., Payne, S. L. and Vickaryous, M. K.** (2014). The anatomy and histology of caudal autotomy and regeneration in lizards. *Physiol. Biochem. Zool.* **86**, 631–644.
- Goldstein, R. S. and Kalcheim, C.** (1992). Determination of epithelial half-somites in skeletal morphogenesis. *Development* **116**, 441–445.
- Gomez, C., Ozbudak, E. M., Wunderlich, J., Baumann, D., Lewis, J. and Pourquié, O.** (2008). Control of segment number in vertebrate embryos. *Nature* **454**, 335–339.
- González, A. and Kageyama, R.** (2010). Automatic reconstruction of the mouse segmentation network from an experimental evidence database. *BioSystems* **102**, 16–21.

- Goodrich, E. S.** (1930). *Studies on the structure and development of vertebrates*. London: MacMillan.
- Goulding, M. D., Chalepakis, G., Deutsch, U., Erselius, J. R. and Gruss, P.** (1991). Pax-3, a novel murine DNA binding protein expressed during early neurogenesis. *EMBO J.* **10**, 1135–1147.
- Goulding, M., Lumsden, A. and Paquette, A. J.** (1994). Regulation of Pax-3 expression in the dermomyotome and its role in muscle development. *Development* **120**, 957–971.
- Graham, A., Papalopulu, N. and Krumlauf, R.** (1989). The murine and Drosophila homeobox gene complexes have common features of organization and expression. *Cell* **57**, 367–378.
- Grobben, K.** (1908). Die systematische Einteilung des Tierreiches. *Verh. Zool. Bot. Ges. Wien.* **58**, 491—511.
- Grotmol, S., Kryvi, H. and Nordvik, K.** (2003). Notochord segmentation may lay down the pathway for the development of the vertebral bodies in the Atlantic salmon. *Anat. Embryol. (Berl)*. **207**, 263–272.
- Grotmol, S., Nordvik, K., Kryvi, H. and Totland, G. K.** (2005). A segmental pattern of alkaline phosphatase activity within the notochord coincides with the initial formation of the vertebral bodies. *J. Anat.* **206**, 427–436.
- Haeckel, E.** (1874). *Anthropogenie oder Entwicklungsgeschichte des Menschen*. Leipzig: Engelmann.
- Hamburger, V. and Hamilton, H. L.** (1951). A series of normal stages in the development of the chick embryo. *Dev. Dyn.* **195**, 231–272.
- Hamilton, H. L.** (1953). *Lillie's Development of the Chick- an Introduction to Embryology*. 3rd ed. New York: H. Holt & co.
- Hamilton, H. L. and Hinsch, G. W.** (1956). The developmental fate of the first somite in chick. *Anat. Rec.* **125**, 225–245.
- Hannibal, R. L. and Patel, N. H.** (2013). What is a segment? *Evodevo* **4**, 35.

- Harding, K., Wedeen, C., Mcginnis, W. and Levine, M.** (1985). Spatially Regulated Expression of Homeotic Genes in *Drosophila*. *Science*. **229**, 1236–1242.
- Harima, Y., Takashima, Y., Ueda, Y., Ohtsuka, T. and Kageyama, R.** (2013). Accelerating the Tempo of the Segmentation Clock by Reducing the Number of Introns in the *Hes7* Gene. *Cell Rep*. **3**, 1–7.
- Harland, R. and Gerhart, J.** (1997). Formation and function of Spemann's organizer. *Annu. Rev. Cell Dev. Biol.* **13**, 611–667.
- Hayashi, S., Shimoda, T., Nakajima, M., Tsukada, Y., Sakumura, Y. and Kim, J.** (2009). Sprouty4, an FGF Inhibitor, Displays Cyclic Gene Expression under the Control of the Notch Segmentation Clock in the Mouse PSM. *PLoS One* **4**, e5603.
- Helker, C. S. M., Schuermann, A., Pollmann, C., Scng, S. C., Kiefer, F., Reversade, B. and Herzog, W.** (2015). The hormonal peptide Elabela guides angioblasts to the midline during vasculogenesis. *Elife* **4**, e06726.
- Henry, C. A., Urban, M. K., Dill, K. K., Merlie, J. P., Page, M. F., Kimmel, C. B. and Amacher, S. L.** (2002). Two linked hairy/Enhancer of split-related zebrafish genes, *her1* and *her7*, function together to refine alternating somite boundaries. *Development* **129**, 3693–3704.
- Hensen, V.** (1876). Beobachtungen über die Befruchtung und Entwicklung des Kaninchens and Meerschweinchens. *Z Anat Entwickl Gesch* **1**, 213–273 und 353–423.
- Herrgen, L., Ares, S., Morelli, L. G., Schroter, C., Julicher, F. and Oates, A. C.** (2010). Intercellular Coupling Regulates the Period of the Segmentation Clock. *Curr. Biol.* **20**, 1244–1253.
- Hirano, S., Hirako, R., Kajita, N. and Norita, M.** (1995). Morphological analysis of the role of the neural tube and notochord in the development of somites. *Anat. Embryol. (Berl)*. **192**, 445–457.
- Holland, P. W. H. and Hogan, B. L. M.** (1986). Phylogenetic distribution of Antennapedia-like homeo boxes. *Nature* **321**, 251–253.

- Holley, S. A., Geisler, R. and Nusslein-Volhard, C.** (2000). Control of her1 expression during zebrafish somitogenesis by a Delta -dependent oscillator and an independent wave-front activity. *Genes Dev.* **14**, 1678–1690.
- Hornbruch, B. A., Summerbell, D. and Wolpert, L.** (1979). Somite formation in the early chick embryo following grafts of Hensen's node. *J. Exp. Morphol.* **51**, 51–62.
- Huang, R., Zhi, Q., Wilting, J. and Christ, B.** (1994). The fate of somitocoel cells in avian embryos. *Anat. Embryol. (Berl)*. **190**, 243–250.
- Huang, R., Zhi, Q., Neubuser, A., Muller, T. S., Brand-Saberi, B., Christ, B. and Wilting, J.** (1996). Function of Somite and Somitocoel Cells in the Formation of the Vertebral Motion Segment in Avian Embryos. *Acta Anat. (Basel)*. **155**, 231–241.
- Huang, R., Zhi, Q., Ordahl, C. P. and Christ, B.** (1997). The fate of the first avian somite. *Anat. Embryol. (Berl)*. **195**, 435–449.
- Huang, R., Zhi, Q., Schmidt, C., Wilting, J., Brand-saberi, B. and Christ, B.** (2000a). Sclerotomal origin of the ribs. *Development* **532**, 527–532.
- Huang, R., Zhi, Q., Brand-Saberi, B. and Christ, B.** (2000b). New experimental evidence for somite resegmentation. *Anat. Embryol. (Berl)*. **202**, 195–200.
- Huang, R., Zhi, Q., Patel, K., Wilting, J. and Christ, B.** (2000c). Contribution of single somites to the skeleton and muscles of the occipital and cervical regions in avian embryos. *Anat. Embryol. (Berl)*. **202**, 375–383.
- Imura, T. and Pourquié, O.** (2006). Collinear activation of Hoxb genes during gastrulation is linked to mesoderm cell ingression. *Nature* **442**, 568–571.
- Incardona, J. P., Gaffield, W., Kapur, R. P. and Roelink, H.** (1998). The teratogenic Veratrum alkaloid cyclopamine inhibits Sonic hedgehog signal transduction. *Development* **125**, 3553–3562.
- Ishikawa, A., Kitajima, S., Takahashi, Y., Kokubo, H., Kanno, J., Inoue, T. and Saga, Y.** (2004). Mouse Nkd1, a Wnt antagonist, exhibits oscillatory gene expression in the PSM under the control of Notch signaling. *Mech. Dev.* **121**, 1443–1453.

- Janvier, P.** (1999). Catching the first fish. *Nature* **402**, 21–22.
- Johnson, R. L., Laufer, E., Tabin, C. and Riddle, D.** (1994). Ectopic Expression of Sonic hedgehog Alters Dorsal-Ventral Patterning of Somites. *Cell* **79**, 1165–1173.
- Jostes, B., Walther, C. and Gruss, P.** (1991). The murine paired box gene, Pax7, is expressed specifically during the development of the nervous and muscular system. *Mech. Dev.* **33**, 27–37.
- Jouve, C., Palmeirim, I., Henrique, D., Beckers, J., Gossler, A., Ish-Horowicz, D. and Pourquié, O.** (2000). Notch signalling is required for cyclic expression of the hairy-like gene HES1 in the presomitic mesoderm. *Development* **127**, 1421–1429.
- Kappen, C., Schughart, K. and Ruddle, F. H.** (1993). Early evolutionary origin of major homeodomain sequence classes. *Genomics* **18**, 54–70.
- Kessel, M. and Gruss, P.** (1991). Homeotic transformations of murine vertebrae and concomitant alteration of Hox codes induced by retinoic acid. *Cell* **67**, 89–104.
- Kessel, M., Balling, R. and Gruss, P.** (1990). Variations of Cervical Vertebrae after Expression of a Hox7.1 Transgene in Mice. *Cell* **61**, 301–306.
- Keynes, R. J. and Stern, C. D.** (1984). Segmentation in the vertebrate nervous system. *Nature* **310**, 786–789.
- Keynes, R. J. and Stern, C. D.** (1986). Somites and Neural Development. In *Somites in Developing Embryos* (ed. Bellairs, R., Ede, D. A., and Lash, J. W.), pp. 289–299. New York: Plenum.
- Kieny, M., Mauger, A. and Sengel, P.** (1972). Early Regionalization of the Somitic Mesoderm as Studied by the development of the Axial Skeleton of the Chick Embryo. *Dev. Biol.* **28**, 142–161.
- Kimelman, D. and Bjornson, C.** (2004). Vertebrate Mesoderm Induction: From Frogs To Mice. In *Gastrulation: From Cells To Embryo* (ed. Stern, C. D.), pp. 363–371. New York: Cold Spring Harbour Laboratory Press.
- Kölliker, A. von** (1861). *Entwicklungsgeschichte des Menschen und der höheren Thiere*. Leipzig: Engelmann.

- Kollman, J.** (1891). Die Rumpfsegmente Menschlicher Embryonen von 13-35 Urwibelm. *Arch. Anat. Physiol.* **1891**, 39–88.
- Koressaar, T. and Remm, M.** (2007). Enhancements and modifications of primer design program Primer3. *Bioinformatics* **23**, 1289–1291.
- Krol, A. J., Roellig, D., Dequéant, M., Tassy, O., Glynn, E., Hattem, G., Mushegian, A., Oates, A. C. and Pourquié, O.** (2011). Evolutionary plasticity of segmentation clock networks. *Development* **138**, 2783–2792.
- Lauri, A., Brunet, T., Handberg-Thorsager, M., Fischer, A. H. L., Simakov, O., Steinmetz, P. R. H., Tomer, R., Keller, P. J. and Arendt, D.** (2014). Development of the annelid axochord: Insights into notochord evolution. *Science*. **345**, 1365–1368.
- Le Douarin, N. M.** (1972). A Biological Cell Labeling Technique and Its Use in Experimental Embryology. *Dev. Biol.* **30**, 217–222.
- Leimeister, C., Dale, K., Fischer, A., Klamt, B., Hrabe de Angelis, M., Radtke, F., McGrew, M. J., Pourquié, O. and Gessler, M.** (2000). Oscillating Expression of c-Hey2 in the Presomitic Mesoderm Suggests That the Segmentation Clock May Use Combinatorial Signaling through Multiple Interacting bHLH Factors. *Dev. Biol.* **227**, 91–103.
- Levin, M., Johnson, R. L., Stern, C. D., Kuehn, M. and Tabin, C.** (1995). Determining Left-Right Asymmetry in Chick Embryogenesis. *Cell* **82**, 803–814.
- Levine, M., Rubin, G. M. and Tjian, R.** (1984). Human DNA Sequences Homologous to a Protein Coding Region Conserved between Homeotic Genes of *Drosophila*. *Cell* **38**, 667–673.
- Lewis, E. B.** (1978). A gene complex controlling segmentation in *Drosophila*. *Nature* **276**, 565–570.
- Lewis, R. A., Kaufman, T. C., Dennell, R. E. and Tollerico, P.** (1980). Genetic analysis of the Antennapedia gene complex (Ant-C) and adjacent chromosomal regions of *Drosophila melanogaster*. I. Polytene chromosome segments 84B-D. *Genetics* **95**, 367–381.

- Lim, T., Jaques, K. F., Stern, C. D. and Keynes, R. J.** (1991). An evaluation of myelomeres and segmentation of the chick embryo spinal cord. *Development* **113**, 227–238.
- Malpighi, M.** (1672). De ovo incubato, (1686). De formatione pulli in ovo. Cited by: I. Needham, (1934). *A history of embryology*, pp. xviii and 274. Cambridge, Cambridge University Press
- Mammoto, T. and Ingber, D. E.** (2010). Mechanical control of tissue and organ development. *Development* **137**, 1407–1420.
- Manner, H.** (1899). Beitrage zur Entwicklungsgeschichte der Wirbelsaule bei Reptilien. *Z. wiss. Zool.* **LXVI-I**, 43–68.
- Mansouri, A., Yokota, Y., Wehr, R., Copeland, N. G., Jenkins, N. A. and Gruss, P.** (1997). Paired-Related Murine Homeobox Gene Expressed in the Developing Sclerotome, Kidney, and Nervous System. *Dev. Dyn.* **210**, 53–65.
- Maroto, M., Dale, J. K. I. M., Dequéant, M., Petit, A. and Pourquié, O.** (2005). Synchronised cycling gene oscillations in presomitic mesoderm cells require cell-cell contact. *Int. J. Dev. Biol.* **49**, 309–315.
- Masamizu, Y., Ohtsuka, T., Takashima, Y., Nagahara, H. and Takenaka, Y.** (2006). Real-time imaging of the somite segmentation clock: Revelation of unstable oscillators in the individual presomitic mesoderm cells. *PNAS* **103**, 1313–1318.
- Maynard Smith, J.** (1960). Continuous, quantized and modal variation. *Proc. R. Soc.* **52**, 397.
- Mcginnis, W., Levine, M. S., Hafen, E., Kuroiwa, A. and Gehring, W. J.** (1984a). A conserved DNA sequence in homeotic genes of the Drosophila Antennapedia and bithorax complexes. *Nature* **308**, 428–433.
- Mcginnis, W., Garber, R. L., Wirz, J., Kuroiwa, A. and Gehring, W. J.** (1984b). A Homologous Protein-Coding Sequence in Drosophila Homeotic Genes and Its Conservation in Other Metazoans. *Cell* **37**, 403–408.
- Mcgregor, A. P., Pechmann, M., Schwager, E. E. and Damen, W. G. M.** (2009). An ancestral regulatory network for posterior development in arthropods. *Commun. Integr. Biol.* **2**, 174–176.

- McGrew, M. J., Dale, J. K., Fraboulet, S. and Pourquié, O.** (1998). The lunatic Fringe gene is a target of the molecular clock linked to somite segmentation in avian embryos. *Curr. Biol.* **8**, 979–982.
- McIntyre, D. C., Rakshit, S., Yallowitz, A. R., Loken, L., Jeannotte, L., Capecchi, M. R. and Wellik, D. M.** (2007). Hox patterning of the vertebrate rib cage. *Development* **134**, 2981–2989.
- McLeod, M. J.** (1980). Differential Staining of Cartilage and Bone in Whole Mount Mouse Fetuses by Alcian Blue and Alizarin Red S. *Teratology* **22**, 299–301.
- McMahon, J. A., Takada, S., Zimmerman, L. B., Fan, C., Harland, R. M. and McMahon, A. P.** (1998). Noggin-mediated antagonism of BMP signaling is required for growth and patterning of the neural tube and somite. *Genes Dev.* **12**, 1438–1452.
- Merchán, P., Bribián, A., Sánchez-camacho, C., Lezameta, M., Bovolenta, P. and de Castro, F.** (2007). Sonic hedgehog promotes the migration and proliferation of optic nerve oligodendrocyte precursors. *Mol. Cell. Neurosci.* **36**, 355–368.
- Mohammadi, M., McMahon, G., Sun, L., Tang, C., Hirth, P., Yeh, B. K., Hubbard, S. R. and Schlessinger, J.** (1997). Structures of the Tyrosine Kinase Domain of Fibroblast Growth Factor Receptor in Complex with Inhibitors. *Science.* **276**, 955–960.
- Moreno, T. A. and Kintner, C.** (2004). Regulation of Segmental Patterning by Retinoic Acid Signaling during *Xenopus* Somitogenesis. *Dev. Cell* **6**, 205–218.
- Morimoto, M., Sasaki, N., Oginuma, M., Kiso, M. and Igarashi, K.** (2007). The negative regulation of *Mesp2* by mouse *Ripply2* is required to establish the rostro-caudal patterning within a somite. *Development* **134**, 1561–1569.
- Morin-Kensicki, E. M. and Eisen, J. S.** (1997). Sclerotome development and peripheral nervous system segmentation in embryonic zebrafish. *Development* **124**, 159–167.
- Morin-Kensicki, E. M., Melancon, E. and Eisen, J. S.** (2002). Segmental relationship between somites and vertebral column in zebrafish. *Development* **129**, 3851–3860.

- Münsterberg, A. E. and Lassar, A. B.** (1995). Combinatorial signals from the neural tube, floor plate and notochord induce myogenic bHLH gene expression in the somite. *Development* **121**, 651–660.
- Neiderreither, K., McCaffrey, P., Drager, U. C., Chambon, P. and Dollé, P.** (1997). Restricted expression and retinoic acid-induced downregulation of the retinaldehyde dehydrogenase type 2 (RALDH-2) gene during mouse development. *Mech. Dev.* **62**, 67–78.
- Neidhardt, L. M., Kispert, A. and Herrmann, B. G.** (1997). A mouse gene of the paired-related homeobox class expressed in the caudal somite compartment and the developing vertebral column, kidney and nervous system. *Dev. Genes Evol.* **207**, 330–339.
- Neubüser, A., Koseki, H. and Balling, R.** (1995). Characterization and Developmental Expression of Pax9, a Paired-Box-Containing Gene Related to Pax1. *Dev. Biol.* **170**, 701–716.
- New, D. A.** (1955). A New Technique for the Cultivation of the Chick Embryo in vitro. *J. Embryol. Exp. Morphol.* **3**, 320.
- Newgreen, D. F., Scheel, M. and Kastner, V.** (1986). Morphogenesis of sclerotome and neural crest in avian embryos: In vivo and in vitro studies of notochordal extracellular material. *Cell Tissue Res.* **244**, 299–313.
- Nicolas, J. F., Mathis, L. and Bonnerot, C.** (1996). Evidence in the mouse for self-renewing stem cells in the formation of a segmented longitudinal structure, the myotome. *Development* **122**, 2933–2946.
- Nicolet, G.** (1965). Etude autoradiographique de la destination des cellules invaginées au niveau du noeud de Hensen de la ligne primitive achevée de l'embryon de poulet. Etude à l'aide de la thymidine tritiée. *Acta Embryol. Morph.* **8**, 213–220.
- Nicolet, G.** (1970a). Analyse autoradiographique de la localisation des différentes ébauches présomptives dans la ligne primitive de l'embryon de poulet. *J. Embryol. exp. Morph.* **23**, 79–108.
- Nicolet, G.** (1970b). Is the presumptive notochord responsible for somite genesis in the chick? *J. Embryol. Exp. Morphol.* **24**, 467–478.

- Nicolet, G.** (1971). The Young Notochord can Induce Somite Genesis by Means of Diffusible Substances in the Chick. *Experientia* **27**, 938–939.
- Nielsen, C.** (2012). The authorship of higher chordate taxa. *Zool. Scr.* **41**, 435–436.
- Nikaido, M., Kawakami, A., Sawada, A., Furutani-Seiki, M., Takeda, H. and Araki, K.** (2002). Tbx24, encoding a T-box protein, is mutated in the zebrafish somite-segmentation mutant fused somites. *Nat. Genet.* **31**, 195–199.
- Niwa, H., Yamamura, K. and Miyazaki, J.** (1991). Efficient selection for high-expression transfectants with a novel eukaryotic vector. *Gene* **108**, 193–199.
- Nomura-Kitabayashi, A., Takahashi, Y., Kitajima, S., Inoue, T., Takeda, H. and Saya, Y.** (2002). Hypomorphic *Mesp* allele distinguishes establishment of rostrocaudal polarity and segment border formation in somitogenesis. *Development*. **129**, 2473-2481
- Noro, M., Uejima, A., Abe, G., Manabe, M. and Tamura, K.** (2009). Normal developmental stages of the Madagascar ground gecko *Paroedura pictus* with special reference to limb morphogenesis. *Dev. Dyn.* **238**, 100–9.
- Norris, W. E., Stern, C. D. and Keynes, R. J.** (1989). Molecular differences between the rostral and caudal halves of the sclerotome in the chick embryo. *Development* **105**, 541–548.
- Nowicki, J. L. and Burke, A. C.** (2000). Hox genes and morphological identity: axial versus lateral patterning in the vertebrate mesoderm. *Development* **127**, 4265–75.
- Oates, A. C. and Ho, R. K.** (2002). Hairy/ E(spl)-related (Her) genes are central components of the segmentation oscillator and display redundancy with the Delta/Notch signaling pathway in the formation of anterior segmental boundaries in the zebrafish. *Development* **129**, 2929–2946.
- Oates, A. C., Morelli, L. G. and Ares, S.** (2012). Patterning embryos with oscillations: structure, function and dynamics of the vertebrate segmentation clock. *Development* **139**, 625–639.
- Oberg, K. C., Pira, C. U., Revelli, J., Ratz, B., Aguilar-Cordova, E. and Eichele, G.** (2002). Efficient Ectopic Gene Expression Targeting Chick Mesoderm. *Dev. Dyn.* **224**, 291–302.

- Olivera-martinez, I., Thelu, J., Teillet, M. and Dhouailly, D.** (2001). Dorsal dermis development depends on a signal from the dorsal neural tube , which can be substituted by Wnt-1. *Mech. Dev.* **100**, 233–244.
- Ordahl, C. P.** (1993). Myogenic lineages within the developing somite. In *Molecular basis of morphogenesis*, pp. 165–176. New York: Liss.
- Ordahl, C. P. and Le Douarin, N. M.** (1992). Two myogenic lineages within the developing somite. *Development* **114**, 339–353.
- Palmeirim, I., Henrique, D., Ish-Horowicz, D. and Pourquié, O.** (1997). Avian hairy gene expression identifies a molecular clock linked to vertebrate segmentation and somitogenesis. *Cell* **91**, 639–648.
- Pauli, A., Norris, M. L., Valen, E., Chew, G., Gagnon, J. A., Zimmerman, S., Mitchell, A., Ma, J., Dubrulle, J., Reyon, D., Tsai, S. Q., Joung, K., Saghatelian, A. and Schier, A. F.** (2014). Toddler: An Embryonic Signal That Promotes Cell Movement via Apelin Receptors. *Science*. **343**, 746–754.
- Pearse, R. V, Vogan, K. J. and Tabin, C. J.** (2001). Ptc1 and Ptc2 transcripts provide distinct readouts of Hedgehog signaling activity during chick embryogenesis. *Dev. Biol.* **239**, 15–29.
- Pearson, M. and Elsdale, T.** (1979). Somitogenesis in amphibian embryos: Emperimental evidence for an interation between two temporal factors in the specification of somite pattern. *J. Embryol. Exp. Morphol.* **51**, 27–50.
- Peel, A. D., Chipman, A. D. and Akam, M.** (2005). Arthropod Segmentation: Beyond the Drosophila Paradigm. *Nat. Rev. Genet.* **6**, 905–916.
- Piekarski, N. and Olsson, L.** (2014). Resegmentation in the mexican axolotl, *Ambystoma mexicanum*. *J. Morphol.* **275**, 141–152.
- Placzek, M.** (1995). The role of the notochord and floor plate in inductive interactions. *Curr. Opin. Genet. Dev.* **5**, 499–506.
- Pourquié, O.** (2011). Vertebrate segmentation: from cyclic gene networks to scoliosis. *Cell* **145**, 650–63.

- Pourquié, O., Coltey, M., Teillet, M. A., Ordahl, C. and Le Douarin, N. M.** (1993). Control of dorsoventral patterning of somitic derivatives by notochord and floor plate. *Proc Natl Acad Sci U S A* **90**, 5242–5246.
- Pourquié, O., Coltey, M., Bréant, C. and Le Douarin, N. M.** (1995). Control of somite patterning by signals from the lateral plate. *Proc. Natl. Acad. Sci. USA* **92**, 3219–3223.
- Pourquié, O., Fan, C., Coltey, M., Hirsinger, E., Watanabe, Y., Bréant, C., Francis-West, P., Brickell, P., Tessier-Lavigne, M. and Le Douarin, N. M.** (1996). Lateral and Axial Signals Involved in Avian Somite Patterning: A Role for BMP4. *Cell* **84**, 461–471.
- Pownall, M. E. and Emerson, C. P.** (1992). Sequential Activation of Three Myogenic Regulatory Genes during Somite Morphogenesis in Quail Embryos. *Dev. Biol.* **151**, 67–79.
- Primmitt, D. R. N., Stern, C. D. and Keynes, R. J.** (1988). Heat shock causes repeated segmental anomalies in the chick embryo. *Development* **104**, 331–339.
- Primmitt, D. R. N., Norris, W. E., Carlson, G. J., Keynes, R. J. and Stern, C. D.** (1989). Periodic segmental anomalies induced by heat shock in the chick embryo are associated with the cell cycle. *Development* **105**, 119–130.
- Prince, V. E., Joly, L., Ekker, M. and Ho, R. K.** (1998a). Zebrafish hox genes: genomic organization and modified colinear expression patterns in the trunk. *Development* **125**, 407–420.
- Prince, V. E., Price, A. L. and Ho, R. K.** (1998b). Hox gene expression reveals regionalization along the anteroposterior axis of the zebrafish notochord. *Dev. Genes Evol.* **208**, 517–22.
- Psychoyos, D. and Stern, C. D.** (1996). Fates and migratory routes of primitive streak cells in the chick embryo. *Development* **122**, 1523–1534.
- Remak, R.** (1855). *Untersuchungen über die Entwicklung der Wirbeltiere*. Berlin: Reimer.
- Richardson, M. K., Allen, S. P., Wright, G. M., Raynaud, A. and Hanken, J.** (1998). Somite number and vertebrate evolution. *Development* **125**, 151–160.

- Rickmann, M., Fawcett, J. W. and Keynes, R. J.** (1985). The migration of neural crest cells and the growth of motor axons through the rostral half of the chick somite. *J. Embryol. Exp. Morphol.* **90**, 437–455.
- Roelink, H., Porter, J. A., Chiang, C. and Tanabe, Y.** (1995). Floor Plate and Motor Neuron Induction by Different Concentrations of the Amino-Terminal Cleavage Product of Sonic Hedgehog Autoproteolysis. *Cell* **81**, 445–455.
- Rufai, A., Benjamin, M. and Ralphs, J. R.** (1995). The development of fibrocartilage in the rat intervertebral disc. *Anat. Embryol.* **192**, 53–62.
- Saga, Y., Hata, N., Koseki, H. and Taketo, M.** (1997). Mesp2: a novel mouse gene expressed in the presegmented mesoderm and essential for segmentation initiation. *Genes Dev.* **11**, 1827–1839.
- Sanders, E. J., Prasad, S. and Cheung, E.** (1988). Extracellular matrix synthesis is required for the movement of sclerotome and neural crest cells on collagen. *Differentiation* **39**, 34–41.
- Sang, H.** (2004). Prospects for transgenesis in the chick. *Mech. Dev.* **121**, 1179–1186.
- Sanz-Ezquerro, J. J. and Tickle, C.** (2000). Autoregulation of Shh expression and Shh induction of cell death suggest a mechanism for modulating polarising activity during chick limb development. *Development* **127**, 4811–4823.
- Sawada, A., Fritz, A., Jiang, Y., Yamamoto, A., Yamasu, K. and Kuroiwa, A.** (2000). Zebrafish Mesp family genes, mesp-a and mesp-b are segmentally expressed in the presomitic mesoderm, and Mesp-b confers the anterior identity to the developing somites. *Development* **127**, 1691–1702.
- Sawada, A., Shinya, M., Jiang, Y., Kawakami, A. and Kuroiwa, A.** (2001). Fgf/MAPK signalling is a crucial positional cue in somite boundary formation. *Development* **128**, 4873–4880.
- Schindelin, J., Arganda-Carreras, I., Frise, E., Kaynig, V., Longair, M., Pietzsch, T., Preibisch, S., Rueden, C., Saalfeld, S., Schmid, B., et al.** (2012). Fiji: an open-source platform for biological-image analysis. *Nat. Methods* **9**, 676–682.

- Schmidt, C., Christ, B., Maden, M., Brand-Saberi, B. and Patel, K.** (2001). Regulation of EphA4 Expression in Paraxial and Lateral Plate Mesoderm by Ectoderm-Derived Signals. *Dev. Dyn.* **220**, 377–386.
- Schmorl, G. and Junghanns, H.** (1968). *Die gesunde und kranke Wirbelsäule in Röntgenbild und Klinik*. 5th ed. Stuttgart: Thieme.
- Schroter, C. and Oates, A. C.** (2010). Segment Number and Axial Identity in a Segmentation Clock Period Mutant. *Curr. Biol.* **20**, 1254–1258.
- Schroter, C., Herrgen, L., Cardona, A., Brouhard, G. J., Feldman, B. and Oates, A. C.** (2008). Dynamics of Zebrafish Somitogenesis. *Dev. Dyn.* **237**, 545–553.
- Schultze, O.** (1896). Ueber embryonale und bleibende Segmentierung. *Anat. Anz. Erg* **12**, 87–93.
- Selleck, M. A. J. and Bronner-fraser, M.** (1995). Origins of the avian neural crest: the role of neural plate-epidermal interactions. *Development* **121**, 525–538.
- Selleck, M. A. J. and Stern, C. D.** (1991). Fate mapping and cell lineage analysis of Hensen ' s node in the chick embryo. *Development* **112**, 615–626.
- Selleck, M. A. J. and Stern, C. D.** (1992a). Commitment of mesoderm cells in Hensen's node of the chick embryo to notochord and somite. *Development* **415**, 403–415.
- Selleck, M. A. J. and Stern, C. D.** (1992b). Evidence for stem cells in the mesoderm of Hensen's node and their role in embryonic pattern formation. In *Formation and Differentiation of Early Embryonic Mesoderm* (ed. Bellairs, R., Sanders, E. J., and Lash, J. W.), pp. 23–31. New York: Plenum Press.
- Sensenig, E. C.** (1949). The early development of the human vertebral column. *Contr. Embryol.* **33**, 23–41.
- Senthinathan, B., Sousa, C., Tannahill, D. and Keynes, R.** (2012). The generation of vertebral segmental patterning in the chick embryo. *J. Anat.* **220**, 591–602.
- Shamim, H. and Mason, I.** (1999). Expression of Fgf4 during early development of the chick embryo. **85**, 189–192.

- Sharpe, J., Ahlgren, U., Perry, P., Hill, B., Ross, A., Hecksher-Sørensen, J., Baldock, R. and Davidson, D.** (2002). Optical Projection Tomography as a Tool for 3D Microscopy and Gene Expression Studies. *Science*. **296**, 541–545.
- Shu, D., Luo, H., Morris, S. C., Zhang, X., Hu, S., Chen, L., Han, J., Zhu, M., Li, Y. and Chen, L.** (1999). Lower Cambrian vertebrates from south China. *Nature* **402**, 42–46.
- Slack, J. M. W.** (1991). *From egg to embryo: Regional Specification in Early Development*. 2nd ed. Cambridge, UK: Cambridge University Press.
- Solursh, B. M., Fisher, M., Meier, S. and Singley, C. T.** (1979). The role of extracellular matrix in the formation of the sclerotome. *J. Embryol. Exp. Morphol.* **54**, 75–98.
- Soroldoni, D., Jorg, D. J., Morelli, L. G., Richmond, D. L., Schinderlin, J., Julicher, F. and Oates, A. C.** (2014). A Doppler effect in embryonic pattern formation. *Science*. **247**, 1451–1455.
- Spemann, H. and Mangold, H.** (1924). Über Induktion von Embryonalanlagen durch Implantation Artfremder Organisatoren. *Roux Arch. Entw. Mech. Org.* **100**, 599–638.
- Spratt, N. T.** (1946). Formation of the primitive streak in the explanted chick blastoderm marked with carbon particles. *J. Exp. Zool.* **103**, 259–304.
- Spratt, N. T.** (1955). Analysis of the organizer center in the early chick embryo. *J. Exp. Zool.* **128**, 121–164.
- Spratt, N. T. and Condon, L.** (1947). Localization of prospective chorda and somite mesoderm during regression of the primitive streak in the chick blastoderm. *Anatomica* **99**, 653.
- Stemple, D. L.** (2005). Structure and function of the notochord: an essential organ for chordate development. *Development* **132**, 2503–2512.
- Stern, C. D.** (1990). Two distinct mechanisms for segmentation? *Semin. Dev. Biol.* **1**, 109–116.

- Stern, C. D.** (1998). Detection of multiple gene products simultaneously by in situ hybridization and immunohistochemistry in whole mounts of avian embryos. *Curr. Top. Dev. Biol.* **36**, 223–243.
- Stern, C. D. and Bellairs, R.** (1984). The roles of node regression and elongation of the area pellucida in the formation of somites in avian embryos. *J. Exp. Morphol.* **81**, 75–92.
- Stern, C. D. and Holland, P. W. H.** (1993). *Essential Developmental Biology: A Practical Approach*. 1st ed. New York: Oxford University Press Inc.
- Stern, C. D. and Ireland, G. W.** (1981). An Integrated Experimental Study of Endoderm Formation in Avian Embryos. *Anat. Embryol. (Berl)*. **163**, 245–263.
- Stern, C. D. and Keynes, R. J.** (1987). Interactions between somite cells: the formation and maintenance of segment boundaries in the chick embryo. *Development* **99**, 261–72.
- Stern, C. D. and Piatkowska, A. M.** (2015). Multiple roles of timing in somite formation. *Semin. Cell Dev. Biol.*
- Stern, C. D., Sisodiya, S. M. and Keynes, R. J.** (1986). Interactions between neurites and somite cells: Inhibition and stimulation of nerve growth in the chick embryo. *J. Embryol. Exp. Morphol.* **91**, 209–226.
- Stickney, H. L., Barresi, M. J. F. and Devoto, S. H.** (2000). Somite Development in Zebrafish. *Dev. Dyn.* **219**, 287–303.
- Storey, K. G., Crossley, J. M., Robertis, E. M. D. E., Norris, W. E. and Stern, C. D.** (1992). Neural induction and regionalisation in the chick embryo. *Development* **114**, 729–741.
- Streit, A. and Stern, C. D.** (1999). Mesoderm patterning and somite formation during node regression: differential effects of chordin and noggin. *Mech. Dev.* **85**, 85–96.
- Streit, A., Berliner, A. J., Papanayotou, C., Sirulnik, A. and Stern, C. D.** (2000). Initiation of neural induction by FGF signalling before gastrulation. *Nature* **406**, 6–10.

- Strudel, G.** (1955). L'action morphogène du tube nerveux et de la corde sur la différenciation des vertèbres et des muscles vertébraux chez l'embryon de poulet. *Arch. Anat. Microsc. Morph. Exp* **44**, 209–235.
- Sunier, A. L.** (1911). Les premier stades de la différenciation interne du myotome et la formation des éléments sclérotomatique chez les acranians, les Sélaciens, et les Téléostéens. *Tijdsh. Nederlansche Dierkd. Ver.* **12**, 75–181.
- Takada, S., Stark, K. L., Shea, M. J., Vassileva, G., McMahon, J. A. and McMahon, A. P.** (1994). Wnt-3a regulates somite and tailbud formation in the mouse embryo. *Genes Dev.* **8**, 174–189.
- Takahashi, Y., Koizumi, K., Takagi, A., Kitajima, S., Inoue, T., Koseki, H. and Saga** (2000). Mesp2 initiates somite segmentation through the Notch signalling pathway. *Nat. Genet.* **25**, 390–396.
- Takahashi, Y., Inoue, T., Gossler, A. and Saga, Y.** (2003). Feedback loops comprising Dll1, Dll3 and Mesp2, and differential involvement of Psen1 are essential for rostrocaudal patterning of somites. *Development* **130**, 4259–4268.
- Takahashi, J., Ohbayashi, A., Oginuma, M., Saito, D. and Mochizuki, A.** (2010). Analysis of Ripply1/2-deficient mouse embryos reveals a mechanism underlying the rostro-caudal patterning within a somite. *Dev. Biol.* **342**, 134–145.
- Takahashi, Y., Yasuhiko, Y., Takahashi, J., Takada, S., Johnson, R. L., Saga, Y. and Kanno, J.** (2013). Metameric pattern of intervertebral disc/vertebral body is generated independently of Mesp2/Ripply-mediated rostro-caudal patterning of somites in the mouse embryo. *Dev. Biol.* **380**, 172–184.
- Takashima, Y., Ohtsuka, T., González, A., Miyachi, H. and Kageyama, R.** (2011). Intronic delay is essential for oscillatory expression in the segmentation clock. *PNAS* **108**, 3300–3305.
- Tam, P. P. L.** (1981). The control of somitogenesis in mouse embryos. *J. Embryol. Exp. Morphol.* **65**, 103–128.
- Tautz, D.** (2004). Segmentation. *Dev. Cell* **7**, 301–312.

- Teillet, M. a and Le Douarin, N. M.** (1983). Consequences of neural tube and notochord excision on the development of the peripheral nervous system in the chick embryo. *Dev. Biol.* **98**, 192–211.
- Teillet, M., Watanabe, Y., Jeffs, P., Duprez, D., Lapointe, F. and Le Douarin, N. M.** (1998). Sonic hedgehog is required for survival of both myogenic and chondrogenic somitic lineages. *Development* **125**, 2019–30.
- Tonegawa, A. and Takahashi, Y.** (1998). Somitogenesis controlled by Noggin. *Dev. Biol.* **202**, 172–82.
- Tonegawa, A., Funayama, N., Ueno, N. and Takahashi, Y.** (1997). Mesodermal subdivision along the mediolateral axis in chicken controlled by different concentrations of BMP-4. **1984**, 1975–1984.
- Tzouanacou, E., Wegener, A., Wymeersch, F. J., Wilson, V. and Nicolas, J. F.** (2009). Redefining the Progression of Lineage Segregations during Mammalian Embryogenesis by Clonal Analysis. *Dev. Cell* **17**, 365–376.
- Untergasser, A., Cutcutache, I., Koressaar, T., Ye, J., Faircloth, B. C., Remm, M. and Rozen, S. G.** (2012). Primer3 — new capabilities and interfaces. *Nucleic Acids Res.* **40**, 1–12.
- Van Eeden, F. J., Granato, M., Schach, U., Brand, M., Furutani-Seiki, M., Haffter, P., Hammerschmidt, M., Heisenberg, C. P., Jiang, Y. J., Kane, D. A., et al.** (1996). Mutations affecting somite formation and patterning in the zebrafish, *Danio rerio*. *Development* **123**, 153–64.
- Vasiliauskas, D., Hancock, S. and Stern, C. D.** (1999). SWiP-1: novel SOCS box containing WD-protein regulated by signalling centres and by Shh during development. *Mech. Dev.* **82**, 79–94.
- Verbout, A. J.** (1976). A Critical Review of the ‘Neugliederung’ the Vertebral Column Concept. *Acta Biotheor.* **25**, 219–258.
- Verbout, A. J.** (1985). The development of the vertebral column. *Adv. Anat. Embryol. Cell Biol* **90**, 1–122.
- Viebahn, C.** (2001). Hensen’s Node. *Genesis* **29**, 96–103.

- Von Ebner, V.** (1889). Urwirbel und Neugliederung der Wirbelsäule. *Sitzungsber Akad Wiss Wien III* **97**, 194–206.
- Wacker, S. A., Jansen, H. J., McNulty, C. L., Houtzager, E. and Durston, A. J.** (2004). Timed interactions between the Hox expressing non-organiser mesoderm and the Spemann organiser generate positional information during vertebrate gastrulation. *Dev. Biol.* **268**, 207–219.
- Waddington, C. H.** (1930). Developmental Mechanics of Chicken and Duck Embryos. *Nature* **125**, 924–925.
- Waddington, C. H.** (1932). Experiments on the Development of Chick and Duck Embryos, Cultivated in vitro. *Philos. Trans. R. Soc. London B* **221**, 179–230.
- Walmsley, R.** (1953). The Development and growth of the intervertebral disc. *Edinb. Med. J.* **60**, 341–364.
- Wang, S., Kryvi, H., Grotmol, S., Wargelius, A., Krossøy, C., Epple, M., Neues, F., Furmanek, T. and Totland, G. K.** (2013). Mineralization of the vertebral bodies in Atlantic salmon (*Salmo salar* L.) is initiated segmentally in the form of hydroxyapatite crystal accretions in the notochord sheath. *J. Anat.* **223**, 159–170.
- Watterson, R. L., Fowler, I. and Fowler, B. J.** (1954). The role of the neural tube and notochord in development of the axial skeleton of the chick. *Am. J. Anat.* **95**, 337–399.
- Wellik, D. M.** (2007). Hox patterning of the vertebrate axial skeleton. *Dev. Dyn.* **236**, 2454–63.
- Wellik, D. M. and Capecchi, M. R.** (2012). Hox10 and Hox11 Genes Are Required to Globally Pattern the Mammalian Skeleton. *Science*. **301**, 363–367.
- Werner, Y. L.** (1971). The ontogenic development of the vertebrae in some gekkonoid lizards. *J. Morphol.* **133**, 41–92.
- Williams, L. W.** (1908). The later development of the notochord in mammals. *Am. J. Anat.* **8**, 251–284.
- Williams, L.** (1910). The Somites of the Chick. *Am J Anat* **2**, 55–100.

Williams, B. A. and Ordahl, C. P. (1994). Pax-3 expression in segmental mesoderm marks early stages in myogenic cell specification. *Development* **120**, 785–796.

Wolpert, L. (1969). Positional Information and Spatial Pattern of Cellular Differentiation. *J. Theor. Biol.* **25**, 1–47.

Yang, X., Dormann, D., Mu, A. E. and Weijer, C. J. (2002). Cell Movement Patterns during Gastrulation in the Chick Are Controlled by Positive and Negative Chemotaxis Mediated by FGF4 and FGF8. *Dev. Cell* **3**, 425–437.

Yardley, N. and Garcia-Castro, M. I. (2012). FGF signaling transforms non-neural ectoderm into neural crest. *Dev. Biol.* **372**, 166–177.

Zhou, W., Hur, W., Mcdermott, U., Dutt, A., Xian, W., Scott, B., Zhang, J., Sharma, S. V, Brugge, J., Meyerson, M., Settleman, J. and Gray, N. S. (2011). A Structure-guided Approach to Creating Covalent FGFR Inhibitors. *Chem. Biol.* **17**, 285–295.

Supplementary Material

The following supplementary movies can be found on the attached CD-ROM.

Movies S1 and S2

Tracing somites adjacent to a notochord graft. Time-lapse movies show development of embryo in which somites are labelled adjacent to a notochord graft using DiO. S1 shows movie in bright field channel overlaid with green fluorescent channel (DiO). S2 shows movie in bright field channel only. Still images from movies S1 and S2 can be seen in Fig. 5.3 A-C and D-F respectively.

Movies S3 and S4

Notochord precursor grafts generate an ectopic notochord that attracts the paraxial mesoderm. Time-lapse movies show two examples of the development of embryos in which a notochord precursor graft from a HH4 quail was placed on the right side of the primitive streak of a HH5-6 chick host. Still images from movies S3 and S4 can be seen in Fig. 6.1H-L and N-R respectively.